Hippocampal circuit dynamics during learning and sleep in freely behaving macaque monkeys

By

Saman Abbaspoor

Dissertation

Submitted to the Faculty of the

Graduate School of Vanderbilt University

In partial fulfillment of the requirements

for the degree of

DOCTOR OF PHILOSOPHY

In

Psychology

May 10th, 2024

Nashville, Tennessee

Approved

Professor Kari Hoffman, Ph.D.

Professor Ivan Soltesz, Ph.D.

Professor Sean Polyn, Ph.D.

Professor Andre Bastos, Ph.D.

to the brave people of Iran and the world

who are valiantly fighting against evil

Acknowledgments

I extend my deepest gratitude to my Ph.D. supervisor, Dr. Kari Hoffman, whose unwavering guidance, support, and expertise was invaluable throughout this transformative journey. Over the last five years, you have patiently taught me the principles, discipline, and rigor needed to be a researcher.

I express my sincere appreciation to my esteemed committee members, Dr. Ivan Soltesz and Dr. Sean Polyn, Dr. Andre Bastos, Dr. Jon Kass, and Dr. Thilo Womelsdorf, for their insightful feedback and contributions to the development of this dissertation.

A special thank you to the former and current members of our lab. I would like to thank Ahmed Hussin, who helped me with my first publication in the lab. I would like to thank Dr. Wolf Zinke and Dr. Daicia Allen for their contribution to developing the Treehouse, which created the pivotal infrastructure for my experimental work. I am grateful to Chrissy Suell and Mitchell Riley, who not only trained me on the many nuances of working with macaques but also provided endless support throughout my time in the Hoffman Lab and Mariana Gabi for helping me with training. I would like to thank Ken Fahmidur, Sarah Cooper, Ayman Aljishi, and Richard Song, whose collaboration, support, and feedback significantly enriched the research process. Finally, I would like to thank Michelle Rumrill for making the lab a cheerful, vibrant environment.

I extend further thanks to members of the Department of Psychology whom I have had the pleasure to interact during my time at Vanderbilt. In the office, I thank Beth Clark, Savannah Crutchfield, Erin Duran, and Cris Zerface. I extend a special thanks to Angel Gaither, whose kindness and patience were invaluable in helping me navigate the US college system. For contributing to the technical aspects of my research, I would like to thank Isaac Haniff, Darin Richardson, Bruce Williams, and Roger Williams. Finally, I would like to thank Adam Neumann for sharing his time and knowledge to help me with my research.

I extend my heartfelt appreciation to Finn and Willow, the monkeys whose contributions were essential to the advancement of our scientific understanding. Their sacrifices have not gone unnoticed and are deeply appreciated.

On a personal note, I extend my gratitude to my parents, Hedayat and Ashraf, and my sister, Sonia, who have consistently supported me through every challenging moment, demonstrating boundless love and kindness. Special thanks go to my friends and family—Mahdi Khadem, Seyyed Javad Saghravanian, Kianoush Banaie Boroujeni, Ramin Abbasi, and Roya Mohammadsadegh and all the members of the Neurosyntax Academy, who have cultivated in me a sense of curiosity and an unwavering desire for knowledge, propelling me forward with relentless determination.

This work would not have been possible without the collective efforts of everyone mentioned above.
Thank you for being an integral part of this academic endeavor.

Table of Contents

List of Figures

List of Tables

1. Background

1.1 The interplay of neural network states and cognitive-behavioral states

The primary aim of systems neuroscience is to comprehend how the nervous system's operations, particularly within neural circuits and networks levels, underlie an organism's capacity to function in its intricate environment. Neurophysiologists often employ statistical methods to unveil associations between neural activity patterns and observable behavior; however, research over the past two decades has revealed that these neural-behavior connections offer only a partial narrative. Neuronal activity, whether at the individual-cell or population level, is not solely influenced by external factors but is also intricately governed by the dynamics of the networks in which they are embedded (Harris et al. 2003; Carrillo-Reid et al. 2015; Dragoi and Tonegawa 2014; Fontanini and Katz 2008). Network activity is described as "states," characterized by a balance of inhibitory and excitatory processes. These states can be observed through recordings of local field potentials (LFPs) which capture the collective electrical activity within local networks (György Buzsáki, Anastassiou, and Koch 2012). The term "network state" denotes the emergence of coherent, often oscillatory, patterns in the activity of interconnected individual neurons (Fontanini and Katz 2008). Theoretical analyses have suggested that alterations in these network states can significantly and non-randomly influence how individual neurons respond to incoming inputs (Başar et al. 2000; Singer 1993; György Buzsáki 2006).

The relationship between network states and cognitive-behavioral states can be explored during the transition from sleep to wakefulness which is marked by significant alterations in neural network states (Fontanini and Katz 2008). These changes can be quantified by shifts in the frequency spectrum of individual LFPs and interactions between multiple LFPs or spike trains (Pesaran et al. 2018). Sleep encompasses various stages, each correlated with distinct LFP patterns, physiological characteristics, and behavior (Klinzing, Niethard, and Born 2019; Diekelmann and Born 2010; Steriade, McCormick, and Sejnowski 1993). Neuronal responses to the same external stimuli differ during different

network states in various sleep stages (Livingstone and Hubel 1981; Edeline et al. 2001). This implies that even in seemingly monolithic situations where the animal remains immobile without apparent movements, neural responses are contingent on subtle distinctions in local and distributed network states. During wakefulness, significant changes in animal behavior or cognitive states coincide with shifts in network states. Similarly, in awake animals, individual neurons' activity is intricately linked to the immediate spatiotemporal dynamics of the network (Mark and Tsodyks 2012; Grinvald et al. 2003; Tsodyks et al. 1999).

Learning can modify an organism's ability to perceive the spatiotemporal dynamics of its environment, comprehend their relevance, and engage with them effectively. At the circuit-level, learning leads to alterations in network states, including variations in the spectral content of spontaneous activity in different areas, along with shifts in functional connectivity within and between regions as learning progresses (Segal, Disterhoft, and Olds 1972; Quirk, Repa, and LeDoux 1995; W E Skaggs and McNaughton 1996; Wilson and McNaughton 1993; Macrides, Eichenbaum, and Forbes 1982). Additionally, the spiking patterns of individual neurons change in response to the environment and in relation to ongoing network states (Benchenane et al. 2010; Hirase et al. 2001; Ji and Wilson 2008). These changes in neuronal responses driven by learning result from widespread patterns of plasticity at multiple levels within the circuit or transient phenomena, such as the phasic activation of neuromodulatory nuclei (Jeffrey C Magee and Grienberger 2020; Abbott and Nelson 2000; Mayford, Siegelbaum, and Kandel 2012; Bocchio, Nabavi, and Capogna 2017). In this manner, network function shapes sensory function, with learning-related synaptic plasticity facilitating the transition of the network into new states. In this context, as behavioral control relies on the functional attributes of neurons operating within a framework of transformed neuronal circuit dynamics, the processing of incoming stimuli continuously evolves through experience. This body of work highlights that experience and internal contexts exert a profound impact on sensory network states, subsequently influencing the processing of specific sensory stimuli. With these insights, cognitive states can be reconceptualized in terms of network states which constraints the way environment can modulate neural dynamics and learning can be defined as a specific shift in the network-level neural states.

In conclusion, it is imperative to investigate the prevailing network states across different cognitive-behavioral states, how these network states organize the patterns of activity at the single cell or population level, and how the emerging neural dynamics supports behavior. In the context of this dissertation, I will focus these questions on the operations of the hippocampus, a brain region renowned for its involvement in learning and memory processes, in macaque monkeys during awake-learning and sleep state transitions.

1.2 An ethological approach to brain and memory research

Both in animals and humans, multiple lines of evidence from anatomical, neuropsychological, and physiological investigations suggest that the hippocampus plays a vital role in the organization and persistence of memory networks. Impairments in memory retrieval, particularly with respect to contextual memories and the sequence of recently visited spatial locations, are prominently observed when the hippocampus is lesioned or inactivated. (Douglas 1967; Hampton and Shettleworth 1996; Sutherland et al. 1989; Maren, Aharonov, and Fanselow 1997; Fortin, Wright, and Eichenbaum 2004; Gaffan 1994; Hampton, Hampstead, and Murray 2004; Lavenex, Amaral, and Lavenex 2006; Scoville and Milner 1957; Ryan et al. 2000; Moscovitch et al. 2005; L R Squire 1992). This highlights the hippocampus's involvement in processing the sequential ordering of events rich in spatiotemporal context (Fortin, Agster, and Eichenbaum 2002; Agster, Fortin, and Eichenbaum 2002). Additionally, the hippocampus support generalization across memories that share item and context information, aligning with its proposed role in transforming detailed memory representations into gist-like and schematic forms (Libby et al. 2019). Furthermore, the hippocampus plays a crucial role in memory consolidation, the process by which newly acquired, initially fragile and interference-prone memories transition into more stable and enduring forms over time (Dudai 2004; Larry R Squire et al. 2015; Bontempi et al. 1999; Frankland and Bontempi 2005; G Buzsáki 1989). While there is a consensus on the hippocampus's critical role in learning and memory, debates persist regarding its precise functional contributions to these processes. In various species, hippocampal single cell activity correlates with

changes in location (J O'Keefe 1976), directions, movement speed (Maurer et al. 2005, 2012; Geisler et al. 2007), time (Mankin et al. 2012; L M Rangel et al. 2014; Kraus et al. 2013), context (Rajji et al. 2006), and event sequences (Manns, Howard, and Eichenbaum 2007; Wood et al. 2000). Because episodic memories inherently contain details about the timing and location of events, these single-cell findings underscore the hippocampus's substantial involvement in representing critical contextual information for event memory. Additionally, insights have been gained into the internal organization of neural activity within the hippocampus, which I will review in the following sections. Many of these findings have primarily originated from rodent studies. Translating the findings of rodent to primates, including humans, is laden with challenges due to differences in perceptual capabilities, exploratory behaviors, brain structures, and functions (Kaas, Qi, and Stepniewska 2022; Passingham 2009; Pine, Wise, and Murray 2021; Thome et al. 2017). Furthermore, electrophysiological studies in primates have predominantly revolved around stationary computerized tasks, rendering direct comparisons with freely-moving rodent findings a complicated endeavor.

While traditional laboratory memory tasks have contributed to our understanding of memory systems, these sterile laboratory paradigms often overlook critical aspects of memory processes and learning, such as dynamic engagement within complex 3D environments (Shamay-Tsoory and Mendelsohn 2019). Evidence suggests that actively engaging with the environment significantly impacts and enhances memory formation, especially for visuospatial and spatial information, potentially due to providing more specific and detailed memories compared to passive experiences (Carassa et al. 2002; Brandstatt and Voss 2014; Koriat and Pearlman-Avnion 2003; Murty, DuBrow, and Davachi 2015; Plancher et al. 2013; Rotem-Turchinski, Ramaty, and Mendelsohn 2019; Brooks et al. 1999; Penaud et al. 2022). These findings align with the embodied views of memory, emphasizing the role of bodily interactions in memory formation (Glenberg 1997). Omitting natural elements such as real contextual information, active participation, and bodily movement diminishes the ecological validity, and hinders our understanding of network and mnemonic states in real-life contexts (Shamay-Tsoory and Mendelsohn 2019).

To address the limitations of stationary memory tasks and bridge the gap between rodent and primate research on the interplay of network states and cognitive-behavioral states, this dissertation will leverage freely behaving macaques within a more natural training environment. The rhesus macaque (Macaca mulatta) shows close genetic homology to humans (Rhesus Macaque Genome Sequencing and Analysis Consortium et al. 2007) and shares numerous structural and functional features with human brains (Orban, Van Essen, and Vanduffel 2004; Nakahara et al. 2002; Vanduffel et al. 2002). They are also capable of performing complex cognitive tests similar to those used in humans (Nagahara, Bernot, and Tuszynski 2010; Peters et al. 1996; Rapp and Amaral 1989; Chau et al. 2011). A memory system like the human episodic memory system can be identified in macaque monkeys (Gaffan 1994; Templer and Hampton 2012; Hampton, Engelberg, and Brady 2020; Brown et al. 2019; Templer and Hampton 2013b). For these reasons, macaques as model organisms represent a holistic and systems approach to studying mechanisms underlying human learning and memory.

1.3 Cytoarchitectonic Organization of the hippocampal CA1

Over the years, the mammalian hippocampal formation has held a fascination for neuroscientists due to its easily distinguishable anatomical characteristics and prominent electrophysiological activity patterns. In the following sections, I will begin by providing an account of the sublayer-specific organization and dynamics of CA1 microcircuits in rodents, as this model has been the most extensively studied. Subsequently, I will establish connections between these dynamics and memory models. For each section, I will take a comparative electrophysiological approach and explore the similarities and differences between rodent and primate models, which serve as the driving force behind the dissertation projects I will present.

The hippocampal formation (HF) consists of three distinct subregions: the dentate gyrus (DG), the hippocampus proper (comprising CA3, CA2, and CA1), and the subiculum (Sub) (Andersen et al. 2006). In this dissertation, my primary focus is on CA1. A feature

of the hippocampus, which greatly facilitates the study of its local field potentials, is its laminar organization. Within CA1, specific sub-layers are clearly delineated: stratum oriens (so), stratum pyramidal (sp), stratum radiatum (sr), and stratum lacunosum moleculare (slm). The stratum oriens, situated deep to the pyramidal cell layer, is a relatively narrow layer with minimal cell density. It houses the basal dendrites of pyramidal cells along with various classes of interneurons. Stratum pyramidal is densely populated with various pyramidal cell types and several categories of inhibitory interneurons (Klausberger and Somogyi 2008; Pelkey et al. 2017). Immediately above the pyramidal cell layer in CA1 lies the stratum radiatum. The stratum oriens and stratum radiatum are the locations for CA3 to CA3 associational connections and the CA3 to CA1 Schaffer collateral connections. The uppermost layer of the hippocampus is referred to as the stratum lacunosum-moleculare, where fibers from the entorhinal cortex make their terminations. Both the stratum radiatum and the stratum lacunosum-moleculare house a diverse array of interneurons.

The hippocampus is composed of various cell classes (Klausberger and Somogyi 2008; Pelkey et al. 2017; Bugeon et al. 2022; Cembrowski and Spruston 2019). While hippocampal CA1 pyramidal neurons were traditionally considered a homogenous population, recent observations have provided strong evidence of within-cell-type heterogeneity, along different axes (Ivan Soltesz and Losonczy 2018). This dissertation focuses on differentiating between superficial (CA1sup) and deep (CA1deep) pyramidal cells along this radial axis. These two distinct groups of pyramidal cells originating at distinct time points developmentally, and exhibit variations in gene expression and can be identified using specific biomarkers (Slomianka et al. 2011). Notably, strongly calbindin-expressing cells are the only ones that tend to occupy a superficial location in the pyramidal cell layer across rodents, macaques, and humans (Seress, Gulyás, and Freund 1991; Seress et al. 1993; Baimbridge and Miller 1982; Rami et al. 1987).
Furthermore, they also diverge concerning their inputs from the entorhinal cortex, with deep CA1 pyramidal cells receiving stronger projections from the medial entorhinal cortex (MEC) in proximal CA1 and superficial CA1 pyramidal cells receiving stronger inputs from the lateral entorhinal cortex (LEC) in distal CA1 (Masurkar et al. 2017). Additionally, CA2 pyramidal cells provide more substantial excitatory inputs to deep CA1 pyramidal cells

compared to their superficial counterparts (Kohara et al. 2014). These differences extend to the dendritic morphology, with deep pyramidal cells extend less of their dendritic tree into stratum radiatum compared to superficial pyramidal cells (Bannister and Larkman 1995). Similarly, macaque monkeys have significantly higher apical dendritic arborization in superficial pyramidal cells compared to those at deeper levels (Altemus et al. 2005). These subclasses of pyramidal cells also vary in their efferent connectivity. Retrograde tracing in rodents and primates have revealed a preference for labeled pyramidal cells to be located either deep or superficial within the cell layer. These include the hippocampo-septal projection (Chronister and DeFrance 1979), projections from deep CA1 pyramidal cells to the prefrontal cortex (Insausti and Muñoz 2001; Barbas and Blatt 1995; Roberts et al. 2007; Harvey et al. 2023), and orbitofrontal cortices (Cavada et al. 2000), as well as projections from superficial CA1 pyramidal cells to the medial temporal cortex (Yukie 2000; Insausti and Muñoz 2001) and medial entorhinal cortex (Harvey et al. 2023).

In contrast to the supposed uniformity of hippocampal pyramidal cells, the diversity of hippocampal GABAergic interneurons has long been recognized (Parra, Gulyás, and Miles 1998; Pelkey et al. 2017; Klausberger and Somogyi 2008; Krook-Magnuson et al. 2012; T F Freund and Buzsáki 1996). Inhibitory interneurons can be distinguished by their anatomical features (e.g. domain-specific innervation of postsynaptic cells), molecular characteristics (e.g.expression of calcium-binding proteins, neuropeptides and transcription factors) and functional properties (e.g. intrinsic electrophysiological properties and the phase-specific firing during hippocampal network oscillations). Moreover, the specialization of inhibitory neurons can further be revealed with respect to their interactions with different subpopulation of pyramidal cells (Krook-Magnuson et al. 2012). Specifically, CA1deep neurons exhibit stronger connectivity with CCK+ basket cells, which, in turn, provide substantial innervation to CA1sup (Valero et al. 2015). Conversely, parvalbumin basket cells (PVBCs) receive increased excitation from CA1sup but deliver stronger inhibition to CA1deep (S.-H. Lee et al. 2014). This intricate organization suggests the presence of distinct microcircuits within the hippocampal network, potentially contributing to the support of various behavioral and cognitive phenomena (Ivan Soltesz and Losonczy 2018).

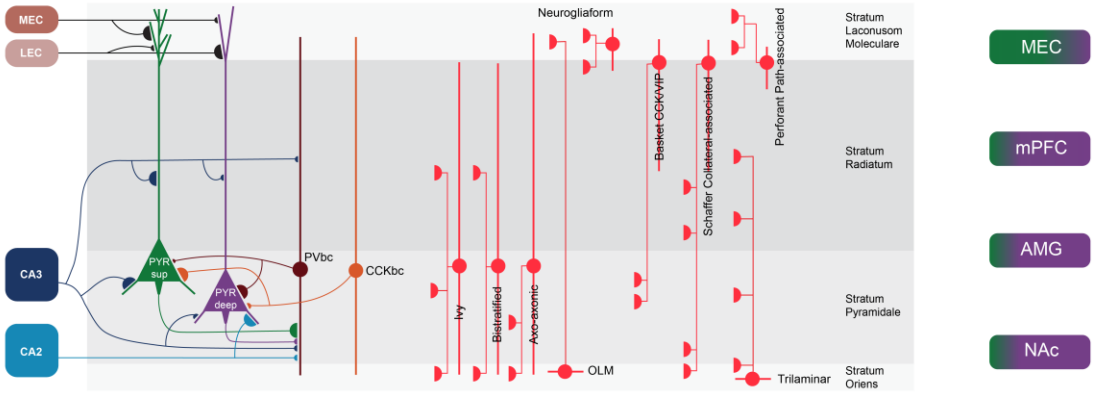

Figure 1-1. Schematic representation of hippocampal pyramidal and interneuron subtypes.

Left. The location of the soma and the axonal target projection for each cell type is illustrated by circles and semicircles respectively. Think lines extending through layers are dendrites. Deep CA1PCs receive stronger feedforward excitation from MEC and from hippocampal area CA2, while superficial CA1PCs receive stronger excitatory drive from LEC. CA3 Schaffer collateral excitation is stronger in calbindin-positive, superficially located CA1PCs. PVBCs provide stronger perisomatic inhibition onto deep CA1PCs and receive stronger excitation from superficial CA1PCs. The second major basket cell class that provides perisomatic innervation to PCs, the regular-spiking cholecystokinin-positive (CCK) basket cells, did not show a preference for either the deep or superficial CA1PCs in mice, although they appeared to provide stronger innervation to superficial PCs in rats. Right. Superficial and deep sublayers provide output both to cortical and subcortical target areas. mPFC, medial prefrontal cortex; AMG, amygdala; NAc, nucleus accumbens. For some of these efferent projections, the soma locations of CA1PCs have been mapped, showing or deep/or superficiall-biased localization of projection neurons. (Modified from (Klausberger and Somogyi 2008; Pelkey et al. 2017; Ivan Soltesz and Losonczy 2018))

1.4 State-dependent oscillatory dynamics in the hippocampus

Intricate spatiotemporal interactions among these cell types in the hippocampus culminates in the emergence of distinct neural oscillatory states. To gain deeper insights into the operations of hippocampus, it is important to understand the physiological properties and underlying mechanisms of these state-dependent oscillations. Moreover, we need to elucidate how these oscillatory states correlate with the local spiking activity of different cell types and the coordination of cell assemblies. This multifaceted endeavor will help our understanding of how the dynamics of the hippocampus contribute to learning and memory.

The hippocampus displays distinctive patterns of neural oscillations in different frequency ranges including theta (6–10 Hz), beta (15-30 Hz), beta2 (23-30 Hz), gamma (~40–100 Hz), and ultra-fast (140–200 Hz) frequency ranges (Vanderwolf 1969; G Buzsáki et al. 2003; Bragin, Jandó, Nádasdy, Hetke, et al. 1995; J Csicsvari et al. 1999b; França et al. 2014; Jayachandran et al. 2023). Our understanding of the underlying cellular and synaptic mechanisms of these hippocampal oscillations and their behavioral significance has mainly come from research conducted in rodents. In this context, I will present an overview of the physiological characteristics and proposed mechanisms underlying various state-dependent oscillations, emphasizing theta, gamma, and ripple oscillations in rodents. Furthermore, I will investigate the divergences between rodents and primates concerning these oscillations.

1.4.1 Mechanisms and physiological properties of Theta oscillations in the hippocampus

1.4.1.1 Rodent models

Ever since its discovery in the rabbit hippocampus by Jung and Kornmuller in 1938 (Jung and Kornmüller 1938) behavioral data have been used to support a role for theta rhythm in one of two main behavioral functions: (1) voluntary movement during arousal/alert states, or (2) learning and memory.

Green and Arduini (Green and Arduini 1954) showed that the theta pattern correlated inversely with neocortical desynchronization, suggesting that it represented the hippocampal arousal pattern. Later, Vanderwolf performed studies correlating theta rhythm with specific behavioral states and argued that theta rhythm was particularly prominent in association with voluntary movement (Vanderwolf 1969; Whishaw and Vanderwolf 1973; Bland and Oddie 2001). The same observation has been replicated during different types of movement (W E Skaggs et al. 1996; Fox, Wolfson, and Ranck 1986). Considerable data support a role of theta rhythm in the sensory-motor interface (Bland and Oddie 2001; Macrides, Eichenbaum, and Forbes 1982; Semba and

Komisaruk 1984; Griffin et al. 2004; Berry and Seager 2001). However, theta rhythm (albeit at lower frequencies) also appears during immobility in rats and mice during fear conditioning (Seidenbecher et al. 2003), or attention to predators (Sainsbury, Heynen, and Montoya 1987; Sainsbury, Harris, and Rowland 1987).

Features of theta rhythm also correlate with learning and memory (Berry and Thompson 1978; Winson 1978; Griffin et al. 2004; Berry and Seager 2001). Adey et al. (1960) (Adey 1960), in their early attempts to correlate the theta rhythm with aspects of learning, reported frequency shifts during simple discrimination learning. The rate of learning is faster in individual rabbits when the hippocampal EEG has the highest amount of theta power (Berry and Thompson 1978). Theta rhythm appears to reset its phase for encoding new stimuli during presentation of visual stimuli in a delayed match to sample task (B. Givens 1996) but not during a reference memory task (McCartney et al. 2004).

Theta consists of rhythmical, asymmetric oscillations that have a narrow frequency power spectrum, with a sharp peak around 8 Hz and often associated with higher harmonics (second peak around 16 Hz) (G Buzsáki et al. 2003). Theta oscillation is most regular in frequency and largest amplitude in the str. lacunosum-moleculare of the hippocampal CA1 region (György Buzsáki 2002). Both the amplitude and phase of theta waves change as a function of depth. Current source density (CSD) analysis of Theta oscillations in the hippocampus reveals a strong sink in the CA1 str. lacunusom-moleculare and a source in the pyramidal layer. These observations lend support to rhythmic excitation of the distal dendrites by the entorhinal afferents as a current generator of theta waves (György Buzsáki 2002). Following surgical removal of the EC, the stratum lacunosum-moleculare dipole disappears (Kamondi et al. 1998). Additional sinks are seen in stratum radiatum that are thought to reflect excitatory inputs from the CA3. Although EC and CA3 are considered the main current generators of the extracellularly recorded theta field, neither of these structures are capable of generating theta activity on their own (György Buzsáki 2002). Numerous intrinsic and extrinsic mechanisms have been postulated to underlie theta rhythm generation and its regulation within the hippocampal CA1(György Buzsáki 2002; Colgin 2013). In vivo, septo-hippocampal projections are the main candidates for generating theta rhythmicity.

About 65% of the projections from the septal region to the hippocampus originate from cholinergic neurons (Sun et al. 2014). These cholinergic neurons fire at relatively low frequencies, around 4 Hz (Simon et al. 2006; Sotty et al. 2003), and are responsible for releasing acetylcholine to the proximal dendrites and cell bodies of pyramidal neurons (Frotscher and Léránth 1985; Sun et al. 2014). The levels of cholinergic signaling in the hippocampus typically increase during exploratory activities, leading to enhanced excitability and firing rates of the neurons (H. Zhang, Lin, and Nicolelis 2010; Stanley, Wilson, and Fadel 2012; Park and Spruston 2012). Due to the distinct distribution of cholinergic receptors on various types of interneurons, different levels of acetylcholine may selectively activate specific subsets of interneurons (McQuiston 2014). This selective activation might engage specific interneuron populations across different hippocampal layers, resulting in a highly state-dependent recruitment of interneurons. For example, the oriens-lacunosum moleculare (O-LM) interneurons, situated in the oriens layer with axonal extensions into the radiatum and lacunosum moleculare layers, become active in response to cholinergic input (Leão et al. 2012). In response, they strongly inhibit the distal dendritic tufts of pyramidal neurons in the lacunosum moleculare layer, counteracting the excitation from the entorhinal cortex through the temporoammonic pathway. When optogenetically stimulated, the septo-hippocampal cholinergic projections increase the strength and coherence of theta oscillations while effectively suppressing slower frequency bands (0.5–4 Hz), higher frequency bands above theta (10–25 Hz), and other competing oscillations such as sharp-wave ripples (150-250 Hz) in actively behaving rodents (Vandecasteele et al. 2014). These effects on gamma oscillations closely resemble the patterns observed in theta oscillations.

The septo-hippocampal glutamatergic projections specifically target alveus/oriens interneurons (INTalv/ori) (Sun et al. 2014) and engage them in a manner influenced by the speed of locomotion (Fuhrmann et al. 2015). When these interneurons are activated during higher-speed running, both the population of CA1 pyramidal neurons and the alveus/oriens interneurons show increased firing rates (Fuhrmann et al. 2015). Consequently, INTalv/ori, which can be activated either by cholinergic or glutamatergic septal input, may have a dual effect: they tend to inhibit the distal dendrites of CA1 pyramidal neurons (via O-LM-mediated dendritic inhibition; (Lovett-Barron et al. 2014;

Maccaferri and McBain 1995) while also having a disinhibitory effect on proximal dendrites (by reducing feed-forward inhibition; (Fuhrmann et al. 2015; Leão et al. 2012)).

The third category of septo-hippocampal projections involves GABAergic neurons. Some of the parvalbumin-positive neurons within the medial septum express HCN channels (V. Varga et al. 2008) and exhibit rhythmic firing patterns that tightly couples to the trough or the peak of theta oscillations and thus are proposed to mediate theta synchronization of the local network (Borhegyi et al. 2004). This rhythmic theta activity is then conveyed to the hippocampus. The septohippocampal GABAergic projections predominantly target hippocampal GABAergic interneurons that also express parvalbumin (T F Freund and Antal 1988; T F Freund 1989). Parvalbumin-positive (PV+) hippocampal interneurons, particularly the basket cells, deliver potent synchronized inhibition to the perisomatic region of CA1 pyramidal neurons (Tamás F Freund and Katona 2007). Thus, the net effect of the rhythmic activation of medial septal GABAergic neurons is the rhythmic disinhibition of the hippocampal pyramidal neuron population (Tóth, Freund, and Miles 1997; Hangya et al. 2009). Optogenetic studies confirm the involvement of PV+ interneurons in generating theta oscillations by showing that these interneurons can effectively entrain hippocampal networks to resonate at theta frequencies in vivo (Stark et al. 2013; Gangadharan et al. 2016). Furthermore, rhythmic optogenetic stimulation of medial septal GABAergic neurons controls the frequency of the hippocampal LFP, although it doesn't significantly impact the oscillation frequency of individual hippocampal cells. Therefore, the inputs from septal GABAergic neurons to the hippocampus appear to influence cellular and circuit mechanisms that enhance the rhythmicity of individual cells rather than directly controlling cellular oscillation frequencies.

In vitro recordings in isolated CA1 slices shows theta oscillations, which suggest that theta rhythms can also be generated intrinsically (Goutagny, Jackson, and Williams 2009). A common feature of interneurons in the hippocampus and pacemaker interneurons in the MS is the expression of HCN channels (Maccaferri and McBain 1996; V. Varga et al. 2008). Neurons expressing these channels can undergo a repetitive sequence of events, starting with an action potential, followed by afterhyperpolarization, depolarization via HCN channels, and another action potential, thus initiating a cycle. Disrupting HCN

channels through pharmacological blockade or genetic deletion interferes with theta frequency membrane-potential oscillations (Dickson et al. 2000; Giocomo and Hasselmo 2009). These findings strongly suggest that HCN channels play a pivotal role in generating theta rhythms. This might suggest that any network of neurons containing HCN channels is predisposed to participate in theta rhythms if the neurons are suitably depolarized to trigger this cycle. Depolarization can result from various sources. Neurons that rhythmically fire can recruit other neurons, leading to the spread of theta rhythms across the network. In this scenario, local neuronal groups function as separate oscillators, and the extent of synchronization depends on the reach of pacemaker projections. Thus, theta oscillations combine inputs from a subcortical pacemaker with local operations to generate complex oscillatory patterns (Colgin 2013).

1.4.1.2 Primate models

Early recordings from the monkey hippocampus suggested that theta activity, 4-8 Hz range, is notably less prominent in behaving or sleeping primates compared to rodents (Green and Arduini 1954). Subsequent studies in macaques further substantiated these findings, demonstrating that hippocampal LFP lack a dominant theta rhythmicity, although brief episodes of rhythmicity within the theta frequency band were observed. These patterns were distinct from the robust and continuous theta rhythms observed in rodents during active locomotion and REM sleep (William E Skaggs et al. 2007). The challenges in observing hippocampal theta in awake monkeys have been associated with the fact that the recording methods typically require immobile, head-restrained monkeys, unlike rodent studies involving freely moving animals (William E Skaggs et al. 2007). It is possible that head restraint, like whole-body restraint in rats, might suppress theta activity (T. C. Foster, Castro, and McNaughton 1989). Recent wireless recordings in freely-moving monkeys, including macaques and marmosets, as they naturally explore their spatial environments, indicate that theta activity in these species is either weak or absent. When present, it occurs in brief episodes rather than continuously and is not significantly influenced by locomotion (Talakoub et al. 2019; Courellis et al. 2019; Martinez-Trujillo et

al. 2023). Thus, immobility cannot explain the absence of strong hippocampal theta during wake states in the primate hippocampus. Intriguingly, distinct hippocampal theta activity patterns emerge during offline behavioral states such as sleep or anesthesia (Stewart and Fox 1991). During sleep, the amplitude of theta oscillations is notably more pronounced during slow-wave sleep compared to REM sleep and the waking state (Takeuchi et al. 2015). Wireless recordings in the macaque hippocampus further affirm the prevalence of stronger theta oscillations during early-stage sleep compared to periods of alert volitional movement, including walking (Talakoub et al. 2019). These collective findings suggest that theta activity in the non-human primate hippocampus emerges in short bursts without displaying the stationary slow wave rhythmicity commonly observed in rodents. Similar to rodents, its occurrence is state-dependent, yet in contrast, it is more pronounced during slow-wave sleep. The question remains whether these observations extend to the human hippocampus.

Human studies of the hippocampal theta oscillation have provided mixed evidence complicated by recording techniques, variations in reported spectral properties, prevalence, and behavioral correlates. Here, I will focus on direct hippocampal recordings from neurosurgical patients because this is the only method for obtaining human brain data that are comparable with laboratory recordings of rodents and other primates.

Early direct recordings in the human hippocampus during various behaviors revealed an irregular rhythmic component at 3-4Hz (Arnolds et al. 1980). Notably, while the spectral characteristics of this slow activity consistently changed during verbal behavior, a significant disparity with rodent data was the absence of a connection between gross motor activity (e.g., walking or sitting) and the spectral properties of low-frequency hippocampal oscillations. A pioneering study on hippocampal recordings during virtual navigation reported episodes of 4-8Hz theta activity, which were influenced by virtual movement (Ekstrom et al. 2005). However, low-frequency oscillations (LFO) in humans exhibited a lower frequency compared to rodents, peaking at around 3.3 Hz during virtual movements in humans as opposed to 7.7 Hz in rats (Ekstrom et al. 2005; Watrous et al. 2013). This difference could be attributed to the argument that virtual reality poorly simulates real spatial navigation due to the absence of body-based input, which

potentially impacts the recording of movement-dependent theta activity. In line with this argument, even in rodents, virtual movement has been shown to reduce theta activity compared to real-world movement, resulting in a lower LFO frequency and the removal of the relationship between movement speed and LFO (G. Chen et al. 2013; Ravassard et al. 2013; Aghajan et al. 2015).

During real-world navigation, one study reported peaks at either lower frequencies, between 1–4 Hz, or alpha range, 7-13Hz (Bohbot et al. 2017). In another study during real-world ambulation, bouts of theta, and lower frequencies (<4Hz) in the medial temporal lobe (MTL) of sighted participants occupied less than 10% of recordings but were significantly modulated by movement in terms of prevalence and bout duration. Interestingly the clearest peaks of theta activity were recorded in a congenitally blind participant (M Aghajan et al. 2017). These findings align with previous results showing that hippocampal theta activity decreased during conditions of resting with open eyes and visuospatial activation compared to resting with closed eyes (Meador et al. 1991). This might suggest that visual inputs suppress theta activity in humans.

Several investigations have pointed out variations in the features of theta activity along the longitudinal axis of the hippocampus and between the two hemispheres. The initial study reported that the left hippocampal low-frequency oscillations (3-4Hz) exhibited smaller amplitude and less rhythmicity compared to the right hippocampus (Arnolds et al. 1980). During virtual movement, oscillations around 8 Hz were observed in the posterior hippocampus, and the precise frequency of these oscillations correlated with movement speed, suggesting their involvement in spatial navigation. On the other hand, slower oscillations at around 3 Hz were more common in the anterior hippocampus, and their frequency remained consistent regardless of movement speed (Goyal et al. 2020). Additionally, the average frequency of theta bouts was found to be higher (~6.0 Hz) in the right hippocampus (RH) compared to the left hippocampus (5.3 Hz, LH). LH theta bouts also had lower amplitudes but were more prevalent when compared to the RH, representing 26% versus 21% of the total time (Penner et al. 2022).

A comparison of theta activity between offline and waking active states in humans reveals similar results to monkeys. During periods of quiet wakefulness, hippocampal theta

activity dominates but diminishes when individuals engage in tasks (Halgren, Babb, and Crandall 1978; Meador et al. 1991). Additionally, electrocorticography (ECoG) recordings in the human medial temporal lobe revealed the presence of Beta-1 activity (10-20Hz) and robust gamma oscillations (30-100Hz) during both wakefulness and rapid eye movement (REM) sleep, while they were absent during slow-wave sleep (SWS). Conversely, delta power (frequencies below 4Hz) was more pronounced during SWS in comparison to wakefulness and REM sleep (Uchida et al. 2001). A more recent study indicated that in awake participants, delta (with a peak around 2Hz) and alpha (with a peak around 12Hz) ranges exhibited stronger power, while theta activity appeared more robust in anesthetized patients (Kleen et al. 2021).

Overall, these findings provide compelling evidence that in the primate hippocampus, theta rhythm is altered in frequency, prevalence and behavioral correlates relative to rodents.

1.4.2 Mechanisms and physiological properties of Gamma oscillations in the hippocampus

1.4.2.1 Rodent models

The historical definition of the gamma frequency band in the hippocampus proper has undergone changes over time, with recent research revealing distinct sub-bands of gamma activity (Zhou et al. 2019). Early observations identified a broad, unified range of activity within 25-70 Hz, which often occurred in conjunction with slower theta oscillations but could also manifest independently (Bragin, Jandó, Nádasdy, Hetke, et al. 1995). Gamma and theta rhythms exhibit strong cross-frequency coupling, where the amplitude and/or phase of gamma oscillations are modulated by the phase of theta oscillations (Bragin, Jandó, Nádasdy, Hetke, et al. 1995; G Buzsáki et al. 2003; Belluscio et al. 2012; Tort et al. 2009; Colgin et al. 2009). Consequently, the power of high-frequency gamma activity was observed to be higher during periods of walking and running compared to immobile or drinking states, (G Buzsáki, Leung, and Vanderwolf 1983; Bragin, Jandó,

Nádasdy, Hetke, et al. 1995). Despite similar levels of theta activity in the CA1 region during rapid eye movement (REM) sleep and wakefulness, CA1 gamma activity significantly decreases during REM sleep (Montgomery, Sirota, and Buzsáki 2008). This coupling between theta and gamma rhythms in CA1 is dependent on inhibitory input to parvalbumin-containing (PV) interneurons (Wulff et al. 2009). Removing GABAA receptors from PV interneurons reduces the amplitude of CA1 theta oscillations but leaves gamma oscillations unaffected, supporting the idea that these two rhythms are independently generated and interact through the actions of specific inhibitory cell types.

Bilateral lesions of the entorhinal cortex attenuate or abolish gamma oscillations in the dentate gyrus but unveil a slower (25–50 Hz), larger amplitude gamma oscillation occurring in the CA3 to CA1 network (Bragin, Jandó, Nádasdy, Hetke, et al. 1995). This observation is the first to demonstrate that there are distinct hippocampal gamma oscillators, one in the dentate gyrus and one in the CA3-CA1 network, with the former requiring input from extrahippocampal regions (Bragin, Jandó, Nádasdy, Hetke, et al. 1995). More detailed studies confirm that gamma oscillations can be categorized into different types based on their origin, spatial localization in CA1, and preferred phase of theta (Colgin et al. 2009; Lasztóczi and Klausberger 2014; Belluscio et al. 2012; Scheffer-Teixeira et al. 2012; Schomburg et al. 2014). CA3 and medial entorhinal cortex projections can generate gamma oscillations with slow (25-50 Hz) and medium (60-90 Hz) frequencies, which can be recorded separately in the stratum radiatum (SR) and stratum lacunosum moleculare (SLM) layers of CA1 (Colgin et al. 2009). Faster gamma (90-130 Hz) oscillations appear to result from local spiking activity in the pyramidal layer of CA1 (György Buzsáki and Wang 2012).

Multiple circuit mechanisms have been suggested for the generation of gamma oscillations in the hippocampus (György Buzsáki and Wang 2012; Whittington et al. 2000). Originally, one proposal was the "PING model," which posited that a recurrent network of pyramidal and inhibitory cells could underlie gamma-frequency population rhythms in the hippocampus. In this model, a full cycle included pyramidal cell excitation, followed by inhibitory cell excitation, pyramidal cell inhibition, inhibitory cell disexcitation, pyramidal cell disinhibition (essentially another form of excitation), and this cycle could

repeat. An alternative model (ING) suggests that gamma band local field potential (LFP) patterns can emerge through the activation of reciprocally connected inhibitory interneurons that mutually regulate each other's activity, primarily via reciprocal inhibition (Bartos, Vida, and Jonas 2007; Leung 1998; X. J. Wang and Buzsáki 1996; Börgers and Kopell 2003). PING-type oscillations rely on phasic synaptic excitatory input to interneurons, whereas ING-type oscillations can occur in sparsely connected interneuron networks with only tonic excitatory drive (Traub et al. 1996; Whittington, Traub, and Jefferys 1995). In vitro examinations of intrinsic CA3 gamma oscillations suggest that these oscillations are generated via PING model because inhibition of pyramidal cells suppresses gamma oscillations in CA3 (Cunningham et al. 2003; Gloveli et al. 2005; Traub et al. 2003; Craig and McBain 2015). Conversely, intrinsically generated gamma oscillations in CA1 persist even during optogenetic inhibition of pyramidal cell firing, indicating an ING-type gamma (Craig and McBain 2015). Interestingly, in contrast to CA3, CA1 gamma oscillations do not appear to require the involvement of fast-spiking basket cells (Craig and McBain 2015). In CA1, the firing of bistratified cells, which target dendrites of pyramidal cells coaligned with the glutamatergic input from hippocampal area CA3, is strongly phase locked to field gamma oscillations (Craig and McBain 2015; Tukker et al. 2007) and thus provide an attractive candidate for being the driver of the locally generated, predominantly interneuron-driven model of CA1 gamma oscillations. Overall, these findings underscore the coexistence of various qualitatively distinct gamma oscillations within hippocampal networks.

1.4.2.2 Primate models

As described, in rodents, theta-nested sub-bands of gamma oscillations emerge during waking mobility states and REM sleep, with both oscillations dissipating during slow-wave sleep. This reflects a tight behavioral coupling between theta and gamma in rodents. In the macaque hippocampus, theta and gamma are also behavioral state-dependent but appear uncoupled. Studies investigating the spectral content of the hippocampus (both

dentate gyrus and CA1) across waking-sleep behavioral states have found that during wakefulness and REM sleep, fast gamma oscillations in the frequency range of 20–80Hz dominate the hippocampal LFP. In the deep stages of non-REM sleep, fast gamma oscillations are partly replaced by continuous, slower oscillations ranging from 0.5 to 8 Hz with high amplitudes (Tamura et al. 2013; Takeuchi et al. 2015; Richardson et al. 2017; Talakoub et al. 2019). The most striking feature of REM sleep-related changes in primate hippocampal activity is the increase in gamma band oscillations (Takeuchi et al. 2015), and the low- and gamma-frequency power ratio defines two clear network states that alternate throughout the night (Richardson et al. 2017). These results suggest that in monkeys, hippocampal theta and gamma are associated with distinct behavioral states, in contrast to rodents. This is supported by cross-frequency coupling (CFC) studies.

Amplitude-amplitude CFC (AA-CFC) between gamma oscillations and slow waves (0.5-2 Hz)/theta (4-10 Hz) reveals a significant negative correlation (Takeuchi et al. 2015; Richardson et al. 2017). When measuring CFC separately for different sleep stages, a significant positive correlation between gamma and theta band amplitudes is detected only in stage N4 (Takeuchi et al. 2015), suggesting a strong cooperative relationship between the gamma and delta/theta bands during this stage. Interestingly, phase-amplitude CFC shows that gamma amplitude is significantly modulated by the phase of delta and theta waves during waking states and N3/N4 sleep stages. This phase-amplitude relationship appears strongest for the delta band compared to theta and shows individual differences among subjects (see (Takeuchi et al. 2015), Figure S5, and (Richardson et al. 2017) Figure 4).

In rodents, different sub-bands of gamma have been documented. In macaques, to the best of my knowledge, only one study has reported a clear bimodality in the gamma power spectrum under ketamine-dexmedetomidine sedation (Richardson et al. 2017). Under this condition, the amplitude distributions of low (30 – 50 Hz) and high (75 – 100 Hz) gamma activity as a function of slow oscillations (0.5-2 Hz) phase showed a consistent phase shift resembling segregated phase-amplitude coupling between different types of gamma and theta rhythms in rodents. This bimodality disappeared during sleep recordings, leaving only high-frequency gamma (~70 Hz). In addition, a separate study

showed that monkey hippocampal neurons tend to have spike-field coherence in low gamma (30–60 Hz) or high gamma (60–100 Hz) (Jutras, Fries, and Buffalo 2009). These findings suggest that distinct gamma oscillations might exist in the monkey hippocampus.

Hippocampal gamma range activity has also been detected in human subjects (Fell et al. 2001; Sederberg et al. 2003, 2007; Chaieb et al. 2015; B. Lega et al. 2016; Staresina et al. 2016; Umbach et al. 2022). Broad-band gamma activity (34-130 Hz) shows phase-amplitude coupling with low-frequency oscillations (2.5-5 Hz), and this phase-amplitude coupling is modulated by success or failure during a memory task (B. Lega et al. 2016). More recently, a study reported the presence of two distinct types of gamma activity in the human hippocampus with segregated interareal relationships with neocortical areas. Neocortical alpha/beta (8 to 20 Hz) power decreases reliably precede and predict hippocampal "fast" gamma (60 to 80 Hz) power increases during episodic memory formation; during episodic memory retrieval, however, hippocampal "slow" gamma (40 to 50 Hz) power increases reliably precede and predict later neocortical alpha/beta power decreases (B. J. Griffiths et al. 2019).

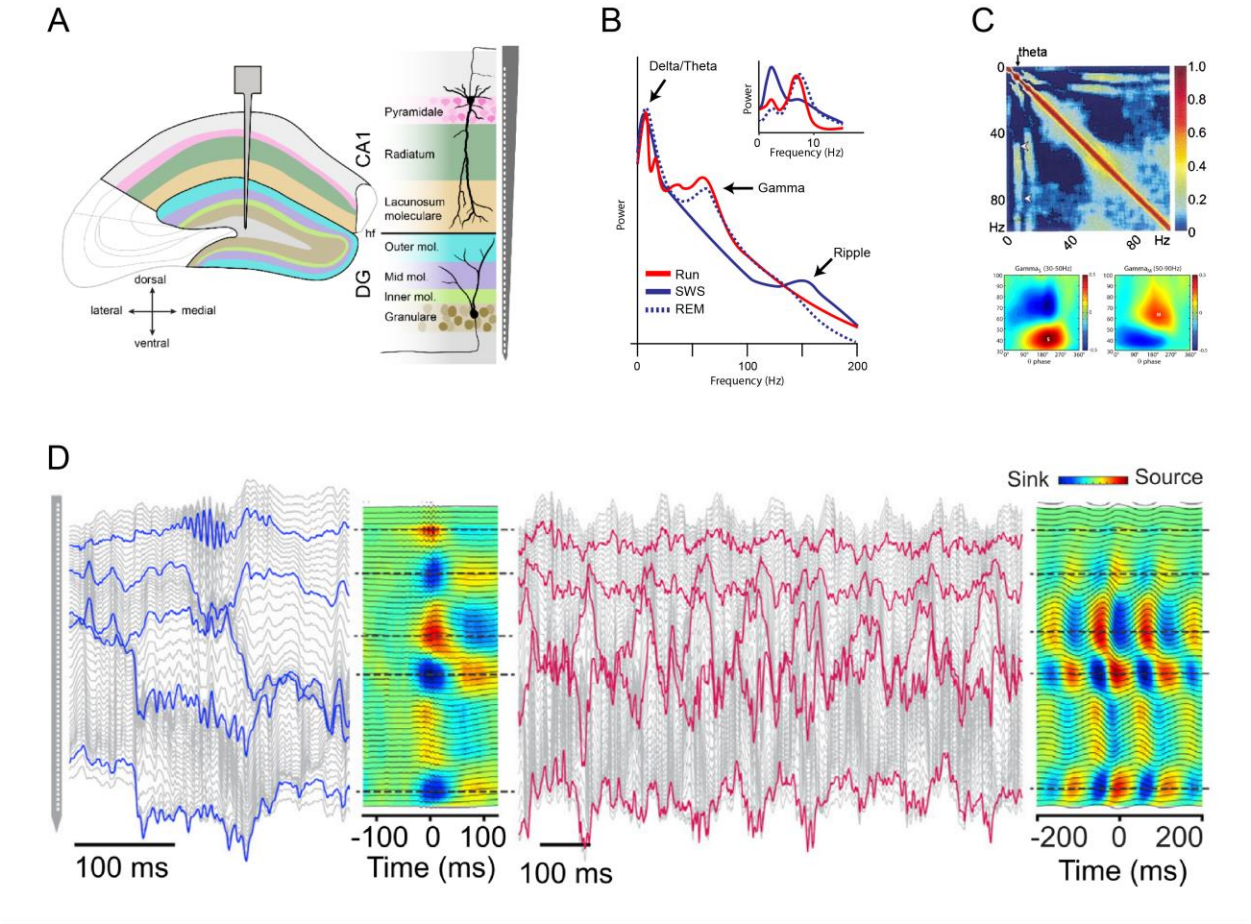

Figure 1-2. Spatiotemporal dynamics of CA1 in the rodents.

A. Schematic representation of different CA1 and Dentate gyrus (DG) layers. B. Power spectral density of CA1 LFP during different stages of sleep (slow-wave sleep, SWS; and rapid-eye movement, REM) and running (RUN). Theta-gamma activity is strongest during RUN and REM and diminishes during SWS. In contrast, sharp-wave ripples emerge during SWS. C. Cross-frequency amplitude-amplitude (TOP) and phase-amplitude (Bottom) coupling showing strong relationship between theta and gamma oscillations in the rodent CA1. D. Examples of laminar recordings in the CA1 and DG in mouse during SWS (blue traces) and RUN (red traces) and current source density showing the position of sinks and sources. A from (Vitor Lopes-dos-Santos, Brizee, and Dupret 2023); B modified from (G Buzsáki et al. 2003; Kang et al. 2017); C from (G Buzsáki et al. 2003; Belluscio et al. 2012); D from (Zutshi et al. 2022) with permission.

1.4.3 Mechanisms and physiological properties of sharp-wave ripples in the hippocampus

1.4.3.1 Rodent models

During offline states of the brain, such as slow-wave sleep and periods of immobility in freely moving animals, the prominent hippocampal "theta state" observed in rodents diminishes or disappears, giving way to the emergence of sharp-wave ripples (SWRs) (G Buzsáki 1986; György Buzsáki 2015). SWRs consist of sharp-waves, which manifest as large-amplitude negative polarity deflections lasting 40–100 ms in CA1 stratum radiatum. These sharp-waves are often, though not consistently, accompanied by a brief fast oscillatory pattern in the local field potential (LFP), referred to as ripples, typically occurring in the range of 130-200 Hz within the CA1 pyramidal layer (György Buzsáki 2015).

Sharp wave-ripple events (SPWs), have a unique depth profile and specific patterns of electrical current sink and source distributions (G Buzsáki, Leung, and Vanderwolf 1983; G Buzsáki 1986; Sullivan et al. 2011). Notably, the most prominent current sinks are localized within the mid-apical dendritic layers of both the CA1 and CA3 regions of the hippocampus (Stark et al. 2014; G Buzsáki et al. 1986). These sinks are accompanied by corresponding current sources within the pyramidal layers of the same regions. These sink-source distributions demonstrate a strong spatial correlation with the evoked LFP responses resulting from electrically induced discharges of CA3 pyramidal neurons (G Buzsáki et al. 1986; G Buzsáki 1989). This correlation implies that SPWs essentially mirror the excitatory depolarization occurring in the apical dendrites of CA1 pyramidal neurons due to the synchronized bursting activity of CA3 pyramidal cells. This synchronized bursting activity in CA3 neurons initiates a series of excitation events directed at CA1 pyramidal cells, which can lead to the local generation of ripples within the CA1 region. Recent research has clarified the temporal sequence of events, indicating that sharp wave-ripples initially manifest in CA3 before propagating to CA1. Interestingly, for a subset of CA1 ripples, the activation of pyramidal cells in CA2 precedes synchronous

firing in CA3 (Oliva et al. 2016). While CA2 neurons contribute to sharp wave-ripple events during both sleep and wakefulness, their role appears to be more pronounced during wakeful states. This finding strongly suggests that CA2 may serve as the primary site for sharp wave-ripple generation. Emerging evidence also points to the significant involvement of the subiculum in the generation of sharp wave-ripples (Oliva et al. 2016). SWRs originating in the subiculum propagate forward into the entorhinal cortex and backward into the hippocampus proper. This observation suggests that structures receiving output from the hippocampus not only facilitate the transmission of sharp wave-ripples to the cortex but also actively participate in their generation (Imbrosci et al. 2021).

Interneurons have been proposed to play a pivotal role in initiating sharp wave-ripple (SPW) bursts through several mechanisms (Ylinen et al. 1995; Schlingloff et al. 2014). First, perisomatic-targeting interneurons can enhance SPW generation by temporarily imposing strong inhibition on a subset of pyramidal neurons. When this inhibition subsides, the synchronized firing of a critical number of pyramidal neurons can start a population burst (Ellender et al. 2010; Stark et al. 2014). In line with this, the optogenetic activation or suppression of parvalbumin-expressing (PV) interneurons has been shown to be sufficient for triggering or interrupting SPW-ripples (Schlingloff et al. 2014; Papatheodoropoulos 2010; Cobb et al. 1995). Notably, whole-cell recordings of postsynaptic current in CA1 pyramidal neurons in awake mice revealed that during SPW-ripples, inhibition prevails over excitation (Gan et al. 2017). Specifically, phasic inhibition, especially by PV+ interneurons, plays a crucial role in shaping SPW oscillations in the hippocampal CA1 region in vivo. These findings support a model in which SPWs are generated through a combination of tonic excitation from CA3 and phasic inhibition within CA1 (Gan et al. 2017). Another potential way in which interneurons may contribute to initiating or sustaining a population burst is through their temporary silencing (György Buzsáki 2015). In this scenario, when CA3 inhibitory cells are silenced, the pyramidal neurons they innervate are released from inhibition, resulting in robust population bursts. A prime candidate for this role is the chandelier or axo-axonic interneuron. Studies in both CA1 and CA3 regions have shown that a subset of axo-axonic neurons exhibit reduced firing rates during SPW-ripples, regardless of whether the subject is anesthetized (Klausberger et al. 2003) or freely moving (Viney et al. 2013; Dudok, Szoboszlay, et al.

2021). The silencing of axo-axonic neurons during SPW-ripples can also be achieved by PV-basket cells and bistratified interneurons. These interneurons exhibit significant increases in discharge rates during SPW-ripples (Ylinen et al. 1995; Klausberger et al. 2003; C. Varga et al. 2014).

1.4.3.2 Primate models

The sharp-wave ripple is a relatively conserved physiological phenomenon of the hippocampal LFP across rodents and primates (A. A. Liu et al. 2022). SWRs have been recorded in different primate species including marmosets (Bukhtiyarova et al. 2022), macaques (William E Skaggs et al. 2007), and humans (Vaz et al. 2019, 2020; Norman et al. 2019, 2021; Y. Y. Chen et al. 2020; Le Van Quyen et al. 2008). Similar to rodents, primate SWRs consist of a high-frequency ripple oscillation, occurring together with a sharp-wave deflection (William E Skaggs et al. 2007). Three notable differences to the rodent are that ripple activity is usually slower in primates than in rodent ripples (William E Skaggs et al. 2007), the slow wave component may not always reverse polarity through the layer, and the post-ripple deflection is more prominent than in rodents (William E Skaggs et al. 2007; Hussin, Leonard, and Hoffman 2020). As in rodents, sharp-wave ripples are more abundant during drowsiness or sleep, although their overall prevalence is less than in rodents, and they can also occur in awake monkeys (Hussin, Leonard, and Hoffman 2020; Leonard and Hoffman 2017; Leonard et al. 2015). In apparent contrast to rodent SWRs, monkey SWRs can occur during active periods of exploration, e.g., while animals searched for a target object in a scene. SWRs were associated with smaller saccades and longer fixations (Leonard and Hoffman 2017; Leonard et al. 2015).

1.4.4 Brain-state- and cell-type-specific firing of hippocampal neurons

The cognitive function of neural oscillations is not inherently determined by their physiological characteristics. The operational advantages and behavioral associations of

a particular oscillation rely on the circuits that generate it. In the hippocampus CA1, extensive research has revealed a remarkable diversity among pyramidal cells and GABAergic interneurons with significant anatomical, molecular, physiological and functional differences (Pelkey et al. 2017; Klausberger and Somogyi 2008; Cembrowski and Spruston 2019; Bezaire and Soltesz 2013; T F Freund and Buzsáki 1996; Ivan Soltesz and Losonczy 2018). Precisely timed inhibition targeting specific somatodendritic regions of pyramidal neurons is essential for maintaining excitation balance, selectively modulating synaptic excitation, regulating the timing of spike output, gain control, governing burst firing and synaptic plasticity (Royer et al. 2012; Topolnik and Tamboli 2022; Kullmann and Lamsa 2007; Dupret, Pleydell-Bouverie, and Csicsvari 2008). Additionally, at the network level, this inhibition plays a crucial role in coordinating cell assemblies by preserving oscillations and synchrony (Dupret, O'Neill, and Csicsvari 2013; Bartolini, Ciceri, and Marín 2013; X.-J. Zhang et al. 2017). A comprehensive understanding of the intricate mechanisms governing local hippocampal operations and their active support of ongoing brain processes necessitates delving beyond oscillations to explore the underlying circuits and the physiological diversity of different cell classes.

1.4.4.1 Rodent models

The firing patterns of different cell classes dynamically change in response to the oscillatory states in the hippocampus. In addition to oscillation-associated alterations in firing rates, hippocampal cell classes also show a specific phase-relationship with different types of local oscillations (Buzsàki and Eidelberg 1983; Klausberger et al. 2003). The phase of firing may fluctuate as a function of the behavioral or brain states (Klausberger and Somogyi 2008). Analyzing the phase relationship between cell types and oscillations offers a valuable tool for understanding network function at a cellular level across species. However, challenges exist. First, rhythms often have a spectrolaminar profile, sometimes with different phases at different locations in hippocampal formation, so the reference waves against which the firing of different neurons are compared must be constant across animals. Secondly, there might exist different kinds of rhythms in a

narrow frequency range, even within a single species (e.g., different types of theta oscillations in rodents). It is crucial to know which kind of rhythm is present and to have data on unit firing in more than one kind. Thirdly, each site in the hippocampal formation harbors different neuron types with distinct relations to the rhythm, emphasizing the need for neuron type identification. Finally, appropriate methods of analysis should be used (Fox, Wolfson, and Ranck 1986).

In terms of firing pattern, hippocampal pyramidal cells are characterized by low average firing rates (<2Hz) and high propensity for generating complex-spike bursts comprising two to seven spikes with interspike intervals of 3–10 ms (Ranck 1973; J Csicsvari et al. 1999b). The physiological properties of pyramidal cells varies as a function of depth in the pyramidal layer. Superficial pyramidal cells display higher firing rates, less burstiness and greater coefficient of variation (Mizuseki et al. 2011; Harvey et al. 2023). Local GABAergic inhibitory cell types in CA1 have a diverse spectrum of firing patterns. Although most of the GABAergic inhibitory cell types have a higher firing rate compared to pyramidal cells (C. Varga, Golshani, and Soltesz 2012; Klausberger et al. 2005, 2003), some inhibitory interneurons, such as Ivy cells, discharge at a low frequency, and have unusually broad waveforms for interneurons, but lack complex spike bursting (Fuentealba et al. 2008). Distinct inhibitory cell classes control the timing, rate and bursts of pyramidal cells (Royer et al. 2012). For example, although silencing PV+ or somatostatin (SOM) expressing interneurons in area CA1 increases the firing rate of pyramidal cells, only SOM suppression, but not PV+, lead to increased burst firing (Royer et al. 2010).

The majority of both pyramidal and inhibitory cell types increase their activity during sharp-wave ripple events (J Csicsvari et al. 1999a; Royer et al. 2012; Geiller et al. 2020; C. Varga, Golshani, and Soltesz 2012); however, the ratio, participation probability, and maximum response time vary among these cell types. Putative pyramidal cells and interneurons typically increase their firing rate during SWRs by approximately sixfold and threefold respectively (J Csicsvari et al. 1999a). The participation probability shows a significantly positive correlation with the firing rate of the cells, with overall inhibitory cell types having higher participation probabilities than pyramidal cell types (Fernández-Ruiz et al. 2019; Nádasdy et al. 1999). Moreover, pyramidal cell types display within-class

variability in participation probability, with CA1deep demonstrating a higher participation probability (Harvey et al. 2023).

In behaving rats, a small population of CA1 cells decrease their firing activity during ripples (J Csicsvari et al. 1999a). Recordings from specific cell classes reveals that these ripple-suppressed cells may include a subset of axo-axonic cells, and CCK-expressing basket cell (Klausberger et al. 2003; Viney et al. 2013; Dudok, Szoboszlay, et al. 2021; Dudok, Klein, et al. 2021). In behaving rats, compared to PVBC and bistratified cells which more reliably and strongly increase their firing during sharp-wave ripples (Katona et al. 2014; C. Varga, Golshani, and Soltesz 2012), O-LM cells show increased firing rate during approximately half of the ripple events (C. Varga, Golshani, and Soltesz 2012) but are otherwise silent or inhibited (Katona et al. 2014). A very small subset of putative pyramidal cells is also suppressed during ripple events (Harvey et al. 2023). The ripple-suppression of a subset of inhibitory cell members or suppression during some but not all ripple events can be due to dynamic reconfiguration of inhibitory circuits to support the expression of distinct behaviorally-relevant pyramidal cell assemblies (Dupret, O'Neill, and Csicsvari 2013). Moreover, if cells are silenced by hyperpolarization, it can create conditions conducive to inducing anti-Hebbian LTP, occurring during negative membrane potentials rather than depolarization. Such synaptic plasticity during sharp-wave ripples in offline states has the potential to influence the phase of pyramidal cell firing and how different afferent input populations contribute to the circuit's population behavior (Kullmann and Lamsa 2007).

Activated pyramidal cells, on average, exhibit their highest firing intensity at the peak of the most prominent ripple amplitudes, (J Csicsvari et al. 1999a; G Buzsáki et al. 1992). Interneurons tend to fire earlier than pyramidal cells, and the decline in their firing frequency is slower than that of the pyramidal cells (J Csicsvari et al. 1999a). Among the group of inhibitory cells, different cell types exhibit varying timing in their discharge patterns. PV basket cells tend to have a high probability of firing right from the beginning of the ripple oscillations, whereas the increase in OLM cell firing occurs with a delayed onset (C. Varga, Golshani, and Soltesz 2012). In behaving rats, during each ripple cycle, the maximum probability of putative pyramidal cell discharge occurs near the trough of

the ripple (J Csicsvari et al. 1999a), with superficial pyramidal cells spiking earlier than deep cells (Stark et al. 2014; Berndt et al. 2023). PVBCs interneurons show strong phase locking to the early ascending phase of the ripple waves. OLM cells preferentially fire during the late ascending phase of the ripple waves (C. Varga, Golshani, and Soltesz 2012). In anesthetized rats, bistratified cells fire with high frequency and in-phase with PVBCs, on average 1–2 ms after the discharges in pyramidal cell somata and dendrites (Klausberger et al. 2004).

During gamma oscillations, modulated CA1 pyramidal cells form a bimodal distribution with one class firing near the trough while the other class fire at early ascending phase of gamma oscillations (Senior et al. 2008). These groups also differ in terms of their spike waveforms, firing rates, and burst firing tendency. Although not directly investigated in the paper, these two pyramidal groups may correspond to the superficial-deep distinctions. In anesthetized rats, bistratified cells, which innervate the dendrites of pyramidal cells aligned with glutamatergic input from hippocampal area CA3, show a strong synchronization with field gamma oscillations while other inhibitory cell types demonstrate a moderate level of synchronization with gamma oscillations (Tukker et al. 2007). This supports the proposal that bistratified neurons might be the main contributors to the local gamma generation in CA1 while PV+ basket cells might not be a requirement in CA1 (Craig and McBain 2015). Cholecystokinin-expressing interneurons tend to fire earliest within the gamma cycle, which aligns with their presumed role in regulating the activity of individual pyramidal cells (Tukker et al. 2007). The firing rate of OLM cells remains relatively constant during gamma oscillations, but these cells synchronize with the gamma rhythm (C. Varga, Golshani, and Soltesz 2012). Notably, the temporal ordering of preferred firing phases among PV and OLM cells remains consistent across different frequencies during fast (>25Hz) network oscillations, typically differing by one or two synaptic delays. Considering that PV and OLM cells target distinct segments of pyramidal cells (perisomatic vs. distal dendrites), this specific temporal arrangement between these two cell types may reflect the regulation of particular inputs in an oscillatory dynamic context (C. Varga, Golshani, and Soltesz 2012).

During theta oscillations, the long-term firing rates of pyramidal cells remain consistent (Csicsvari et al. 1999). PV+ basket cells and oriens-lacunosum-moleculare (OLM) interneurons increase their firing rates during theta states compared to nontheta states (C. Varga, Golshani, and Soltesz 2012). Deep and superficial pyramidal cells exhibit opposite firing phases in the theta cycle (trough vs. peak) (Navas-Olive et al. 2020). Both experimental work and computational modeling propose that perisomatic inhibition, provided by populations of basket cells, plays a pivotal role in shaping the phase-locked preferences of deep and superficial pyramidal cells (Navas-Olive et al. 2020). In behaving mice, PVBCs tend to fire preferentially during the descending phase of theta (C. Varga, Golshani, and Soltesz 2012), followed by OLM cells and bistratified cells which fired strongly phase-coupled to the trough of theta oscillations recorded in strata pyramidale (Katona et al. 2014; C. Varga, Golshani, and Soltesz 2012). Ivy cells have sparse firing during theta oscillations but phase-lock to the trough (Fuentealba et al. 2008) and adjust their firing rate in response to the frequency of theta oscillations (Lapray et al. 2012). CCK-expressing interneurons, while representing a morphologically diverse group of neurons, appear to demonstrate relatively homogeneous and similar phase-locked firing behaviors during theta oscillations in CA1 (Klausberger et al. 2005; Tukker et al. 2007). Extrahippocampal neuronal firing can also align with hippocampal theta. Theta activity recorded in the third layer of the entorhinal cortex (EC3) typically exhibits phase synchrony and high coherence with theta recorded from the CA1 pyramidal layer (Mizuseki et al. 2009). Various cell types within the entorhinal cortex display specific theta phase preferences. EC2 and EC3 principal neurons, serving as the primary afferents to dentate gyrus/CA3 and CA1 neurons, respectively, demonstrate, on average, out-of-phase firing relative to each other. Moreover, their preferred discharge phases tend to be approximately opposite those of their target hippocampal neurons. Interestingly, a small subset of EC3 pyramidal cells fires in phase with the EC2 population, and this subgroup displays the strongest theta phase locking among all EC3 cells. Group cross-correlogram analysis substantiates these findings, indicating that EC2 principal cell-EC2/3 interneuron pairs exhibit small temporal offsets, whereas EC3 principal cell-EC2/3 interneuron pairs display more significant temporal offsets. Additionally, EC2 principal cell-DG/CA3 interneuron pairs and EC3 principal cell-CA1 interneuron pairs also exhibit substantial

temporal discrepancies. These observations imply that population activities in unidirectionally and monosynaptically connected layers/regions display significantly more temporal delays than what a simple drive-integrate model would predict (Mizuseki et al. 2009).

1.4.4.2 Primate models

While a detailed study of spike-LFP phase dynamics for various cell types across diverse frequency ranges is yet to be conducted in the primate hippocampus, spike-field coherence (SFC) analyses suggest that primate hippocampal neurons exhibit oscillatory modulations. In monkeys, SFC peaks during a visual memory task were most prominent in the 1–8 Hz range (delta/theta band), and the 30–100 Hz range (gamma band). Across the population, gamma-band SFC tended to cluster in one of two frequency bands: low gamma (30–60 Hz) and high gamma (60–100 Hz) (Jutras, Fries, and Buffalo 2009). More recent results show that hippocampal neurons show phase-locking to a spectrum of frequencies with prominent peaks in low theta (1-4Hz) and high gamma (60-120Hz) frequency bands (Mao et al. 2021).

In humans, spike timing during ripples is phase locked (Le Van Quyen et al. 2008; Tong et al. 2021) and this relationship is cell-type specific (Le Van Quyen et al. 2008). Putative pyramidal cells fired preferentially at the highest amplitude of the ripple, but interneurons began to discharge earlier than pyramidal cells. Furthermore, a large fraction of cells were phase-locked to the trough of the ripple cycle, but the preferred phase of discharge of interneurons followed the maximum discharge probability of pyramidal neurons (Le Van Quyen et al. 2008). Spiking activity also shows significant phase locking to the trough of the 2–10Hz low-frequency signal. Phase locking in this frequency band is probably due to the strong negative deflections that accompany ripple activity. When measuring the relation between spiking activity and individual frequencies between 2 Hz and 400 Hz, across participants, spiking activity is significantly locked to specific high-frequency bands in the LFP (peak 86.9 Hz) (Tong et al. 2021).

1.4.5 State-dependent subcircuit dynamics of hippocampal CA1 cell assemblies in rodent models

1.4.5.1 Cell assemblies as temporal structures of neural dynamics

Cortical neurons typically exhibit irregular spike trains; however, when these spike trains are examined within the context of other simultaneously recorded neurons and then rearranged to group synchronously firing cells together, structured patterns emerge. These patterns often suggest the presence of a cell assembly organization, wherein different groups of cells consistently display distinct spatio-temporal configurations (Harris et al. 2003; Harris 2005). A cell assembly, in this context, refers to an anatomically dispersed group of neurons in which excitatory connections have been potentiated (Hebb 1949). Furthermore, a sequence of such assemblies, each triggered by the previous one, is termed a “phase sequence”.

Spike trains within a phase sequence exhibit a temporal structure that is modulated by external variables but displays more variability than what would be expected from strict sensory control (Harris 2005). In the hippocampus, neurons increase their firing rate when the animal navigates over a specific locations within the local environment (J O’Keefe 1976). Neighboring place cells fired at different locations such that, throughout the hippocampus, the entire trajectory of the animal is correlated with the temporal ordering of the cells (J O’Keefe 1976; Wilson and McNaughton 1993). Individual place cell activity has a particular temporal relationship to local theta oscillations, in that the phase of the theta cycle at which a place cell emits spikes is negatively correlated with the position of the animal within the place field (J O’Keefe and Recce 1993; W E Skaggs et al. 1996). This phenomenon is known as ‘‘theta precession,’’ because these neurons consistently spike at progressively earlier phases of the theta oscillation as the animal runs forward through the place field. The prediction of spike train of a hippocampal place cell can improve by incorporating peer prediction, estimating spike trains of a cell given the spike times of simultaneously recorded assembly members, compared to models where only

theta phase and place fields are used (Harris et al. 2003). This finding underscores that the firing patterns of the hippocampal population are not solely dictated by external factors but exhibit a high degree of internally generated and coordinated activity. Such interdependence among neuronal ensembles suggests that comprehending the temporal structure of neuronal activity necessitates an analysis at the population level (Harris et al. 2003).

Further experimental support favoring internally-generated versus environment-controlled assembly sequences is derived from the observation that in the rat hippocampus, consistently evolving cell assemblies emerge not only during spatial navigation but also in the absence of alterations in environmental or self-derived inputs (Pastalkova et al. 2008). Additionally, disrupting the internally organized rhythmicity of the hippocampal network by inactivating the medial septum abolishes firing fields during running in the sensory-cue controlled condition but not running in a maze. Nevertheless, theta sequences are abolished in both conditions (Y. Wang et al. 2015). These findings imply the existence of two distinct mechanisms supporting the development of spatial firing fields in the hippocampus, with only the internally organized system facilitating short-term sequential firing.

These internally generated cell assembly sequences are hypothesized to play a crucial role in supporting various cognitive processes, including goal acquisition across multiple timescales, action control, and the formation of learning and memory (György Buzsáki 2010; Pezzulo, Kemere, and van der Meer 2017). Consequently, to gain insights into how system-level operations contribute to cognitive functions, it is essential to concentrate on the population activity of simultaneously recorded neurons and examine their organizational principles. In the following sections, I will explore three distinct forms of temporal structure in hippocampal cell assemblies: theta sequences, preplay, and replay.

1.4.5.2 Theta sequences, preplay, and replay in the hippocampus of rodents

Observation of phase precession in hippocampal place cells led to the prediction of temporal sequences across a population of several neurons (W E Skaggs and

McNaughton 1996; W E Skaggs et al. 1996; Wallenstein and Hasselmo 1997; Dragoi and Buzsáki 2006). Experimental support followed from the demonstration that precise sequences of place cell activity occur during theta-states (D. J. Foster and Wilson 2007). In these theta sequences, spike times are correlated with the rank positions of the place fields of the cells, over a short timescale of tens of milliseconds. Theta sequences represent time-compressed trajectories through space in which a portion of the animal's spatial experience is played out in forwards order (Dragoi 2020; Drieu and Zugaro 2019). What would we observe if we examined the spatiotemporal firing patterns of hippocampal CA1 principal neurons in awake and sleeping rats? During sleep, there is no external perceptual reference or motor behavior to drive hippocampal cells. Therefore, if recurring spike sequences are present during sleep, they are likely to be internally generated.

In an early study, place cells that were exposed to their individual place fields during awake behavior showed significant increases in the spiking activity and rate of bursting during subsequent sleeping states compared to the unexposed place cells (Pavlides and Winson 1989). This finding suggests that neuronal activity of hippocampal place cells in the awake states may influence the firing characteristics of these cells in subsequent sleep. A later study showed that neuron pairs which represented similar parts of the environment in the awake rat and therefore fired together during exploration showed an increased correlation in their firing during the subsequent slow-wave sleep episode compared with the preceding sleep episode (Wilson and McNaughton 1994; W E Skaggs and McNaughton 1996). Examining the temporal structure of an ensemble of hippocampal CA1 principal neurons demonstrated that during sleep, and usually coaligned with sharp-wave ripples, the spatiotemporal pattern of neuronal sequences is self-generated spontaneously that recapitulates previously experienced behavioral trajectories, a phenomenon called replay (Nádasdy et al. 1999; W E Skaggs et al. 1996; Wilson and McNaughton 1994; Z. S. Chen and Wilson 2023; D. J. Foster 2017; O'Neill et al. 2010; Ólafsdóttir, Bush, and Barry 2018). Although replay events were originally reported during sleep, later results established highly robust replay sequences across tens of simultaneously recorded cells occurring during the awake state (Carr, Jadhav, and Frank 2011; Davidson, Kloosterman, and Wilson 2009; D. J. Foster and Wilson 2006).

An important new dimension has been added to this picture with the finding that during pre-run sleep and rest, the hippocampal network of adult naive rats and mice exhibits repertoires of pre-formed firing motifs which precede animals' first ever run on a linear track and can preplay the future place cell sequences and animal trajectories on the track (Diba and Buzsáki 2007; Dragoi and Tonegawa 2011, 2013). This indicates that a new spatial experience can be formed, in part, by the selection of blocks of preexisting cellular firing sequences from a larger internal repertoire identifiable during the preceding sleep and rest, rather than by exclusively forming all the sequences in response to the external cues, even in experimentally naive animals (Dragoi and Tonegawa 2014). The rapid selection of pre-existing cellular firing sequences could be essential to the role of the hippocampus in rapid encoding and learning (Tse et al. 2007; McClelland, McNaughton, and O'Reilly 1995). How are aspects of navigational experience encoded such that they modify the pre-existing default patterns to better represent and consolidate the experience during replay compared with preplay?

A series of experimental studies have demonstrated that in the absence of detectable robust theta sequences in the hippocampus during navigation, the expected experience-dependent replay during sleep is abolished (Drieu, Todorova, and Zugaro 2018; Chenani et al. 2019). More interestingly, developmentally, although preplay and non-plastic replay with similar characteristics before and after the navigational experience exist from early stages, it is only during late stages that locations experienced sequentially become uniquely bound into larger trajectories within hippocampal theta sequences during navigation; consequently, their replay during the following slow wave sleep became stronger than their preplay preceding the experience (Farooq et al. 2019; Muessig et al. 2019). Three types of changes in cell-assembly dynamics from preplay to replay have been recently proposed to underlie the replay plasticity including 1) increases in firing rates and coactivation of contributing neurons specifically within the preferred cell assembly, 2) increased precision of firing of these neurons within preferred cell-assemblies during sleep replay (i.e., decreased spike dispersion and increased tuning to preferred cell assembly), 3) amplification of number of repeats for short neuronal motifs specifically encoding the prediction-error signal during navigation (Dragoi 2020). These changes in cell-assembly dynamics could primarily support an increased trajectory

representation during replay at the (tens of) millisecond activation lifetime of cell assemblies.

Overall, these observations indicate that early in development experience–independent assembly of preconfigured trajectory-like sequences emerge. During behavior, an assembly is selected from the repertoire of pre-existing cell assemblies to support the novel experience. Novel experience induces plasticity in trajectory experience–dependent replay during sleep.

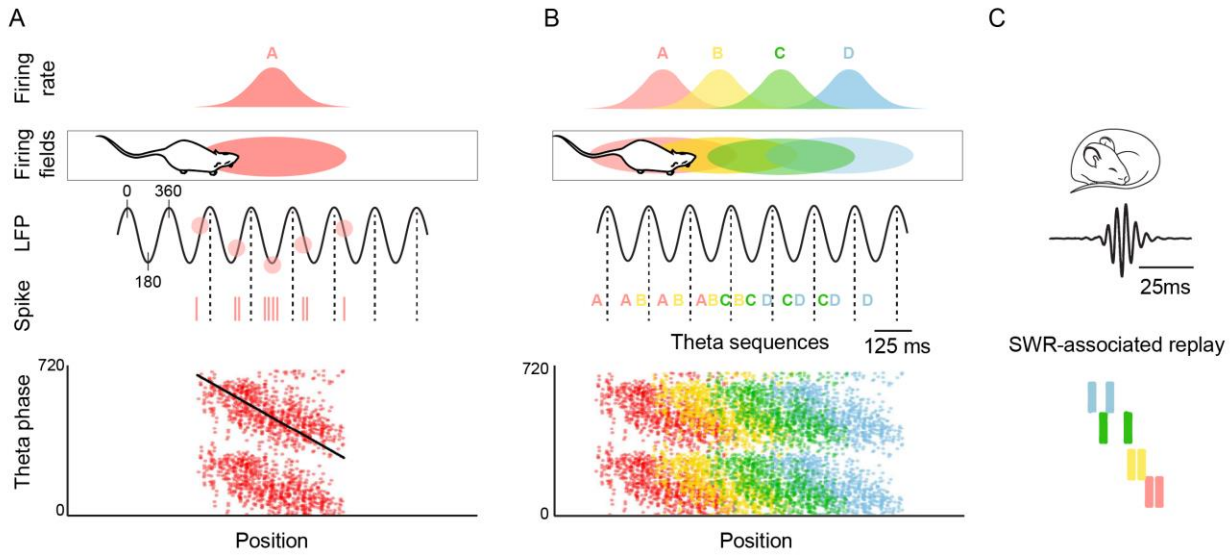

Figure 1-3. The emergence of theta sequences and sharp-wave ripples the hippocampus.

A. Theta spike phase precession. Top, schematic representation of the temporal organization of successive place cell bursts relative to theta as a rat runs along a linear track. When the rat enters the firing field (pink ellipse), the cell fires near the end of the theta cycle, i.e., with a phase of ∼360◦. As the rat progresses through the field, bursts occur on earlier and earlier phases (red vertical ticks, action potentials; black numbered dots, mean burst times within individual theta cycles). Bottom, phase precession plot. For each spike, phase is represented as a function of position (tilted black line, best linear-circular regression line). B. Top, four schematic overlapping firing fields. Middle, in their overlap region the cells discharge in sequence (A, AB, ABC, etc.) within each theta cycle, reflecting the order of field traversal at a compressed time-scale. Bottom, these past-present-future “sweeps” may require coordination between individual phase precessing cells. C. During slow-wave sleep sharp-wave ripple events, sequences that occur during track running are replayed in reverse order. (Modified from (Drieu and Zugaro 2019))

1.4.6 Linking physiology to behavior

The extensive physiological data on hippocampal rhythms provide an opportunity to evaluate hypotheses about the role of these rhythms for hippocampal network function. Here, I will review work on network models in which hippocampal rhythms contributes to the following functions: (1) two-stage model of memory formation (2) separating the dynamics of encoding and retrieval, (3) facilitating the context-dependent retrieval of sequences. I should emphasize that these models were largely motivated by findings in rodents and as such might not readily be translatable to primate behavior. Still, the core ideas can provide insights into how brain rhythms can structure the temporal dynamics of cell assemblies that support behavior.

1.4.6.1 Two-stage model of memory formation

The prevailing understanding is that the formation of memories relies on experience-driven synaptic plasticity, which allows the modification of connections between neurons (Bailey, Kandel, and Harris 2015). This idea emerged shortly after the discovery of synapses, with various models suggesting that information is represented by patterns of individual neuron firing (Hebb 1949, Lynch 1986). In these models, memory results from changes in neuronal connections driven by activity, which subsequently leads to an enhanced occurrence of the same activity pattern during recall. The exploration of this concept gained traction when the phenomenon of long-term potentiation (LTP) was demonstrated, revealing enduring synaptic changes following strong, preferably burst-like, high-frequency activation (Bliss and Lomo 1973). To induce LTP, certain conditions must be met, including intense synaptic stimulation, the coactivation of multiple converging input pathways, and high rates of neuronal firing associated with synchronized population discharges (Henry Markram, Gerstner, and Sjöström 2011). These conditions are met during temporally-compressed sequential activation of cell assemblies in the hippocampus during different behavioral states.

During wakefulness, increased levels of neuromodulators like acetylcholine in the hippocampus enhance the influence of external sensory inputs compared to intrinsic neural activity. This amplification of external inputs favors sensory processing and promotes the flow of information from the neocortex to the hippocampus (M E Hasselmo 1999). As animals explore their environment, they sequentially traverse successive place fields, and the corresponding place cells activate in a sequence reflecting the ongoing trajectory at the behavioral timescale (Drieu and Zugaro 2019). Embedded in these slow sequences, due to the overlapping nature of place fields, overlapping place cells fire within a sub-theta-cycle which leads to the emergence of time-compressed sequences in each cycle of the ongoing theta rhythm (D. J. Foster and Wilson 2007; J O'Keefe and Recce 1993; W E Skaggs et al. 1996). This fast temporal organization, continually repeated in successive theta cycles, brings together and links cell assemblies within a temporal range where they can be modulated by synaptic plasticity (William E. Skaggs et al. 1996; J C Magee and Johnston 1997; György Buzsáki and Draguhn 2004; Wójtowicz and Mozrzymas 2015). In line with this, targeted lesions of the medial septum and fornix reduce hippocampal theta power or alter its frequency (Rawlins, Feldon, and Gray 1979; Winson 1978; S Leutgeb and Mizumori 1999; Peter Christian Petersen and Buzsáki 2020) which further leads to impairments in various memory-guided tasks, (B. S. Givens and Olton 1990; Aggleton et al. 1995; Numan and Quaranta 1990; S Leutgeb and Mizumori 1999). Medial septum inactivation results in the elimination of theta sequences, while preserving the firing field of neurons during navigation. Under this condition, the performance of the animals in the memory task becomes significantly impaired (Y. Wang et al. 2015). These results suggest that theta structuring of cell assemblies is vital for normal memory formation.

During subsequent episodes of slow wave sleep (SWS), the brain becomes effectively isolated from external sensory inputs, and the reduced levels of acetylcholine in the hippocampus facilitate recurrent effective connectivity which results in the expression of endogenous activity recapitulated in sharp-wave ripple (SWR) events (Gais and Born 2004b; M E Hasselmo 1999). During SWR events, temporally structured population-level events within the hippocampus often appears in which the pattern of neural activity correspond to the behaviorally-related theta sequences on a compressed timescale that

is conducive to Hebbian plasticity (J C Magee and Johnston 1997; Silva, Feng, and Foster 2015). Several studies have provided confirmation of the role of slow-wave sleep in the consolidation of memories (Gais and Born 2004a; Peigneux et al. 2004; Plihal and Born 1997). Interventions aimed at enhancing specific aspects of slow-wave sleep, including the content of neuronal activity, have been shown to result in improved performance in memory tasks that were learned prior to sleep (Marshall et al. 2006; Rasch et al. 2007). Furthermore, the selective disruption of sharp-wave ripples during sleep or quiet wakefulness leads to memory deficits (Ego-Stengel and Wilson 2010; Jadhav et al. 2012; Girardeau et al. 2009). In parallel, increases in sharp wave-ripple events have been observed following learning in both humans and rats (Axmacher, Elger, and Fell 2008; Eschenko et al. 2008). Artificially prolonging these ripple events enhance memory performance, while truncating the late part of ripples has the opposite effect (Fernández-Ruiz et al. 2019). These findings strengthen the notion that the critical attribute of slow-wave sleep for memory consolidation is the presence of sharp wave-ripple events.

Based on these observations, it was proposed that behavior-dependent electrical changes in the hippocampus, specifically theta and sharp-wave ripple (SPW)-associated states, might underlie a two-stage process of information storage (G Buzsáki 1989). In stage 1, a labile form of memory trace is created through the convergence of excitatory inputs from fast-firing granule cells onto CA3 pyramidal neurons during theta-associated behavioral states, resulting in a weak and transient heterosynaptic potentiation of CA3 pyramidal cells. This process is influenced by subcortical inputs. In stage 2, a long-lasting form of memory trace is established through the long-term modification of synaptic efficacy, facilitated by SPW-population bursts that occur at the end of theta behaviors. The highly synchronous population bursts in CA3 lead to the long-term enhancement of synaptic efficacy in CA3 and some of their CA1 target neurons. From this perspective, both theta and SPW states are considered essential for normal memory trace formation.

1.4.6.2 Separating the dynamics of encoding and retrieval

The formation of new memories requires new information to be encoded in the face of proactive interference from the past. SPEAR model (Separate Phases of Encoding And Retrieval) has been proposed as a solution. Based on this model, encoding preferentially occurs at the pyramidal-layer theta peak, coincident with input from entorhinal cortex, and retrieval occurs at the trough, coincident with input from CA3, consistent with theta phase-dependent synaptic plasticity (Michael E Hasselmo, Bodelón, and Wyble 2002; Michael E Hasselmo 2005). Physiological data on theta rhythm are consistent with the encoding/retrieval model, including phase changes in membrane potential dynamics, inhibition, synaptic input, long-term potentiation, and gamma coupling.

In the encoding phase, dendrites are depolarized (Kamondi et al. 1998) by entorhinal input, allowing for the encoding of information. However, the cell body is hyperpolarized in this phase to prevent spiking and interference from the retrieval of previously stored associations (Michael E Hasselmo, Bodelón, and Wyble 2002). On the other hand, during the retrieval phase of the theta cycle, the external input from the entorhinal cortex is weaker, but the excitatory input from region CA3 is stronger. In this phase, CA1 cell bodies are depolarized by the input from region CA3, enabling the spread of activity across previously modified synapses to retrieve stored associations. This is supported by the fact that spiking in region CA1 follows spiking in region CA3 and does not coincide with spiking in entorhinal layer III (Mizuseki et al. 2009). These changes in membrane potential align with the patterns of synaptic currents during theta, as revealed by current source density analysis (G Buzsáki et al. 1986; Kamondi et al. 1998).

Phase fluctuations in membrane potential during theta cycles may be attributed to distinct types of inhibitory interneurons that spike at different phases of the theta rhythm (Klausberger and Somogyi 2008). Computational models propose functional roles for various phases of interneuron firing in segregating the processes of encoding and retrieval (Cutsuridis and Hasselmo 2012; Kunec, Hasselmo, and Kopell 2005). Inhibitory axo-axonic and basket cells, for example, can suppress the cell bodies and axons of excitatory cells, reducing spiking activity during the encoding phase (Cutsuridis and

Hasselmo 2012). Conversely, during the retrieval phase, the spiking of oriens lacunosum-moleculare cells inhibits the layer where entorhinal input connects with the distal dendrites, thereby diminishing external input as associations from previously modified synapses in the stratum radiatum are retrieved (Kunec, Hasselmo, and Kopell 2005; Michael E Hasselmo, Bodelón, and Wyble 2002). During this phase, the cell body receives minimal inhibition, allowing the retrieval process to drive neuronal spiking activity. Fluctuations in membrane potential give rise to dynamic changes in long-term potentiation (LTP). During the encoding phase, there is robust synaptic modification at the synapses located in region CA1, resulting in the strengthening of synapses containing NMDA receptors. This process encodes associations between the presynaptic activity in CA3 and the postsynaptic activity induced in CA1 neurons by input from the entorhinal cortex (Michael E Hasselmo and Stern 2014). Experimental evidence from physiological data indicates that LTP can be induced at the synapses originating from region CA3 when synaptic transmission is relatively weak at these CA3–CA1 synapses, but postsynaptic dendrites become depolarized due to input from the entorhinal cortex (Hölscher, Anwyl, and Rowan 1997; Huerta and Lisman 1995; Hyman et al. 2003).

Studies of gamma oscillations in rats further substantiates the proposed model. Gamma oscillations are observed during specific phases of the theta rhythm in both the hippocampus (Bragin, Jandó, Nádasdy, Hetke, et al. 1995) and the entorhinal cortex (Chrobak and Buzsáki 1998; Tort et al. 2009). Aligning with the encoding phase of the model, high-frequency gamma oscillations exhibit synchronization between the entorhinal cortex and region CA1 during a particular phase of theta (Colgin et al. 2009). In contrast, during a different phase of theta, region CA1 displays coherence of low-frequency gamma with region CA3 (Colgin et al. 2009), in line with the concept of a retrieval phase.

Several studies have directly tested the SPEAR model's predictions. Empirical evidence indicates that in novel environments, the preferred theta phase of CA1 place cell firing shifts closer to the peak of the CA1 pyramidal-layer theta cycle, tilting the balance more toward encoding. Notably, this shift during encoding in novel environments is disrupted by the administration of cholinergic antagonists. In contrast, in familiar environments, the cholinergic antagonism push the preferred theta firing phase closer to the theta trough,

shifting the encoding-retrieval balance even further toward retrieval (Douchamps et al. 2013). These findings align with the anticipated outcomes from the SPEAR model. Moreover, applying phase-specific closed-loop inhibition to dorsal CA1 during the endogenous theta rhythm in freely moving mice resulted in improved performance on a spatial navigation task that required both encoding and retrieval of reward-related information in each trial. The effectiveness of this intervention was contingent on both the specific phase of theta and the task phase at which the stimulation occurred. Stimulation during the encoding phase enhanced performance when synchronized with the theta peak, while stimulation during the retrieval phase was more effective when aligned with the theta trough. Taken together, these observations indicate that in rodents, processes related to encoding and retrieval of task-relevant information are preferentially active at distinct theta phases, and the cholinergic system plays a pivotal role in orchestrating these phasic transitions (Siegle and Wilson 2014).

1.4.6.3 **Facilitating the context-dependent retrieval of sequences**

Episodic memory is the primary cognitive function often associated with hippocampal activity (Tulving and Markowitsch 1998). Episodic memories are contextual-rich experiential phenomena that contain temporally-ordered spatiotemporal configurations (Allen and Fortin 2013). Episodic memories are impaired in animals or patients with hippocampal lesion (Aggleton and Brown 1999). Furthermore, a substantial and continually evolving body of research indicates that the dynamics of single hippocampal cells or assemblies are linked to factors like the animal's location, time, and spatial context (György Buzsáki and Llinás 2017; Howard Eichenbaum 2017b). This suggests that the hippocampus plays a role in processing contextual information. Nevertheless, there is ongoing and extensive debate regarding the precise contribution of the hippocampus to episodic memories.

While the activity of individual hippocampal cells is associated with both spatial and nonspatial aspects of the environment, the cognitive map theory proposes that hippocampal processing is fundamentally rooted in spatial information and that nonspatial

information is integrated within a primary spatial framework in the hippocampus (John O'Keefe and Lynn Nadel 1978). According to this view, place-related features are created within the hippocampus itself, whereas nonspatial inputs originate from other sources and are incorporated into these place representations within the hippocampus (John O'Keefe and Krupic 2021).

Some have argued that the apparent prioritization of spatial representation in hippocampal activity is a consequence of ever-present spatial regularities associated with various behavioral episodes (H Eichenbaum et al. 1999). This means that locations where events take place typically exhibit distinct patterns that can be included in most event-related coding. At the same time, nonspatial events are incorporated in situations where they occur with regularity and can provide a pervasive influence when the events occur across many places (Wood, Dudchenko, and Eichenbaum 1999). Based on this perspective, it has been inferred that the neural activity of individual hippocampal neurons reflects a multidimensional association between relevant object and spatial dimensions, essentially creating a system for relational memory (Howard Eichenbaum 2017a). To illustrate, in a nonspatial 'transitive inference' task, rats were trained to distinguish between pairs of overlapping odors (e.g., odor A > odor B; odor B > odor C, and so on). After mastering these paired associations, the rats were able to construct a sequence that allowed them to deduce relationships between pairs of odors not directly learned, such as odor A > odor C. Rats with hippocampal lesions were capable of learning individual discriminations but struggled to correctly infer the relationship between a novel pair, like odor A > odor C (Bunsey and Eichenbaum 1996; Dusek and Eichenbaum 1997; Devito, Kanter, and Eichenbaum 2010). In a context-guided object associations task, hippocampal neuronal networks demonstrated a hierarchical organization that interconnected overlapping elements of related memories, encompassing both spatial and nonspatial aspects of separate experiences. Features associated with events that dictated divergent behaviors and reward expectations were segregated into distinct hippocampal representations (McKenzie et al. 2014). These findings support the idea that the hippocampus plays a role in a broad relational memory capacity, serving two main functions: 1) systematically organizing multiple overlapping memories to establish relational networks among items to be remembered and 2) enabling the flexible

expression of memories through inferences about indirectly related items (N. J. Cohen, H. Eichenbaum 1993).

The above hypothesis does not address the issue of how the brain organizes its memory content and the role of the hippocampus in this process. The Index theory posits that incoming sensory information is initially processed and stored in unique assemblies of cortical modules within distributed sensory and association areas throughout the cortex (Teyler and DiScenna 1986). The function of the hippocampus, according to this theory, is to map functional units of the neocortex and other brain structures activated by experiential events. This concept assumes that neocortical memory networks are content-addressable. Content addressability implies a systematic relationship between the content of an experience and the specific brain networks responsible for representing it (Nadel and Hardt 2011). An intriguing aspect of content-addressable systems is their reliance on pattern completion mechanisms for accurate information retrieval. Pattern completion involves the ability to retrieve complete memories or associations from partial or incomplete cues (Marr, Willshaw, and McNaughton 1991). The unique circuits within the hippocampus, particularly the recurrent networks of CA3-CA3 synapses, are believed to be the subcellular basis for pattern completion (Guzman et al. 2016; Bennett, Gibson, and Robinson 1994). Recall in the neocortex is achieved through a reverse hierarchical series of pattern association networks facilitated by the hippocampo-cortical backprojections. Each of these networks performs pattern generalization to retrieve a complete pattern of cortical firing in higher-order cortical areas (Rolls 2013).

The accurate recall of event memories necessitates preserving the temporal order of events. So, how does the hippocampus maintain this temporal order during pattern completion? As mentioned earlier, hippocampal circuits can activate cell assemblies in a specific temporal sequence that corresponds to the behavioral trajectory. This sequential activation of these cell assemblies is the leading candidate for preserving the temporal order of events. Therefore, as an extension of the Index theory, it has been proposed that the role of the hippocampal system is to generate content-limited cell assembly sequences without encoding the details of specific events. In this framework, the hippocampus, acting as a sequence generator, essentially points to items (such as a

percept or 'what') stored in the neocortex in the same order they were experienced during learning (Friston and Buzsáki 2016; György Buzsáki, McKenzie, and Davachi 2022; György Buzsáki and Tingley 2018). Evidence supporting this hypothesis comes from physiological data that indicates when the temporal sequence among hippocampal neurons is disrupted at the theta oscillation timescale, without affecting place fields, the animal's memory is impaired (Robbe et al. 2006; Y. Wang et al. 2015).

2. Chapter 1: Learning of object-in-context sequences in freely-moving macaques[1]

2.1 Abstract

Flexible learning is a hallmark of primate cognition, which arises through interactions with changing environments. Studies of the neural basis for this flexibility are typically limited by laboratory settings that use minimal environmental cues and allow restricted behaviors for actively sensing and interacting with the environment. To address this, we constructed a 3-D enclosure containing touchscreens on its walls, for studying cognition in freely moving macaques. To test flexible learning, monkeys completed trials consisting of a regular sequence of selections across four touchscreens. On each screen, the monkeys had to select the sole correct item ('target') from a set of four available items. Each item was the target on exactly one screen of the sequence, making correct performance conditioned on the spatiotemporal sequence rule. Both monkeys successfully learned multiple 4-item sets (N=14 and 22 sets), totaling over 50 and 80 unique, conditional item-context memoranda, with no indication of capacity limits. The enclosure allowed freedom of movements leading up to and following the touchscreen interactions. To determine whether movement economy changed with learning, we reconstructed 3D position and movement dynamics using markerless tracking software and gyroscopic inertial measurements. Whereas general body positions remained consistent across repeated sequences, fine head movements varied as monkeys learned, both within and across sequence sets, demonstrating learning set or "learning to learn". These results demonstrate monkeys' rapid and flexible learning within a true 3-D space. Furthermore, this approach enables the measurement of continuous behavior while ensuring precise experimental control and behavioral repetition of sequences over time. Overall, this approach harmonizes the design features that are needed for electrophysiological studies from within tasks that showcase fully situated, flexible cognition.

[1] This chapter is adapted from Learning of object-in-context sequences in freely-moving macaques available in bioRxiv and has been reproduced with the permission of my co-authors KF Rahman, W Zinke, KL Hoffman.

2.2 Introduction

Emulating natural learning conditions in laboratory tasks should increase the external validity of behavioral results. In addition, it can help to pinpoint those neural mechanisms that will also generalize outside the laboratory environment. Examples of naturalistic elements in learning tasks for non-human primates typically include either photorealistic stimuli or complex visuospatial stimuli, but under reduced spatial and/or temporal dimensions, or else the animals are tested under spatially extended contexts, albeit with simplified stimuli and/or temporal demands (Bachevalier, Nemanic, and Alvarado 2015; Gaffan 1994; Elisabeth A. Murray, Baxter, and Gaffan 1998; Froudist-Walsh et al. 2018; Templer and Hampton 2013a; Hampton, Hampstead, and Murray 2004, 2005; Lavenex, Amaral, and Lavenex 2006; Parkinson, Murray, and Mishkin 1988). Furthermore, the dependent variables to operationalize learning in such tasks have traditionally been limited to percent correct or error count and error type. Technological advances make it possible to incorporate greater contextual richness and variety, and factor in a wider range of behaviors that occur during learning, including the range of movements and behaviors exhibited by macaques. In addition, increasing temporal resolution enhances the opportunity to capture some species-typical macaque behaviors, including foraging in space and visuomotor reaching for manipulable and visually-distinct 3-D (real) objects.

Traditional neurophysiological studies came at the direct cost of species-typical affordances and active sensing, due to requirements for stationarity of the recording apparatus. More recently, some of the technological improvements for neurophysiological studies can free these restrictions and capitalize on the natural multisensory richness of stimuli-in-context (Mao et al. 2021; Schwarz et al. 2014; Berger, Agha, and Gail 2020; Voloh et al. 2023; Courellis et al. 2019; Stangl, Maoz, and Suthana 2023). Using chronically implanted arrays and wireless recordings, neurophysiology has been possible under conditions of mobility, offering more direct comparisons with neurophysiological studies in freely moving rats and mice (Abbaspoor, Hussin, and Hoffman 2023; Mao et al. 2021; Courellis et al. 2019). Furthermore, implementing a more naturalistic behavioral context strengthens the generalizability of the results for understanding human memory

as it exists in the natural world, beyond experimental settings (Shamay-Tsoory and Mendelsohn 2019). Indeed, memory can be impaired in humans tested under more restricted movements and impoverished multisensory and visual environments, further emphasizing the importance of naturalistic learning settings (Brandstatt and Voss 2014; Carassa et al. 2002; Koriat and Pearlman-Avnion 2003; Murty, DuBrow, and Davachi 2015; Plancher et al. 2013; Rotem-Turchinski, Ramaty, and Mendelsohn 2019). Thus, while recognizing the benefits of precisely timed experimental control and the strengths of a reductionist approach, there remains a need to conduct neurophysiology under more naturalistic settings (Miller et al. 2022; Krakauer et al. 2017; Gomez-Marin et al. 2014).

The growing adoption of large-scale wireless recordings in monkeys and the emergence of interactive computer control of environments offers the potential to reconcile neurophysiological and neuroethological demands for a broader range of studies. Specifically, in this study, our aim was to create an environment that meets electrophysiological demands (precise timing and experimental control, and repetition for comparison to rodent neurophysiology studies) while allowing conditional, complex stimulus arrays extended in space and time, and within the situated context of naturalistic movements and exploratory behaviors that are native to learning in this species.

We constructed an enclosure for macaques that allows exploratory movements and affords exposure to numerous and diverse combinations of contexts and visual objects through the use of computer touchscreen displays distributed throughout the enclosure. By conditionally rewarding the selection of objects as a function of their spatiotemporal position, we created structured, sequential, goal-directed journeys. We asked i. can macaques learn items in context under this complex conditional structure, replete with protracted delays and action sequences prior to reward, ii. can repeated discriminanda be learned without prohibitive interference/memory capacity issues, and iii. do movements track with learning? The answers to these questions will inform not only the utility of the task and enclosure for understanding learning, but also its suitability for use in electrophysiological studies, to understand the neural mechanisms driving task performance.

2.3 Results

2.3.1 Learning sequentially-presented item-context associations

Two macaques learned stimulus sets whereby each set consisted of a four-item sequence of target objects-in-context, spanning across the four different touchscreens of one corner (i.e., 4 item-screen associations) per trial. Monkey F completed 22 sets, Monkey W completed 14 sets, with 3 sets excluded based on unclear learning estimates (i.e. possible learning failures or forgetting). Each target occurred in the face of 3 distractors, but the objects designated distractors on any one screen would be targets in exactly one of the other screens, i.e. 'context-conditional'. Figure 2A and 2B present the mean learning curves and learning trial statistics for each animal subject separately. Both monkeys showed performance improvement within sets, and both learned according to the learning state-space model. The learning trial was defined as the trial in which the lower bound of the performance confidence interval surpassed the chance level for each set (P = 0.25, dotted grey lines on lower plots).

Completion of this task required a series of decisions and extensive movement in the enclosure prior to reward. Trial duration (the elapsed time from touch on the 1st screen cue to when animals completed performance on the 4th screen, triggering reward) was, on average, 40.5 and 29.0 s for W and F, respectively (N: 1408, and 2157 trials, s.d. 11.0 and 5.5 s).

We designed this task to offer several means to learn the correct responses. These include learning 4 distinct spatial/temporal/visual-contextual associations, or adopting a non-matching working memory rule that would eliminate as a candidate object any confirmed target object from the previous screens on that trial. These two possible strategies would lead to different performance probabilities across screens, as a function of trial repetition. The second strategy would appear as a linear performance improvement across screens within each trial, reflecting the shifting chance performance as targets are eliminated: 1/(4-# previous screens); Figure 2C, dotted line with square markers, by the time animal arrives at the 4th screen, she had eliminated 3 objects as

target so the probability of success should be 1.0). Importantly, this strategy does not require long term memory across trials i.e. is as effective on the first as on the last trials, distinguishing it from the associative-learning strategies that are ineffective on the first trial, but become optimal strategies if the associations can be learned with repeated exposure. To test these two possibilities, we computed the proportion of success on the first trial across sets for each screen and for each animal separately (Figure 2C). The performance of neither animal subject follows the linear trend that would be expected from an ideal process of elimination. Although this doesn't rule out the possibility that animals sporadically used this strategy over the course of learning, it shows that this was not a prepotent strategy.

The two monkeys, W and F learned 14 and 22 sets of 4-item sequences for over 50 and 80 unique item-context memoranda. In practice, proactive interference would be a sign of reaching capacity limits. We tested for signs of proactive interference by comparing learning points for the new sets presented over time. Neither animal showed worsening performance over the sets based on a linear regression of learning trial over set number, suggesting that additional sets could have been introduced (i.e. no observable proactive interference): (W: $t(62) = -3.85$, $p < 0.001$; F: $t(86) = 1.4$; $p > 0.1$). On the contrary, one of the animals (W) showed significant improvement over time, potentially reflecting learning set or schema learning.

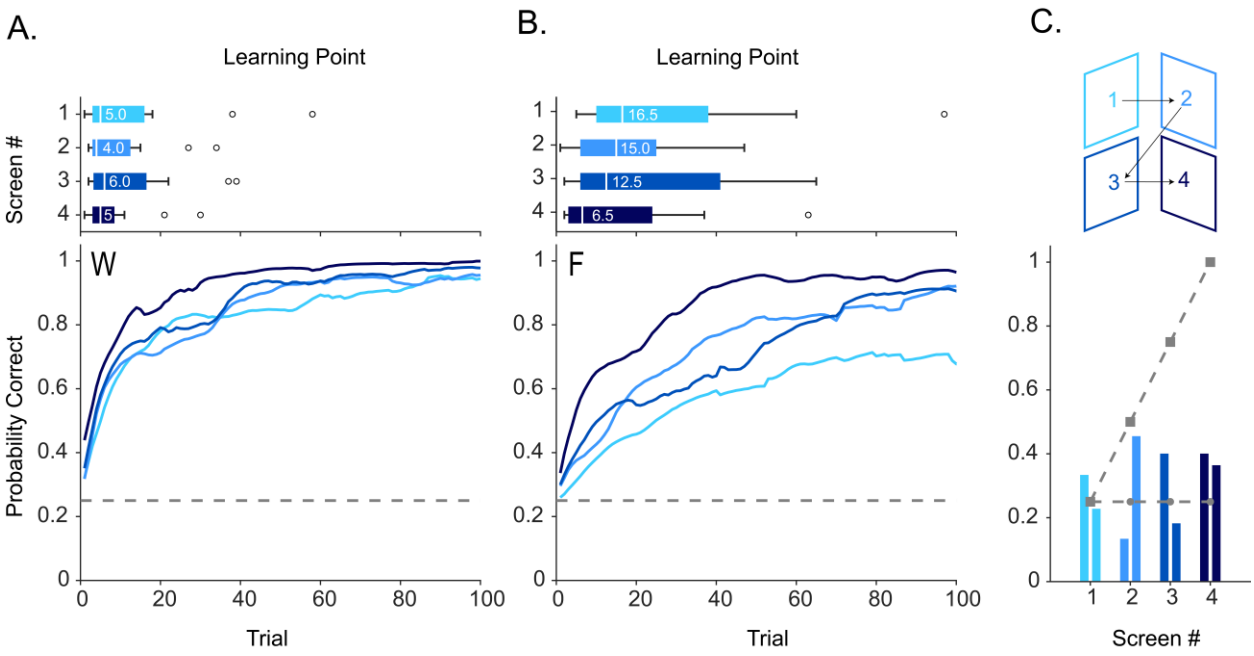

Figure 2-1. Monkeys learn sequentially-presented associations between objects and context.

(A) *Top* learning points in monkey W across different sets of object context associations, shown for each screen in the trial sequence. White bars and numbers indicate the median (N = 14 sets). Circles show outliers. *Bottom* Mean learning curves across sets for each screen. The dotted grey line indicates the chance level at 0.25. (Please see the methods section for more details on the learning point estimation) (B) Same as A for monkey F (N = 22 sets). (C) The proportion of correct choices for the first trial across sets for each screen for both animals (right bars for each screen correspond to the second monkey in B). The dotted line with circle markers shows the chance level at 0.25. The dotted grey line with square markers indicates the expected performance if monkeys were using only a non-match, working memory strategy across items in the trial sequence.

2.4 Markerless motion capture for macaques using Jarvis and accelerometer data

Adopting more naturalistic, unconstrained behavior increases potential benefits but also burdens for quantifying movements that have more degrees of freedom (Gomez-Marin et al. 2014; Juavinett, Erlich, and Churchland 2018). It was of interest, therefore, to determine how consistent the animal's position was across learning, during key task epochs and in general, during performance. We trained a CNN model for each corner and each animal, owing to different camera views and camera calibrations needed per animal (see Methods for details). Simultaneously we obtained accelerometer data sampled at 3 kHz, for greater temporal precision. Although the outward facing animal and

slow (30 fps) cameras made reach trajectories difficult to measure in all cases, most other body parts were tracked qualitatively well. Figure 3A shows the markerless location of the headpost position for one complete block, out of two blocks completed in that corner for that session. Figure 3B expands to include all trials, with the head position at the time of touch highlighted with black dots, revealing a relatively consistent position at the time of screen engagement. Using the IMU, we screened for the most relevant axis during the decision epoch specifically, for each animal. Comparing the trials leading up to the learning point (N(W)=507, N(F)=1443) with the final trials after learning ('post-learning' N(W)=519, N(F)=840), both animals showed a decrease in head movements following learning (Figure 3D,E; Mann-Whitney U test (W: $z = 5.80$, $p < 0.001$; F: $z = 4.87$, $p < 0.001$). To explore whether this effect emerged with learning set (as the animals continued to perform new sets) we separated out the first 5 ('early') and last 5 ('late') sets learned for each animal, (Figure 3D,E, insets). Qualitatively, the low amplitude differences were more visible across animals in the late sessions, suggesting a 'learning to learn' the effective changes in movements with learning. To explore the changes in finer temporal detail, example IMU traces were selected from the distribution extrema. Whereas the late learning traces will, per definition, be smaller overall, the changes over the course of the choice epoch suggests specific attributes may be indicative of learning (e.g. addressing when the larger excursions occur, relative to selection.) Drawing from an example trial (Figure 3C), we see from the head label compared to the mid-shoulder label that early learning contains some 'waffling' or 'scanning' head movements relative to the body, consistent with viewing the wide object spatial array. This opens up the possible future benefit to use head movements and video labels to assess gaze (visual point of regard), when visual items are made sufficiently distant in the viewpoint of the animal. More work will be required to determine the unique contributions of these metrics in evaluating reaction time, learning, gaze, and attention during deliberative decision making and possible vicarious trial and error behaviors.

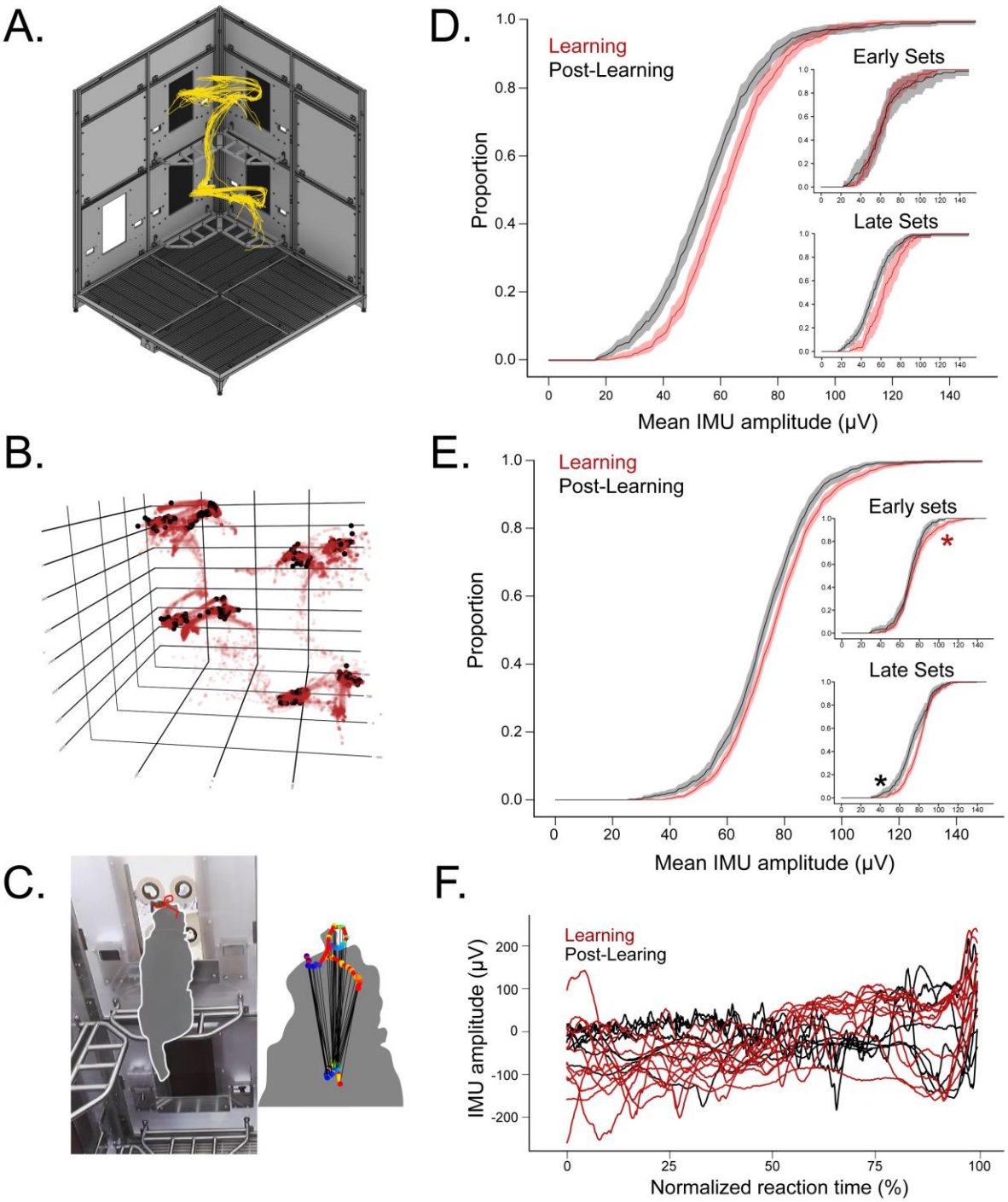

Figure 2-2. Body movements during the task.

Body movements during the task. (A) Markerless tracking during repeated trials of one training block. The top of the head is tracked across cameras to generate a 3-D position estimate in the enclosure during one block of trials, shown in yellow (see methods). (B) Positions across both corners' sequences in a session. As in A., but depicting each position point in red, and the positions at the time of any touchscreen touch, in black. Qualitatively consistent positions are shown, based on the clustering of black points into 8 discrete

locations, at the touchscreens. (C) A series of labeled points from the head and shoulder, selected during the choice (deliberation) epoch early in learning (from a trial in E.) Head oscillation may reflect vacillation. (D) Average IMU movements during the choice epoch in monkey W, as a function of learning. Shown is the cumulative distribution of average movement amplitude during the choice epoch from trials preceding the learning point (Learning) in red (N=507), and from trials after the learning point ('Post-Learning') in black (N=519); shaded areas indicate the bootstrapped 95% confidence intervals. There was, on average, more movement during learning than after the sequence was learned, (Mann-Whitney U test, $z = 5.80$, $p < 0.001$). Top inset: the same cumulative distributions as in the main plot, but only for data obtaind from the first 5 sets learned by this monkey. Bottom inset: the same as the top inset but for the final 5 sets. (E) The same as in D., but for monkey F. Learning trials N = 1443; Post-Learning trials N = 840; Mann-Whitney U test (F: $z = 4.87$, $p < 0.001$). Asterisks in insets indicate the subset of data selected for the plot in F. (F) Example IMU movements during the choice epoch. A selection of example traces to illustrate the movement over the course of the epochs exemplifying the larger movement early in learning (red) relative to late in learning (black). Because the choice epochs vary in duration, the responses are shown in proportional elapsed time from the choice array onset to the selection touch. The body positions in C. are taken from one example during the choice epoch.

2.5 Discussion

In this study we introduced monkeys to a 3D task environment designed to test cognitive skills and track unconstrained, continuous behavior while preserving elements of precise temporal and stimulus control and trial structure. To demonstrate the utility of this enclosure, we designed an object-in-context associative learning task whose items were presented sequentially. Both exposed monkeys learned the structure of the task and completed multiple sets of unique item-in-context sequences, including memory for two different sets presented in opposite corners within the same session. Markerless tracking of multi-camera recordings allowed 3D pose reconstruction. Furthermore, we collected IMU data and observed that movement patterns varied with different stages of learning. These results demonstrate the feasibility of training monkeys on complex cognitive tasks and tracking their behavior under naturalistic conditions, while preserving precisely timed behavioral contingencies needed for wireless electrophysiological recordings.

As a new apparatus, the experimental design must weigh theoretical advances against the uncertainty of obtaining viable behaviors from the test subjects. In the present experiment, we prioritized the enrichment of "routes", including primate specializations, while encouraging sufficient repetition of cues, contexts, and actions to support use with wireless neural recordings in the relevant brain structures. We held a secondary interest

in exploring the multiple modalities for assessing behaviorally-relevant movements, for future elaboration of pose and possibly embodied memory in the enclosure.

2.5.2 Route enrichment

We incorporated several common features from studies of freely-moving rats and mice involved in memory or navigation studies, adapting them to be more relevant to the macaque. First, we include temporal context (a sequential 'route'), which had been used to bridge rodent hippocampal place field studies and human list learning and item sequences (Pastalkova et al. 2008; Howard Eichenbaum 2014; Fortin, Agster, and Eichenbaum 2002; Allen et al. 2014; Salz et al. 2016; Long and Kahana 2019; Hsieh et al. 2014; Jang and Huber 2008). We additionally incorporate visual objects into the sequences as relevant material for primate species (Ranganath 2010; Libby et al. 2019). The objects on a background scene are reminiscent of hippocampal-dependent object-context memory tasks to assess hippocampal and MTL function in monkeys (Gaffan 1994; Froudist-Walsh et al. 2018; Basile et al. 2020; Templer and Hampton 2013b; Chau et al. 2011), but in this case, we require the 3-D screen location in the environment as the spatial associate; finer, 2-d position on the screen must be ignored, adding another level of flexibility to the task. These attributes are important for creating event memories that demonstrate flexible learning through the layered spatio-temporal contingencies and rules (or features) that need to be ignored. The cost of this task structure is that we require sufficient changing elements to be learned in parallel, before reward, and it was not clear at the outset if the monkeys would succeed. Furthermore, electrophysiological studies of replay or that measure trajectories, typically require repeating sequences (Z. S. Chen and Wilson 2023). To encourage learning and to encourage resampling of behaviors/positions through a common sequence, we incorporated a correction trial. This complicates reinforcement learning modeling and could have led to 1-pass learning, in principle. In practice, the monkeys take the serial equivalent of ~1-5 trials to learn, even in the face of the distractors. This rate of learning suggests they did not come to rely on the correction in favor of responding appropriately to the choice array. Empirically, they learned and did

so rapidly considering the multiple strategies and conditionals that could have impeded progress. Having demonstrated learning, future studies may isolate different cues and rules to encourage different learning strategies. For example, contingencies could be based on the background image, temporal sequence (order), spatial sequence, or item sequence. Capacity and memory generalization could be assessed by varying the similarity and relationship among cues to be grouped or discriminated. Prospective and retrospective replay could be probed by varying the spatial trajectories just completed with those that are about to commence. Meanwhile, proceeding with the present design offers a convergence of spatiotemporal cues, each of which can drive differentiable neural responses, to facilitate neural decoding of the different trial trajectories.

2.5.3 Tracking pose across learning

In the present experiment, we placed the touchscreens as the primary behavioral assessment tool, using cameras and IMU to augment those measures, unlike other freely-moving monkey setups (Bala et al. 2020). As a consequence, the animal shows a regular outward positioning to react to screens, limiting the visibility of face and limbs during the task epochs. As such, this task structure is not optimized for assessing reach and eye movements, therefore other design strategies could be added for tasks designed to study reaching and facial movements (Womelsdorf et al. 2021) Our use of touches on the screen, however, was effective at ensuring spatiotemporal and physical (vision and reach) points of alignment, each funneling into lower degrees of freedom than the full continuous behaviors would offer. This suggests that for predictable goals, the range of movements and poses has far fewer degrees of freedom and is therefore more tractable to analyze than random foraging and exploration. It also helps dissociate performance differences due to movements versus perceptual or mnemonic differences. If more complete foraging or spontaneous behaviors are desired, changing the structure of the environment and experimental contingencies will prevent ‘settling’ into a regular goal-directed path. Future experiments should expand on the curiosity, free foraging, and more

diverse response strategies of macaques to capitalize on the full benefits of such enclosures.

2.5.4 Learning set, or 'learning to learn'

The use of richer task structures offers an opportunity to assess whether and how subjects use previously learned structure to inform new decisions. In the present study, monkeys changed head movements with learning. Specifically, the head 'toggling' during deliberation was reduced post-learning, and further, over set repetition. This may be an analog of saccadic scan paths that invoke fewer checks and re-checks before a decision is made. Tracking the animal's body, head, and eyes may be useful to detect the embodiment of learning (Gottlieb and Oudeyer 2018; Yang, Lengyel, and Wolpert 2016; Yang, Wolpert, and Lengyel 2018; Gomez-Marin and Ghazanfar 2019; Gomez-Marin et al. 2014). In addition, one of the monkeys showed improved performance across sets. Because the monkeys have different overall levels of performance and different levels of experience viewing visual objects, further work will be needed to reveal the conditions that are conducive to learning greater movement economy versus correct flexible-associative learning, across set repetition.

In the present study, we do not measure explicitly whether movement itself improves learning speed, robustness to interference, or capacity; however, numerous studies restricting movement or using virtual and 2-D visual environments make a compelling argument for the use of maximal immersion and bodily agency in experiments (Aghajan et al. 2015; Carassa et al. 2002; T. C. Foster, Castro, and McNaughton 1989). In particular, to understand flexible learning, maximize the capacity of memory, and to understand the neural circuits as they have developed to aid the individual, we must endeavor to use the organism's defaults: natural movements within 3-D naturalistic settings. The present example is one demonstration of this, within the nascent but vital field studying primate neurophysiology through a freely-moving, ethological lens.

2.6 Materials and Methods

All animal procedures were approved by the Vanderbilt Institutional Animal Care and Use Committee, in compliance with the policies of the United States Department of Agriculture and Public Health Service on the humane care and use of laboratory animals. Experimental subjects were two adult female rhesus macaque monkeys (*Macaca mulatta*).

2.7 Behavioral Testing

Testing environment. The testing apparatus consisted of a custom-made enclosure (1.52 x 1.52 x 2.13 m; the 'Treehouse', Figure 1a,b), equipped with modular panels organized into upper and lower levels. Among the panels, 8 were designated as testing stations, each equipped with a touchscreen (ViewSonic 24" 1080p 10-Point Multi Touch Screen Monitor, models 2421 and 2455) and a perch. These stations were arranged symmetrically in two opposed corners (e.g., northwest and southeast) with a 2-level x 2-side arrangement in each corner. Fluid reward was delivered by peristaltic pumps (Campden Instruments Precision Liquid Feed Pump) placed in both active corners. The pumps were controlled with a Measurement Computing Corporation USB DAQ (OM-USB-1208FS) that was connected to the Experimental Control System.

Behavioral tracking We monitored and recorded animals' behavior in using 8 side cameras and 1 overhead camera (Figure 1A; 5 e3Vision, WhiteMatter cameras, https://white-matter.com/products/e3vision/, and 4 Logitech webcams) set up around the enclosure. Video frames from all cameras/webcams were collected at 30Hz with HD resolution. e3Vision frames from all cameras were sent to the e3Vision hub and synchronized online before recording. Logitech video frames were synced to e3Vision

frames manually by aligning a reference frame (a simultaneous change of background on all screens). In addition to video recordings, we recorded movements, with a wireless 9-axis Inertial Measurement Unit (IMU, Freelynx, Neuralynx, Inc.) to previously-implanted titanium cranial fixtures (Double-Asymmetric Head Post, Gray Matter Research or similar custom fixtures from Rogue Research). The IMU data were acquired at 3kHz and saved directly to the acquisition computer's disk. To synchronize IMU and camera frames, TTL pulses for the start and end of the e3Vision frames were sent from the e3Vision hub to the acquisition system where IMU data were recorded.

Experimental control. Experiments were controlled by a single computer equipped with two AMD graphics cards (Cape Verde PRO FirePro W600) that connected to the eight touchscreens, plus one control monitor. A MATLAB toolbox based on PLDAPS (Eastman and Huk 2012) was developed in house ('TreeTop' at https://github.com/hoffman-lab/TreeHouse)(Wagner 2006). This toolbox uses Psychtoolbox functionality (Brainard 1997; Pelli 1997) to control stimulus selection and presentation on each monitor independently with precise timing, of stimulus presentations and monitoring multi-touch activations of the screens with exact locations, and control of reward delivery. To achieve the precision and independence in stimulus timing and touch monitoring, the toolbox relies on object oriented programming using a finite state system approach (Wagner 2006) as outlined for the PLDAPS (Eastman and Huk 2012) and Opticka packages (Andolina 2023). The TreeTop system also sent event codes to the IMU DAQ, allowing experimental control, cameras, and IMU to be synchronized.

Trial structure. As shown in Figure 1C and D, the task started with the presentation of a *start cue* (black circle) that designated the active screen for the animal. Upon touching the cue, and after a 1 s delay, the *array onset* consisted of the appearance of 4 objects presented in a 2 by 2 grid on a background scene providing context specific for that set of objects. *Selection*: If monkeys touched the correct item ('Target') - the item associated with that screen - a 'correct' tone was played and the target reappeared at the center of the screen. *Confirmation*: The subject had to touch the target again to proceed to activate

the next screen. If, instead, she selected one of the 3 non-target objects ('distractors'), an 'error' tone was played along with the disappearance of the stimuli for 2-4 seconds. Then, the correct target was shown in isolation in the originally presented location in the background context (i.e. *Correction*). Monkeys had to touch the target in isolation to proceed to the confirmation where they had to select the target once again. Occasionally, only the target was displayed, with no distractors, to help maintain motivation. These were equally likely across screens, and were excluded from all learning analyses. As shown in Figure 3D, subjects proceeded through the trial sequence on all 4 screens, in order, before receiving fluid reward. For Subject W, the total reward was calculated based on the performance of the animal within a trial (e.g. 2 drops of juice per correct selection and 0 drops for incorrect touched) and delivered at the reward receptacle. For subject F, a fixed reward amount was delivered, but the reward type (flavor) was switched in the middle of the session to maintain motivation. For the presented data, both subjects always traversed an identical sequence starting with screen 1 (upper left) to screen 4 (lower right) on one corner of the environment.

Session design. Although a given stimulus set was restricted to one corner of the apparatus, sets could be assigned to either of the two touchscreen corners. Within a given session, monkeys were trained on both corners of the apparatus, using different sets of stimuli, in an alternating block design of 2 repetitions. For monkey W, only one corner contained a new set; the other corner contained a set that had been learned previously. Presentation of new sets was staggered across corners in this way. For monkey F, earlier sessions consisted of two new sets on opposite sides of the apparatus, but later sessions were similar in setting to monkey W. We continued training on the same sets across days until monkeys learned the novel sets and then introduced new different sets. For the current study, we only used learning on the novel sets.

Visual stimuli. Objects and background images were chosen from colored photorealistic fruits/vegetables and natural scenes, respectively. The isolated object images were scaled to approximately the same size and placed on a black circle background of 73 mm diameter with a gray ring of 117 mm diameter around it, to make objects distinct from the

screen background image (Figure 1). Different types of fruits/vegetables were included in any a set of four objects, and images were never reused across sets.

2.7.5 Experimental subject pretraining

First, the monkeys were pretrained to use touch screens. Subject W was then required to select by touching a correct synthetic object paired with a specific scene background in the booth setup, while seated in a transport chair. Subject F was required to touch one of two possible item colors, or one of two spatial positions as a function of the screen location screen in the treehouse. When training started in the Treehouse, both monkeys were therefore naïve to screen-contingent object association tasks, but were familiar with learning selection rules on touchscreens. After the animals learned the location of all the reward spouts, we introduced an operant cue touch on a single screen for reward, followed by selection from among an increasing number of items in an array. Finally, we increased the number of active screens in which the animal had to perform the same actions, but across the multiple screens in a predetermined order before receiving reward until a sequence of all 4 screens from a given corner was achieved.

2.7.6 Behavioral analysis

Learning assessment. We concatenated all completed trials per stimulus set, including all responses in which the animals selected from among the 4 objects in the array. We then used a latent-process model to calculate individual learning curves for each screen of each set, by subject (Smith et al. 2004). The process includes a 2-step state-space filtering followed by a smoothing algorithm to estimate the learning curve and its confidence intervals. The estimation used an Expectation Maximization algorithm with an initial background probability of 0.25 and convergence criterion of 1e-8. The maximum number of steps was set to 5000, and a significant epsilon (square root of the variance of the learning state process) of 0.005 was used. The initial conditions were fixed, and the

learning trial was defined for each animal as the first trial where the 95% confidence interval of the estimated probability of correct performance exceeded and remained above chance. To estimate changes in learning rate across sets (i.e. over time) for each animal, we fit a linear regression to the learning rate of each screen of each set, according to the ordinal position of the set.

Markerless pose labeling of videos. For 3D movement reconstruction, we used JARVIS (https://jarvis-mocap.github.io/jarvis-docs/). In the first step, we used a 7x4 checkerboard to record one calibration video for each camera. 20 frames per camera were used to compute all the camera-specific parameters that were used for 3D reconstruction including focal length, principal point offset, and distortion parameters. Next, we used JARVIS annotation tool to annotate 26 points on the animal's body in the apparatus which included the center shoulder, tailbone, tail tip, nose tip, joints such as elbow, wrist, fingertip, knee, ankle on both sides, and 2 LEDs on the recording cover, and the headpost. Initially, a subset of frames was uniformly extracted for manual labeling, followed by training and testing the model. We improved the model's performance by replacing faulty frames where the model did not work well with similar frames. We trained separate models based on the camera views of each two active corners of the apparatus. The model for each corner was trained on frames from 3 cameras that maximized the projection of the animal for that corner. For each camera, 500 frames were labeled. For both models, we used HybridNet with 3D-CNN (convolution neural network) based network architecture containing 88 layers (medium size). HybridNet models achieved an accuracy of 29mm on the training set and 32mm on the test set. After initial reconstruction, we applied a 3D median filtering with a window length of 7 frames for smoothing. In addition, for illustration purposes, we applied a second Savitzky-Golay filter with a window length of 30 frames and polynomial order of 1.

IMU tracking. The IMU data tracked the linear acceleration and angular velocity of head movement. Angular velocity measures roll, pitch, and yaw, and linear acceleration measures linear movements. These data can augment behavioral assessments by

providing higher temporal resolution (3000 Hz) than video markerless tracking (33 Hz). Our interest was in the relative movement of the head at different learning points. To analyze head movement differences with learning, we extracted and rectified IMU data, in microvolts, from the choice epoch of each trial, (I.e. the onset of choice array appearance to selection). During this time, the animals need to choose among four options, and this choice is the target of learning in the present experiments. The resulting average movement value per trial was grouped according to learning (pre-learning point and the final trials, after the learning point), for each set. Because of the different placement and orientation of the IMU on the animal, we are showing the angular velocity for one animal and the linear acceleration of the other. For the cumulative distribution functions, we bootstrapped the data over 1000 trials, taking out 40 samples per trial, to generate a 95% confidence interval. A 2-tailed Mann-Whitney U test was used to compare the early and late learning movement distributions of each animal.

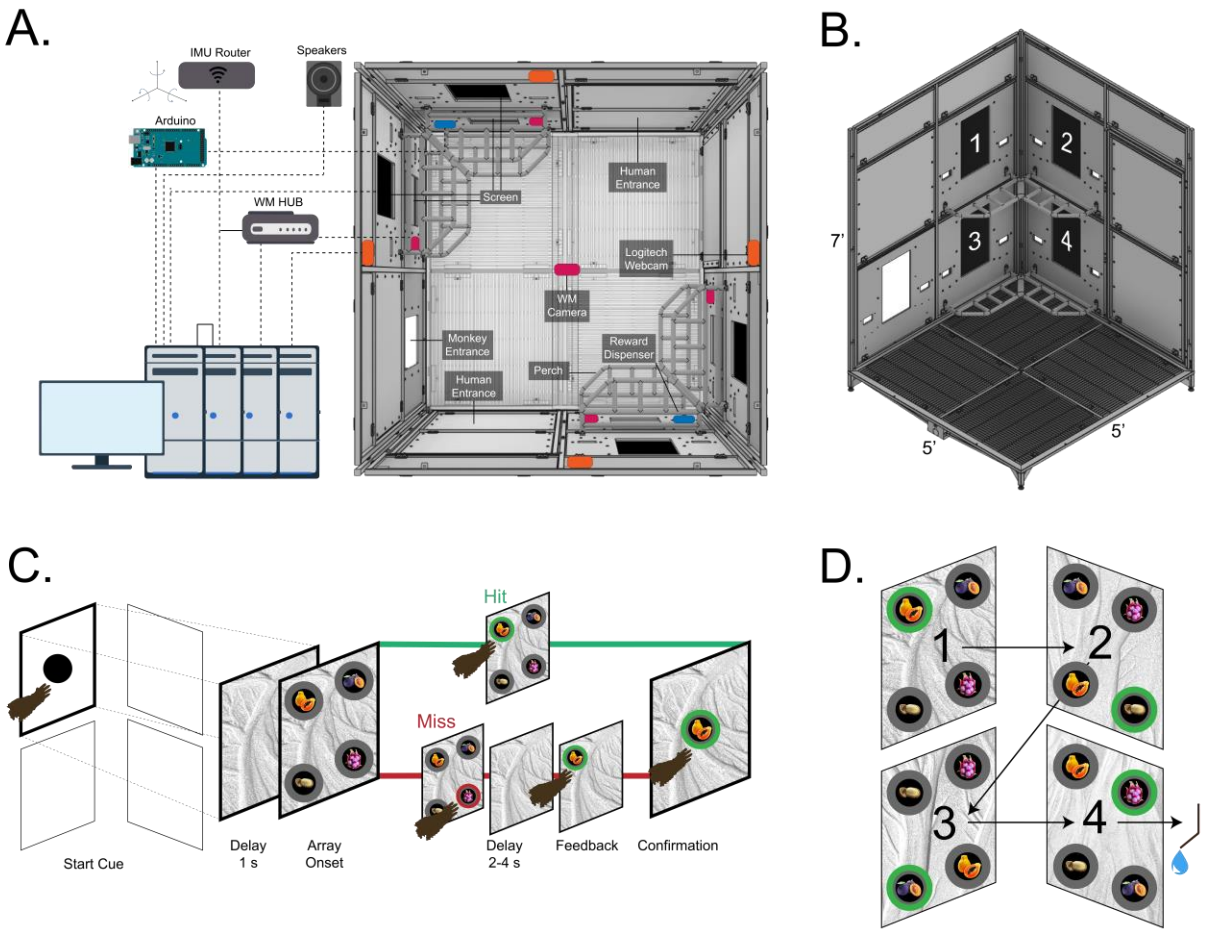

Figure 2-3. Sequential object-in-context association task in the 3-D 'Treehouse' enclosure.

(A, B) renderings of the enclosure, including a schematic of peripheral devices that enabled timed stimulus delivery and behavioral measurements. (A) overhead view of the task environment. Black squares depict touchscreens, white squares show the monkey entrance, blue rectangles show reward dispenser locations, and pink rectangles show the camera positions. (B) One corner of the enclosure, revealing the four stations comprising one trial (stations are numbered in presentation order). The opposite corner has been hidden for visibility. (C)Trial sequence depicted for the first screen in the sequence. Bold black = active screen; green ring = correct target; red ring = incorrect distractor. Following completion of one screen's association, the trial continues to the next screen in the sequence. (D) *O*bjects and their location on the screen in an example trial. Green rings indicate associated targets of screens. The position of the 4 objects in the 2 x 2 array is randomized across screens and trials, and the background image was simplified for the purpose of illustration.

Funding. This work was funded by the Whitehall Foundation, NEI P30EY008126, and NI R01 NS127128.

Acknowledgements. The authors wish to thank the veterinary staff for maintaining the well-being of animals, Daicia Allen, Mitchell Riley, and Chrissy Suell for animal training support, and Sergey Motorny, Supeng Wu, and Richard Song for their technical support for pose tracking.

Conflict of interest. The authors declare that the research was conducted in the absence of any commercial or financial relationships that could be construed as a potential conflict of interest.

3. Chapter 2: Theta- and gamma-band oscillatory uncoupling in the macaque hippocampus[2]

3.1 Abstract

Nested hippocampal oscillations in the rodent give rise to temporal dynamics that may underlie learning, memory, and decision making. Although theta/gamma coupling in rodent CA1 occurs during exploration and sharp-wave ripples emerge in quiescence, it is less clear that these oscillatory regimes extend to primates. We therefore sought to identify correspondences in frequency bands, nesting, and behavioral coupling of oscillations taken from macaque hippocampus. We found that, in contrast to rodent oscillations, theta and gamma frequency bands in macaque CA1 were segregated by behavioral states. In both stationary and freely-moving designs, beta2/gamma (15-70 Hz) had greater power during visual search whereas the theta band (3-10 Hz; peak ~8 Hz) dominated during quiescence and early sleep. Moreover, theta band amplitude was strongest when beta2/slow gamma (20-35 Hz) amplitude was weakest, instead occurring along with higher frequencies (60-150 Hz). Spike-field coherence was most frequently seen in these three bands, (3-10 Hz, 20-35 Hz and 60-150 Hz); however, the theta-band coherence was largely due to spurious coupling during sharp-wave ripples. Accordingly, no intrinsic theta spiking rhythmicity was apparent. These results support a role for beta2/slow gamma modulation in CA1 during active exploration in the primate that is decoupled from theta oscillations. The apparent difference to the rodent oscillatory canon calls for a shift in focus of frequency when considering the primate hippocampus.

3.2 Introduction

Hippocampal oscillations are heralded as canonical examples of how oscillations support cognition by coordinating neural circuit dynamics (Klausberger and Somogyi 2008; Colgin

[2] This chapter is adapted from Theta-and gamma-band oscillatory uncoupling in the macaque hippocampus published in eLife and has been reproduced with the permission of the publisher and my co-authors AT Hussin, KL Hoffman.

2016; György Buzsáki and Draguhn 2004; Hahn et al. 2019). In turn, behavioral states constrain and entrain specific neural oscillations. In rodents, locomotion and other exploratory movements elicit an ~8 Hz theta oscillation in hippocampal CA1, (Whishaw and Vanderwolf 1973; Kramis, Vanderwolf, and Bland 1975; Vanderwolf 1969; György Buzsáki 2002) and a faster gamma oscillation (25-100 Hz) that nests within theta (Colgin 2016; Colgin and Moser 2010; Bragin, Jandó, Nádasdy, van Landeghem, et al. 1995; Jozsef Csicsvari et al. 2003; I Soltesz and Deschênes 1993). In contrast, during quiescent states, theta and gamma oscillations are suppressed and sharp-wave ripple complexes emerge, the latter consisting of large high-frequency oscillations (150-250 Hz) in CA1 that occur within a slower (sharp-wave) deflection (György Buzsáki 2015; Ylinen et al. 1995). Although the occurrence of sharp wave ripples during quiescence is highly conserved across species (György Buzsáki 2015), its dichotomy with theta is questionable (Hussin, Leonard, and Hoffman 2020; Leonard et al. 2015). This may stem from differences in how and when theta oscillations appear across phylogenetic order (Ulanovsky and Moss 2007; Green and Arduini 1954), particularly among primates, including humans (Halgren, Babb, and Crandall 1978; Green and Arduini 1954; Stewart and Fox 1991; Tamura et al. 2013; Talakoub et al. 2019; Courellis et al. 2019; Jacobs 2014; Herweg, Solomon, and Kahana 2020; Mao 2022). Consequently, gamma coupling to hippocampal theta (Bragin, Jandó, Nádasdy, Hetke, et al. 1995; Colgin 2016; Lisman and Jensen 2013), and the presence – as postulated – of sub-bands of gamma (Colgin et al. 2009; Colgin 2016; Jozsef Csicsvari et al. 2003; György Buzsáki and Wang 2012), could understandably be affected by the scarcity and/or brevity of theta oscillations in monkeys during species-relevant exploration (Talakoub et al. 2019; Leonard et al. 2015; Hoffman et al. 2013; Jutras, Fries, and Buffalo 2013; Courellis et al. 2019; Mao et al. 2021; William E Skaggs et al. 2007). In the present study, we therefore adopted a hypothesis-generating (data-driven) approach to identify i. which oscillatory bands emerge in macaque hippocampal CA1 as a function of the behavioral state; ii. whether these oscillations coalesce or compete, and iii. to what extent local single units are modulated at these rhythms.

3.3 Results

3.3.1 Spectral analysis of hippocampal LFP during active visual search and quiescence

We recorded 42 sessions (M1: 26 sessions, M2: 16 sessions) in the hippocampal CA1 subfield of two macaques (Figure 1; Figure 1- figure supplement 1) during active visual search and quiescence (henceforth: 'rest'). As a control for the effects of the stationary animal, we recorded from one of the above animals (M2) and a third animal (M3) in freely moving and overnight sleep conditions (Figure 1 – figure supplement 2). Consistent with previous reports (Leonard et al. 2015; Leonard and Hoffman 2017), we observed bouts of roughly 20-30 Hz oscillations predominantly during search, and slower-frequency, larger-amplitude local field potentials (LFPs) during rest (Figure 1A, C). To visualize the relationship between spectral power across frequency bands, we sorted quantiles of ~1 s segments based on their average power in the 20-30 Hz frequency band, revealing an antagonistic relationship between 20-30 Hz and <10 Hz frequencies (Figure 1B) i.e. when power at 20-30 Hz was greatest, <10 Hz power was qualitatively weakest. In contrast, stronger power at <10 Hz was accompanied by stronger power at > 80 Hz. To determine whether the spectrum varies with behavioral epoch, as it does in rodents (G Buzsáki 1996; Whishaw and Vanderwolf 1973), we calculated the power spectrum for each behavioral state (Figure. 1D). To identify power beyond the 1/f background, we used the aperiodic-adjusted power spectrum (Demanuele, James, and Sonuga-Barke 2007; Donoghue et al. 2020). We found stronger 7-10 Hz power during rest compared to active search (Figure. 1D, Middle). In contrast, power in the higher frequencies from 15-70 Hz was stronger during active search compared to rest, with a peak in the 20-30 Hz range (both, $p<0.05$ Wilcoxon signed rank test with FDR correction). In most non-rodent species examined, including humans, hippocampal theta band oscillations during alert wakefulness are described as occurring intermittently, in short-lived bouts, unlike the protracted and predictable trains of theta oscillations seen in the rodent hippocampus (Jutras, Fries, and Buffalo 2013; Talakoub et al. 2019; M Aghajan et al. 2017; Watrous et al. 2013; Jacobs 2014; Ulanovsky and Moss 2007; Green and Arduini 1954). To identify oscillations that are rare and short-lived, and to allow for a more direct comparison to

conventions used in human iEEG/macroelectrode studies, we used the BOSC method (Hughes et al. 2012; Caplan et al. 2001; M Aghajan et al. 2017). This method quantifies the fraction of time that band-limited power exceeds amplitude and duration thresholds. The amplitude threshold is set after fitting the signal to a log-log linear regression to account for the spectral tilt ($1/f^x$) of the distribution under consideration and accepting only residuals with at least 3 cycles exceeding 95% of the χ^2 distribution. This classifies the graded power spectral measure into discrete 'hits' and 'misses' across time. Consistent with continuous power spectral results, we found that theta bouts ('hits') were more prevalent during rest/sleep compared to online active behavioral states. The pattern was the opposite for beta2/gamma frequencies, which were more prevalent during active states (Figure 1-figure supplement 2, $p<0.05$ Wilcoxon signed rank test with FDR correction).

In rodents, the frequency and the amplitude of theta oscillation are related to the speed of locomotion (McFarland, Teitelbaum, and Hedges 1975; Fuhrmann et al. 2015; György Buzsáki 2002; Sheremet, Burke, and Maurer 2016) although theta activity is also observed during awake immobile states of alertness (Sainsbury 1998; Tai et al. 2012; Vanderwolf 1969; Kramis, Vanderwolf, and Bland 1975). Theta-movement correlates raise the concern that the scarcity of theta during active behaviors in the present study might be attributed to the animals' immobility. To address this concern, we recorded wirelessly from the hippocampal CA1 of the second monkey (M2) and a third adult female macaque (M3) during freely-moving active states including immersive visual search and during overnight rest/sleep (M3: 15 sessions, M2: 3 sessions). The results match those of the previous experiment, thereby demonstrating that the decrease in theta-band power and the increase in gamma power during active behaviors generalize, i.e. they were not merely due to the immobile state of the animals (Figure 1-figure supplement 3, Video 1). Furthermore, the duration and consistency of theta bouts during early sleep indicate that these methods (recording sites, electrode signal, and states) are capable of detecting theta oscillations, but that they appear during different epochs than those for recordings in rats and mice, (Figure 1-figure supplement 3, Video 1, Figure 1-figure Supplement 4).

3.3.2 Hippocampal cross-frequency coupling

To assess the coupling of theta and gamma oscillations at a finer temporal scale, we computed the cross-frequency power correlations across the spectrum. Consistent with the qualitative pattern shown in Figure 1B, power at 3-8 Hz and 20-35 Hz were negatively correlated (Fig. 1E, $p<0.05$, using a cluster-based permutation test corrected for multiple comparisons). In addition, power in the slower, 3-8 Hz band was positively correlated with that of a much faster, 80-150 Hz band. We next applied a complementary approach, comparing the amplitude envelopes of these two bands (theta and slow gamma) over time, to track the finer temporal structure of power correlations. The results supported the epoched-data results (Figure 1-figure supplement 2).

To estimate phase-amplitude coupling in the LFP, we performed bicoherence analysis (Kovach, Oya, and Kawasaki 2018; Hyafil 2015; Giehl, Noury, and Siegel 2021), revealing a peak cluster around the 25 Hz frequency range which confirms an interaction between the activity at this frequency and its second harmonic. In addition, the 3-8 Hz band was coupled to high frequencies of 95-150 Hz ($p<0.05$, cluster-based Monte Carlo statistical test). This is consistent with the cross-frequency amplitude coupling results and indicates that the correlated envelopes in Fig. 1E are driven by the phase-specific coupling of the high frequencies (Figure 1B). In contrast, our bicoherence results showed no significant phase-amplitude coupling between theta and gamma frequency ranges.

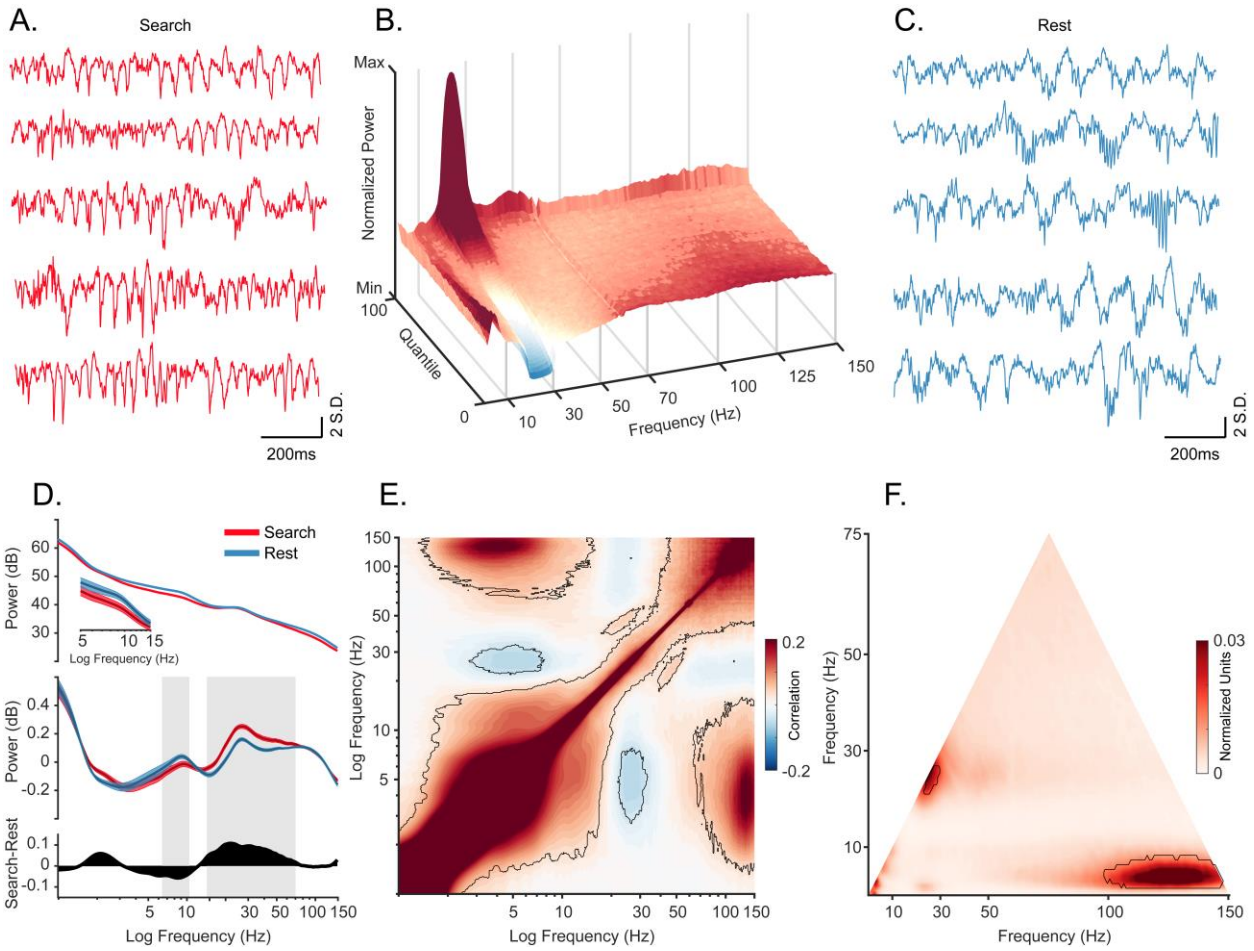

Figure 3-1. Oscillatory decoupling in CA1 field potentials.

A. Example traces of broadband LFP in CA1 during search. Data segments were taken from epochs with characteristic high 3-200 Hz power, shown in B (traces were linearly detrended for visualization). B. Spectral density sorted by 20-30 Hz power. The surface plot shows data segments sorted into quantiles according to 20-30 Hz power, revealing an apparent increase in 5-10 Hz power when 20-30 Hz power is weakest. See Methods for details. C. Example traces of wideband LFP in CA1 during the rest epoch showing characteristic interactions between <10 Hz and >60 Hz oscillations. Conventions as in A. D. Top. Mean power spectral density during search (red), and rest (blue). Inset: mean power for low frequencies of the main plot, with shaded 95% bootstrap confidence interval (N=42 sessions). Middle. Power spectral density after fitting and subtracting the aperiodic 1/f component during search and rest, with shaded 95% bootstrap confidence intervals. Gray areas show significant differences in power across behavioral epochs ($p<0.05$, Wilcoxon signed rank test, FDR corrected) Bottom. Power difference between search and rest. E. Average cross-frequency power comodulogram (N=42 sessions). Dark outline represents areas that were significant in at least 80% of samples ($p < 0.05$, cluster-based permutation test corrected for multiple comparisons). F. Average bicoherence of the CA1 LFP (N=42 sessions). The dark outline represents areas that were significant in at least 80% of sessions ($p < 0.05$, Monte Carlo test corrected for multiple comparisons). The decoupling is preserved when applying analysis methods sensitive to transient oscillations (Figure 1-figure supplement 2), and when analyzing CA1 LFPs from an additional monkey who moved freely in a search task, and during night-time rest (Figure 1-figure supplement 3).

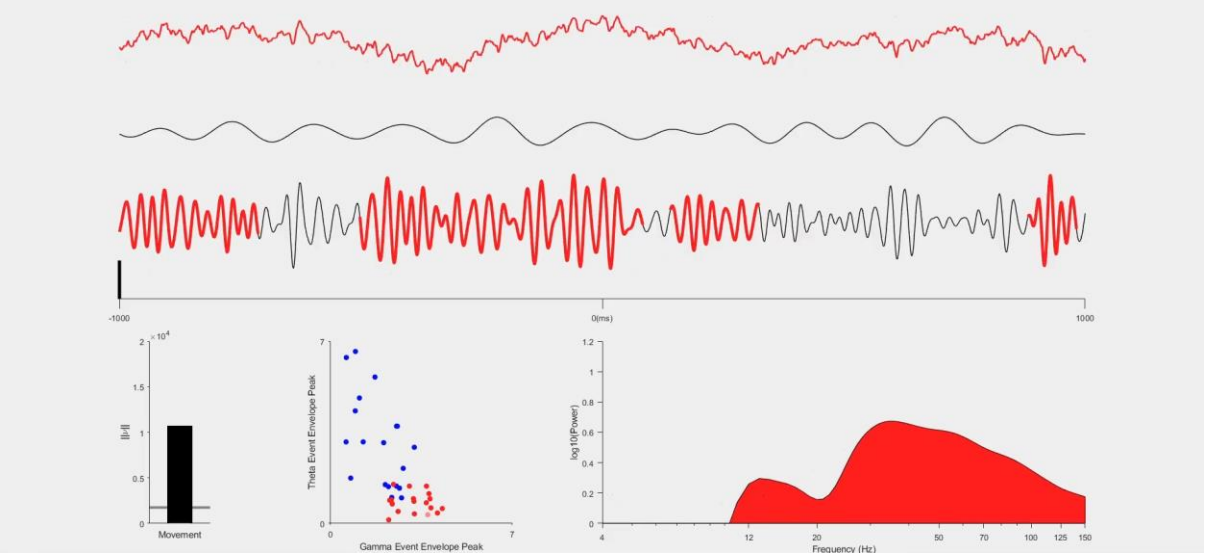

Figure 3-2 (Video) Oscillatory dynamics in monkey CA1 during sleep and waking states

(Top) Two-second segments of broadband LFP during sleep (blue), and free movement in an enclosure during a search task (red), the 4-8 Hz bandpass filtered LFP, and the 25-50 Hz LFP, shown top to bottom, respectively. Detected bouts in each frequency band are highlighted with blue (sleep) and red (waking). The black vertical line shows 3 S.D. above the mean. (Bottom) Left: Movement, expressed as the vector norm of angular velocity. The grey horizontal line shows the threshold for movement. Middle: The envelope peak of detected theta (4-8 Hz) bouts plotted as a function of the gamma (25-50 Hz) peaks. Right: 1/f corrected (fitted residual) power spectrum. The distribution of power shifts to higher frequencies during awake compared to sleep.

3.3.3 Oscillatory modulation of spiking activity

Peaks in spectral power do not necessarily indicate the presence of oscillations in the underlying neural activity (Buzsáki and Wang 2012; Pesaran et al. 2018; Herweg et al. 2020; Jones 2016). If oscillations are present in the local neural population, regular comodulation between spikes and local field oscillation phases should occur. We measured the spike-field coherence for the whole duration of the sessions by calculating pairwise phase consistency (Vinck et al. 2010) for well-isolated units (N=404). Individual cells phase locked to multiple frequencies (Figure 2A; $p<0.05$, permutation test and Rayleigh test $p<0.05$), with the population showing the full range of spike preferred frequencies of modulation (Figure 2C).

One of the caveats of spike-field coherence measures is that they can be sensitive to large amplitude non-periodic deflections. Sharp-wave ripples (SWRs) have a non-

oscillatory amplitude envelope within the frequency range of 0.1 to 10Hz in rodents and non-human primates (Maier, Nimmrich, and Draguhn 2003; Rex et al. 2009; Leonard et al. 2015; Hussin, Leonard, and Hoffman 2020; William E Skaggs et al. 2007).

Furthermore, we previously observed that SWRs occur in primates during active visual exploration (Leonard et al. 2015; Leonard and Hoffman 2017) and that the probability of firing of cells increases during these events, for putative pyramidal and inhibitory cells alike (Hussin, Leonard, and Hoffman 2020; Leonard et al. 2015; William E Skaggs et al. 2007). Given the limitations of spike-field coherence, the frequency characteristics of SWRs, spiking activity profile of neurons around these events, weaker power at 7-10 Hz during active search, and the strong coupling between bands matching the SWR events (3-8 Hz and >95 Hz), we hypothesized that spike-LFP coherence at low frequencies might be partly produced as a byproduct of the slow deflection of sharp-wave ripples (Hussin, Leonard, and Hoffman 2020) rather than via harmonic oscillations. To test this, we extracted peri-SWR spikes, computed PPC only for these spikes in each cell [PPCswr], and then compared this to the PPC for spikes outside the SWR windows [PPCresidual]. Figure 2B shows an example cell that exhibits stronger spike-LFP coherence at 8 Hz during SWR than outside the SWR window ($p<0.05$, permutation test with FDR correction). At the population level, coherence at lower frequencies (2-10 Hz) was greater during SWR than in the SWR-removed distributions. In contrast, the higher frequencies (10-200Hz) maintained a greater coherence outside of the SWR time window (Figure 2D). This led to weaker mean spike-field coherence restricted to the < 10 Hz range, after removing the influence of SWRs, suggesting a contribution of the non-oscillatory slow deflections in the SWR complex to the apparent cross-frequency interactions.

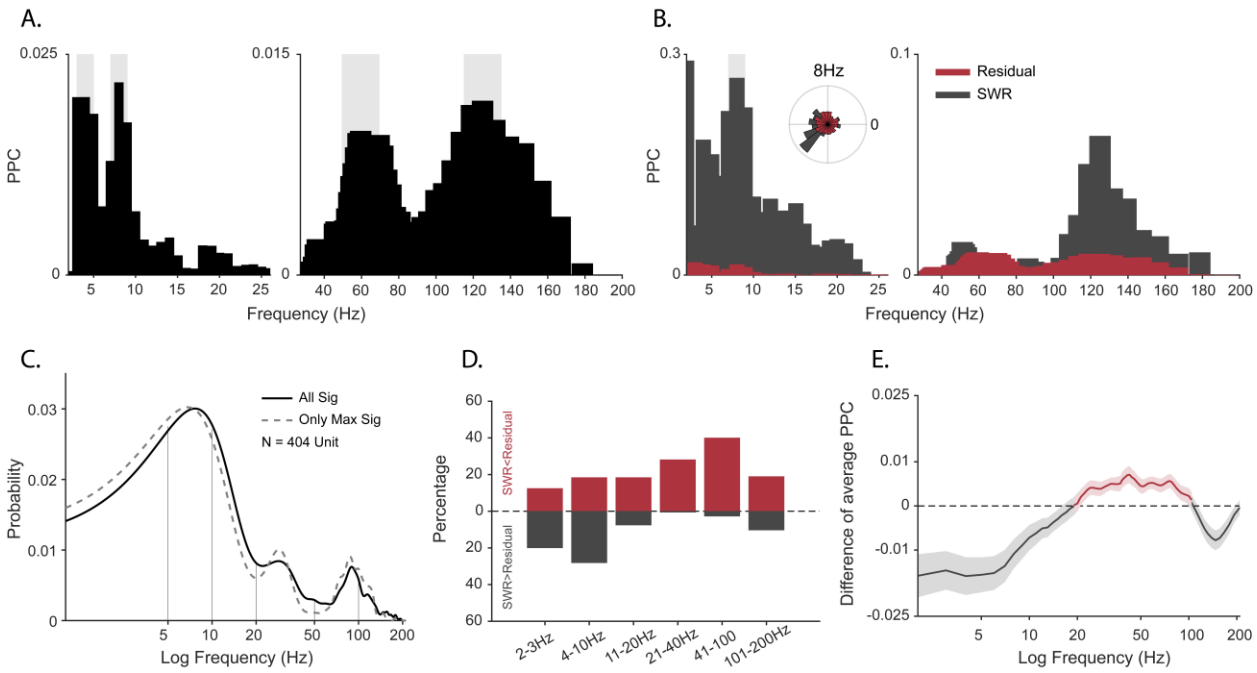

Figure 3-3. Spike-field coherence and its influence by sharp-wave ripples.

A. Spike-LFP Pairwise phase consistency (PPC) spectra for an example unit. Shaded gray shows significant values ($p<0.05$, permutation test, and Rayleigh test $p<0.05$). **B.** Spike-LFP coherence for spikes during detected SWRs (dark gray) and for spikes remaining after extracting the SWR epochs ('residual', red). Light gray shading shows a significant difference at $p < 0.05$ in the FDR-corrected permutation test for the SWR group. Inset: Normalized histogram of the phase values at 8 Hz, obtained from the spike-LFP coherence analysis shown in A. **C.** Probability distribution of observing significant PPC values across all frequencies (solid black line), and only for preferred frequency (frequency with maximum PPC value) before adjusting for SWRs (N = 404 units). **D.** Difference in the proportion of cells with greater spike-LFP coherence for SWR (grey) and SWR-removed residual (red), for 6 frequency bands (N=185 units). **E.** SWR-residual difference of mean Spike-LFP coherence. Shading shows 95% bootstrapped confidence interval. Positive values indicating greater PPC for residual than SWR groups are shown in red, negative values (SWR>residual) in dark gray.

To ensure that oscillations were local and to avoid the influence of aperiodic deflections, we generated spike autocorrelograms. Periodic peaks of the spike autocorrelograms demonstrate theta rhythmicity in rat and mouse CA1 (Cacucci et al. 2004; Royer et al. 2010; J O'Keefe and Recce 1993). To directly compare theta rhythmicity in our cell population with observations in the rodent, we computed the autocorrelogram for a complete population of well-isolated cells with at least 100 spikes for the whole session and for the complete cell population from homologous subregions of CA1 in rodents, also across the whole session. Figure 3A shows an autocorrelogram of the theta spike-field coupled cell in Figure 2A (black, monkey) overlaid onto a theta-rhythmic cell from the homologous CA1 region of a rat (i.e. temporal CA1) shown in gray. To quantify theta

autocorrelogram rhythmicity, we calculated the theta modulation index (52). Compared to modulations seen in the rat (Figure 3B in gray), monkey cells typically showed near zero index values i.e. were not modulated (Figure 3B in black), which was also evident in the sorted-cell and mean population autocorrelogram (Figure 3C, inset shows rat distribution). For a given firing rate, higher frequencies are less likely to demonstrate cycle-by-cycle periodicity due to their shorter periods; nevertheless, we observed a few examples of >20 Hz spike modulation in the spike-triggered averages and autocorrelograms of several cells (Figure 4).

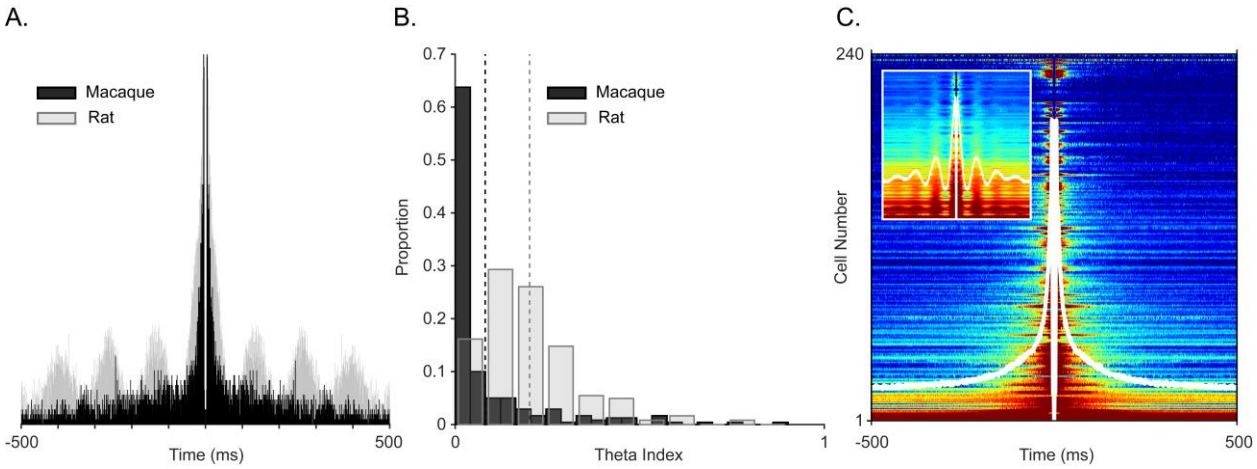

Figure 3-4. Examining spiking periodicity for theta modulation in macaque hippocampus.

A. Autocorrelogram of an example “theta” unit from Figure 2A (black, N= 945 total spikes) and a theta-modulated unit from the rat (grey, N= 5655 total spikes). **B.** Distribution of the theta index in CA1 units from this study (black, N=240 units), and CA1 units of rat (gray, N=197 units). Dashed lines show mean values, color-coded by species. **C.** Sorted autocorrelograms of CA1 units, with mean population ACG shown as a white trace. Inset: same as the main plot but for rats.

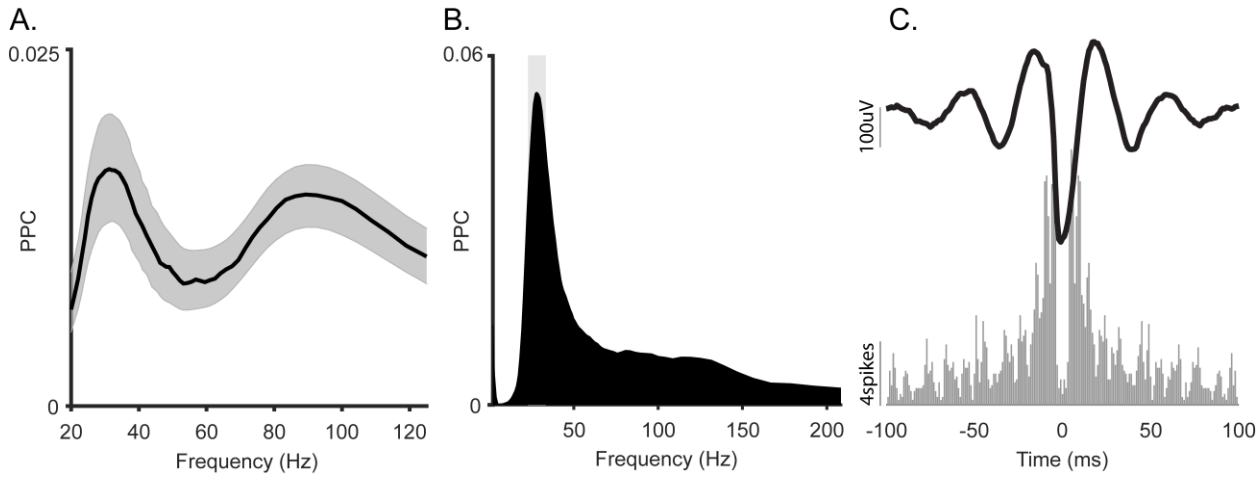

Figure 3-5. Spike-LFP coherence of the slow gamma oscillation in macaque hippocampus.

A. Average spike-LFP coherence in gamma frequency range. Shading shows 95% bootstrap confidence interval. **B.** Spike-LFP coherence for a representative gamma-locked unit. This unit had a significant peak at 30Hz ($p<0.05$, permutation test and Rayleigh test $p<0.05$). **C. Top:** Spike-triggered average LFP of the unit in B. **Bottom**: Autocorrelogram of the same unit.

3.4 Discussion

In this study we evaluated the oscillatory dynamics of primate hippocampus during two general behavioral states: first, during 'online' states of awake active behavior and second, during offline states. The waking-behavior recordings included stationary monkeys who were engaged in memory-guided visual exploration, and freely-moving monkeys exploring their environment. The offline-state recordings included post-task quiescent states in the darkened booth, and the early stages of overnight sleep, respectively. The most prominent oscillation in amplitude and prevalence during alert active behavior was in the beta2 / slow gamma band (~20-35 Hz for stationary search and ~20-50Hz in freely-moving subjects). In contrast, theta-band (3-10 Hz, peak at ~8 Hz) amplitude and bout prevalence were greater during offline states of rest and sleep than during online active states. This bimodal oscillatory profile was also evident in finer temporal scales. Theta and beta2/gamma bands were decorrelated in the cross-frequency amplitude coupling, and in phase-amplitude bicoherence, quite unlike that observed in rodents (Zhou et al. 2019). Spike modulation by LFP frequency was seen in both bands; however, only the theta band effect appeared to be partially due to non-

oscillatory field events, such as the sharp-wave ripple. Despite longer and more prevalent theta oscillations in rest, overall, we found no clear evidence of theta-periodic modulation. This contrasts with the strong and prevalent modulation seen using the same analysis methods applied to signal from the rat in homologous regions of CA1. Across several measures we found consistent or compatible results in the coalescence among frequency bands, and between bands and behavioral states within this study. These patterns differ from well-established spectral-behavioral coupling in rodents.

3.4.4 Dormant theta

In rat and mouse hippocampal LFPs, theta activity (centered at 6-9 Hz) is most consistently present during activated cortical states, i.e., during alert aroused behaviors and REM sleep (György Buzsáki 2002; Vanderwolf 1969; Colgin 2013; Nuñez and Buño 2021). In contrast, theta gives way to sharp-wave ripples and irregular slow activity during quiescence and NREM sleep (G Buzsáki 1989; György Buzsáki 2015). Further, theta 'nests' different frequencies of gamma in a phase-specific manner during these 'active' cortical states(Lasztóczi and Klausberger 2014; Lisman and Jensen 2013; Colgin and Moser 2010; Colgin 2016). And finally, most classes of cells in CA1 are modulated by the theta rhythm(Klausberger et al. 2003; Klausberger and Somogyi 2008; Royer et al. 2010). Indeed, theta is so reliably present and so spectrally dominant in fields, spikes, and intracellular currents during the active states when gamma occurs, that studies of hippocampal gamma oscillations and spikes are commonly conditioned on them.

Monkey CA1 LFPs also show reliable, durable theta oscillations with peak frequencies at 6-9 Hz; however, where measured across states, they do not demonstrate the above characteristics of theta. Instead, they show divergent brain-behavior coupling to that seen in rodents. Much of the literature in humans and monkeys has focused on brief epochs of alert, goal-directed behaviors within stationary visual and visuospatial tasks and may therefore be suboptimal for detecting theta oscillations. Yet where rest or sleep have been measured, stronger, more durable theta field-potential oscillations appear during quiescence and NREM sleep (or anesthetized states (Kleen et al. 2021)) than during

alert/task-on states or REM sleep (Bódizs et al. 2001; Moroni et al. 2007; Tamura et al. 2013; Uchida et al. 2001; Cox et al. 2019). Whereas these behavioral-state correlates of field potential oscillations apparently differ by species, local control of unit activity may nevertheless reveal strong underlying rhythmic motifs.

To better understand local modulation, we measured CA1 spiking activity as a function of LFP oscillatory phase. All tested frequencies had at least some units that were preferentially phase locked to them, but the most common preferred frequencies were roughly matching the 3-10 Hz, 20-30 Hz, and 60-150 Hz bands. The lowest band would be consistent with theta modulation of local spiking, which has been reported using a few different methods in humans and macaques. Spike-field coherence in the theta frequency range was seen for microelectrode bundles including microwires in unspecified subregions of the human hippocampus (Rutishauser et al. 2010), and for recording sites estimated to be within the hippocampus proper of the freely-moving macaque (Mao et al. 2021), though in the latter case, the higher gamma bands and delta bands were several times more likely to show SFC. Within the theta band, spurious coherence may arise in response to nonrhythmic deflections (de Cheveigné and Nelken 2019; Aru et al. 2015; Jones 2016; Vinck, Uran, and Schneider 2022), such as the slow components of the SWR which is especially prominent in macaques and human (Hussin, Leonard, and Hoffman 2020; A. A. Liu et al. 2022). Indeed, we found that SWRs (Figure 2-figure supplement 1) disproportionally influenced the 2-10 Hz band (Figure 2B, D, E), whereas the gamma frequency range was largely unaffected. Because SWRs occur infrequently, it was somewhat surprising that SWR removal affected the overall results; however, the population activity during ripples typically includes 2-10x firing rate increases in nearly all cell types (György Buzsáki 2015; Hussin, Leonard, and Hoffman 2020; William E Skaggs et al. 2007; Leonard et al. 2015). As such, each ripple is likely contributing disproportionately to the spike-locked activity. In addition, we know that visual (Katz et al. 2020; Rey, Fried, and Quian Quiroga 2014; Roux et al. 2022) and saccade-elicited ('ERP-like') responses in the hippocampus (Hoffman et al. 2013; Jutras, Fries, and Buffalo 2009; Katz et al. 2022) increase theta-band power without necessarily producing harmonic oscillations. This would presumably only affect the segments from search, not sleep. Future human and monkey hippocampal studies should factor out the contributions

of SWRs and to the same end stimulus-locked transients, when evaluating low-frequency (<10 Hz) oscillations for non-stationary signals and when using methods that do not discriminate oscillations from transient deflections, as with spike-field coherence. The present results found residual coherence, and in addition, the typical duration of sleep theta bouts would well exceed the SWR envelope, (as shown in Video 1 and Figure 1-figure Supplement 4), therefore we consider the observed spectral peaks during rest likely reflect true oscillations and not simply collections of evoked transients.

The spike autocorrelogram is a more stringent measure of oscillatory modulation, not susceptible to LFP spectral analysis artifacts. The <10 Hz range including the theta band failed to show clear examples of theta modulation (Figure 2 supplement 2). This was not simply due to low firing rates: even high firing rate cells, which should include 'theta-on' interneurons, failed to show theta modulation. Indeed, the same analysis applied to units from a homologous region of rat CA1 (Royer et al. 2010) showed a predominance of theta modulation (even after pooling functional cell types). In light of our rest-related theta power and SWR-removed spike-field coherence, this was somewhat surprising, but consistent with the results in free-flying bats (Yartsev, Witter, and Ulanovsky 2011), monkeys (Courellis et al. 2019; Mao et al. 2021) and humans (Qasim, Fried, and Jacobs 2021). In such cases, to observe spike timing regularity to field potentials, the aperiodic – i.e. non oscillatory – slow fluctuations in the LFP must first be warped to 'fit' one another, to create a pseudo-oscillation (Eliav et al. 2018; Mao et al. 2021; Qasim, Fried, and Jacobs 2021; Bush and Burgess 2020). Due to the different criteria used, compared to the theta-rhythmic spiking reported in rodents, the theoretical or computational roles ascribed to the theta oscillations may need to be re-evaluated, or, more precisely defined in terms that do not depend on periodicity.

Slower oscillations, or irregular low frequency components at 1-4 Hz 'delta' band, are more frequently correlated with spatial or associative memory effects (Goyal et al. 2020; Watrous et al. 2013; Vivekananda et al. 2021), leading to the supposition that rodent hippocampal theta is simply faster than in primates (Mao 2022; Jacobs 2014). If our present results were based on two distinct oscillations – the faster 'offline' theta and the slower 'online/memory' delta band – we would have predicted anti-correlations or

segmentation in the power plots into sub-bands. We have yet to see such a segmentation, but we would stress that this remains a candidate for closer inspection. Finer task behaviors might help to uncover this possible alert-behavior correlate. Even if this proves to be the case, it would raise further questions about which bands become considered homologous across species. If 1-4 Hz is envisaged as relating to septal-cholinergic theta in rats, what is the equivalent of the classic 8-Hz theta band in rats? Compounding this problem is a separate 1-4 Hz oscillation that was observed in rat hippocampus (Jesse Jackson et al. 2014; Schultheiss et al. 2020). When trying to consider homology across species, the LFP signals are only proxies for the underlying circuit activity. Identifying the local circuit motif, including receptor-specific neuromodulation in primates (Stewart and Fox 1991) may help differentiate among various low-frequency oscillations and their functional roles across species.

3.4.5 Decoupled gamma

Gamma oscillations in rat and mouse CA1 comprise a wide high-frequency band (initially 40 -100 Hz but more recently 20 or 30 – 100 Hz) known for tight coupling within the theta oscillation (G Buzsáki, Leung, and Vanderwolf 1983; Bragin, Jandó, Nádasdy, Hetke, et al. 1995; Tort et al. 2008; Colgin et al. 2009; Colgin and Moser 2010; I Soltesz and Deschênes 1993). In line with this coupling, gamma shares behavioral state correlates with theta: waking exploratory states and REM sleep. We found that the slower part of the gamma range (<~70 Hz) is decoupled from theta. Consistent with this finding, gamma power is seen as a relatively strong oscillation in monkeys and humans during REM sleep (Cantero et al. 2003; Takeuchi et al. 2015; Tamura et al. 2013; Uchida et al. 2001), as in rodents. Gamma oscillations, when measured, are often associated with hippocampal processing (e.g. memory-guided search (Leonard et al. 2015; Montefusco-Siegmund, Leonard, and Hoffman 2017), and retrieval (Montefusco-Siegmund, Leonard, and Hoffman 2017) or subsequent memory effects (Jutras, Fries, and Buffalo 2009) in monkeys, or spatial coding and memory in rodents. In addition, a band-limited 20-40 Hz oscillation is seen in rodent CA1 (and is synchronized with LEC (Igarashi et al. 2014)) during discrete

item cueing or retrieval such as in olfactory associative place and sequence learning (Allen et al. 2016; França et al. 2014; Lansink et al. 2016; Lopes-Dos-Santos et al. 2018), and when exploring novel environments (França et al. 2021; Trimper et al. 2017). This frequency band is associated with activation of the trisynaptic pathway (DG and CA3, (Lara M Rangel, Chiba, and Quinn 2015; Hsiao, Zheng, and Colgin 2016; Colgin 2016; Fernández-Ruiz et al. 2021)), but is also seen in coherent oscillations between CA1 and LEC (Igarashi et al. 2014) implicating direct, temporoammonic pathways, thus the origin of the observed gamma oscillations in primates will be an important topic for future research.

3.4.6 Gamma and theta coupling

The results of the current study show that theta oscillations are not prominent during awake behavior and do not couple with gamma, and thus, are not a good candidate for structuring possible gamma sub-bands. Although most studies in humans focus on coupling via slower or faster bands outside this range, we note two exceptions that ostensibly find increases in hippocampal theta-gamma coupling associated with active processing in the theta band (Axmacher et al. 2010; Stangl et al. 2021) and a third that included 5-11 Hz, for which the low-frequency-granting signal may have included the alpha band (Roux et al. 2022). Both of the former studies use macro-electrode iEEG with >1 mm contacts and 3-10mm spacing between contacts, along with MR/CT coregistration, which are estimated to be in some regions of the hippocampus proper in only a subset of participants. Thus, any apparent discrepancies to the present findings may involve the inclusion of extra-hippocampal signals, though this would still be interesting to understand. Signal localization notwithstanding, the first study of working memory reported that 6-10 Hz medial temporal lobe theta phase was coupled with gamma oscillations (Axmacher et al. 2010). Although modulation strength was not associated with performance, modulation width predicted reaction time. Pertinent to the state correlates of theta, they show that the intertrial interval - i.e. a potentially offline state - shared a strong modulation, similar to that seen during the memory epoch, except at the

onset of the WM epoch, where intertrial coherence was strongest. In the second study, recording MTL iEEG in ambulating patients, theta power did not increase with movement speed (if anything, it nominally decreased), and search during movement was associated with weaker theta; however, when stationary, some theta modulation was seen and in addition, general theta-gamma coupling was reported between 6-10 Hz and high gamma during movement and 6-10 Hz and a slower gamma when stationary and observing others (Stangl et al. 2021). The effects of eye movement evoked responses on this theta were not reported but saccade-locked increases in reported theta power, thus, it remains unclear what effect saccadic responses may have had on the reported theta gamma coupling. In the third study, using microwires, the most applicable measures to our study produced generally consistent results, including decreased theta and increased gamma power associated with successful associative memory, and no difference in low-frequency spike field coherence for locally measured fields and spikes (Roux et al. 2022). Here, unlike the first study (Axmacher et al. 2010), the modulation of gamma power by peak 5-11 Hz phase was greater with successful memory (hits vs. misses). This might suggest that a theta or alpha oscillation is regulating gamma magnitude; however, the MI measure of phase-amplitude coupling does not require a strong or periodic phase-granting signal to cluster gamma (Tort et al. 2010). Future studies may help to disentangle the role of periodic theta in contrast to saccadic or other evoked response waves, in clustering gamma oscillations during active behaviors. At present, we suggest that gamma oscillations – across species - can nevertheless work as a standalone rhythmic activity to select among inputs by virtue of laminar specificity, including those of other hippocampal fields (e.g. CA3-dentate gyrus) or extrahippocampal areas (e.g. entorhinal cortex).

Our findings offer a hypothesis-generating framework for future analysis in (human and non-human) primate hippocampal physiology. The present results suggest that theta oscillations were not prevalent during search in primates and did not consistently modulate single unit activity, but rather form the strongest oscillatory marker of offline or quiescent states. Instead, beta2/slow gamma oscillations constitute the chief, self-contained oscillation that arises during active exploration in the primate hippocampus and stands as the most likely oscillation for organizing local dynamics during exploration.

Aside from understanding the nature of these cross-species differences, future work may focus on the better-conserved aspects of CA1 activity, including gamma synchrony during exploration, locking of spiking to exploratory movements, and aperiodic spike timing measures that don't require autocoherent oscillations. Despite several surface differences in hippocampal-behavioral coupling across phylogenetic orders, the underlying neural-circuit activity giving rise to these oscillations may yet reveal fundamentally conserved mechanisms.

3.5 Methods

3.5.7 Subjects and task

Two adult female macaques (Macaca mulatta, ‘M1, M2’) were used in the main, visuospatial search experiments whose results are shown in all figures except those of the control task/recordings from Figure 1-figure supplements 3. Data from M1 and M2 have been reported previously (Leonard and Hoffman 2017; Leonard et al. 2015; Hussin, Leonard, and Hoffman 2020). The apparatus, training procedure, and task have also been described previously (Leonard et al. 2015; Leonard and Hoffman 2017), and are summarized briefly here. During search, animals performed a hippocampally-dependent visual target-detection task. In the task, seated, head-fixed monkeys were placed in front of a monitor and were required to identify a target object from nontargets in unique visual scenes presented on a monitor positioned in front of them, and report their selection of scene-unique target objects by holding their gaze on the target region for a prolonged (≥800 ms) duration. Target objects were defined as a changing item in a natural scene image, where the original and changed images were presented in alternation, each lasting 500 ms, with a brief grey screen (50 ms) shown between image presentations. An inter-trial interval (ITI) of 2–20 s followed each trial. The daily sessions began and ended with a period of at least 10 min when no stimulus was presented within the darkened booth and animals could sleep or sit quietly (‘rest’). All procedures associated with this task were conducted with approval from the local ethics and animal care authorities (Animal Care Committee, Canadian Council on Animal Care). Two adult female monkeys (Macaca mulatta, ‘M2’ and ‘M3’) were used in a separate experiment to extend the analysis to include freely-behaving conditions. The search epochs of M2 were observational (identified post-hoc) and of M3 were experimentally controlled. M2 was placed in an enriched environment where she could actively forage, play with toys (manipulanda), walk, climb, self-groom, and groom another animal. Blind raters denoted the times of foraging, walking, and exploratory ‘search’ behaviors. M3 was placed in a testing enclosure equipped with multiple touchscreens around the periphery that presented spatially distributed arrays of objects. To obtain fluid reward the monkey was required to locate and select (touch) designated objects in a global spatial sequence across the

enclosure, thereby requiring visual search, reaches, and walking/climbing during a trial. For M3 search data analysis, we extracted the trial sequence duration + 2 seconds beyond the first/last touches of the sequence which included goal-directed walking but excluded the intertrial intervals containing reward consumption or idle time prior to the animal's approach and trial initiation. For both M2 and M3, rest epochs consisted of 40 minutes of recordings in the housing area during the start of the "night" cycle of the room's automatic lighting system. A total of 18 sessions (M3: 15, M2: 3) were analyzed for both task and rest epochs. All procedures for M3 were conducted in accordance with the approved protocols and authorized procedures under the local animal care authorities (Institutional Animal Care and Use Committee).

3.5.8 Electrophysiological and movement recordings

For monkeys M1, and M2, indwelling bundles of moveable platinum/tungsten multicore tetrodes (96 µm outer diameter; Thomas Recordings) were implanted into the anterior half of the hippocampus and lowered into CA1. In M3 we recorded from an indwelling active multichannel probe on an adjustable microdrive ('Deep Array' probe, beta-test design, Diagnostic Biochips, Inc.). Recording sites were verified with postoperative CT co-registered to pre-operative MRI and using functional landmarks that changed with lowering depth, including the emergence of depth-specific sharp-wave ripples in a unit-dense layer, as described in the previous studies (Figure 1-figure supplement 1, Figure 2-figure supplement 1). Post-explant MRI verified the electrode locations in M1 (Leonard et al. 2015). For the current study, we detected channels within the pyramidal layer based on the strongest amplitude of ripples during SWRs and single unit activity and only used these channels for unit and local field potential (LFP) analyses. LFPs were digitally sampled at 32 kHz using a Digital Lynx acquisition system (Neuralynx, Inc.) and filtered between 0.5 Hz and 2 kHz for M1 and M2. LFPs for M2 and M3 that were used for results shown in Figure 1-figure supplement 2 were sampled at 30kHz using a Cube/Freelynx wireless recording system (Neuralynx, Inc.) to SD card (for rest) or using wireless transmission to the Cheetah acquisition system (for the task). Single-unit activity was

filtered between 600 Hz and 6 kHz, recording the waveform for 1 ms around a threshold-triggered spike event. Spike sorting was performed semi-automatically using KlustaKwik based on wave shape, principal components, energy, and peak/valley across channels. This was followed by manual curation of clusters in MClust (A.D. Redish). We used the 3D accelerometer in Freelynx data acquisition system to record the movement of freely-behaving animal subjects during active search and rest. Angular velocity (AV) traces were recorded at 3kHz and samples were synchronized with the neural recording. For movement detection, we first calculated the vector norm of the 3 AV axes using vecnorm function in MATLAB. Then we thresholded the vector norm to find periods of time when the animal was moving. The threshold was calculated based on the vector norm of AV recordings when Freelynx was placed statically on a flat surface. In addition to the accelerometer data, we used recorded videos to detect animal behavioral states (e.g. sleep).

3.5.9 Sharp wave ripple detection

Sharp wave ripple (SWR) detection was performed on the tetrode channels of M1 and M2 with the most visibly apparent ripple activity using the previously described method (Leonard et al. 2015). Raw LFPs recorded from the tetrode channel were filtered between 100-250 Hz. To determine the SWR envelope, filtered LFPs were transformed into z-scores and rectified, and subjected to a secondary band-pass filter between 1-20 Hz. Events with a minimum amplitude exceeding 3 SDs above the mean with a minimum duration of 50 ms, beginning and ending at 1 SD were designated as potential ripples. High-frequency energy is present for non-SWR events such as EMG and other non-biological noise, though these artifacts are distinct from ripples because the latter are restricted to the regions near the pyramidal layer. For artifact (non-ripple-event) rejection, a distant tetrode channel was selected as a ‘noise detecting’ channel (Talakoub et al. 2016). Events that were concurrently detected on the noise channel and the ‘ripple-layer’ channel were removed from the ripple pool. High gamma (80-120 Hz) and high-frequency oscillations (HFO, 110-160Hz) events were similarly identified, but with the filter criterion

set at 80 –120 and 110 –160 Hz, respectively, and in both cases identifying peaks as those > 1 SD. Duplicate High gamma/HFO and SWR events were labeled as SWRs. Events with a repetition rate <125 ms were considered a single event.

3.5.10 Power Spectral Parametrization and Fitting

To compare the spectral content during search and rest, we selected successfully completed trials lasting longer than 1 second. For rest segments in M1 and M2, we extracted the LFP signals that were recorded before the start of the task and after the end of the task when the animal was in a dark environment in a quiescent or inactive state. For rest segments in M3, we extracted LFP signals recorded during the evening after the task, during the dark cycle of the housing area. We used Welch's method with a 50%-overlapping 1024-sample sliding Hanning window to estimate power spectra for the frequency range of 1 to 150 Hz with a frequency resolution of 0.25 Hz.

To identify spectral peaks and compare between search and rest states, we parameterized power spectra using the method described by Donoghue et al. (2020). This method models power spectra as a combination of the 1/f frequency components (aperiodic) in addition to a series of Gaussians that capture the presence of peaks (periodic components). The model was fit to a frequency range between 1 to 200 Hz with a frequency resolution of 0.5 Hz. Settings for the algorithm were set as: peak width limits: (0.5, 12); max number of peaks: infinite; minimum peak height: 0; peak threshold: 2.0; and aperiodic mode: 'Fixed'.

To assess the statistical significance of the difference in parametrized spectra at each frequency, we used Wilcoxon signed rank test at $p < 0.05$ with FDR correction for multiple comparisons.

3.5.11 20-30 Hz sorted spectral density map:

We estimated the power spectral density using Welch's method described in the previous section to obtain (frequency * PSD segments) matrix. We then sorted the PSD segments based on the mean power in the 20-30 Hz frequency range and normalized each segment by dividing it by its median. We clustered all sorted segments into 50 total segments of equal size (frequency * 50 segments) by averaging original PSD sorted segments. We repeated this procedure across sessions and animals separately.

3.5.12 Cross-frequency Power Correlation

On continuous LFP time-series data, Welch's method with a 50%-overlapping 1024-sample sliding Hanning window was used to estimate the spectrogram for the frequency range of 1 to 150 Hz with a frequency resolution of 0.25 Hz.

We computed the pairwise correlation between cross-frequency power using the following formula (Masimore, Kakalios, and Redish 2004):

$$corr_{ij} = \frac{\sum_k (S_k(f_i) - \overline{S(f_i)})(S_k(f_j) - \overline{S(f_j)})}{\sigma_i \sigma_j}$$

where $S_k(f_i)$ is the PSD at the frequency f_i in time-window k, $\overline{S(f_i)}$ the averaged PSD at the frequency f_i overall sliding window, σ_i the standard deviation of the PSD at the frequency f_i, and k ranges over all sliding windows. In M3 this procedure was applied to the data segments extracted during task performance.

To test the null hypothesis that the power spectral time series of two different frequencies, f_i and f_j , are not coupled in the data, we performed a non-parametric surrogate data method with cluster-based multiple comparison correction (Thammasan and Miyakoshi 2020). This method preserves the original data's statistical properties while generating time series that are randomized such that any possible nonlinear coupling is removed. In this method, we randomized time-window k differently for each frequency bin to build surrogate time-frequency time series' and computed the surrogate cross-frequency power correlation. This process was repeated 5000 times to produce distributions for the

dataset in which the null hypothesis holds. The original, non-permuted data are then compared to the surrogate distribution to obtain uncorrected p-values. The significance threshold was selected to be 0.05. For cluster-based multiple comparison correction, all samples were selected whose p-value was smaller than 0.05. Selected samples were then clustered in connected sets based on their adjacency and the cluster size was calculated. This procedure was performed 5000 times to produce the distribution of cluster sizes. If cluster sizes in the original correlation matrix were larger than the cluster threshold at 95-th quantile, they were reported as significant. We performed this statistical procedure at the level of single channels per animal. We consider as robust significance those areas that were significant for at least 80% of all samples.

3.5.13 Hilbert amplitude envelope correlation

We applied a 3rd order Butterworth filter at each frequency of the LFP with a 2Hz bandwidth. We then Hilbert transformed the bandpass-filtered LFP and estimated the continuous amplitude envelope. We computed the pairwise correlation between cross-frequency amplitude envelope using previously described correlation method.

3.5.14 Bicoherence

For Bicoherence, we used the HOSA toolbox. Bicoherence was estimated for frequencies f_1 (1 to 75 Hz) and f_2 (1 -150 Hz) in steps of 1 Hz according to the following formula (Bullock et al. 1997):

$$B(f_1, f_2) = \frac{|\langle F_t(f_1)F_t(f_2)F_t^*(f_1+f_2)\rangle_t|}{\langle|F_t(f_1)F_t(f_2)F_t^*(f_1+f_2)|\rangle_t}$$

Where $F_t(f)$ is the signal's time-frequency transformation at time t, | | represents the absolute value, and ⟨ ⟩ is the average over time. We set the segment length to 1024 samples for this analysis.

Bicoherence has a higher spectral resolution for disentangling harmonic from non-harmonic cross-frequency coupling. Additionally, bicoherence relaxes the artificial spectral constraints introduced by conventional PAC, corrects for its poor biases, and accounts for asymmetry in the rhythms (Sheremet, Burke, and Maurer 2016; Kovach, Oya, and Kawasaki 2018; Giehl, Noury, and Siegel 2021).

Theoretically, the bispectrum is statistically zero for linear systems with mutually independent Fourier coefficients. For nonlinear systems, the bispectrum will exhibit peaks at triads (f_n, f_m, f_{n+m}) that are phase correlated, measuring the degree of three-wave coupling (Sheremet, Burke, and Maurer 2016). In practice, however, bicoherence has a positive bias The background activity of LFP signals can be estimated by properties of red noise which can then be used for significance testing (Torrence and Compo 1998; Bédard and Destexhe 2009). To calculate the statistical significance of the local autobicoherence, we generated red noise with the same length of our original signals and computed Bicoherence for the red noise sample. We repeated this procedure 5000 times to obtain the null distribution. We then compared the original data to the null distribution to obtain uncorrected p-values, thresholded for significance at 0.05. We then performed cluster-based multiple comparison correction as described in the Cross-frequency Power Correlation section.

3.5.15 Detection and prevalence of transient oscillatory events

We used the BOSC algorithm (Hughes et al. 2012; Caplan et al. 2001) to detect transient bouts of heightened frequency-specific power using a joint amplitude and duration thresholding procedure. A specific concern we wished to address was that the 1-s windowed power spectral method may result in false negatives (i.e. missing brief theta epochs) therefore we set a maximally-permissive duration threshold of three cycles, and an amplitude threshold using 6th order wavelets passing the 95th percentile of model fit distributions. From these detected events, we computed the occupancy rate using the formula:

$$Occupancy\ rate\ (\%) = \frac{Total\ duration\ of\ detected\ events}{Duration\ of\ the\ original\ signal} \times 100$$

Occupancy rate is a measure of prevalence, showing the percentage of time spent in an oscillatory event of a specific frequency, also referred to as $P_{episode}(f)$.

The BOSC algorithm provides a logical matrix of the form [number of frequencies * timepoint] where values are 1 when an event was detected and 0 otherwise. For bout duration distributions we summed values across frequency ranges of interest and then performed the logical operation larger than 1, thus in MATLAB it will be, where detected is the BOSC output:

```
thresholded = sum(detected(ThetaRange,:))>=1;
```

We found start (thresholded switches from 0 to 1) and stop (thresholded switches from 1 to 0) of events and removed events that were incomplete, only had one start or stop, and computed duration. We then fitted a kernel probability distribution to the duration values using fitdist function in MATLAB. We used bandwidths of 50 and 10 for theta and gamma oscillations respectively.

3.5.16 Spike-Field Synchronization

To quantify spike-field synchronization, we used fieldtrip toolbox (MATLAB) to compute pairwise phase consistency (PPC) which is unbiased by the number of spikes (Vinck et al. 2010). Raw continuous recordings were resampled with a 1000 Hz sampling rate. The spectral content was estimated with a frequency-dependent Hanning window with 5 cycles per frequency and a frequency resolution of 1Hz. All detected spikes of a unit during the session were included. To assess the statistical significance of spike-field synchronization, we first used a non-parametric permutation test with minimal assumptions. In this procedure, the distribution of PPC values was estimated from 1000 iterations of shuffled spike times of each cell. We used the PPC distribution of shuffles to compute the PPC threshold for significance at each frequency. We applied a threshold of uncorrected $p < 0.05$ to determine the significant synchronization at each frequency. Only

PPC values that exceeded the statistical threshold and had a Rayleigh test $p<0.05$ and a minimum peak and peak prominence of 0.005 were reported as significant. To obtain the probability distribution of observing significant PPC values at a frequency, we fitted a kernel probability distribution to significant frequency values using fitdist function in MATLAB. We used a bandwidth of 4.

To compare spike-field synchronization during SWRs, we extracted spikes inside a 600ms window centered around the SWR events and computed PPC [PPCSWR]. These spikes were then excluded from the unit spike timestamps and PPC was calculated for the remaining 'residual' spikes [PPCresidual]. PPCSWR was then compared with PPCresidual. Only cells with at least 20 spikes during ripple time windows were included in this analysis.

To test the significance of differences in spike-field coupling within SWR epochs or excluding them, on a per-unit basis, spikes were randomly selected and assigned to SWR and residual conditions. In this random selection, spike counts were controlled to correspond to the original condition. We performed the random selection 1000 times and measured the difference between PPC in each iteration to obtain the null distribution. Then, we grouped frequencies into 5 bands 2-3, 4-10, 11-20, 21-40, 41-100, 101-200 Hz. In each frequency band, we found the peak frequency at which the absolute PPC difference was largest and only tested these for significance. If the p-value of the PPC difference was less than 0.05 (two-tailed) after FDR correction, it was labeled as significant.

3.5.17 Theta modulation index (TMI) Estimation

We used the method described by Royer et al. (2010) to quantify the degree of theta modulation in single units. For all units, we first computed the autocorrelogram of the cell, in 10 ms bins from -500 to +500 ms, normalized to the maximum value between 100 and 150 ms (corresponding to theta modulation), and clipped all values above 1. We only

included autocorrelograms with at least 100 counts for further steps (N=240 units). We then fit each autocorrelogram with the following function:

$$y(t) = [a(sin(\omega t) + 1) + b] \ * \ \mathrm{e}^{-|t|/\tau_1} + c \ * \ \mathrm{e}^{-t^2/\tau_2^2}$$

Where t is the autocorrelogram time lag from -700 to 700ms, and $a - c$, ω, and τ_{1-2} were fit using the $fminsearch$ optimization function in MATLAB. The theta indexes were defined as the ratio of the fit parameters a/b. For best-fitting performance, we restricted possible values for ω to (4, 10), for a and b to non-negative values, for c to (0, 0.2), and for τ_2 to (0, 0.05).

3.5.18 Additional single unit datasets

To generate example plots of theta rhythmic cells (Figure 3), recordings from the Buzsáki laboratory were included (https://buzsakilab.nyumc.org/datasets/).

3.5.19 Acknowledgments

The authors wish to thank A. Maurer for thoughtful comments on the manuscript and W. Zinke and I. Hayes for technical support for the wireless recordings. This work was funded by the Krembil Foundation, Brain Canada, NSERC, the Whitehall Foundation, NEI P30EY008126, and NIH R01 NS127128.

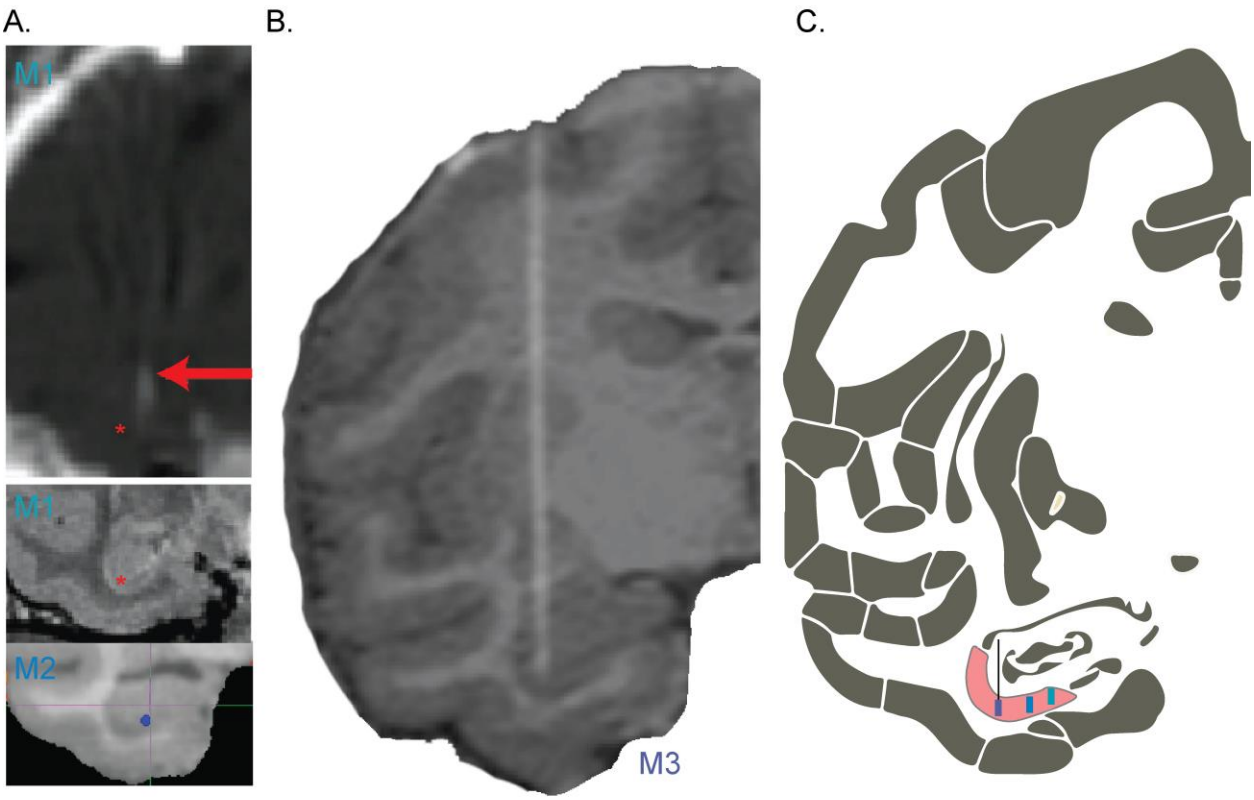

Figure 3-6. Supplement 1. Electrode localization.

A. Coronal MR and CT images of hippocampal electrode trajectories. CT image of implanted electrode bundle (top) shows the electrode tracts (white puff, red arrow) with deepest electrodes targeting CA1, confirmed in post-explant MR and via functional localization to the pyramidal layer (middle, M1). Red asterisk shown laterally displaced at the depth of probe tip, for visibility. Bottom shows the location of the electrode tip from the CT image placed in a coronal plane of the coregistered MR image for M2. B. Coronal view of CT-MR coregistered image showing the location of the electrode for M3. C. Schematic coronal slice showing the location of the CA1 subfield in the hippocampus (pink) with M1, M2, and M3 probe locations from right to left, collapsing across the coronal slab for visualization. Features were adapted from the Saleem and Logothetis atlas (2012). All electrodes used in this study were chronically implanted and individually micro-adjusted in depth to the pyramidal layer.

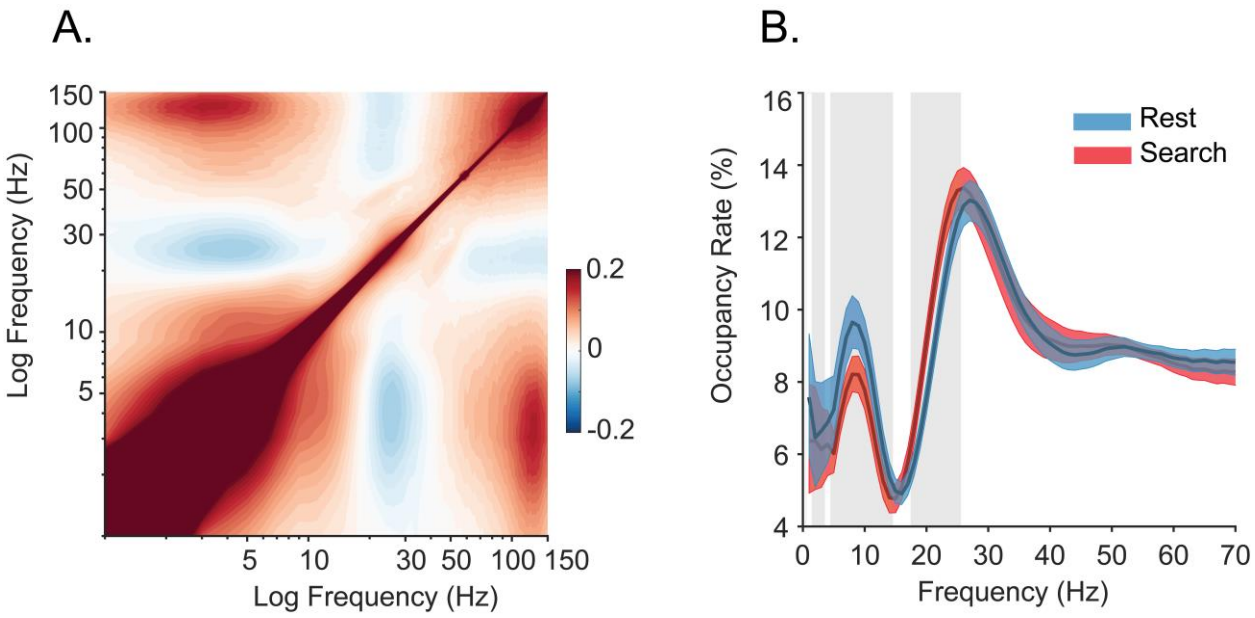

Figure 3-7. Supplement 2. Spectral strength and coupling using alternate analysis methods.

A. Cross-frequency pairwise correlation of Hilbert (amplitude) envelope (N = 42 sessions), which is sensitive to finer temporal coupling resolution than that of the methods used in the main Figure 1. The spectral correlation structure is preserved even at finer temporal resolution. B. Prevalence of frequency-specific bouts during search (red), and rest (blue) with shaded 95% bootstrap confidence intervals (N = 42 sessions, $p<0.05$, Wilcoxon signed rank test, FDR corrected). Occupancy rate is the percent time spent in a detected bout of the specified frequency (also called 'Pepisode').

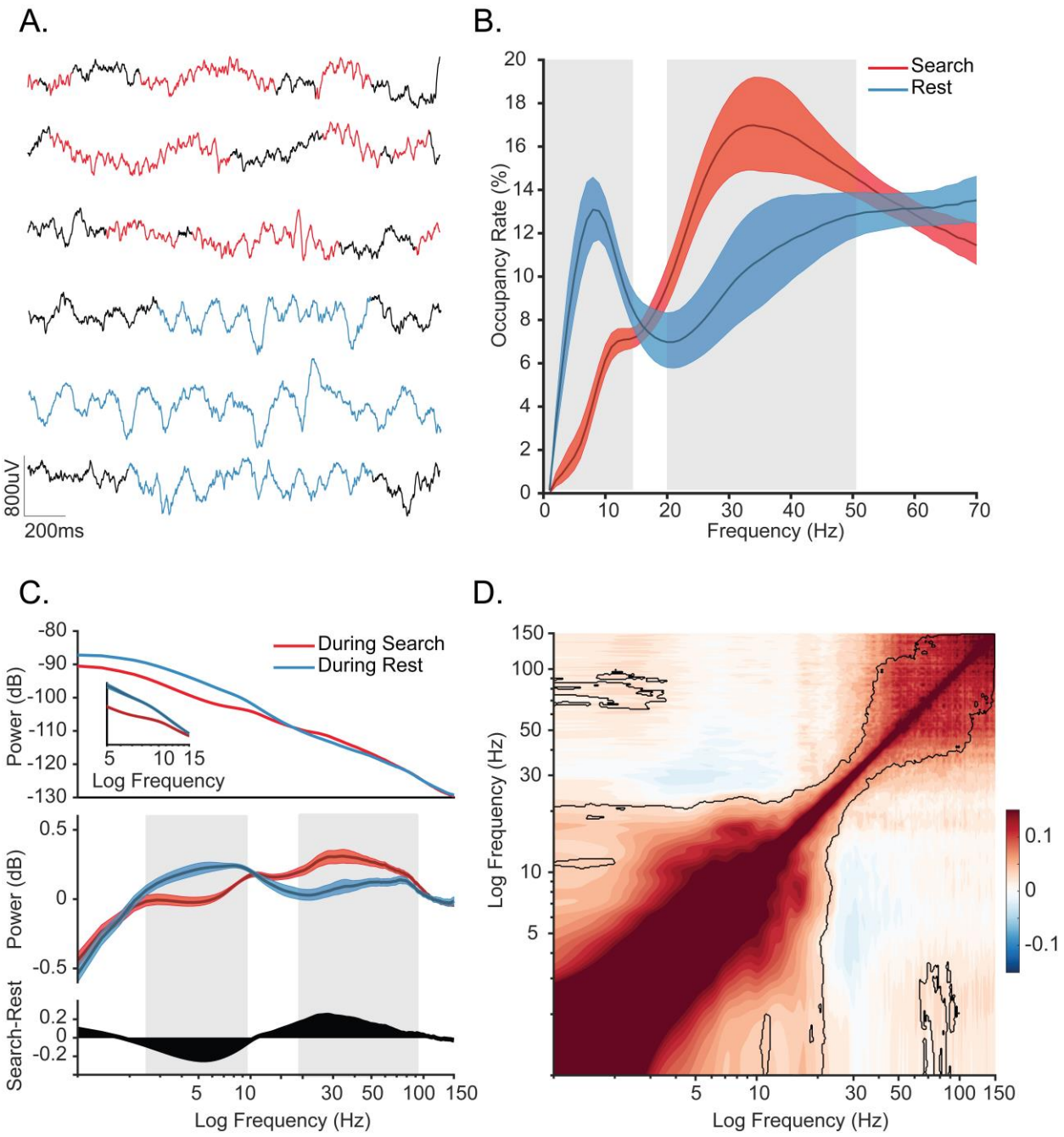

Figure 3-8. Supplement 3. Oscillatory decoupling in CA1 of freely-behaving monkeys

A. Example detected oscillations in 4-8 Hz and 25-40 Hz frequency bands during awake, free behavior (red), and sleep (blue) shown on the wideband LFP in CA1. B. Prevalence of frequency-specific bouts during search (red), and rest (blue) with shaded 95% bootstrap confidence intervals (N = 18 sessions, $p<0.05$, Wilcoxon signed rank test, FDR corrected). C. Top. Mean power spectral density during search (red), and rest (blue). Inset: mean power for low frequencies of the main plot, with shaded 95% bootstrap confidence interval (N=18 sessions). Middle. Power spectral density after fitting and subtracting the aperiodic 1/f component during search and rest, with shaded 95% bootstrap confidence intervals. Gray areas show significant differences in power across behavioral epochs ($p<0.05$, Wilcoxon signed rank test, FDR corrected) Bottom. Power difference between search and rest. D. Average cross-frequency power

comodulogram (N=18 sessions). Dark outline represents areas that were significant in at least 80% of samples ($p < 0.05$, cluster-based permutation test corrected for multiple comparisons).

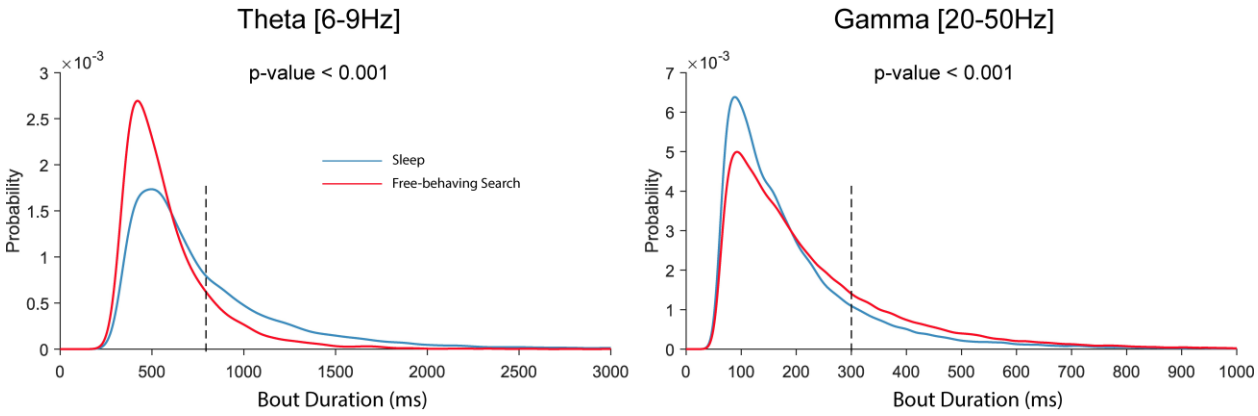

Figure 3-9. Supplement 4. Relative probability distribution of bout durations.

Left Distribution of detected bout durations for theta (6-9 Hz) oscillation. Red, and blue show distribution for detected bouts during active search and offline behavioral states respectively ($p<0.05$, Wilcoxon signed-rank test). For reference, the black dotted line indicates 800ms, which reflects ~3-6 cycles at 4-8 Hz and is more than twice the duration of the slow SWR components (see Figure 2-figure supplement 1). Right same as the left plots but for gamma oscillations (20-50 Hz). The black dotted line indicates 300ms, indicating durations that would exceed two typical 8-Hz cycles. The lower end of the duration distribution is bounded by the duration threshold in the BOSC algorithm.

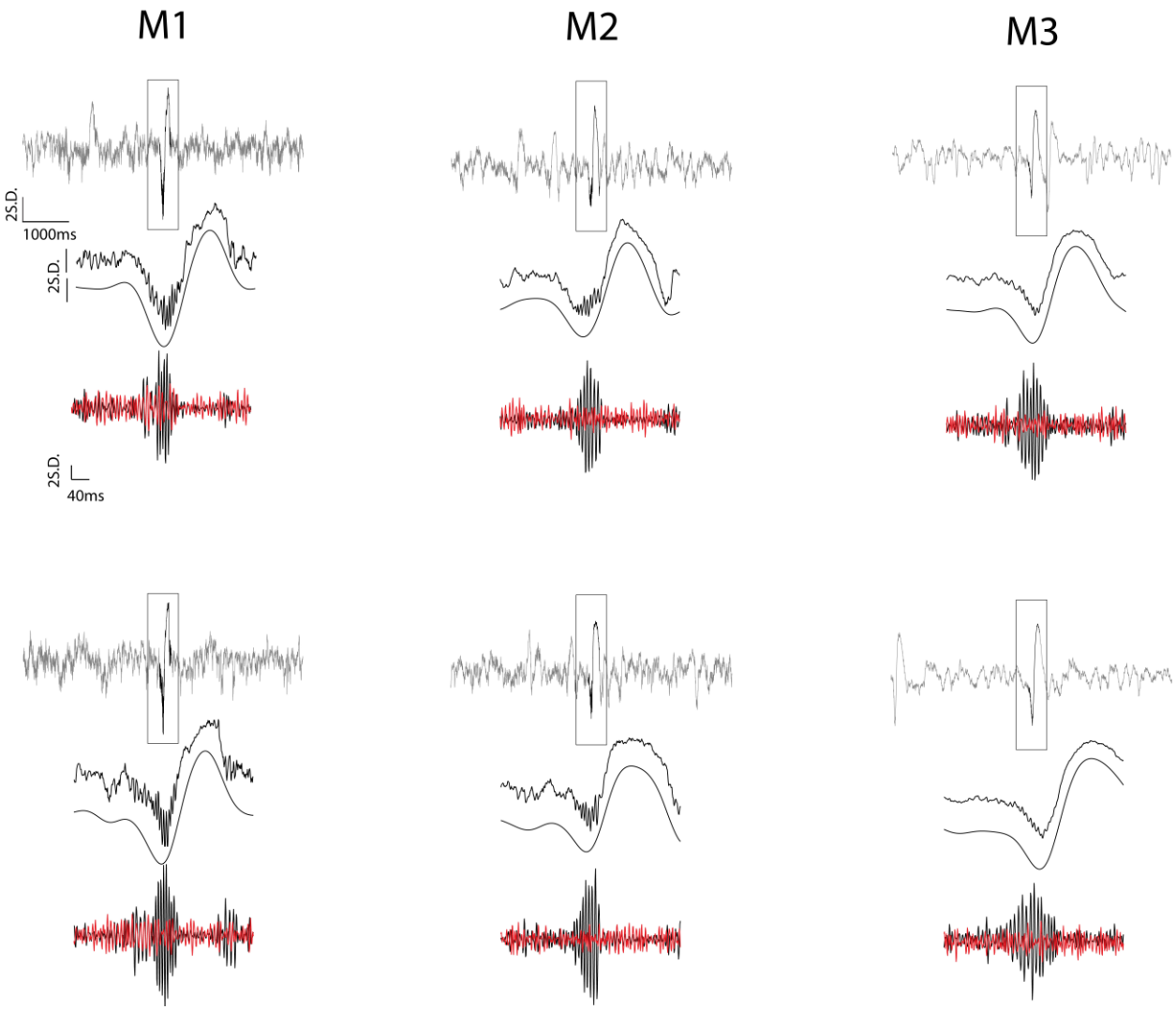

Figure 3-10. Supplement 5. Examples of detected ripple events.

For each example, the first row shows 6 seconds of z-normalized broadband signal centered at a ripple peak. The second row illustrates the zoomed-in (400 ms) broadband LFP locked to the ripple peak and the narrow-band (<10 Hz) filtered signal. Note this large amplitude deflection accompanying ripples contains aperiodic spectral energy in the theta band. The third row shows a bandpass (100-250 Hz) filtered trace of the ripple (black) and of a simultaneously-recorded signal from a hippocampal channel outside the layer (red), revealing the spatial localization of the ripples. The distant channels were used during ripple detection, to selectively remove high-frequency noise that shares the ripple frequency band, but that are apparent across channels due to volume conduction.

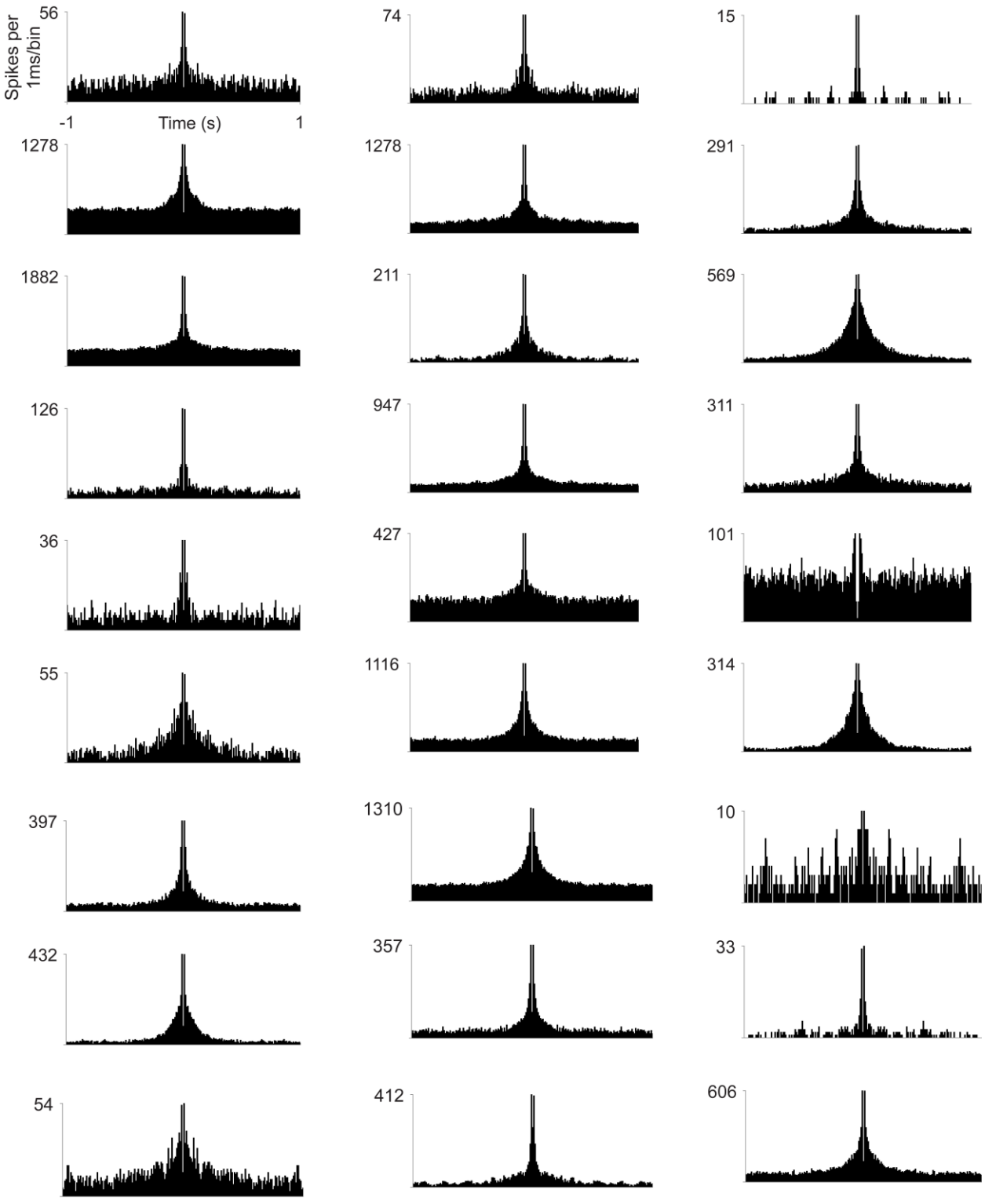

Figure 3-11. Supplement 6. Spike-train autocorrelograms of example hippocampal cells.

Examples were selected to represent different baseline firing rates. Note the absence of any clear temporal modulation in the theta range, including higher firing rate cells that are predicted to show the strongest modulation. Bin size = 1 ms.

4. Chapter 3: State-dependent circuit dynamics of superficial and deep CA1 pyramidal cells in macaques[3]

4.1 Abstract:

A great diversity of neuron classes in CA1 has been identified through their heterogeneous cellular/molecular composition. It is unclear how this cellular diversity relates to the hippocampal network dynamics that support behavior in primates. Here we report a range of functional cell groups in macaque CA1 with distinct firing profiles relative to the spectral phase preferences of pyramidal cells. Within the pyramidal cell layer, superficial and deep pyramidal cells showed robust differences in their firing rate, burstiness, and sharp-wave ripple associated firing. Most notably, these subtypes of pyramidal cells have differential interactions with the inhibitory cell groups. Furthermore, we detected cell assemblies in the macaque hippocampus for the first time and show that the laminar position of pyramidal cells is a major organizing principle of CA1 assembly dynamics. These results suggest a sublayer-specific circuit organization in the macaque hippocampal CA1 that may support dissociable contributions across cognitive and behavioral processes in the primate.

4.2 Introduction

Circuit dynamics specific to the hippocampus govern its role in navigation, memory, and social/motivational behaviors across species (H Eichenbaum et al. 1999; Colgin 2016; Michael E Hasselmo 2005; Oliva, Fernandez-Ruiz, and Karaba 2023; He, Wang, and McHugh 2023; G Buzsáki, Leung, and Vanderwolf 1983; György Buzsáki and Moser 2013). Based on studies in rats and mice, these dynamics arise from a well-described and diverse range of cell classes (Harris et al. 2018; Franjic et al. 2022; T F Freund and Buzsáki 1996; Klausberger et al. 2003). For example, the pyramidal cell layer is organized into radial strata (Slomianka et al. 2011), each receiving distinct afferents

[3] This chapter is adapted from State-dependent circuit dynamics of superficial and deep CA1 pyramidal cells in macaques available on bioRxiv and has been reproduced with the permission of my co-authors KL Hoffman.

(S.-H. Lee et al. 2014; Masurkar et al. 2017; Valero et al. 2015; Kohara et al. 2014), bearing different intrinsic and task-related response characteristics (Mizuseki et al. 2011; Valero et al. 2015; Geiller et al. 2017; Sharif et al. 2021; Danielson et al. 2016; Gu et al. 2023; Harvey et al. 2023; Berndt et al. 2022), and projecting to different target structures (Harvey et al. 2023; Slomianka et al. 2011). The dynamics of these pyramidal cells are precisely regulated by inhibitory cell classes (Klausberger and Somogyi 2008; Pelkey et al. 2017; T F Freund and Buzsáki 1996) that differ from each other in their behaviorally-specific firing patterns and roles in shaping network oscillations (Klausberger et al. 2003, 2005; Lasztóczi and Klausberger 2014; C. Varga, Golshani, and Soltesz 2012; Dudok, Klein, et al. 2021; Forro and Klausberger 2023). Because these cell classes differently segregate pyramidal cell assembly patterns in space and time (Dudok, Klein, et al. 2021; Dupret, O'Neill, and Csicsvari 2013; McKenzie 2018) they may be fundamental determinants of the role of these assemblies in memory and navigation.

Although many aspects of hippocampal physiology are conserved between rodents and primates, differences in oscillatory dynamics (Abbaspoor, Hussin, and Hoffman 2023; Talakoub et al. 2019; Leonard et al. 2015; Green and Arduini 1954; Tamura et al. 2013; Bódizs et al. 2001) and behavior-specific modulation (Mao et al. 2021; Gulli et al. 2020; Courellis et al. 2019; Rolls 1999; Ringo et al. 1994; "Unable to Find Information for 13050334," n.d.) suggest there may be phylogenetic specializations that an understanding of the underlying functional cell composition may uncover. A first-pass bisection of hippocampal (and medial temporal lobe) cells in primates into putative inhibitory and excitatory classes (or four groups: (Hussin, Leonard, and Hoffman 2020)) reveals characteristic responses at both the circuit-level (William E Skaggs et al. 2007; Leonard et al. 2015; Le Van Quyen et al. 2008) and cognitive/behavioral levels (Katz et al. 2022; Ison et al. 2011). Yet a more fulsome description of primate CA1 functional cell types, that can bridge what is known from anatomy and rodent physiology to circuit function and behavior, remains lacking. To gain a better understanding of the degree of functional conservation in the hippocampal CA1 region, we sought to identify potential functional cell types, delineating their characteristic laminar and spectral profiles during active wakefulness and sleep. Additionally, we describe CA1 pyramidal cell activity in primates along their previously-unexplored superficial and deep strata, including basic

physiological responses, pairwise activity among the pyramidal groups and relative to putative inhibitory cell groups, and finally, in relation to network properties including oscillations and synchronized assemblies of activity.

4.3 Results

4.3.1 Identification of functional cell groups in laminar recordings of freely-behaving macaque CA1

We recorded from hippocampal CA1 layers in two freely-behaving macaques, as they performed a sequential memory task and during rest/sleep (Figure 1, A and B). Across 35 daily sessions (M1: 17 sessions, M2: 18 sessions) we measured the local field potentials and activity in ensembles of units. To align recording depths across these sessions and animals, we calculated for each session the current source density (CSD) during sharp-wave ripple (SWR) events. SWRs are known to evoke sinks in the Stratum Radiatum and sources in the Stratum Pyramidale layers of CA1 ((A. A. Liu et al. 2022); Figure 1C). Within this region, we found the slope of the slow component of sharp-wave ripples, which crossed zero across all sessions and animals, and we aligned to that zero-crossing. To validate that alignment, we measured ripple power, which peaks within the central region of the pyramidal layer. We found maximal power just below the zero crossing, consistent with the anatomy of the pyramidal cell layer in macaques (Figure 1C). After identifying single unit activity typically consisting of waveforms across several adjacent channels (Figure 1B), we selected the electrode contact with the largest spike amplitude for each unit as the best estimate of the location of the cell body. This reduced some of the known within-cell variability in waveshape. The regular linear distribution of these recording sites on the probe shanks allowed us to determine the relative depths of the cell bodies of the simultaneously-recorded neurons (Figure 1D).

We classified various cell groups with a semi-supervised approach according to their normalized waveform (E. K. Lee et al. 2021; Trainito et al. 2019) and their interspike interval (ISI) distributions, to capture several of the principal intrinsic physiological characteristics that differ by cell type. This led to 10 separate cell groups (Figure 1D, see Methods; overall between-group distances exceeded within-group distances: $p < 0.001$, Kruskal-Wallis, Figure S1A). We use the term “cell groups” throughout to refer to these 10 clusters, and note that these groups are clustered based on extracellular physiological features only, and thus may differ from the formal “cell classes” or “cell types” as identified through molecular/immunohistochemical methods or cytoarchitectonics.

The incorporation of the ISI distributions as features along with spike waveforms, qualitatively drew out cells with bursting activity, low-firing rates, and broad waveforms, characteristic of pyramidal cells (J Csicsvari et al. 1999a; Ranck 1973). These comprised the first cell group (Figure 1D, far left, black, notably well-localized to the ripple layer i.e. Stratum Pyramidale). The other negative-deflecting groups were therefore considered putative inhibitory cells, because pyramidal cells are the only excitatory cell class in CA1. As expected from these features, firing rates of these cell groups differed ($p<0.001$, Kruskal-Wallis, Fig. 1D, Figure 1D and S1C inset); and in addition, 3 neuron types selectively decreased firing during sleep compared to waking behavior ($p<0.001$, permutation test, Figure S1B). The ISI-conditioned coefficient of variation, CV2, measures the intrinsic variability of local spiking intervals, irrespective of global firing rate changes like those seen across behavioral epochs (Holt et al. 1996). As expected, cell groups also showed differences in CV2 ($p<0.01$, Kruskal-Wallis test with post-hoc permutation test FDR corrected, Figure S1C), leading to distinct, cell group-characteristic joint ISI histograms (Figure S1D).

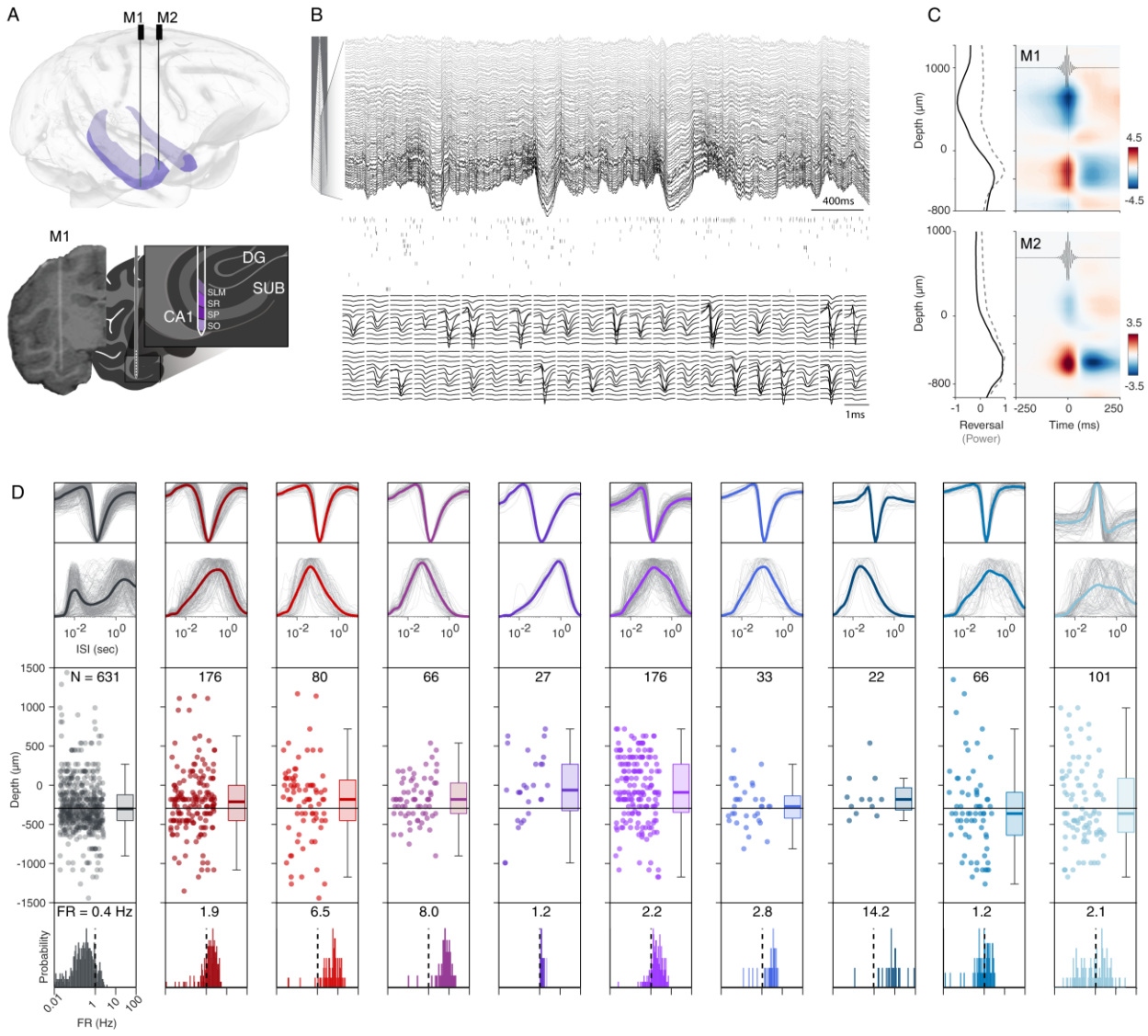

Figure 4-1. Single units from macaque CA1 characterized by depth and physiological parameters.

(A) Top: schematic rendering of the electrode arrays localized to anterior hippocampal CA1. Dark purple: CA1. Bottom: Coronal view of the CT coregistered to MR for one electrode trajectory, targeting the hippocampal CA1, and schematic of hippocampal CA1 layers.

(B) Top: LFP traces across 64 of 128 recorded channels (40 micron spacing) spanning different layers of hippocampal CA1. Middle: Spike raster of simultaneously recorded neurons (N = 48). Bottom: Example spike waveforms for selected units from this recording.

(C) Top, left: Ripple slope reversal (black) and ripple power (light gray) across channels (depth). Top, right: Current source density of average ripple LFP (blue: sink, red: source). Bottom: The same as top but for the 2nd animal.

(D) 1st Row: Mean (colored) and individual (gray) waveforms (1.5 ms) for different cell groups. 2nd Row: Mean (colored) and individual (gray) ISI distributions (0-10 s) for different cell groups. 3rd Row: Estimated depth of units aligned to ripple reversal (0 µm, $p < 0.001$, Kruskal-Wallis) and superficial-deep pyramidal split (black horizontal line, -330 µm). N= number of units per group. 4th Row: Distribution of overall firing rates (Hz; $p < 0.001$, Kruskal-Wallis), dashed line at 1Hz.

4.3.2 Spectrolaminar profiles and spike-phase coupling by cell group

To better understand oscillatory composition across layers, we computed aperiodic-corrected power spectra (Figure 2A). Despite inter-subject differences in absolute peak frequencies across the spectrum, both subjects showed reduced theta-band power (5-10 Hz) during active wakefulness in comparison to rest or early sleep overnight, across all recorded channels (Figure 2A, $p<0.05$, cluster-based permutation test), in line with previous studies (Talakoub et al. 2019; Abbaspoor, Hussin, and Hoffman 2023; Leonard et al. 2015). Furthermore, the contrast with active wakeful states showed increases peaking in the pyramidal layer in the mid frequencies of 15-40 Hz (Figure 2A), and each animal had a preferred higher gamma band apparent during active waking (Figure S2A). These general profiles were also evident in the spike-phase coupling across units, measured as the pairwise phase consistency (PPC; Figure 2B and Figure S2B). Comparing across states, spike-field coherence within the theta frequency range (5-10 Hz) was greater during sleep ($p<0.05$, two-sample permutation test) seen across all cell groups (Figure S3B). Conversely, spike-field coherence in the slow (25-35 Hz) and higher (50-75 Hz) gamma ranges were significantly higher during wakefulness (Figure 2B, $p<0.05$, two-sample permutation test), across cell groups, though with differing gamma-band peaks (Figure S3B).

Focusing only within band-limited bouts of high power, cells showed a generally large bandwidth, showing significant phase-locking to, on average, 4.4 of the 8 frequency bands. The grand mean phase angle per cell group revealed that these groups typically clustered within a limited range of preferred phases (~90 degrees) that shifted by frequency (Figure 2C), but nevertheless differed reliably in mean phase-of-firing values for all but the lowest frequencies (Figure S3C, except for 1-4Hz, 4-7Hz, and 7-13Hz, $p < 0.001$, multi-sample Watson-Williams test). Using the pyramidal cell group as a reference, the other cell groups deviated in phase angle as function of frequency and cell group (Figure S2C, S2D; $p < 0.05$, two-sample Watson-Williams). Cells exhibiting significant phase locking ($p<0.001$, Rayleigh test) within each frequency group produced the largest

resultant vectors in the following order: 1-4Hz, (100-180Hz and 4-7Hz), 60-90Hz, (30-60Hz and 20-30Hz), (7-13Hz and 13-20Hz) ($p<0.05$, Kruskal–Wallis test with Tukey-Kramer correction); therefore the strongest global spectral peaks were not necessarily those yielding the strongest phase-locking during band-limited bouts.

4.3.3 Cell type-specific ripple-associated activity

Most cells increased their firing during ripples, across all cell groups ($p<0.05$, one-sample randomization test, figure S2A) though to differing degrees (ripple ratio, during/baseline FR, $p<0.001$ Kruskal-Wallis test, Figure S3B), and with differences in participation rate across ripple events ($p<0.001$ Kruskal-Wallis test, Figure S2B). The pyramidal cell group showed the highest ripple ratios but the lowest participation rate ($p<0.001$, pairwise permutation test, FDR corrected, Figure S2B). Putative inhibitory cell groups showed a striking range of participation probability and timing: some groups' members participated in all ripple events (Figure S2B), and some restricted firing to a specific time relative to ripple peak (Figure S2C; $p < 0.001$, Bartlett's test). A small population of cells had suppressed activity during the ripple, and these were comprised mainly of the inhibitory (non-pyramidal) cell groups ($p < 0.05$, one-sample randomization test, Figure 2E).

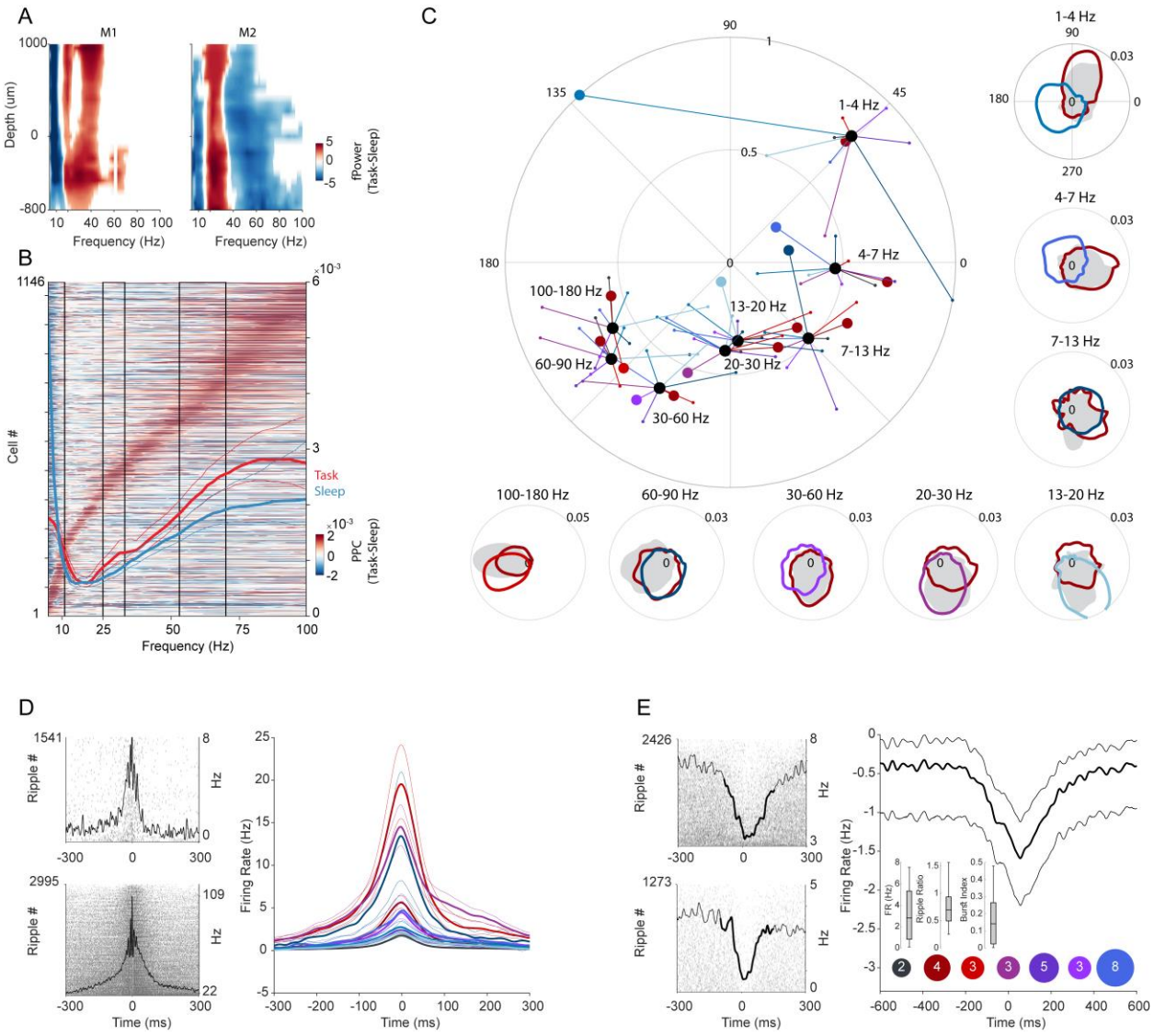

Figure 4-2. Local field potential dynamics and spike-field relationships across cell groups.

(A) Color difference plot of 1/f corrected power spectrum between alert, task-related (red) and rest/sleep states (blue) across depth of recordings for each animal. Color indicates significance ($p < 0.05$, cluster-based permutation test).

(B) Color difference plot of pairwise phase consistency (PPC) between task and rest/sleep states sorted based on preferred frequency. Red lines indicate mean + bootstrap 95% CI for PPC during task. Blue lines indicate mean + bootstrap 95% CI for PPC during rest/sleep. Black boxes indicate frequency ranges with significant difference across states ($p<0.05$, two-sample permutation test with Tmax multiple comparison correction).

(C) Center: Phase plot for grand average phase and resultant vector for different frequency bands. Thick black dots show central tendency of phase locking values across the different cell groups per frequency band. Thick color dots indicate grand mean phase and resultant vector per cell group and frequency band, colored according to cell group. Off-center: Phase plots of selected individual neuron examples in different frequency bands. Examples are colored according to group membership; gray = group 1.

(D) Right: Lines show mean + bootstrap 95% CI for baseline-corrected ripple-associated activity for ripple-activated neurons ($p < 0.05$, one-sample randomization test) in different cell groups. Left: Example raster and PETHs of individual neuron activity during ripple.

(E) Right: Lines show mean + bootstrap 95% CI for baseline-corrected ripple-associated activity for ripple-suppressed neurons ($p < 0.05$, one-sample randomization test) in different cell groups. Left: Example raster and PETHs of individual neuron activity during ripple.

4.3.4 Stratification into superficial and deep CA1 pyramidal cells reveals physiological heterogeneity

To extend findings from the rodent literature, we examined whether CA1 pyramidal cells recorded in different depths of Stratum Pyramidale differ in their spiking properties and circuit-level dynamics. For each session, cells in the 'Pyramidal' group (meeting firing rate and burst criteria), were median split according to depth, creating the CA1sup group (closer to Stratum Radiatum) and the CA1deep group (closer to Stratum Oriens). Compared to CA1deep cells, the firing rates of CA1sup cells were higher overall and during ripples, and they had a greater CV2 (Figure 3A-3C, Figure S1C; $P < 0.05$, permutation test), though they were less 'bursty' than their deeper peers (Figure 3B; $P < 0.001$, permutation test).

To investigate whether these cells interact differently, either within their subgroups, or in their coupling with the inhibitory groups, we analyzed their pairwise co-firing statistics. We found that pyramidal cells of the same sublayer were more likely to fire together compared with cells of different sublayers (Figures 3D), and they showed differences in co-firing strength with several of the inhibitory cell groups ($p<0.001$, permutation test; Figure 3E). The finer-grained temporal dynamics revealed greater detail in these interactions: baseline-normalized cross-correlograms (CCGs) also showed preferential within-sublayer firing ($p<0.01$, two sample permutation test with Tmax correction, Figure 3D), and among the inhibitory groups, CA1sup and CA1deep differed in their lead/lag spike timing and strength ($p<0.01$, two sample permutation test with Tmax correction, Figure 3E). Finally, CA1sup and CA1deep cells have somewhat opposite timing interactions with the ripple-suppressed cells: for CA1deep cells, the interactions peak at 0ms, when

CA1sup cell interactions are near their nadir; CA1sup cells' peak is at approximately 7ms lag ($p<0.01$, two sample permutation test).

During ripples, CA1sup had a higher participation probability and fired more than CA1deep ($p<0.01$ two sample permutation test, Figure 3G). Relative to pre-ripple firing, CA1sup cells they fire more post-ripple compared to CA1deep ($p<0.05$ cluster-based permutation test, Figure 3F). Finally, CA1deep cells are more strongly locked to the ripples and fire at a slight but significant phase advance compared to CA1sup ($p<0.01$ permutation test, $p<0.001$ Kuiper's test, Figure 3G).

4.3.5 CA1 cell assembly membership by strata and cell group

We used unsupervised detection of recurrent co-activity to identify cell assemblies during sleep epochs, using established methodologies (Figure 3J and Figure S4A, Methods). Assemblies that included pyramidal cell contributions were assigned to "within superficial," "within deep," or "across", based on the category membership of those pyramidal cells. Our findings revealed that "within CA1sup" assemblies exhibited significantly stronger activation during ripple events in comparison to "within CA1deep" assemblies ($p<0.05$ cluster-based permutation test, Figure 3I). Furthermore, assembly membership depended on layer, with most having all members belonging to the same sublayer (Figures 3K). Importantly, these results held after accounting for the priors (the observed exceeded expected sampling distributions of eligible cells by layer), and when only considering assemblies detected during balanced sessions, where an equal number of CA1sup and CA1deep cells were recorded (Figures 3K).

A cell's selectivity across assemblies can be defined as the inverse of its participation rate (the proportion of assemblies to which a neuron significantly contributed, divided by all detected assemblies in a session). The majority of cells demonstrated a propensity for participating in specific assemblies, with a mean participation rate of 7% (Figure S4B). Participation varied by cell group (Figure S4C, $p<0.001$, Kruskal-Wallis test), and considering the firing rates of these groups, this effect was not otherwise accounted for

by the overall negative correlation between the firing rate of neurons and their participation rate (p<0.001, t-test Figure S4D).

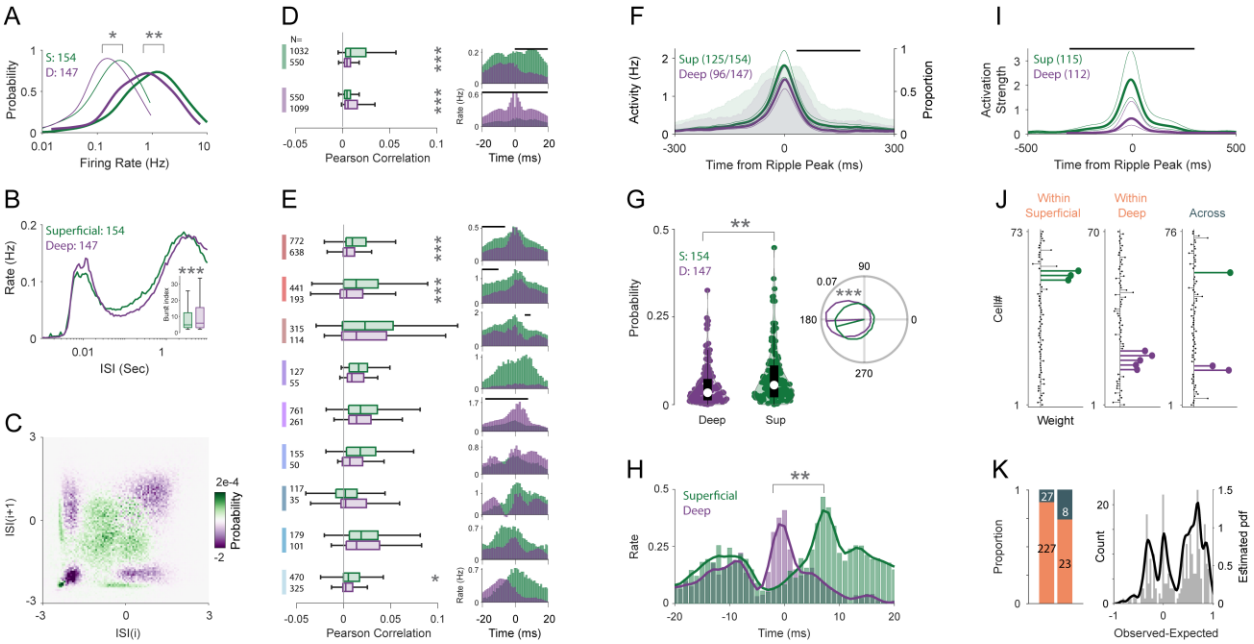

Figure 4-3. Sublayer-specific circuit dynamics of hippocampal pyramidal cells in macaque CA1.

(A) Overall (thin lines) and ripple (thick lines) firing rate distribution for superficial (green, N= 154) and deep (purple. N= 147) pyramidal cells.

(B) Mean ISI distribution. Inset: burst index distribution.

(C) Difference (Sup-Deep) plot of joint probability density of previous ISIs versus next ISIs.

(D) Left: Pairwise cofiring of sup/deep pyramidal cells with other pyramidal cells of within and across groups. Right: Mean cross-correlograms of sup/deep pyramidal cells. Mean CCG values from -50 to -20ms were subtracted from all bins. Black lines indicate significant difference (p<0.05, two-sample permutation test with Tmax multiple comparison correction).

(E) Left: Pairwise cofiring of sup/deep pyramidal cells and putative inhibitory cell groups. Mean cross-correlograms of sup/deep pyramidal cells and inhibitory cells. Mean CCG values from -50 to -20ms were subtracted from all bins. Black lines indicate significant difference (p<0.05, two-sample permutation test with Tmax multiple comparison correction).

(F) Ripple-aligned spike density (mean + 95% CI) for significantly modulated cells (N = 125 superficial, and 96 deep), black horizontal line shows significant difference (p < 0.05 cluster-based two-sided permutation tests). Distribution of significantly modulated units (shaded area plots, p<0.05, one-sample cluster-based permutation test).

(G) Left: Distribution of the ripple participation probability. Right: Phase concentrations and mean resultant vector for significantly phase locked units (N = 74 superficial, 98 deep, p = 1e-3 Kuiper two-sample test/p=2e-4 permutation test, N = 5000).

(H) Mean cross-correlograms of sup/deep pyramidal cells and ripple-suppressed inhibitory cells (p<0.05, two-sample permutation test with Tmax multiple comparison correction).

(I) SWR-triggered average activation strength in post-task sleep for CA1deep (N = 115) and CA1sup (N = 112) cell assemblies.

(J) Example assembly weights for assemblies in which all members belonged to the same sublayer (N =227, “within layer”) or to different ones (N=27, “across layer”). Length indicates weight. Significant members are colored.

(K) Left: Fraction of within (N =227, orange) and across (N=27, dark gray) assemblies for all sessions and assemblies (N = 254) and for balanced sessions where the number of recorded deep and superficial were equal and assemblies that had at least 2 significant pyramidal members (N = 31). For a, b, c, d, e, and g, P values were computed using a two-sided permutation test (N = 5000).

4.4 Discussion

Currently, any detailed microcircuit mechanism of the primate hippocampus thought to underlie its cognitive and behavioral functions must be extrapolated from the hippocampus of rodents. In this study, we sought to forge a link between the extensive understanding of CA1 microcircuit function from rats and mice (Bezaire and Soltesz 2013) to the network dynamics and brain-behavior states seen during naturalistic experiences in primates. To accomplish this, we recorded in vivo, in freely-moving monkeys during species-typical behaviors. To this we added high-density laminar recordings that identified depth-localized populations of isolated single units fully embedded in their network context. Physiologically-defined pyramidal cells were concentrated in the SWR CSD source layer, and additional cell groups arose from the unsupervised clustering of waveform and ISI distribution, building on previous work (E. K. Lee et al. 2021; Trainito et al. 2019). The novel addition of the ISI distribution had the advantage of incorporating features that human experts often use in evaluating cell firing characteristics. In addition, it allowed for the full ISI range to inform the clustering, as opposed to thresholding into discrete burst/non-burst groups. The inclusion of ISI may help mitigate some potential limitations of using single-channel waveshape as a sole grouping criterion, such as extracellular waveshape variance due to different positions relative to the cell soma (Henze et al. 2000; György Buzsáki, Anastassiou, and Koch 2012), and differences in absolute waveshape that may arise across preparations due to differences in electrochemical and physical properties of the recording electrode and of acquisition filter characteristics.

Here, we describe in the primate hippocampus a spectrum of 10 identified cell groups that constrain the CA1 microcircuit through i. their intrinsic firing characteristics, ii. their different engagement with pyramidal cells, iii. their firing prevalence and temporal

organization relative to local field fluctuations, and to some degree, iv. their distribution in depth. Mesoscopic CA1-population/hippocampal spectrotemporal activity shows considerable differences in macaques relative to rats and mice (Leonard et al. 2015; Abbaspoor, Hussin, and Hoffman 2023; Jutras, Fries, and Buffalo 2013; Hoffman et al. 2013; Brincat and Miller 2015). For example, some aspects of gamma and sharp-wave ripples appear well conserved across species, whereas the multiple circuit mechanisms driving hippocampal theta-band oscillations in rats and mice have yet to be dissected in primates. Conversely, the rodent circuits that could generate the equivalent to the hippocampo-cortical alpha or beta band, and their gamma coupling, as seen in monkeys (Hussin, Abbaspoor, and Hoffman 2022; Brincat and Miller 2015; Leonard et al. 2015), is yet to be firmly established in rodents (though see (Allen et al. 2016; Jayachandran et al. 2023; Lansink et al. 2016)). Our finding of wide bandwidths of spike-field locking among the cell groups of CA1 suggests that in general, cells have the flexibility to participate in a wide range of frequencies. Within this range, three specializations were nevertheless evident. First, cell groups' peak beta/gamma frequencies tiled the range of these frequencies (Figure S2B). Second, spike-phase timing in the weaker, mid-band frequencies of 7-30 Hz spanned the greatest range of phases (~90°) and exhibited the most groups with firing phases different from the pyramidal cells' phase (Figure S2C). Third, groups differed in their assembly participation, and this was not merely a function of firing rate (Figure S4C). These differences constrain the available functional space in primate CA1, which was previously limited to considering broad classes, such as excitatory and inhibitory groups (Le Van Quyen et al. 2008; Ison et al. 2011; Leonard et al. 2015; Hussin, Leonard, and Hoffman 2020).

Despite some degree of mismatch in hippocampal brain-behavioral states across clades, it is nonetheless tempting to identify possible correspondences between the present groups and identified cell classes in rodent CA1, particularly for generally conserved oscillations, such as SWRs (A. A. Liu et al. 2022; György Buzsáki 2015). We found a small number of ripple-suppressed neurons, primarily among the interneuron groups. In rodents, OLM and axo-axonic cells under anesthesia (Klausberger et al. 2003), and a subset of axo-axonic cells in behaving rats (Viney et al. 2013; Dudok, Szoboszlay, et al. 2021) decrease their firing rate during ripples, too (n.b. the the OLM class activation

depended on the preparation (C. Varga, Golshani, and Soltesz 2012)). At the other extreme, the rare TORO inhibitory cells dramatically increase firing rate leading into and during ripples (Szabo et al. 2022). We had two groups showing unusually strong ripple modulations, despite overall lower firing rates, and one in particular had disproportionate ripple participation and the highest proportion of cells showing strong assembly participation; however, these tended to fire maximally at, not before, the ripple peak, unlike TORO cells. Beyond ripple modulation, PV basket cells show strong theta-locking, and strongly regulate and phase-lead pyramidal cells (Amilhon et al. 2015). The cell groups we observed with strongest 4-7 Hz phase locking, however, matched pyramidal cells' phase locking and angle, and had somewhat lower overall firing rates than classic theta-locked cells. Since PV inhibitory cells are thought to play a role in memory function, mediated through hippocampal network dynamics (Ognjanovski et al. 2017; Raven and Aton 2021; Xia et al. 2017), their recasting to fit the network dynamics of the primate brain will be an important future direction. Although the precise mapping across species is yet to be reconciled, our observations of systematic phase relationships between groups with varying frequency, offers the opportunity to identify putative groups as they arise with recent transcriptomic and synaptic-connectomic profiles in monkeys and humans, as demonstrated in rodent models (Bugeon et al. 2022; Schneider et al. 2023).

Perhaps the most exciting finding was that CA1 pyramidal cells show different attributes by superficial/deep allocation. Similar to findings in rodents, (Mizuseki et al. 2011; Harvey et al. 2023), macaque CA1 pyramidal cells in superficial and deep layers differ in average firing rate, bursting, and coefficient of variation. They showed different pairwiseinteractions with the inhibitory cell groups and with fine temporal specificity within several of these groups. This included deep-pyramidal cell suppression, in the context of increased superficial-cell responses, and a tightly-timed superficial-deep tradeoff among the ripple-suppressed cells, presumably arising from somatodendritic inhibitory mechanisms known to differently target pyramidal cells by depth (S.-H. Lee et al. 2014; Valero et al. 2015; Royer et al. 2012; English et al. 2017). Inhibitory-cell switching can determine the precisely-timed expression of independent cell types or assemblies, creating parallel channels for information transmission (Lapray et al. 2012; Krook-Magnuson et al. 2012; Ivan Soltesz and Losonczy 2018). Evidence for parallel

channels can be seen in their participation in cell assemblies, which are composed of either superficial or deep neurons but rarely both (Harvey et al. 2023). When added to differences in connectivity, this enables both layer-biased processing of different elements of behavioral tasks and selective coordination of extrahippocampal activity (Harvey et al. 2023). We discovered that primate CA1 also demonstrates this cell assembly bias by strata. Because macaques also show extra-hippocampal projections that are organized by CA1 pyramidal depth (Barbas and Blatt 1995; Insausti and Muñoz 2001), this suggests separable hippocampo-cortical networks may be organized through parallel channels within primate CA1. These findings, together with strata-specific differences in experience-dependent plasticity and in memory formation, (Stark et al. 2014; Valero et al. 2015; Harvey et al. 2023; Berndt et al. 2023; Gu et al. 2023), suggest that their detection in primates may prove to be key to understanding how the hippocampus structures activity during memory formation.

4.5 Methods

4.5.6 Subjects and Behavioral Conditions

Two adult female macaques (Macaca mulatta, referred to as 'M1' and 'M2') were subjects in this study. Both monkeys underwent training in a 3D testing enclosure, which allowed them to move freely. This enclosure was equipped with multiple touchscreens distributed around its periphery. To receive a fluid reward, the monkeys needed to move sequentially to each of four touchscreens placed in one corner of the environment. On each screen, they had to touch designated objects associated with that screen, avoiding distractor objects. Their overall performance in completing the four-screen sequence determined their reward. The screens were arranged in a 2x2 array on opposite corners of the 3D space, necessitating visual search, reaching, and walking or climbing during each trial. The monkeys completed various trial blocks, which took place in both screen array corners of the testing apparatus. Following their training session, the monkeys were returned to their housing. For monkey M2, sleep recordings started immediately after the training session. For monkey M1, there were sometimes 1-2 hour gaps. Sleep epochs occurred with the monkeys in their normal housing area, with their usual social housing accommodations, in complete darkness, following the automated lighting system's overnight dark cycle. All procedures were conducted in accordance with the approved protocols and authorized procedures under the local animal care authorities (Institutional Animal Care and Use Committee).

4.5.7 Electrode placement and Electrophysiological recordings

Active multichannel probes were inserted into a chronically implanted base (Talakoub et al. 2019), including a 128-channel probe (DA128-1, linear configuration with 40µm contact spacing) for Monkey M1 and a 64-channel probe (organized into 4 parallel shanks

with 40 channels at 90 μm spacing and 3 shanks with 8 channels at 60 μm spacing) for Monkey M2 ('Deep Array' design, by Diagnostic Biochips, Inc). The probes were affixed to adjustable microdrives (M1, M2: Nano Drives, Cambridge Neurotech, Inc.; M1: custom, Rogue Research, Inc.) to facilitate precise depth positioning adjustments post-implantation, and allowing the raising and relowering (max. 7 mm or 5 mm, respectively) into target areas while remaining implanted. Post-operatively, the probes were incrementally advanced through these drives in 125mm steps until the target positions were achieved. The localization of recording sites was verified through postoperative CT scans, coregistered with pre-operative MRI data, and also by referencing functional landmarks that changed with increasing depth. Notably, the emergence of depth-specific sharp-wave ripples (SWRs) within unit-dense layers served as a key reference point. To align the 4 shanks in M2, we employed cross-correlation analysis of LFP signals observed during ripple activity across the channels. Local field potentials (LFPs) were digitally sampled at a rate of 30 kHz using the FreeLynx Wireless Acquisition system (Neuralynx, Inc) and subsequently bandpass filtered within the 0.1 Hz to 7500 Hz range. During task performance and sleep recordings for Monkey M2, data were wirelessly transmitted to the Freelynx acquisition system (Neuralynx, Inc). To optimize battery life, sleep recordings for Monkey M1 were stored on an SD card within the acquisition system. A high-frequency noise signal at approximately 6 kHz marked the point at which the battery capacity reached 10%. The onset of this noise was detected by calculating the root mean square (RMS) envelope of the band-passed filtered signal between 5800-6200Hz. The noise initiation point was defined as the timestamp at which the RMS envelope exceeded 110% of the median value, and sleep data following this point was excluded. For the purpose of merging task and sleep recordings, data was initially converted to microvolt units, bitVolts were standardized to 0.195, and the data was subsequently transformed into binary files encoded as 16-bit integers. Sessions that exhibited no signal loss during recording were exclusively included in the analyses. In LFP-related analyses, the raw signal was subjected to third-order Butterworth filtering with a low-pass cutoff frequency set at either 350Hz or 450Hz, and the data was downsampled to 1 kHz.

4.5.8 CT-MRI image processing and coregistration

The General Registration tool, Elastix, in the Slicer (version 4.11), was used to perform the registration of post-operative CT scans with pre-operative MRI images. The registration process maintained default parameters. Preceding registration, the CT images were cropped to encompass solely the skull region.

4.5.9 Power spectral parametrization and fitting

To estimate the layer-specific spectral content of the hippocampal and neocortical recordings, we used Welch's method with a 50%-overlapping 1024-sample sliding Hanning window to estimate power spectra for the frequency range of 1–150 Hz with a frequency resolution of 0.25 Hz. To identify spectral peaks and compare between search and rest states, we parameterized power spectra using the method described by (Donoghue et al. 2020). This method models power spectra as a combination of the 1/f frequency components (aperiodic) in addition to a series of Gaussians that capture the presence of peaks (periodic components). The model was fit to a frequency range between 1 Hz and 200 Hz with a frequency resolution of 0.5 Hz. Settings for the algorithm were set as: peak width limits: (0.5, 12); max number of peaks: infinite; minimum peak height: 0; peak threshold: 2.0; and aperiodic mode: 'Fixed'.

4.5.10 Detecting hippocampal Sharp-wave ripples

A single hippocampal LFP channel with largest ripple amplitude was selected for ripple detection. The wide-band signal was band-passed filtered between 100-180Hz using a 3rd order Butterworth filter, and squared signal was calculated. The squared signal was further band-passed filtered in 1-20Hz range and z-normalized. SWR peaks were detected by thresholding the normalized squared signal at 3SDs above the mean, and

the surrounding SWR start and stop times were identified as crossings of 1 SDs around this peak. SWR duration limits were set to be between 20 and 400 ms. Detected events with a time interval shorter than 40ms were merged.

Exclusion Criteria: In addition to assessing amplitude and duration, we employed several criteria to identify and exclude potential false-positive ripple events. **Channel Noise Exclusion:** A 'noise' channel, defined as one devoid of detectable sharp-wave ripples (SWRs) in the local field potential (LFP), was designated. Any events simultaneously detected on this channel were considered as potential false-positives, likely originating from artifacts such as electromyography. **Spectral Analysis:** We conducted spectral analysis of each detected ripple event to further scrutinize its characteristics. The data was spectrally decomposed using Morlet wavelets, allowing us to compute the frequency spectrum for each event. This was achieved by averaging the normalized instantaneous amplitude within ±50ms of the ripple peak over the frequency range of 50-200 Hz, normalized by multiplying the amplitude by the frequency. We then analyzed the number and properties of spectral peaks in each detected ripple frequency spectrum. These peaks were identified using the findpeaks function in MATLAB, considering parameters such as peak height, prominence, peak frequency, and peak width. This analysis aimed to ensure that the detected ripple events genuinely reflected high-frequency, narrowband bursts within the ripple band range. We applied multiple criteria to achieve this: first, authentic ripple events were expected to exhibit a predominant spectral peak within the ripple band range. Therefore, if no single prominent peak (corresponding to the ripple band) was identified, the event was rejected. Additionally, authentic ripple events were anticipated to display a limited narrowband burst; thus, if the ripple-peak had an excessively wide peak width (indicating more broadband spectral changes) or prominent high-frequency activity, the event was considered for rejection (see (Y. Y. Chen et al. 2020)). **Visual Inspection:** Finally, all detected ripples underwent visual inspection, and any events flagged as false-positives during this process were subsequently removed from the dataset.

4.5.11 Spike sorting

Spike sorting was performed using Kilosort 1.0 ((Pachitariu et al. 2016), https://github.com/cortex-lab/KiloSort). The process involved applying a 300-Hz high-pass filter to the raw signals, followed by whitening the data in blocks of 32 channels. Parameters relevant to automated sorting are detailed in the accompanying table.

Removing putative double-counted spikes (Lecoq et al. 2021)***.*** The Kilosort algorithm will occasionally fit a template to the residual left behind after another template has been subtracted from the original data, resulting in double-counted spikes. Such double-counted spikes could artificially inflate inter-spike interval (ISI) violations for a single unit or create erroneous zero-time-lag synchrony between neighboring units. Consequently, spikes with peak times within a 5e-4 second interval and peak waveforms detected on the same channels were systematically removed from the dataset.

Removing units with artefactual waveforms. Kilosort1 generates templates of a fixed length (2 ms) that matches the time course of an extracellularly detected spike waveform. However, there are no constraints on template shape, which means that the algorithm often fits templates to voltage fluctuations with characteristics that could not physically result from the current flow associated with an action potential. The units associated with these templates are considered ‘noise’ and are removed on the basis of spread (waveform appears on many channels), and shape (e.g. no peak and trough or sinusoidal waveform) criteria and autocorrelogram function.

Manual curation and re-clustering with Phy. Manual curation and re-clustering were performed using Phy (https://github.com/kwikteam/phy). Kilosort-derived clusters were imported into Phy for manual curation. Units that were poorly isolated according to the initial Kilosort results were re-clustered using Klusta with custom-designed plugins (https://github.com/petersenpeter/phyplugins) to obtain well-isolated single units. The quality of these clusters was evaluated based on refractory period violations and Fisher's linear discriminant metrics. Noise clusters and poorly isolated units were subsequently excluded from the analysis.

Kilosort Parameters

ops.datatype	'dat'
ops.fs	30000
ops.Nfilt	1024
ops.whitening	‘full’
ops.nSkipCov	1
ops.whiteningRange	32
ops.criterionNoiseChannels	0.2
ops.Nrank	3
ops.nfullpasses	6
ops.maxFR	20000
ops.fshigh	300
ops.ntbuff	64
ops.scaleproc	200
ops.NT	32*1024+ ops.ntbuff
ops.Th	[4 10 10]
ops.lam	[10 30 30]
ops.nannealpasses	4
ops.momentum	1./[20 400]
ops.shuffle_clusters	1
ops.mergeT	0.1
ops.splitT	0.1
ops.initialize	'fromData'
ops.spkTh	-4
ops.loc_range	[3 1]
ops.long_range	[30 6]
ops.maskMaxChannels	5
ops.crit	0.65
ops.nFiltMax	10000

4.5.12 Hippocampal CA1 layer estimation and localization of neuronal somata in the CA1 layers

To estimate the location of the linear-array channels relative to CA1 layers, we used features of the sharp wave ripple. The sharp wave component of the SWR arises from CA3 Schaffer collateral inputs that generate a current sink in stratum radiatum (SR) with a return source centered in stratum pyramidale (Sullivan et al. 2011). In the relatively closed fields of rat or mouse CA1, this is evident as a polarity reversal between SR and the deeper layers, where the envelope flattens, distorts and ultimately reverses (G Buzsáki, Leung, and Vanderwolf 1983). The source/sink gradient has been used as a depth reference to identify superficial/deep pyramidal cells (Harvey et al. 2023), and should be more sensitive to local generators (more tolerant of open-fields) than the raw fields (Mitzdorf 1985; Tenke et al. 1993; Steinschneider et al. 1992). On this basis, we first estimated the radiatum/pyramidale transition using current source density (CSD), the second spatial derivative, of ripple-trigger averaged signal across the regularly-spaced LFP channels. This identified the general regions of SR and SP. Next, we calculated ripple power and the slope of sharp-wave envelope peak, both of which have been used to center the pyramidal layer in previous studies (Mizuseki et al. 2011; Harvey et al. 2023), respectively. For each session, we set the channel closest to the LFP slope zero-crossing as 0, and the depth of the other channels in relation to that point, considering the fixed inter-electrode distance. No additional scaling was made to the inter-channel distances. This reversal point fell in the middle of sinks and sources of CSD and above the depth of maximum ripple power. For the side-shank linear sites (in M2), we adjusted the physiological depth based on the correlational similarity of mean sharp-wave ripple LFP. For all isolated units, the site with the largest spike amplitude for each unit was regarded as the location of the cell body.

4.5.13 Cell type classification

To establish the feature space for cell type classification, we leveraged single-unit waveforms and interspike interval (ISI) distributions of the cells. The filtered single-unit waveforms (comprising 48 samples at 30 kHz) were first normalized within the range of 0 to 1 and aligned. Subsequently, we used the Uniform Manifold Approximation and Projection (UMAP) to reduce the dimensionality of the waveform matrix to 2 components. In a parallel process, the log10 ISI distributions within the range of 0-10 seconds were subjected to UMAP analysis to obtain 2 components as well. For these UMAP procedures, we employed a custom UMAP function implemented in MATLAB (McInnes, Healy, and Melville 2018). The selection of UMAP parameters was guided by consultation with (E. K. Lee et al. 2021). To generate the feature space for clustering, the four attributes (two from waveform and two from ISI) were concatenated. Clustering was performed using Spectral Clustering in MATLAB, with Mahalanobis distance serving as the primary metric. Initially, we set the number of clusters to 20, based on the criteria of AIC and BIC applied to Gaussian mixture models (GMM) built on the feature space. Subsequent refinements were carried out on the initial clusters using either spectral or GMM clustering techniques, with similar clusters being merged.

UMAP Parameters:

min_dist	0.1
n_neighbors	20
n_components	2
n_epochs	5000
metric	euclidean

4.5.14 Classification of deep and superficial CA1 pyramidal cells

The first group was designated the pyramidal cell group, because these cells demonstrated the low firing rates, high propensity for bursting, and dense localization within the Stratum Pyramidale that are the hallmarks of CA1 pyramidal cells (Ranck 1973; William E Skaggs et al. 2007; J Csicsvari et al. 1999a). For the superficial and deep analyses, we removed from this group the spatial outliers (with relative depths falling outside the 5-95th depth percentile range), and cells with mean firing rates > 1 Hz or a burst index exceeding 3, before calculating the median depth of these units to segregate into superficial and deep categories. The spatial distribution of CA1sup neurons spanned from -300 to 540 μm, and for CA1deep neurons, it extended from -630 to -330 μm.

4.5.15 Burst Index

We used a burst index that captured the propensity of neurons to discharge in bursts. The amplitude of the burst was estimated from the mean of spike auto-correlogram (1-ms bin size) measured between 1 and 10 ms normalized by the baseline, the mean value between 200 and 300 ms (Royer et al. 2012; Peter C Petersen et al. 2021).

4.5.16 Ripple-associated spike content analysis

Within-SWR firing rate was calculated as the number of spikes during SWRs divided by the cumulative duration of the SWRs between the first and last spike fired by the cell. The ripple participation probability of individual units was defined as the fraction of SWRs in which that neuron fired at least one spike. Ripple ratio was defined as firing rate during ripple events divided by the overall firing rate.

To calculate spike density functions, spike vectors of individual cells were binned with 1ms binsize and peri-event time histograms (PETHs) were computed locked to ripple peaks and converted to rate. Then a gaussian kernel with a 10 ms S.D. was applied to the PETHs to obtain spike densities. For each cell, we calculated the baseline activity as

the mean firing rate of a shuffled surrogate dataset created for that cell and subtracted this value from the original PETH.

To test the hypothesis that spiking activity of single cells are modulated surrounding the ripple peak, we derived nonripple event surrogates. These surrogates were created for individual cells using timestamps selected randomly without replacement from recording epochs when ripples were not detected. We matched the number of ripple and nonripple surrogate events (n observed ripple events = n nonripple events). Furthermore, to ensure that signal properties were maximally matched between target events and surrogates, surrogates were drawn only from a 10-min time window before and after the corresponding ripple event. To test the significant difference between the ripple-locked and surrogate spike densities, we used a cluster-based permutation procedure using 5000 permutations and a cluster threshold of $p < 0.05$ and a final threshold for significance of $p < 0.05$.

4.5.17 Spike-field synchronization

To quantify spike-field synchronization, we used the pairwise phase consistency (PPC) measure, which is unbiased by the number of spikes (Vinck et al. 2010). For hippocampal recordings, we selected the sharp-wave ripple channel in the Stratum Pyramidal of the CA1 across sessions. If the unit spikes were from this channel, we used an adjacent channel to measure the PPC. The spectral content was estimated with Morlet wavelet decomposition method using a constant number of cycles (7) per frequency for frequencies between 1 and 200 Hz with a frequency resolution of 1 Hz. We measured PPC values separately for spikes during wakeful and rest/sleep states, and only for neurons that fired at least 100 spikes (Vinck et al. 2010). One caveat of this approach is that it assumes signals to be oscillatory and, additionally, sinusoidal. This can distort preferred phase estimations. We used an alternative approach to estimate phase of modulation in restricted time windows of presumed oscillatory bouts, across frequency ranges. For each frequency group, LFP signal was filtered in the specified frequency band using a 3rd Butterworth filter. Next, instantaneous phase and power were derived from

Hilbert transform. A phase value was assigned to each action potential during significant periods (power of filtered LFP > 2 S.D. above the mean) using linear interpolation. Peaks are at 0° and 360° and troughs at 180° throughout the paper. Then we calculated the mean phase and resultant vector using the circular statistics toolbox on MATLAB ((Berens 2009), https://github.com/circstat/circstat-matlab). To find the grand mean phase and resultant vector of a cell group in a specific frequency, we measured the mean phase of firing for included members of that cell group and then calculated the mean phase and resultant vector of the mean phases. The grand mean phase and resultant vector determines the consistency of phase of firing among the members of a cell group. For the calculation of the grand mean phase, we included only cells that had at least 20 spikes during significant epochs of interest. We set a significance threshold of $p = 0.01$ using the Rayleigh test for phase locking.

4.5.18 Pairwise cell interaction

We employed two complementary approaches to estimate pairwise cell interactions in our analysis. First, recordings were segmented into 25 ms time bins, and for each neuron, the number of spikes within each bin was counted and converted to firing rate. Subsequently, we convolved the spike vectors with a Gaussian kernel, with a standard deviation calculated as binsize / (2 * sqrt(2 * log(2))) (converted to Full Width at Half Maximum, FWHM). Pearson's correlation coefficients were then calculated between the spike density vectors of different neurons, serving as a measure of their co-firing tendencies.

Due to potential recording instabilities, some cells might have appeared or disappeared during the recording. To prevent periods of inactivity from influencing the Pearson's coefficients, we only considered correlations during overlapping windows of activity if two conditions were met: 1) the overlapping window extended beyond 5 minutes, and 2) both cells fired at least 100 spikes within the overlapping time window.

Additionally, cross-correlograms (CCGs) were computed between pairs of neurons with a 1 ms bin resolution and converted to rate (CCG divided by the reference cell's number of spikes per time bin). These CCGs were smoothed using a zero-lag partially hollowed Gaussian filter with a convolving window of 5 ms and a hollow fraction of 0.6 (English et al. 2017; Stark and Abeles 2009).

The mean activity in a baseline window (-50 to -20 ms) was subtracted from the original CCGs to account for any baseline activity. For assessing the statistical significance of CCGs, we employed a surrogate approach by shuffling the inter-spike intervals of the cells (Nádasdy et al. 1999) and calculating the CCGs between the surrogate cells. This process was repeated 5000 times to generate a surrogate distribution of CCGs. P-values were computed for each time bin of the CCG (-20 to 20 ms) and subjected to multiple-comparison correction using the Benjamini and Hochberg False Discovery Rate (FDR) procedure. Only cells with at least one significant time bin were included in the calculation of the mean CCG. To compare CCGs between the CA1sup and CA1deep groups, a two-sample permutation test with Tmax correction was used (Blair and Karniski 1993).

4.5.19 Assembly pattern identification and activation strength

Cell assemblies were identified during sleep recordings as previously described (Vítor Lopes-dos-Santos et al. 2011; Vítor Lopes-dos-Santos, Ribeiro, and Tort 2013; van de Ven et al. 2016; Peyrache et al. 2010; Harvey et al. 2023; Boucly et al. 2022). Significant co-firing patterns were detected using an unsupervised statistical method based on independent component analysis (ICA). The spike trains for each neuron were binned into time windows of 90-ms (corresponding to max duration of ripple events at 90 percentile) and z-score transformed to eliminate biases due to differences in average firing rates. Next, a principal component analysis was applied to the binned spike matrix (Z). The correlation matrix of Z was given by $C = \frac{1}{n}ZZ^T$ and the eigenvalue decomposition of C was given by:

$$\sum_{j=1}^{n} \lambda_j p_j p_j^T = \frac{1}{n} ZZ^T$$

where λ_j is the j[th] eigenvalue of C and p_j is its corresponding eigenvector. The Marcenko-Pastur law was used to estimate the number of significant patterns embedded within Z. For a nXB matrix, an eigenvalue exceeding λ_{max}, defined by $\lambda_{max} = (1 + \sqrt{n/B})^2$, signifies that the pattern given by the corresponding principal component explains more correlation than would be expected if the neurons were independent of each other. The number of eigenvalues exceeding λ_{max} was defined as N_A and therefore represents the minimum number of distinct significant patterns in the data. The significant principal components were then projected back onto the binned spike data

$$Z_{PROJ} = P_{SIGN}^T Z$$

where P_{SIGN} is the nXN$_A$ matrix with the N$_A$ principal components as columns.

Independent component analysis (ICA), using the fast ICA algorithm (http://research.ics.aalto.fi/ica/fastica), was then applied to the matrix Z_{PROJ}. That is, an N$_A$XN$_A$ unmixing matrix W was found such that the rows of the matrix $Y = W^T Z_{PROJ}$ were as independent as possible. The arbitrary signs of the Independent component (IC) weights were set so that the highest absolute weight was positive. The unmixing matrix W was then used to derive each cell's weight within each assembly $V = P_{SIGN} W$ where the columns of V $(i.e., v_1, \dots, v_{NA})$ are the weight vectors of the assembly patterns.

To determine the strength of the expressed assemblies, we tracked each assembly pattern v_k over time by:

$$R_k(t) = z(t)^T P_k z(t)$$

where $z(t)$ is a smooth vector-function containing for each neuron its z-scored instantaneous firing-rate and P_k is the matrix projecting $z(t)$ to the activation-strength of the assembly pattern k at time t.

4.5.20 Organization of cell assemblies

The majority of the identified assembly patterns exhibited a characteristic distribution where a few neurons displayed high weights, while a larger group of neurons had weights approximating zero. To determine the significant membership corresponding to each assembly pattern, we used the criteria that the member neurons of an assembly should have weights exceeding the mean weight by at least two standard deviations. It's

important to note that all subsequent analyses were conducted directly on the assembly patterns themselves, using the weight vectors derived from the contribution of all recorded neurons. Based on the configuration of significant assembly members, the assemblies were classified into three distinct groups: **Within Assemblies:** These assemblies were defined as having at least one significant member from the pyramidal cell group. If all significant pyramidal members were exclusively from the superficial or deep regions, we labeled the assembly as "within superficial" or "within deep," respectively. **Across Assemblies:** These assemblies included at least one significant member from both the superficial and deep pyramidal cell groups. **Assemblies with No Recorded Pyramidal Members:** This category comprised assemblies that did not contain any recorded pyramidal cell members.

To estimate the probability of realization of a specific assembly organization, we used the binomial probability density function (binopdf in MATLAB). Observed and expected probabilities were computed as:

$$ObservedProb = binopdf(sigDeep, sigSup + sigDeep, NDeep/(NSup + NDeep));$$

$$PallDeep = binopdf(sigSup + sigDeep, sigSup + sigDeep, NDeep/(NSup + NDeep));$$

$$PallSup = binopdf(sigSup + sigDeep, sigSup + sigDeep, NSup/(NSup + NDeep));$$

$$ExpectedProb = 1 - (PallSup + PallDeep);$$

Where $sigDeep$ and $sigSup$ represent the number of significant CA1deep and CA1sup members within the assembly, respectively. $NDeep$ and $NSup$ denote the total number of recorded CA1deep and CA1sup neurons within the session. $ObservedProb$ signifies the probability of encountering the specific organization of the assembly. $PallDeep$ and $PallSup$ indicate the probability that all significant pyramidal members exclusively belong to either CA1deep or CA1sup. $ExpectedProb$ reflects the anticipated probability that the assembly could belong to the "across" category.

Assembly participation probability was calculated for all cells per session and it was defined as the number of assemblies where a cell participated as a significant member divided by the total number of detected assemblies in a session.

4.5.21 Statistical analysis

Data collection was not conducted under blinded conditions and data analysis and behavioral experiments did not necessitate manual scoring. No specific methodology was employed to estimate the minimum required population sample, but the number of animals, trials, and recorded cells exceeded or was comparable to those used in prior studies. All statistical analyses were performed using MATLAB R2021a, utilizing non-parametric methods for comparisons of means and variances, including Kruskal-Wallis analysis of variance, two-sample permutation tests, one-sample randomization tests.

Two-sample permutation test: A two-sample permutation test is a statistical method used to compare two independent groups or samples in a hypothesis testing framework. It is particularly valuable when the data do not meet the assumptions of parametric tests like the t-test. For comparison where each sample had a single data point, we simply shuffled the membership assignments 5000 times and computed the mean difference between the surrogate samples each time to create a surrogate probability distribution of mean differences. The original, non-permuted data are then compared to the surrogate distribution to obtain uncorrected p-values.

For **cluster-based multiple comparison correction**, all samples with p-values smaller than 0.05 were selected. These selected samples were subsequently clustered into connected sets based on their adjacency, and the size of each cluster was calculated. This process was repeated 5000 times to generate a distribution of cluster sizes. Clusters with sizes exceeding the cluster threshold at the 95th quantile were reported as significant.

For CCG analyses we controlled family-wise error rate (FWER) using the Tmax correction method (Blair and Karniski 1993). This method provides strong control of FWER, even for

small sample sizes, and is much more powerful than traditional correction methods (Gondan 2010; Groppe, Urbach, and Kutas 2011a). It is also rather insensitive to differences in population variance when samples of equal size are used (Groppe, Urbach, and Kutas 2011b).

One-Sample Randomization Test: This test, akin to the permutation test, involved comparing a time series against a surrogate dataset created from randomly selected timestamps.

For all other posthoc tests, either Tukey-Kramer or the Benjamini & Hochberg (1995) multiple comparison correction was applied, as specified in the main text.

Boxplots were used to present data, with the median, 25th, and 75th percentiles represented within the box, and the whiskers illustrating the data range. In cases where boxplots did not display individual data points, outliers were excluded from the plots but were consistently included in the statistical analysis.

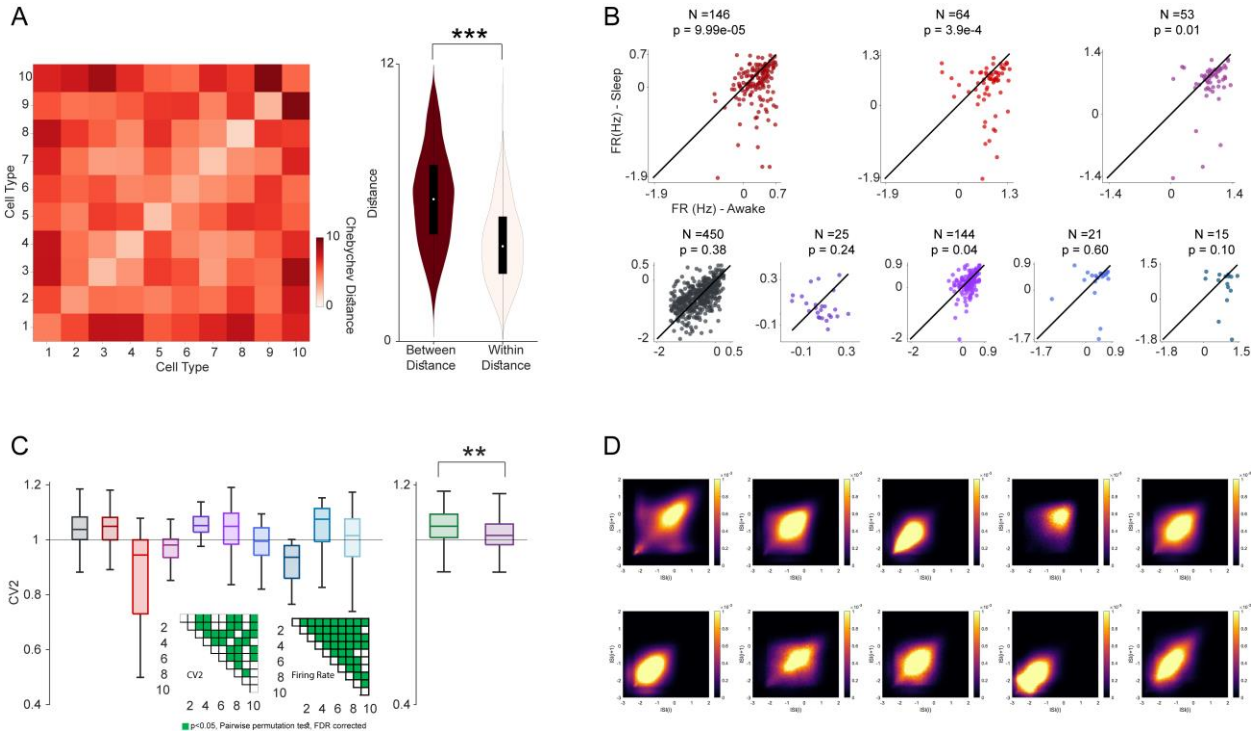

Figure 4-4. Physiological features of different cell groups in the macaque hippocampal CA1

(A) Left: Chebyshev distance matrix for feature space of recorded cells. Note that the diagonal values are smaller than off-diagonal indicating that within-group members were closer together in the feature space compared to between-group members. Right: Distribution of between-group (red), and within-group (bone white) of distance values ($p<0.001$, two-sample permutation test)

(B) Firing rate of neurons during sleep and wakeful states for different cell groups (N: number of cells, pval = result of a two-sample permutation test).

(C) Left: ISI-based coefficient of variance (CV2) for different cell groups ($p<0.001$, Kruskal-Wallis test). Matrices show the result of pairwise permutation tests for firing rate and CV2 (dark pixels indicate $p<0.01$, two-sample permutation test + FDR correction). Right: CV2 for superficial versus deep pyramidal cell group ($p<0.001$, two-sample permutation test)

(D) Joint ISI histograms showing the next interval (ISI_{i+1}) as a function of the previous interval (ISI_i) for different cell groups.

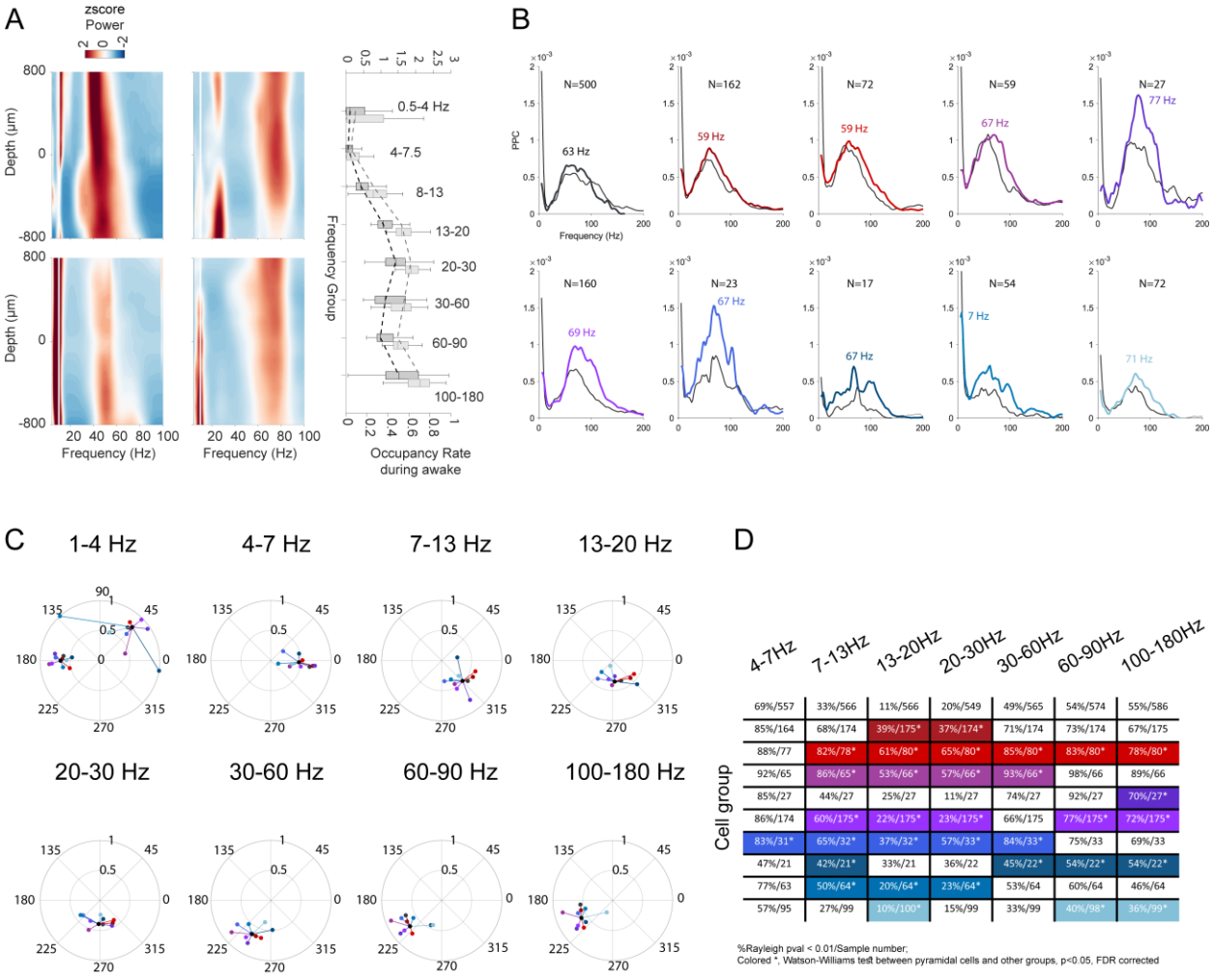

Figure 4-5. Oscillatory dynamics and spike-field relationship

(A) Left: 1/f corrected FOOOF power spectrum across depths of recording during task (top) and rest/sleep (bottom) for two animals subjects. Right: Corrected (black) and balanced (grey) proportion of detected oscillatory bouts during task versus sleep states in different frequency bands. LFP channels was selected from Stratum Radiatum.

(B) Mean PPC values during task (colored) and rest/sleep (grey).

(C) Phase plots showing grand mean phase and resultant vector for cell groups and frequency bands. Note that for the 1-4Hz group, we separated the results for the 2 animal subjects due to conspicuous differences between them. Matrix shows percent (%) of cells with significant phase locking (p<0.01, Rayleigh's test) in each frequency and cell group; total number of cells included for this analysis (all cells with less than 20 spikes during significant oscillations were excluded); and the results of pairwise permutation tests between pyramidal cell group and other groups for different frequency bands (Significant differences are depicted by *colored, p<0.05, two-sample Watson-Williams test, FDR corrected)

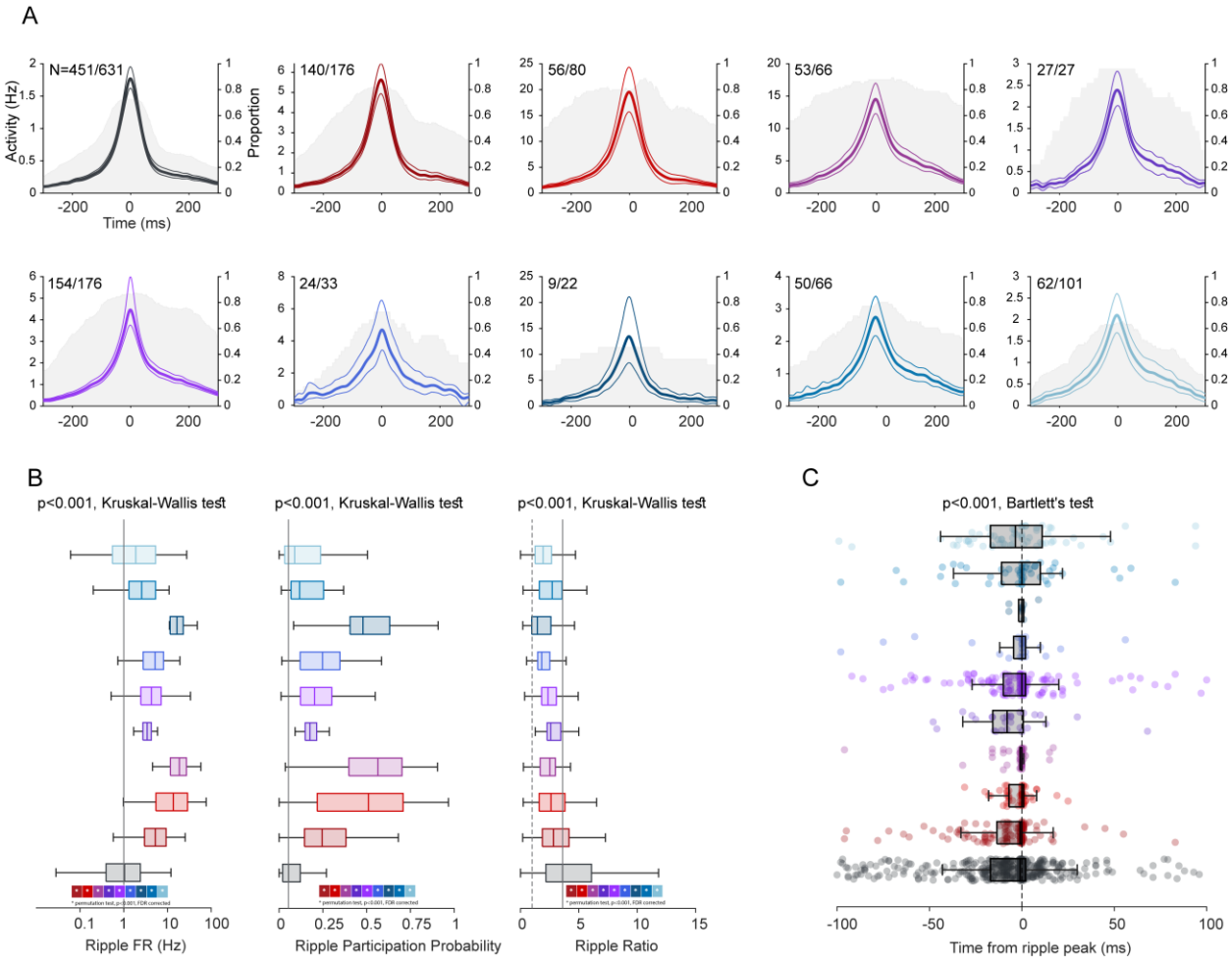

Figure 4-6. Sharp-wave ripple-associated spiking dynamics

(A) Ripple-aligned spike density (mean + 95% CI) for significantly modulated cells of different groups. N: Significantly modulated/total cells in the group. Distribution of significantly modulated units (shaded area plots, p<0.05, one-sample cluster-based permutation test).

(B) Left: Ripple firing rate for different groups. (p<0.001, Kruskal Wallis test). Middle: Ripple ratio (average firing rate during ripples / overall firing rate, p<0.001, Kruskal-Wallis test). Right: Ripple participation probability (p<0.001, Kruskal-Wallis test). Color coded asterisks show the result of post-hoc pairwise permutation test between pyramidal cell group and all other cell groups (* p<0.001, FDR corrected).

(C) Distribution of peak response times around the ripple peak (p<0.001, Bartlett's test for equality of variances).

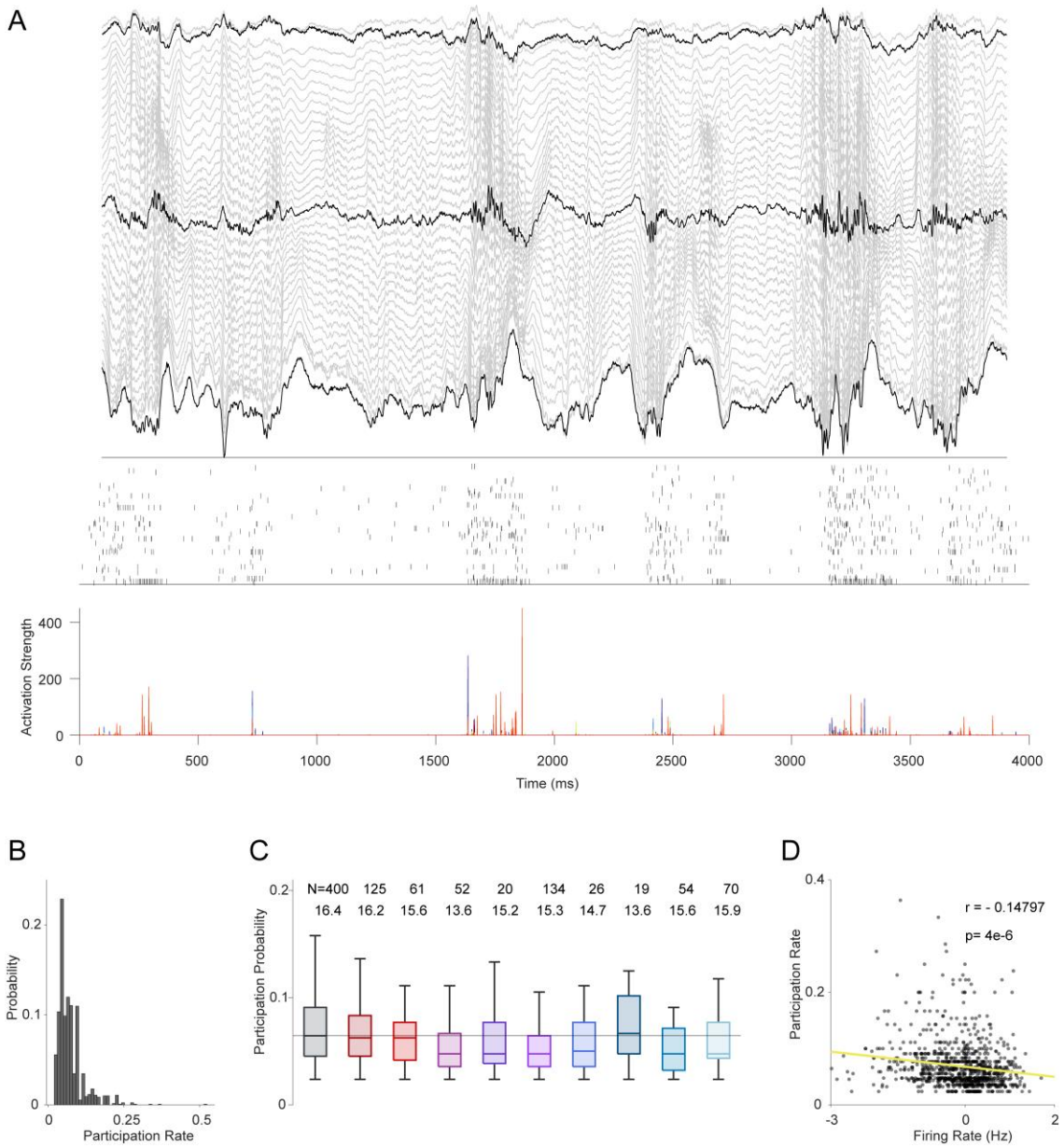

Figure 4-5. Anatomical organization of assembly dynamics in the macaque hippocampal CA1

(A) Top: Example LFP traces across depth of recording in CA1 during sleep for M2. Middle: Raster plot of simultaneously recorded units. Bottom: Assembly activation strength of different assemblies.

(B) Distribution of assembly participation rate for cells. Cells with a participation rate of 0 were removed from the analysis.

(C) Distribution of assembly participation probability for different cell groups ($p<0.001$, Kruskal-Wallis test). The first row of text shows the number of cells with a participation rate greater than 0. The second row of text show average available assemblies to participate in for different cell groups across sessions.

(D) Relationship between firing rate of neurons and assembly participation rate showing a significant inverse correlation ($r = -0.14$, $p < 0.001$ ttest)

5. General Discussion

In the past couple of decades, we've witnessed significant progress in recording techniques for rodents, ranging from high-density extracellular recordings to in vivo juxtacellular recordings, functional transcriptomics, and genetic cell tagging. These advances have unveiled a distinct functional organization of diverse cell classes in various layers of the CA1 region (Klausberger and Somogyi 2008; Harris et al. 2018). The state-of-the-art technologies in primate electrophysiology, however, still lags behind and consequently, many of our theories on neural mechanisms of learning and memory heavily rely on rodent studies. While these findings in rodents have revolutionized our understanding of the brain, the direct translation to primates may not be straightforward due to differences in their behavioral repertoire and brain structure.

From a cognitive perspective, it is increasingly recognized that the limited ecological validity found in many paradigms and settings in the field can artificially constrain our theories about the cognitive processes involved (Miller et al. 2022). In most cases, there's a significant gap between the spatiotemporal scale of naturalistic episodic memories and the often artificial laboratory memory tests, which usually overlook the crux of the processes that underlie these functions such as dynamic and flexible embodiment in 3D complex physical spaces (Shamay-Tsoory and Mendelsohn 2019). This disparity can impact our understanding of how memory systems are organized, their capacity, and their underlying mechanisms across animal species.

To address these challenges, my dissertation aimed to investigate the neural dynamics of the hippocampus in freely-moving macaques within more ecologically relevant memory task settings. I used multi-channel laminar recordings to sample local field potentials (LFP) and spiking activity from different layers of the CA1 region and used similar analytical techniques to those used in rodent studies, to facilitate the comparison of findings between macaques and rodents. These approaches enabled me to create a more detailed microcircuit picture of the primate hippocampus and compare it to the rodent models. Such comparative electrophysiological approaches across two species

with notably different exploratory behaviors can provide insights into how the hippocampus supports the distinctive behavioral repertoires of these species.

6. Chapter 1: Exploring event memories in freely-behaving macaques

One of the main goals of this dissertation was creating a task enclosure suitable for cognitive tests in freely behaving macaques. This enclosure, the Treehouse, was designed to facilitate intricate interactions with the environment, offering conditional stimulus arrays that extend across both space and time, all within the context of naturalistic movements and exploratory behaviors. These features are crucial parts of the contextual episodic memories, a topic I will delve into. Simultaneously, this apparatus meets the electrophysiological requirements by delivering precise timing, experimental control, and repetition necessary for studying the neural dynamics of memories within these behavioral conditions.

Episodic memories include details about the spatiotemporal context of events, seamlessly integrated into a sequence of unified and coherent representations. These memories can be flexibly expressed to facilitate adaptive behavior in novel situations (Crystal 2021; Allen and Fortin 2013). Despite observations on the capacity of animal models to learn complex spatiotemporal contingencies and to form sequence memory at the behavioral level, much of our understanding of the neural dynamics of contextual episodic memory primarily stems from the contextual fear conditioning paradigm in rodents. In this paradigm, animals associate a spatial context with an unpleasant experience. This paradigm offers a single memory within a limited spatiotemporal context. Although valuable insights have been gained into the neural organization of such memories, it's crucial to recognize that memory is diverse, with organization varying based on specific content. Therefore, studying the neural organization of memories across species and under different cognitive conditions spanning various spatiotemporal scales and stimulus complexities is essential.

Laboratory paradigms designed to assess episodic memories frequently impose restrictions on the spatial and temporal scales of memories, typically to exert control over the subject's behavioral state. The neural and cognitive structures underlying memories are sensitive to the spatiotemporal characteristics of the items to be remembered. Therefore, careful consideration must be given to the specific demands placed on the subject and the conditions under which assessments are conducted. Temporal scale assessment involves two key aspects: 1) the length of a sequence that a subject needs to learn and 2) remoteness, measuring the time elapsed from the original exposure to information before the retention/retrieval test. Episodic memories are constructed from sequences of events, with events defined by their specific contextual arrangements in terms of space and time. Both animal models and humans exhibit the ability to remember a list of items in their correct temporal order. In rats, selective lesions in the hippocampus impairs remembering the sequential ordering of odors while sparing the capacity to recognize odors that recently occurred (Fortin, Agster, and Eichenbaum 2002; Agster, Fortin, and Eichenbaum 2002). Similarly, patients with medial temporal lobe (MTL) damage exhibit no special difficulty remembering spatial details in comparison with nonspatial details but the order in which patients recalled the events is unrelated to the order in which they occurred (Dede et al. 2016). Interestingly, a recent study shows that monkeys with hippocampal lesions were impaired only transiently, if at all, in memory for temporal order (Basile et al. 2020), however, order judgments are sensitive to fornix transection in monkeys (Charles, Gaffan, and Buckley 2004). This suggests that other regions in the MTL might be supporting the memory for order. Electrophysiological studies in rodents and neuroimaging studies in humans also demonstrate that hippocampal activity patterns differentiate between overlapping object sequences and between temporally adjacent objects that belonged to distinct sequence contexts (Hsieh et al. 2014; Gelbard-Sagiv et al. 2008; Lehn et al. 2009; Davachi and DuBrow 2015). These results caution against over-generalizing from human correlational studies or rodent experimental studies and might suggest that the organization of memories is different across these species, emphasizing causal tests of hippocampal function in nonhuman primate models.

Space is another dimension which is an inseparable part of a contextual memory because all memories are formed somewhere. But not all spaces are equal (Banta Lavenex and Lavenex 2009). Cognitive tests in monkeys, and even humans, is typically restricted to chaired subjects where the relevant space for memory is on a monitor, focusing on the spatial layout of stimuli. Under these conditions, we have a high level of control over the subject and the experimental settings, but the behavioral repertoire is limited, doesn't incorporate body movement and sensation, and is less ethologically relevant. Removing naturalistic components of everyday experience as they pertain to presented stimuli, real contextual information, active participation, and bodily movement may reduce ecological validity to the extent that it precludes us from understanding behavioral and neural elements of memory in real life (Shamay-Tsoory and Mendelsohn 2019). The main argument is that interfering with the ability of participants to act on the environment may reduce their sense of control over the environment, in turn affecting their sense of agency—the experience of controlling one's actions (Haggard and Chambon 2012). That the actions of participants do not affect the experience may diminish the engagement of participants in the tasks and leave basic cognitive faculties dormant. In agreement with this, in natural and virtual environments (VE) spatial learning depends on several factors including the spatial goal, environmental complexity, and mode of learning. A factor influencing the mode of learning is the extent to which exploration is self-governed (Carassa et al. 2002). Memories of experiences are formed whether the individual is a passive part of the occurrence or an active agent. The question at hand is whether the degree of perceived control over the environment may affect memory properties associated with relevant experiences. There are now several lines of evidence supporting the notion that actively interacting with the environment can affect memory formation (Brandstatt and Voss 2014; Carassa et al. 2002; Koriat and Pearlman-Avnion 2003; Murty, DuBrow, and Davachi 2015; Plancher et al. 2013; Rotem-Turchinski, Ramaty, and Mendelsohn 2019). For instance, in humans, active exploration, self-movement, and self-referencing in natural complex environments enhance memory of visuospatial scenes and spatial memory in virtual environments (Brooks et al. 1999; Carassa et al. 2002; Plancher et al. 2013; Penaud et al. 2022). It has been suggested that additional movement traces provide supplementary specificity to the formed memories and hence enhance them

compared to passively acquired memories (Brooks et al. 1999; Plancher et al. 2013). These observations are in line with the embodied views of memory that denote memories operate in the service of perception and action, and hence memory representations must arise from bodily interactions with the world (Glenberg 1997). Interestingly, one of the main findings in the current dissertation was that as monkeys underwent the learning process, the kinetics of their head movements altered. In primates, the combination of eye and head movements plays a central role in acquiring information about the environment's structure (active sensing) and externalizing internal beliefs or deliberations (embodied cognition) (Zhu, Lakshminarasimhan, and Angelaki 2023). The outcomes of this behavioral experiment consequently imply that learning not only modify an animal's internal cognitive states but also influence how these cognitive states are expressed through their bodily actions. This adjustment in active sensing likely assists the animal in more effectively gathering pertinent information from the surroundings and translating it into purposeful actions. Such findings are not possible under restrained conditions.

The hippocampus plays a central role in processing the spatial arrangement of items in the visual scene. In monkeys, while hippocampal lesion leaves the capacity to learn discrete objects-reward associations intact, it significantly impairs the memory retrieval if subject require to know not only the objects, but also something about their spatial arrangement in the scene (Gaffan 1991, 1994). The involvement of hippocampus in spatial learning depends on the frame of reference (allocentric vs. egocentric). Lesion of the hippocampus in freely-behaving monkeys results in significant memory impairment in the absence, but not the presence, of local cues (Lavenex, Amaral, and Lavenex 2006). These results suggest that the monkey hippocampal formation is critical for the establishment or use of allocentric, but not egocentric, spatial representations. Specifically, any task in which subjects always approach a testing apparatus from the same direction, which is the condition for most of the computerized tasks of memory, cannot rid the task of its egocentric component, and therefore cannot be considered purely spatial relational. It has been argued that egocentric strategies employed in shorter-time windows might render the task hippocampal-independent (Banta Lavenex and Lavenex 2009). Lastly, restricting animals' movement alters the network state dynamics of the hippocampus, and reduces not only the number of activated cells but

also their response selectivity (Thome et al. 2017; Aghajan et al. 2015; T. C. Foster, Castro, and McNaughton 1989). The findings from my dissertation and prior research underscore the importance of developing behavioral experiments that contain a broader range of elements from natural behaviors. These elements might include aspects like those that depend on the subject (e.g., free navigation, situated perception) and aspects that vary according to the situation (e.g., environmental sensory enrichment and temporal sequencing). Embracing a more naturalistic approach to behavior can potentially lead to a profound transformation in our understanding of the relationship between the brain and behavior.

Appreciating the importance of spacetime features, active sensing, and body movements in memory processing, I devised a task in the Treehouse to assess memory in freely moving macaques, which incorporates a distinctive combination of features designed to closely mimic memory processes in natural settings. In this sequential item-in-context associations task: 1) events are embedded in unique spatial and temporal contexts within a 3D real environment, 2) each trial unfolds sequentially, 3) it necessitates flexible learning of contingent associations, and 4) it facilitates the testing of multiple item-context sets on distinct niches (e.g., sides of the Treehouse) within the same session. The monkeys adeptly learned multiple sets of 4-item sequences, including numerous unique item-context associations, with no apparent limitations related to interference-based capacity. While not discussed in this dissertation, I also evaluated their long-term memory of remote sets, which the animals learned 2-5 weeks prior to the retention test and had not encountered since. Both animal subjects exhibited significantly higher task performance (success probability) on early trials (first 10 trials) and overall, indicating memory savings for remote sets even after weeks of no exposure (unpublished data).

The arbitrary nature and the spatiotemporal contingencies of associations in this task can put it in the category of event/episodic memories. Episodic memory was originally described as unique to humans (Tulving and E 1972), however, decades of research now demonstrate convincingly that animals share some of the core features of episodic memory in humans (Allen and Fortin 2013; Nicola S Clayton, Bussey, and Dickinson 2003; Crystal 2021). Although still a matter of debate, some of the more established

features are content and structure. Episodic memories include information about the (spatiotemporal) context of events integrated into a sequence of unified coherent representations, and these memories can be flexibly expressed to facilitate adaptive behavior in novel situations (Crystal 2021; Allen and Fortin 2013).

Potential cases of episodic memory in nonhumans have been documented in a diverse range of species. Clayton and Dickinson operationally defined episodic memory as one that provides information about the 'what' of events as well as 'when' and 'where' they happened (N S Clayton and Dickinson 1998; D. Griffiths, Dickinson, and Clayton 1999). They showed that food-caching scrub jays can remember what foods they hid in which locations at which points in time providing the first evidence of what-where-when memory in nonhumans. Later a similar paradigm was used for freely moving rhesus monkeys. Although monkeys demonstrated long-term (~25hrs) memory for the type and location of food, they failed to demonstrate sensitivity to when they acquired that knowledge (Hampton, Hampstead, and Murray 2005). Other studies in primates that only addressed the where component, testing memory for food locations, provided evidence of long-term spatial memory revealing a capacity to remember the positions of accessible and non-accessible baited sites for periods up to months. Similar what-where-when approaches have also been adapted to other species including humans (Allen and Fortin 2013). It has been argued that the integrated what-where-when approach may be overly restrictive and as such other forms of memory for events in context should also be considered episodic, such as memories involving a subset of the two (e.g., what-where). The what-where approach focuses on the memory for the spatial context of episodic memory and asks animals to remember specific what-where associations (i.e., specific items in specific places). In computer-based stationary item-in-context task paradigms which is a version of what-where, the “what” component refers to the presentation of specific objects, and where refers to the unique visual scene in the background and the task of the animal is to learn what object is rewarded on which visual context. Using this paradigm, early studies demonstrated that monkeys can learn a list of what-where problems (Gaffan 1994; Elisabeth A. Murray, Baxter, and Gaffan 1998). Our previous results also showed that monkeys can learn to associate objects embedded in more naturalistic images to reward (Chau et al. 2011; Hussin, Abbaspoor, and Hoffman 2022) and demonstrate

memory savings for these unique scenes after a year of no exposure (Hussin, Abbaspoor, and Hoffman 2022). Other studies in monkeys demonstrate their ability in learning spatial discrimination, object discrimination, object recognition, and relational tasks, all of which can be considered important prerequisites for episodic memory (Angeli, Murray, and Mishkin 1993; Hampton, Hampstead, and Murray 2004; Lavenex, Amaral, and Lavenex 2006; Malkova and Mishkin 2003; E A Murray and Mishkin 1998; Parkinson, Murray, and Mishkin 1988). The findings of this dissertation add to this body of knowledge by showing that macaques are capable of learning distinct sets of arbitrary associations in face of great interference from other elements in the environment, flexibly switch their choices depending on the context they are situated in and remember this information after weeks.

7. Chapter 2: Interspecies differences in hippocampal theta oscillation: the case for its role in active sensing

In chapter two, I looked into the network state dynamics of macaque hippocampal CA1 in 3 macaque monkeys and under different behavioral conditions. The results showed that in both head-restrained and freely-behaving subjects that were engaged in a hippocampal-dependent memory-task, beta2/gamma oscillations dominated the oscillatory mode of the CA1. In contrast, during offline states of rest or sleep, the dominant gamma oscillations were replaced by a strong theta activity. It is noteworthy that I found bouts of theta activity also in awake behaving macaques, but these theta episodes were less prevalent and weaker than theta during offline states. Consistent with this behavioral segregation, cross-frequency coupling also revealed negative (or no) correlation between these two rhythms.

I also showed that spiking pattern of hippocampal neurons phase lock to the local oscillations peaking at theta (3–10 Hz), beta2/slow gamma (20-35Hz), and high-gamma/ripple band (60-150Hz). Because spike-field coherence was measured during behavior, the strong peak on the theta frequency band was surprising; however, I further demonstrated that the spike-theta coherence partially arise from the non-oscillatory slow component of sharp-wave ripples not theta rhythms. The same phenomenon has also

been observed in the human hippocampus (Tong et al. 2021). Because in primates, the negative deflection of SWRs contain spectral power within low frequencies (2-10Hz, (Tong et al. 2021; Leonard et al. 2015)), it is imperative to account for these non-oscillatory events before reporting the strength and prevalence of theta activity. In primates, duration of reported bouts of theta during freely-moving behavior is on average ~400ms (~3 cycles of a 8Hz oscillation (Abbaspoor, Hussin, and Hoffman 2023; M Aghajan et al. 2017) which roughly correspond to the duration of negative deflections accompanying SWRs (Abbaspoor, Hussin, and Hoffman 2023). It is important to note that SWRs also occur during active exploration/memory retrieval in primates (Leonard et al. 2015; Leonard and Hoffman 2017; Norman et al. 2019, 2021). This suggest that some of the previously reported power in theta band might have been contaminated with the power in non-oscillatory negative deflections.

Previously, several other studies have investigated the oscillation modes during awake and sleep in macaques (Talakoub et al. 2019; Takeuchi et al. 2015). In chapter 2, I built upon those reports and extended them. First, I performed the recordings in a targeted part of the hippocampus (pyramidal layer of CA1), in freely-moving macaques that were engaged in a memory task. These elements are important because, as discussed in the introduction, the strength of theta rhythms changes as a function of layer, area of recording, and behavior. Strongest theta in rats/mice is recorded during running, and restraining these animals can hinder or abolish theta activity (T. C. Foster, Castro, and McNaughton 1989). Therefore, it was imperative to characterize the theta dynamics in moving macaques. For recordings, we have used microelectrodes that were also used in rodents for such investigations. This is important because it has been argued that differences in theta rhythms in primates and rodents might be due to methodological differences in recordings (impedance, macro vs micro (Ulanovsky and Moss 2007)). Differences in analytical methods can lead to changes in results and therefore leading to unfair comparisons. As such, to characterize the oscillations and also to make a fair comparison, I also used the same methods that were previously used in rodent studies. Finally, we also recorded spiking activity. Genuine strong oscillations usually entrain local spiking activity. We showed that spiking activity in hippocampal neurons of macaques, in contrast to rats, doesn't show theta rhythmicity. A finding that supports the interpretation

that theta activity might not readily be engaged in processes that were described in rodents. So, what is theta activity doing in primates? I think to answer this question, we should put the primate findings in the context of cross-species analysis.

A comparative analysis across various animal species unveils disparities in the rhythmicity, power, prevalence, and behavioral contingencies of hippocampal theta oscillations. Different animal species exhibit specialized and distinct forms of locomotion and exploration strategies. In natural behavior, motor behaviors associated with information gathering play a crucial role in the active sensing process, defined as actively locating and acquiring sensory information using a motor sampling routine (Schroeder et al. 2010). The role of hippocampus in learning and memory have been linked to various types of active sensing across animal species (Fotowat et al. 2019; Meister and Buffalo 2016; Zhu, Lakshminarasimhan, and Angelaki 2023; Bland and Oddie 2001). Is it possible that variations in theta oscillations might, at least in part, be accounted for by differences in the expression of behavior, active sensing, and cognitive demands?

Here, I will examine the research on hippocampal theta oscillations across various animal species, aiming to provide a context for the findings in the current dissertation. I will draw two primary conclusions: 1) during active behavioral states, theta rhythms are associated with different forms of active sensing across species, and 2) the mechanisms underlying theta activity during sleep or immobility may differ from those observed during wakefulness.

7.1 Rat/Mouse

Rats and mice are nocturnal animals with poor visual abilities that heavily rely on their proximal senses, namely olfaction and somatosensory sensations (Kaas, Qi, and Stepniewska 2022; Burn 2008). Their exploration of the environment involves a combination of sensory activities, such as sniffing for acquiring odor information, whisking to gather tactile information, and walking (Ranade, Hangya, and Kepecs 2013). These activities show strong synchronization (Ranade, Hangya, and Kepecs 2013) and their regularity all fall within the frequency range of the hippocampal theta rhythm (Ranade, Hangya, and Kepecs 2013; Berg, Whitmer, and Kleinfeld 2006; Grion et al. 2016; Joshi

et al. 2023). As have been posited before (Komisaruk 1970) sniffing and whisking show a strong phase synchronization with ongoing theta rhythms in the hippocampus, and this relationship can vary as a function of learning state (Macrides, Eichenbaum, and Forbes 1982) or environmental-behavioral conditions (Grion et al. 2016; Berg, Whitmer, and Kleinfeld 2006).

A recent rat study addresses the question of whether hippocampal local dynamics can be influenced by or coordinated with the detailed structure of locomotor processes. The findings of this study reveal a strong synchronization between the ongoing steps of the animals and various aspects of hippocampal dynamics, including hippocampal theta rhythms, multiunit activity (MUA), and the microstructure of spatial representations. What's particularly interesting is that this coordination swiftly adapts to changes in cognitive demands. These results strongly indicate the existence of a dynamic coordination between the cognitive representations and the peripheral motor processes (Joshi et al. 2023).

Overall, these findings implies that the coherence between sensory-motor systems and hippocampal theta rhythms is particularly enhanced during periods when the rat is actively gathering sensory information. This coherence might, in turn, improve the efficiency of integrating stimulus information into memory and decision-making centers . The dynamics synchronization between movement-related active sensing parameters and hippocampal local oscillations have been reported in other species.

7.2 Bats

Echolocating bats have two distinct modes of exploratory behavior: (i) "exploration without locomotion," characterized by low velocity and the use of echolocation for environment exploration while nearly stationary, and (ii) "exploration by locomotion," where the bat is actively moving and employs lower call rates. Hippocampal recordings in bats reveal the presence of a clear theta oscillation, peaking between 5-7 Hz, but this phenomenon is exclusively observed during the first behavioral mode, which corresponds to echolocation. Theta oscillations in bats manifest in short (1-2 seconds), intermittent bursts with significant amplitudes and exhibit a depth profile similar to that observed in rodents, with

increasing theta amplitude toward the hippocampal fissure. Interestingly, theta bouts can also be recorded during sleep; however, the power spectrum analysis shows no prominent theta spectral peak when computed over the entire sleep session. This suggests that theta oscillations are only sporadically present during sleep and occupy a relatively small percentage of the sleep duration. Neuronal firing rates exhibit a slight reduction during theta episodes compared to non-theta periods, although there is a discernible moderate influence of theta bouts on neural firing patterns (Ulanovsky and Moss 2007).

7.3 Ferret

A recent study explored hippocampal theta rhythms in rats and ferrets under comparable behavioral situations (Dunn et al. 2022). In ferrets, prominent hippocampal theta waves are observed during locomotion, exhibiting a depth profile and speed/power (frequency) relationship similar to those observed in rats. However, there are notable differences in the characteristics and behavioral associations of theta activity in ferrets when compared to rats and mice. Firstly, the frequency of theta waves during locomotion in ferrets (4 – 7 Hz) is lower than the typical range seen in rats (5 – 12 Hz). Secondly, in rats, theta oscillations transition into large irregular activity during periods of immobility, whereas in ferrets, hippocampal theta oscillations remain robust during both movement and immobility. Significantly, theta oscillations are stronger during immobility periods associated with rewards, in contrast to holding or spontaneous immobility outside of the task, and this effect is primarily observed in the SLM layers of the hippocampus. Interestingly, error trials exhibit a similar pattern of peak range values across the probe, suggesting that reward consumption may not be necessary for the observed enhancement.

Theta oscillations during immobility (hold or reward) and movement display distinct features in ferrets. While theta activity during movement exhibits a characteristic sawtooth shape, similar to rats, immobility-related theta oscillations lack the sawtooth waveform and display a more sinusoidal pattern. Moreover, the administration of atropine suppresses theta oscillations during immobility, with significant reductions in peak range

observed in all animals and regions around the cell layer. However, during movement, atropine has no effect on the prevalence of theta oscillations. Furthermore, immobility-related theta during both the Hold and Reward epochs appears to be generated from common mechanisms. Power spectral densities (PSDs) in the Reward and Hold epochs do not display the harmonic peaks evident in Run epoch PSDs, suggesting that the oscillations during both Hold and Reward epochs have similar waveforms. Additionally, the application of atropine abolishes theta during both Hold and Reward epochs, with significantly reduced peak range values for both epochs.

The findings of this research are important because they show that, even under similar behavioral conditions, differences in the relationship between theta activity and behavioral states exist across species.

7.4 Sheep

During periods of alert wakefulness in sheep, the hippocampus exhibits a prominent theta oscillation ranging from 4 to 10Hz, alongside gamma band oscillations. Notably, the power of theta oscillations is more pronounced during phases of higher locomotion speed compared to slower moments. However, when examining the entire spectrum of movement speeds, a regression analysis of theta power only revealed weak correlations with speed or acceleration. Additionally, there is a robust phase-amplitude coupling between the theta frequency band and high gamma range (55-90Hz), but this coupling is not observed with low gamma frequencies (30-50Hz). It's important to note that the strength of this relationship depends on the speed of locomotion. While the study recorded a small population of cells, the majority of them exhibited synchronization with theta oscillations. An intriguing finding was the variability in the activation of theta-modulated cells during different types of movements. For instance, when the sheep was guided through the arena with its head directed upward, a theta-modulated neuron displayed preferential activity. In contrast, when the same path was traversed with the head facing forward or downward, the cell remained silent (Perentos, Krstulovic, and Morton 2022).

7.5 Nonhuman and human primates

Primates possess high acuity color and stereovision, granting them the ability to perceive distant objects in during daylight (Kaas, Qi, and Stepniewska 2022). Consequently, their environmental exploration primarily relies on visual inputs, utilizing the specialized mechanism of saccadic eye movements, the rapid and repetitive displacement of a high-acuity region of the retina to sample different locations in the visual environment (Fuchs 1967).

In macaques, the initiation of saccadic eye movements is linked to a transient alignment of theta (3–8 Hz) rhythms (Hoffman et al. 2013; Jutras, Fries, and Buffalo 2013; Doucet et al. 2020). This phase clustering (PC) phenomenon varies depending on the specific task and the visual stimuli present in the field of view (Hoffman et al. 2013; Doucet et al. 2020). For instance, saccades made on a solid gray background exhibited significant PC values at approximately 4 Hz, while saccades towards specific targets predominantly showed significant PC values in the 4 to 8 Hz range. Additionally, saccade characteristics were found to correlate with the phase and amplitude of local field potentials (LFPs): saccade direction correlated with delta (≤ 4 Hz) phase, and saccade amplitude correlated with theta (4 – 8 Hz) power (Doucet et al. 2020). The reliability of this phase reset is indicative of subsequent recognition (Jutras, Fries, and Buffalo 2013). Conversely, frequencies in the alpha/beta range (8 – 16 Hz) exhibited higher clustering around the onset of fixations (Doucet, Gulli, and Martinez-Trujillo 2016). These findings suggest that hippocampal LFPs are modulated at specific frequencies during saccade-fixation sequences, influenced by both sensory and motor components. However, despite the synchronization between step timing and hippocampal theta activity in rats, the frequency of PC is not a direct consequence of saccade rate (Jutras, Fries, and Buffalo 2013; Hoffman et al. 2013). Interestingly, single-unit neuronal activity increased only at the onset of saccades directed at a visual target, not during saccades to a solid background (Doucet et al. 2020). This implies that saccade-related signals, likely originating outside the hippocampus, influence the phase of LFPs in the hippocampus without necessarily altering the firing rate of individual neurons. It's worth noting that a previous study demonstrated changes in hippocampal unit activity during spontaneous saccadic eye movements in complete darkness (Ringo et al. 1994). Intriguingly, similar saccadic

modulations were also observed in the medial septum (S Sobotka and Ringo 1997). Finally, delivering hippocampal stimulation immediately after a saccade in monkeys resulted in larger late components in the local evoked potentials of extrahippocampal areas compared to stimulation without a saccade, suggesting that saccadic modulation can also alter functional connectivity between the hippocampus and other brain regions (Stanislaw Sobotka, Zuo, and Ringo 2002).

More recently the relationship between hippocampal theta rhythms, free navigation, and saccadic eye movements have been addressed in freely moving macaques (Mao et al. 2021). Power spectral analysis during free navigation revealed two peaks at 1-4Hz and 12-30Hz suggesting that rodent-like theta (4-10Hz) is not the dominant mode of oscillation in freely moving macaques. This is consistent with previous reports (Talakoub et al. 2019) and the results of the current dissertation (Abbaspoor, Hussin, and Hoffman 2023). Despite this, intermittent brief bouts of theta activity were recorded during the movement onset and during saccadic eye movements. Hippocampal LFP consistently showed modulation linked to saccade events. Consistent with studies in headfixed monkeys (Doucet et al. 2020), theta band power was positively correlated with saccade magnitude. Based on these findings, it was suggested that the relationship between theta activity and saccade in macaques may be analogous to that between theta and locomotion in rodents. In addition, although a large number of neurons showed spike-LFP phase locking with theta activity, theta phase precession was only present in a minority of cells (12/599 neurons for low theta and 13/599 neurons for theta), which were all tuned to various spatial variables (Mao et al. 2021).

Much like the findings in macaques, humans also exhibit significant hippocampal phase clustering within the theta frequency range (4-8 Hz) following the onset of visual images or saccades (Katz et al. 2020). This phenomenon is accompanied by modulations in single-unit neuronal activity both before and during the saccade (Katz et al. 2022; Andrillon et al. 2015). These modulations are characterized by an increase in inhibition, leading to reduced firing rates in potential pyramidal cells and increased firing rates in potential inhibitory cells (Katz et al. 2022). The amplitude of the post-saccade event-related potential (ERP) is correlated with the magnitude of firing rate reduction in putative

inhibitory cells during the peri-saccadic period (Katz et al. 2022). These observations suggest the presence of a corollary discharge signal that reaches the hippocampus, potentially activating parvalbumin interneurons, which, in turn, effectively inhibit pyramidal cells, resulting in the phase resetting of membrane potential oscillations (Katz et al. 2022; Martinez-Trujillo 2022).

Moreover, the ERPs associated with saccades and image onsets exhibit distinct characteristics, with the response to image onset peaking in a lower-frequency range (delta, 1-3 Hz) (Katz et al. 2020). The population of neurons modulated by image onset is separate from those influenced by saccade-related events and the neurons responsive to image onset show a peak increase in firing rates a considerable time after the modulation observed in saccade-related units (Katz et al. 2022). This indicates that, within the medial temporal lobe (MTL), the units processing visual information following image onset differ from those responding to saccade-related information. If the peri-saccade modulation were solely due to extraretinal signals, it should persist in the absence of light. Prior research with humans and non-human primates suggests that saccade-related ERPs and neuronal activity modulation can be observed in darkness or on blank screens (Andrillon et al. 2015).

Further evidence supporting the coordination of movements related to active sampling and hippocampal oscillations comes from studies on marmosets. Marmosets frequently execute rapid head-gaze shifts to explore their visual environment. When aligning local field potentials (LFPs) with the peak velocity of these head movements, the 4-15 Hz frequency range, with a peak in the theta frequencies (4-10 Hz), is most prominent around the onset of head movement. This theta phase-resetting is accompanied by the modulation of neuronal firing in both potential interneurons and pyramidal cells. Differences in activation latencies and the proportion of various modulation types suggest that phase resetting may be causally linked to interneuron activation, followed by a range of modulations in pyramidal cells (Martinez-Trujillo et al. 2023).

7.6 Conclusion

In 1972, Johnathan Winson published a paper in which he conducted a review of the behavioral correlates of hippocampal theta activity in various species based on the data available at that time. He concluded that "It is suggested that the plethora of theories and the contradictions that have arisen reflect a core difficulty in the interpretation of the data in this field due to the implicit assumption that there must be a correlation of theta activity with specific behaviors that will hold across species. It is concluded that this assumption is untenable and that the data indicate that there is a distinct set of theta-correlated behaviors for each species. These behaviors may correspond to important natural behaviors of the species." (Winson 1972)".

In this context, I have examined the characteristics and behavioral connections of hippocampal theta rhythms across different species, taking into account the latest research findings. This comparative approach yields several key findings: 1) theta activity is consistently observed in the hippocampus of all recorded mammalian species, 2) the properties of theta rhythm, including its frequency, power, waveform, and prevalence, exhibit significant diversity across species, 3) more importantly, on the surface, the behavioral contingencies of theta rhythms seem to be distinct across species.

Variations in behavioral training approaches, analytical methodologies, and data recording methods pose challenges when attempting to make a fair comparison across studies. It's important to acknowledge that some of the inconsistencies in findings may be due to these variations. However, even when experiments are conducted under identical conditions, distinctions in the correlation between theta activity and behavioral states persist among different species (Dunn et al. 2022). The question then arises whether we can identify shared behavioral principles that could help explain the observed differences in theta across species?

Traditionally, influenced by extensive research on rodents, it was theorized that theta rhythms is linked to spatial navigation and memory processes (encoding and retrieval) (György Buzsáki and Moser 2013). However, findings from different species challenge this perspective on theta activity. For instance, many spatial navigation and memory

models are built on the assumption of continuous theta oscillations. Yet, evidence from bats, nonhuman, and human primates indicates that theta oscillation occurs in brief bursts (<2sec), and accounts for less than 15% of the awake recording time. It seems unlikely that memories are encoded and retrieved only a couple of times a minute. Thus, in these species, models of oscillatory encoding and retrieval of memories via the theta cycle may not be applicable (Michael E Hasselmo, Bodelón, and Wyble 2002).

Furthermore, in some species, theta activity is recorded during awake immobility (e.g. ferrets, cats and restrained primates during visual search), and in some of the species theta doesn't show correlation with speed/acceleration (e.g. sheep) and in others it is too infrequent during free navigation (e.g. primates), to be significantly involved in their navigational mechanisms. Nevertheless, despite differences in the dynamics of theta rhythms, the presence of place cells has been documented in some nonrodent species including bats (Ulanovsky and Moss 2007), nonhuman primates (Courellis et al. 2019; Hori et al. 2003; Mao et al. 2021; Hazama and Tamura 2019), and humans (Poo et al. 2016). Additionally, in line with the advanced distant vision of primates, a substantial population of spatial view cells has been observed in macaques (Rolls 1999), marmosets (Martinez-Trujillo et al. 2023), and humans (Rolls 2023). These cells exhibit maximum activity when the animal focuses on a specific area of the environment. The discovery of place/spatial view cells in the hippocampus of these species supports the idea that hippocampal pyramidal neurons play a role in spatial processing. However, in non-rodent species like bats and nonhuman primates, the interaction between theta oscillations and place-cell activity in the hippocampus of freely moving animals is rather limited and weak. Hippocampal neurons can encode self-position without a significant influence from this oscillation (Courellis et al. 2019; Eliav et al. 2018; Ulanovsky and Moss 2007). Based on these findings, it has been suggested that two aspects of spatial navigation should be distinguished: exploration and self-position. Exploration pertains to actions related to building a mental representation of the environment, whereas self-position refers to determining one's location within that environment (Courellis et al. 2019). In the case of nocturnal burrowing animals like rodents, these two aspects of navigation are closely linked because there are fewer distant sensory cues available to construct a spatial map before moving through it. Notably, in rodents, the relationship between these neural

signals is not fixed but influenced by behavioral characteristics that may reflect the differentiation between exploration and self-position. In species where these two navigational components are less temporally intertwined, the association between theta oscillations and place cell activity is also weaker. For instance, in primates, the typical pattern is to visually explore the surroundings before actively moving through them.

Based on the emerging comparative data regarding hippocampal theta oscillations, a more comprehensive framework can be formulated, wherein the variations in theta rhythms among different species are influenced by how these animals utilize their sensory systems to explore the environment. Across species, a strong correlation appears to exist between recorded hippocampal theta rhythms and active sensory engagement. While sensory processing was once viewed as a passive mechanism where biological receptors like photoreceptors and mechanoreceptors convert physical stimuli into neural signals, recent discoveries suggest otherwise (Schroeder et al. 2010). It's becoming clear that most sensory processing is actually an active process, primarily shaped by motor and attentional sampling routines. Due to the rhythmic nature of these motor routines and their synchronization with ambient rhythms in sensory regions, sensory input tends to exhibit a rhythmic pattern. Such active rhythmic sampling of the environment might coordinate with ongoing brain rhythms or influence their expression. Given the distinct structural organizations of bodies across species, active sensing involves unique sensory-motor processes in different animals. As a results, if hippocampal theta rhythms are associated with or dependent on active sensing in animals, theta activity is expected to emerge during various behavioral expressions and specific conditions. But generally, during awake states, we might expect maximal theta activity when sensory information arrives at high rates or changes rapidly.

The above explanation appears to conflict with certain observations, including the findings of the present dissertation, which indicate that in primates, theta activity becomes a prominent rhythmic oscillation during sleep periods when the influence of sensory systems is reduced. It's plausible that the mechanisms generating sleep-associated theta rhythms differ from those responsible for theta rhythms during alert wakefulness. In rodents, hippocampal theta oscillations have been categorized into two types: type 1,

termed 'atropine-resistant' theta, which occurs during locomotion, and type 2, labeled 'atropine-sensitive' theta, which is present during immobility in response to sensory stimuli (Kramis et al. 1975, Robinson, T.E. 1980, Bland et al. 2001). Type 2 theta has been proposed to play a role in sensory processing relevant to the initiation and maintenance of voluntary motor behaviors (Bland et al. 2001). Similarly, recent observations in ferrets revealed that atropine disrupted theta during immobility while leaving theta during locomotion unaffected. It's conceivable that a similar differentiation between different types of theta coexists in the primate hippocampus through different mechanisms.

8. What shall the primate hippocampus do in the absence of continuous theta activity?

The findings of chapter 2 show that during awake active behavioral states, macaque CA1 is dominated by supratheta oscillations such as beta and gamma. Gamma oscillations are involved in spike-time dependent plasticity, intra-areal dynamic reconfiguration, and cell assembly formation, all of which are postulated to be critical for memory formation. I will discuss how gamma can engage in these operations and how these operations are linked to memory.

8.1 Gamma and episodic memory

Numerous studies across species indicate that gamma oscillations in the hippocampus (30 – 90 Hz) play a crucial role in both the formation and retrieval of memories. The connection between memory and gamma oscillations can be generally classified into two categories: 1) enhancement of gamma oscillation power or alterations in its characteristics during memory formation or retrieval, and 2) memory-related modulation of the intra- and inter-areal synchronization of gamma oscillations. I will delve into the findings of several of these studies.

8.1.1 Local hippocampal gamma oscillations and memory

In rats, distinct subtypes of gamma oscillations have been recorded. It has been suggested that entorhinal cortex-associated fast gamma oscillations in the SLM of CA1 facilitates memory formation, while CA3-indued slow-gamma oscillations in the SR can support memory retrieval (Colgin and Moser 2010). Several pieces of evidence support these theories. These studies have collectively discovered: 1) an increase in the power of CA3-slow and EC-fast gamma during moments indicative of memory retrieval and encoding (M. Takahashi et al. 2014; Cabral et al. 2014), 2) variations in the phase-amplitude coupling between local theta rhythms and slow and fast gamma during retrieval and encoding (Tort et al. 2009; Shirvalkar, Rapp, and Shapiro 2010), 3) distinct spatial sequence coding during slow and fast gamma rhythms, with slow gamma power and phase locking of spikes increasing during prospective coding, and fast gamma power and phase locking increasing during retrospective coding (Bieri, Bobbitt, and Colgin 2014; Zheng et al. 2016). Additionally, Scopolamine, a drug that impairs memory encoding but not memory retrieval, has been observed to reduce fast gamma rhythms (~60–120 Hz) while leaving slow gamma rhythms (~20–40 Hz) unaffected (Newman et al. 2013). More recently, it has been shown in a mouse model of Alzheimer's disease, that reduced slow gamma amplitude, and phase-amplitude coupling to theta oscillations coincide with spatial memory loss. Restoring the slow gamma oscillations in the hippocampus by frequency-specific (40Hz but not 80Hz) optogenetic stimulation of medial septal parvalbumin neurons rescued spatial memory in mice (Etter et al. 2019). It's worth noting that there are also studies with results that don't align easily with the idea of slow, and fast gamma serving distinct memory functions (Yamamoto et al. 2014; Trimper, Stefanescu, and Manns 2014; Kemere et al. 2013).

In monkeys, gamma-band LFP power is enhanced during successful memory formation (Jutras, Fries, and Buffalo 2009). Additionally, the synchronization between local spiking activity and gamma oscillations strengthens as a function of repetition in a memory task (Montefusco-Siegmund, Leonard, and Hoffman 2017), and this modulation during encoding predict greater subsequent recognition memory performance (Jutras, Fries, and Buffalo 2009).

Intracranial studies of human memory also report increases in the power of gamma frequencies during successful compared with unsuccessful memory operations (B. J. Griffiths et al. 2019; Herweg, Solomon, and Kahana 2020). This is sometimes associated with a decrease in theta power. (Fellner et al. 2019; Greenberg et al. 2015; Herweg, Solomon, and Kahana 2020; Long and Kahana 2015; Sederberg et al. 2003, 2007; B. C. Lega, Jacobs, and Kahana 2012; Burke et al. 2014; Weidemann et al. 2019).

8.1.2 Interareal gamma phase synchronization and memory:

Along with changes in the power of hippocampal gamma oscillations, elevation in inter-areal gamma-band phase synchronization has also been reported in rats, monkey, and human (Fell et al. 2001).

Recently, we recorded neural activity in the hippocampus and retrosplenial cortex of macaques as they visually selected targets in year-old and newly acquired object-scene associations. We found that although hippocampal activity was unchanging with memory age, remote retrieval was associated with decreased gamma-band synchrony between the hippocampus and each neocortical area (Hussin, Abbaspoor, and Hoffman 2022). Another study found functional differences and frequency-specific interactions between HPC and PFC of monkeys learning object pair associations. Theta-band HPC-PFC synchrony was stronger after errors, was driven primarily by PFC to HPC directional influences and decreased with learning. In contrast, alpha/beta-band synchrony was stronger after correct trials, was driven more by HPC and increased with learning (Brincat and Miller 2015).

In humans, neocortical alpha/beta (8 to 20 Hz) power decreases reliably precede and predict hippocampal “fast” gamma (60 to 80 Hz) power increases during episodic memory formation; during episodic memory retrieval, however, hippocampal “slow” gamma (40 to 50 Hz) power increases reliably precede and predict later neocortical alpha/beta power decreases (B. J. Griffiths et al. 2019).

The reviewed evidence suggests that distinct forms of gamma oscillation, and other types of supra-theta oscillations such a beta oscillation, can be found within the hippocampal, each of which might have a complementary role in the neural processes of memory in primates. What are the mechanisms through which gamma oscillations can facilitate the formation and expression of memories?

8.2 The mechanistic link between gamma oscillations and episodic memory

8.2.3 Gamma oscillations and spike timing-dependent plasticity

Our ability to form memories hinges upon long-term potentiation of synaptic transmission in the hippocampus, a process through which synaptic connections between two neurons are strengthened (Bliss and Collingridge 1993; Lynch 2004; Malenka and Nicoll 1999). Spike timing-dependent plasticity (STDP) is a specific form of synaptic plasticity whereby the synaptic modification depends on (i) a presynaptic spike leading to the release of presynaptic glutamate, which promotes the opening of postsynaptic NMDA receptors; and (ii) the backpropagation of a postsynaptic spike leading to the unblocking of the Mg2+ block from the same postsynaptic NMDA receptors (Bliss and Collingridge 1993; Caporale and Dan 2008; H Markram, Gerstner, and Sjöström 2012). It has been suggested that the presynaptic action potential must precede the postsynaptic action potential by ~10–20 ms for STDP to occur (H Markram et al. 1997; Levy and Steward 1983; Bi and Poo 1999); please note that this is mostly a crude estimate, the exact temporal window can depend on cell types, affected dendritic compartment, and brain area). Although STDP depends upon correlated pre- and postsynaptic spiking, a solitary presynaptic spike is unlikely to induce postsynaptic spiking; Instead, convergent input is required (Bliss and Collingridge 1993; Sjöström, Turrigiano, and Nelson 2001).

Gamma oscillations can establish the necessary conditions for STDP. Their cycle duration falls within the optimal time frame for STDP. Furthermore, gamma oscillations can enhance the coordination of convergent inputs by synchronizing the firing of multiple presynaptic neurons, leading to a more potent depolarizing effect on the target

postsynaptic neuron than what would occur with isolated firing. Although theoretically, oscillations of any frequency could synchronize neuronal activity, gamma oscillations stand out as particularly suitable. They provide a relatively brief window of excitability, ensuring near-perfect synchronization of neuronal firing, while also featuring oscillatory cycles of adequate length to allow neurons to return to their resting state before the next excitatory phase of the oscillation (B. J. Griffiths and Jensen 2023). In vitro studies demonstrate that in neuronal networks that are engaged in high-frequency oscillations, synaptic modifications remain highly sensitive to the phase relation between periodic presynaptic and postsynaptic activity. When postsynaptic neurons receive synchronized, oscillatory inputs, synapses undergo long-term potentiation (LTP) when EPSPs coincided with the peaks of the oscillations but exhibited long-term depression (LTD) when EPSPs coincided with the troughs (Wespatat, Tennigkeit, and Singer 2004). These results suggest that precise phase synchronization of discharges in distributed networks is critical for the direction of synaptic modification. We showed that similar to previous studies, in the hippocampal CA1, the coupling between local field potential (LFP) oscillations and the spiking of single neurons can be highly precise across cell types. Neural networks simulation show that such precise spike-LFP coupling can be achieved, in the face of heterogeneous membrane properties and total input, under quite general conditions by the combination of STDP, and neuronal ensemble oscillations invariant to differences in initial excitation (Muller, Brette, and Gutkin 2011). More direct support for the idea that gamma oscillations may play an important role in hippocampal function comes from the finding that experimentally induced gamma oscillations produce a prolonged enhancement of recurrent excitatory connections between CA1 pyramidal neurons (Whittington et al. 1997). These observations suggest that gamma oscillations may be an important factor determining the temporal activity relationships that are critical for the function synaptic plasticity which further can support memory.

8.2.4 Gamma oscillations and dynamic coordination

Perception and cognition rely on context-dependent selection of relevant inputs and the control of flexible interareal brain interactions on behavioral time-scales that are faster than structural synaptic changes. In particular, strength and direction of influences between areas, must be reconfigurable even when the underlying structural connectivity is fixed (Varela et al. 2001; Bressler and Kelso 2001).

Simulations of interacting circuit models with oscillatory behaviors and fixed structural connectivity demonstrate that the same structural motifs can produce a variety of effective motifs with distinct strengths and directions of connectivity organized into different families of interactions (Battaglia et al. 2012). Due to nonlinearity in dynamics, the symmetrical relationships between the nodes in the structural system can be disrupted, resulting in dynamics with multiple stable states. This dynamic multi-stability enables the controlled transition between effective motifs within the same family without requiring any structural modifications. This means that, without making modifications to the long-rage excitatory or local connections, the flow of information can rapidly switch from A→B to B→A. Shifting between effective motifs belonging to different families, however, cannot happen without changes in the strength of the delay of inter-areal couplings, even if the overall topology of the underlying structural motif needs to remain unaltered. Such rapid dynamic reconfiguration of functional connectivity can facilitate the regulation of both the efficiency and the directionality of information transfer in short-time scales which is critical for cognition.

Experimental work on such rapid reconfiguration comes from observations that information flow can change around the time of high-frequency oscillations. For example, in hippocampus, during sleep, there is a rapid cortical–hippocampal–cortical loop of information flow around the times of SWRs (Rothschild, Eban, and Frank 2017). Patterned spiking in auditory cortex (AC) precedes and predicts the subsequent content of hippocampal activity during SWRs, while hippocampal spiking patterns during SWRs predict subsequent AC activity. It has been proposed that such loop in information flow

can bias the content of experiences being replayed and thus consolidated into long-term stores.

In the primary visual cortex, the local phase of gamma-band rhythmic activity exerts a stimulus-modulated and spatially-asymmetric directed effect on the firing rate of spatially separated populations within the primary visual cortex. The relationships between gamma phases at different locations, often described as phase shifts, corresponded to a stimulus-modulated propagation of gamma-band waves along spatial directions that maximized information transfer. Transient changes in the spatial arrangement of phase patterns linked to the direction of gamma wave propagation, coinciding with an increase in the amount of information flowing along the instantaneous direction of the gamma wave. These effects were specific to the gamma-band frequency. Based on these, it was proposed that the evolving relationships between gamma phases at different sites may serve as a potentially causal mediator in the dynamic reconfiguration of functional connections (Besserve et al. 2015).

Several concerns have been raised with regard to the function of gamma oscillations in dynamic reconfiguration and rerouting of information. Gamma synchronization occurs in brief episodes lasting approximately around 100 milliseconds, and these oscillatory episodes are not autocoherent (phase conserving) and exhibit strong characteristics of stochasticity (Burns, Xing, and Shapley 2011; Xing et al. 2012). As such, gamma activity cannot be used as a clock meaning that neuronal networks cannot use gamma activity as a regular temporal signal on which to base time-dependent calculations. This result calls into question theories of “binding” by coherence using gamma-band oscillations that rely on regular, rhythmic, or autocoherent oscillations (Burns, Xing, and Shapley 2011). Furthermore, interareal synaptic transmission delays are long and diverse and may counteract reliable phase synchronization. Lastly, the frequency of the transient oscillatory bursts fluctuates over time and varies between recording sites (Ray and Maunsell 2010) making effective phase synchronization difficult. Given these factors, it would initially appear unlikely for intra-areal gamma bursts to spontaneously align with each other.

These concerns were effectively addressed through a series of simulations using various circuit models (Palmigiano et al. 2017). These models naturally exhibited significant variability in terms of power, frequency, and timing, while also encompassing crucial forms of heterogeneity, including the presence of diverse transmission delays. Within these models, specific parameters were fine-tuned to produce collective gamma oscillations that were short-lived, lasting only a few cycles, weakly synchronized, and characterized by stochastically drifting frequencies. Notably, these features closely resembled the characteristics of local field potentials observed in behaving animals. When multiple circuits with these defined features were interconnected by long-range excitatory connections, the resulting large-scale dynamics spontaneously generates temporally co-occurring bursts of synchrony. The drifting frequencies of each region harmonized with one another, leading to transient phase-locking within the gamma bursts. This coordination occurred not only between bursts with exactly matching main frequencies but also extended to cross-frequency interactions. The precision of phase-locking notably increased within the periods of high cross-covariance between LFPs from the two circuit models. During these windows of high cross-covariance and peaked phase synchronization, significant information transfer, measured using transfer entropy, occurred. The direction of information transfer was dependent on the phase difference between the two circuits. It's crucial to highlight that even during periods of coarse phase synchronization, there remained a high degree of information transfer. This implies that the emergence of information transfer requires only a minimal degree of phase-locking. The outcomes of these simulations affirm that dynamic frequency-matching among interacting neuronal populations with transient synchrony is a robust and inherent characteristic.

Thus, gamma oscillations can create rhythmic states that facilitate dynamic interaction across different brain areas.

8.2.5 Gamma oscillations and cell assembly formation

As it was discussed previously, the induction of post-synaptic spiking and pursuing STDP requires a large convergent input, probably from different presynaptic neurons, in a short time window of 10-20ms. Based on this, a reader-neuron-defined cell assembly have been proposed which is defined as “a group of presynaptic neurons, whose spike discharges occur within the window of the membrane time constant of the reader-integrator neuron and trigger an action potential in the reader neuron” (György Buzsáki 2010). The optimal time constant of cell assemblies should correspond to the temporal window of spike-timing-dependent plasticity, and as such it falls within the period of gamma and higher frequency oscillations. According to the ‘reader-centric’ framework, assemblies should effectively elicit discharges in downstream reader neurons. This has two implications: first, activation of an assembly should precede that of its reader within a brief time window, occurring more frequently than expected by chance; and second, this relationship should be dependent on the collective activation of the assembly.

Recent evidence suggests that assembly–reader communication exist in amygdala-prefrontal cortex network (Boucly et al. 2022). Studying assembly-reader pairs, it was shown that at time amygdalar assembly activations were consistently followed by prefrontal spikes, and vice versa, suggesting a bidirectional interaction between these two regions. More importantly, spiking in downstream neurons were selective for the collective activation of upstream assemblies with specific cell identities. The results also yielded an endogenous time scale of up to ~20-25 ms for effective cell assemblies. Consistent with this, previous hippocampal recordings in rodents and humans also indicated that organized firing occurs on time scales of roughly 10-30 ms (the period of the hippocampal gamma oscillation; (Harris et al. 2003; Umbach et al. 2022)). In humans, hippocampal cell assemblies were detected during a memory task. During cell assembly activations, gamma oscillatory power at 40 Hz peaked. The influence of this gamma oscillation on the cell assembly organization was demonstrated by showing that the majority of the cell assembly member neurons phase locked to this oscillation (Umbach et al. 2022).

Recently, direct evidence supporting the role of gamma in orchestrating cell assemblies within the hippocampal formation has been presented (Fernández-Ruiz et al. 2021). Extracellular recordings were performed in the entorhinal cortex-dentate gyrus-CA3 networks in rodents that were trained in two different tasks. Cell assemblies were detected during task performance. While approximately half of the assemblies comprised cells of the same type, others featured combinations of GCs, MCs, and CA3pyr cells. The composition of neuronal assemblies was task-specific, with GCs playing a more prominent role during spatial learning, and CA3pyr cells contributing more during object learning. Optogenetic gamma perturbation disrupted the learning-induced organization of target neuron assemblies, emphasizing the crucial role of gamma in task-specific assembly dynamics (Fernández-Ruiz et al. 2021).

In conclusion, the findings presented here underscore the critical role of gamma oscillations in facilitating learning through the precise synchronization of specific cell populations in a task-specific context. This synchronization mechanism allows multiple presynaptic neurons to fire in a coordinated manner, resulting in a collectively stronger depolarizing impact on the target postsynaptic neuron compared to isolated firing events. This aligns with the idea that the coordination of firing over extended time scales hinges upon the integration of multiple neural assemblies orchestrated by the rhythmic dynamics of gamma oscillations.

9. Chapter 3: The organization of cell assemblies in the hippocampus

For the final chapter of this dissertation, I performed multi-channel laminar recordings within the hippocampal CA1 region of two female macaques while they engaged in a freely-behaving sequential memory task, as well as during sleep. Laminar recordings of local field potentials (LFPs) and ensemble unit activity provided several advantages, enabling me to achieve the following objectives: 1) Identify distinct layers within the CA1 region in macaques and estimate the cell bodies of the recorded units with respect to the layers. This led to the stratification of the pyramidal cell groups and characterization of different putative inhibitory cell groups. 2) Detect hippocampal cell assemblies and

investigate the composition of these assemblies at a cellular level. Collectively, these allowed for the in-depth exploration of sub-layers specific dynamics within the macaque's CA1 region. In the next section, I will interpret the results of chapter 3 within the framework of cell assembly theory.

9.1 Cell assembly theory: what Donald Hebb had dreamed

Hebb recognized that beyond the level of individual synapses and neurons, several higher-order levels of organization in the brain, particularly neural assemblies, played a crucial role. Hebb proposed that neurons forming these cell assemblies, collectively respond to sensory input, and create a transient closed-loop system in which activation reverberates after the initial stimulus subsided. While Lorente de No´ had previously observed reverberatory activity lasting for around half a second (Sejnowski 1999), Hebb took this notion further by suggesting that the activity generated by each cell assembly could propagate and sequentially activate connected cell assemblies, forming what he termed a phase sequence. He posited that this phase sequence was at the core of how the brain represents perceptual information derived from sensory stimuli (Wallace and Kerr 2010).

The quest to identify cell assemblies presents significant technical challenges, primarily due to the vast number of neurons that have the potential to contribute to these assemblies, the exact count or locations of which remain largely unknown. Consequently, the increasing ability to record a growing number of neurons simultaneously is advantageous, as it supplies the necessary dataset to investigate the simultaneous firing of neuron populations and the constitution of cell assemblies. This is the primary reason why direct tests of Hebb's hypotheses were significantly delayed, only becoming feasible after large-scale brain recordings became accessible several decades later (György Buzsáki 2004). Today, there are numerous studies on cell assemblies conducted in different brain regions (Luczak, Barthó, and Harris 2009; Nicolelis et al. 1995; Laubach, Wessberg, and Nicolelis 2000; Harris et al. 2003). However, it is worth noting that even in the present day, studies on hippocampal cell assemblies in primate brains remain limited

in number. There's only 1 study that directly test cell assemblies in human hippocampus (Umbach et al. 2022) and none in the monkey hippocampus. Therefore, the current results present the first evidence on cell assembly formation in the nonhuman primate hippocampus.

While much attention has been dedicated to exploring the connection between the activation of cell assemblies and memory, less focus has been directed toward investigating the internal organization of these assemblies, including their topology, and cellular composition. Determining features of cell assemblies like their dimensions, cellular membership, connectivity, dynamics, and the relevance of these features to perception and cognition, continues to be an engaging field of research. In my dissertation, I explicitly investigated the cellular composition of detected cell assemblies in terms of their member pyramidal and inhibitory cell types.

A prominent hallmark of these cell assemblies is the synchronized activity among a network of interconnected neurons. Despite the typical irregularity in the firing patterns of individual neurons, it has been postulated that at least a portion of information transmission takes place through synchronous activity within these cell assemblies (Stevens and Zador 1998; Luczak, Barthó, and Harris 2009; Salinas and Sejnowski 2001). The methods used in the current dissertation were designed to identify cell assemblies and their constituent neurons based on the criteria of precise spike synchronization exceeding chance levels. However, it's important to acknowledge the limitation of these methods, which require defining a specific temporal window for synchronization. Alternative methods have been developed that can detect assembly structures at multiple temporal scales, with arbitrary constellations of time lags, levels of precision, and with arbitrary internal organization (Russo and Durstewitz 2017). The deliberate choice of the method was made to enable a meaningful and fair comparison between the current findings and those from rodent studies.

9.2 Cell assembly activations during sleep

Sleep constitutes an essential part of our daily life, and among its numerous functions, memory formation emerges as a vital function (Klinzing, Niethard, and Born 2019). Memory formation is an active process that involves selecting novel experiences to integrate into an existing memory structure, which must be preserved and modified simultaneously (Robin and Moscovitch 2017; Gilboa and Marlatte 2017). While we are awake, this process takes place amid a continuous influx of new sensory information, however, sleep offers a unique opportunity for the brain to organize and reinforce newly acquired memories without the constant input of external information (Girardeau and Lopes-Dos-Santos 2021). According to the two-step theory, during an experience, a specific group of coordinated CA3 and CA1 cells form interconnected cell assemblies linked to the new information. Subsequently, during sleep, these CA3 assemblies spontaneously trigger SWR events, reactivating the associated CA1 ensembles and enhancing their connections, ultimately leading to memory consolidation (G Buzsáki 1989). Disturbing the synchronized activity during sleep, particularly the sharp-wave ripple, significantly impairs memory (Ego-Stengel and Wilson 2010; Girardeau et al. 2009). The emergence of sharp-wave ripple events during offline states and the accompanying phase-locked increase in cell firing rates has previously been documented in nonhuman and human primates during sleep (Bukhtiyarova et al. 2022; Kaplan et al. 2016; Skelin et al. 2020; Y. Y. Chen et al. 2020; William E Skaggs et al. 2007; Le Van Quyen et al. 2008; Hussin, Leonard, and Hoffman 2020). Chapter 3 replicated these findings for different cell types and extended these results by showing that the synchronous activation of cells during sharp-wave ripples form member-specific cell assemblies. The specific recruitment of cells into cell-assemblies may be able to support the specificity of memories at the cognitive level.

Although it's tempting to relate this cell assembly activation during sleep to rodent replay studies, several important distinctions should be made. Cell assembly activation/reactivation is methodologically, and biologically separate from cell assembly replay (Tingley and Peyrache 2020; Z. S. Chen and Wilson 2023). Activation/reactivation

refers to population-level synchronization episodes in which groups of cells with specific identity, cell assemblies, show correlated spiking activity; however, this correlated activity does not need to be temporally ordered. In replay, cell assembly activations should maintain a specific temporal order which correspond to the same sequential activity during experience. A recent study directly investigated the functional dissociation between reactivation and replay in the hippocampus (C. Liu et al. 2023). Optogenetic stimulation was used to perturb the fine temporal coordination of hippocampal place cell firing in a novel environment while maintaining global network dynamics, single-cell spatial tuning and rate coding properties. During sleep after the novel experience, task-related cell assemblies encoding discrete maze locations were reactivated in SWRs, unaffected by the manipulation. However, their sequential structure did not reproduce the order in which they were active in the task, resulting in impaired sequential replay for the perturbed trajectories. At the behavioral level, while context-reward associative learning in a conditioned place preference task was unaffected, flexible memory–guided navigation in a foraging task was impaired, suggesting that sequential replay might only be instrumental for some but not all types of learning and memory. The same manipulation did not disrupt replay of familiar trajectories, suggesting that the precise temporal coordination of place cell firing during learning mediates initial plasticity required for subsequent replay (C. Liu et al. 2023). Consistent with this, an earlier study showed that disrupting theta sequences, but not behavioral time scale sequences, during novel experience results in impaired subsequent sleep replay (Drieu, Todorova, and Zugaro 2018). These findings support the view that nested temporally ordered sequences during experience underlie the initial formation of memory traces subsequently consolidated during sleep. Recently, in the human hippocampus, it was shown that during awake assembly activations in a memory task, the participating members of a cell assembly fire in a consistent temporal order. The strength of this temporal ordering was positively correlated with the recall fraction observed during the corresponding session supporting the mnemonic relevance of firing order consistency (Umbach et al. 2022). The evidence for phase sequence of cell assemblies and replay during offline states is yet to be recorded in the primate hippocampus.

9.3 Topology of cell assemblies in the CA3-CA1 and memory

How is assembly-specific synchronous activity generated in CA1? In vivo studies in behaving rats reveals that that CA2/CA3 cells fire synchronously preceding CA1 (Oliva et al. 2016). In the hippocampal CA3 region, synaptically connected neurons exhibit a notably higher likelihood of engaging in synchronized spiking activity compared to other pairs of neurons (N. Takahashi et al. 2010). Interestingly, the primary factor influencing this synchronization appears to be not the direct synaptic connection between neurons, but rather the correlated synaptic inputs originating from multiple shared presynaptic neurons. This is reinforced by the observation that, in contrast to unconnected pairs, synaptically linked neurons share a greater number of common presynaptic neurons and receive more correlated excitatory synaptic inputs (N. Takahashi et al. 2010). Based on these observations, CA3 cell assemblies are formed from the synchronized activity of synaptically connected neurons that share common inputs.

CA3 units within functional assemblies send convergent projections onto the selective population of CA1 neurons (N. Takahashi et al. 2010). However, this doesn't mean that CA3 activation can always lead to CA1 spiking outputs. The reason is that it is very unlikely that a single CA3 spike depolarizes every target cell beyond threshold (Sayer, Redman, and Andersen 1989; Sayer, Friedlander, and Redman 1990), since it forms few contacts on each of them (Li et al. 1994). Consistent with this, it has been shown that only a fraction of spikes of a single CA3 pyramidal cell are monosynaptically related to the micro-field EPSPs of CA1 neuron populations (Fernández-Ruiz et al. 2012). These findings suggest that to generate an output response in CA1 neurons, CA3 neurons in a cell assembly should emit synchronous spikes (N. Takahashi et al. 2010; Fernández-Ruiz et al. 2012). Additionally, under some behavioral conditions, CA1 ensemble activity appear before CA3 indicating that CA1 ensemble activity can also emerge independently of CA3, probably via the direct projections from entorhinal cortex (Stefan Leutgeb et al. 2004).

Another feature of population synchrony in CA3-CA1 network is the power-law scaling of synchronization (Mizuseki and Buzsáki 2013; György Buzsáki and Mizuseki 2014; N. Takahashi et al. 2010). This implies that most of the time, synchronization results from the simultaneous firing of a relatively small proportion of neurons, whereas the network occasionally exhibits larger synchronous events. This dissertation provides multiple lines of evidence that reinforce the existence of such small-world network organization in the primate hippocampus. In the context of SWR, the participation probability of many CA1 pyramidal cells was less than 10%, indicating a highly selective recruitment of these cells. While certain inhibitory cell types exhibited a relatively higher participation probability, only a few specific groups had members with participation probabilities exceeding 50%. More directly, the rate of assembly participation among neurons from all cell groups averaged less than 10% with inhibitory cell groups showing lower participation rate than the pyramidal cells. These findings suggest that at any given time, only a limited number of neurons play a role in the synchronization episodes.

The activation of different cell assemblies in CA3-CA1 is task specific (Fernández-Ruiz et al. 2021; Dragoi and Buzsáki 2006; Guzowski, Knierim, and Moser 2004), and disrupting the learning-induced assembly organization by gamma oscillations perturbation can lead to impairments in spatial and object learning tasks (Fernández-Ruiz et al. 2021). Hebb postulated that, during memory formation, connections between population of neurons that fire together should strengthen (Hebb 1949). In line with this, a recent study used novel genetic tagging tools to investigate the synapses between engram cells in the CA3 and CA1 regions, which were activated during a contextual fear conditioning task in rats (Choi et al. 2018). While the total number of engram cells remained unchanged during memory formation, there were notable modifications in the structural connectivity between CA3 and CA1 engram cells. Specifically, the density of synapses between CA3 and CA1 engram cells increased, and this was not observed in non-engram cells. Additionally, the size of the dendritic spines associated with these synapses increased, and this enlargement was positively correlated with the strength of memory. As a result, the presynaptic transmission between CA3 and CA1 engram cells enhanced suggesting increased release probability from CA3 engram inputs to CA1. These results

demonstrated that synaptic populations that fired together during memory formation showed the strongest connections.

By considering the CA3-CA1 circuit as an illustration, we can understand that during memory formation, a coherent input (possibly sensory from entorhinal cortex) can converge on a selective population of cells that form a cell assembly by virtue of their synaptic connectivity and activate them synchronously. These segmentally synchronized pulse packets can then propagate to target specific cell assemblies in downstream areas. This coactivation can result in structural changes that strengthen the memory. This raises the question of whether the coordinated activity of cell assemblies extends across diverse brain regions and whether this interplay between inter-areal cell assemblies is associated with memory.

In a recent study, multi-regional large-scale electrophysiology were performed in the amygdala, ventral hippocampus, and prefrontal cortex during a fear memory in rats. The local ensembles activated during the acquisition of fear memories and displayed inter-regional coactivation during subsequent sleep which relied on brief bouts of fast network oscillations. During memory retrieval, the coactivations reappeared, together with fast oscillations (Miyawaki and Mizuseki 2022). In another study, ensemble dynamics in Amygdala and mPFC were shown to form selective cell assemblies that are dynamically reconfigured. These inter- regionally coupled cell assemblies were selectively modified upon associative learning, indicating that they were plastic and could become bound to behaviorally relevant variables (Boucly et al. 2022). Using brain-wide high-throughput phenotyping across 247 regions in mice during a contextual fear memory, 117 cFos+ brain regions were identified holding engrams with high probability (Roy et al. 2022). These brain-wide neuronal ensembles were reactivated during recall. Optogenetic manipulation revealed that many of these local neuronal ensembles were functionally connected to hippocampal or amygdala engrams. Simultaneous chemogenetic reactivation of multiple engram ensembles conferred a greater level of memory recall than reactivation of a single engram ensemble.

These results indicate that locally detected cell assemblies associated with a specific memory may be coordinated across multiple brain regions, making a unified engram complex.

9.4 Cellular composition of cell assemblies and segregated functional circuits

The hippocampus assumes a critical role in various cognitive domains, including tasks such as spatial navigation, temporal associations, and contextual learning. Therefore, a fundamental question arises as how are hippocampal cell assemblies organized to effectively underpin learning and memory across highly distinct experience-specific contexts? One possibility is that hippocampal pyramidal cells form segregated functional modules with parallel channels of information processing to accommodate a broad spectrum of cognitive demands (Ivan Soltesz and Losonczy 2018). This possibility can be put to the test by comparing various attributes of pyramidal cells in the hippocampus, including their fundamental physiological characteristics, their interactions with inhibitory microcircuits, their connectivity within and beyond the hippocampus, their behavior-related firing patterns, and their engagement in cell assemblies. Nonuniformity in these metrics can indicate that hippocampal pyramidal cells constitute distinct subpopulations tailored to different functions.

Along the radial axis of the rodent hippocampus, superficial (CA1sup) and deep (CA1deep) pyramidal cell types demonstrate sublayer-specific dynamics (Mizuseki et al. 2011; Harvey et al. 2023; Gu et al. 2023; Berndt et al. 2023). The findings of this dissertation demonstrates that, similarly, in the monkey hippocampus superficial and deep pyramidal cells have distinct basic physiological properties such as firing patterns, burstiness, sharp-wave ripple depth of modulation and phase of firing. One important question is to what extent the circuit-level organizational differences between CA1 pyramidal cell type populations are relevant to behavior. Ca2+ imaging in head-fixed mice demonstrated that superficial CA1 pyramidal cells (CA1sup) form more stable spatial maps compared to their deep counterparts, with more reliable discrimination of contexts at both single-cell and population levels (Danielson et al. 2016). Silicone probe recordings

further indicated that CA1deep firing fields were tightly linked to individual sensory stimuli, while the superficial layer contained cells representing a global spatial context (Geiller, Royer, and Choi 2017; Harvey et al. 2023). Recent in vivo recordings of molecularly identified pyramidal cell subclasses highlighted the efficient spatial information representation by Calbindin-positive (CB+) cells, mainly corresponding to CA1sup, compared to CB− place cells, albeit with lower firing rates during running epochs (Gu et al. 2023). In a learning task, CA1deep exhibited greater stability than during random foraging, and the representation of the goal by CA1deep proved more predictive of task performance than that by superficial neurons (Danielson et al. 2016). Additionally, deep CA1 place cells track changes in reward configuration (Harvey et al. 2023).

Among intrahippocampal afferents, deep and superficial CA1PCs receive stronger inputs from the region CA2, and CA3 respectively. Novel object presentation induces global remapping of place fields in CA2 (Alexander et al. 2016), making CA2 ensembles more responsive to subtle contextual changes compared to CA1 and CA3 (Wintzer et al. 2014). The strong connectivity between CA2 and CA1deep may explain why deep cells show instantaneous responses to landmark manipulations, persist through change of context, and encode landmark identity and saliency (Geiller et al. 2017). In addition, in proximal CA1, strong MEC and weak LEC inputs favor CA1deep, whereas in distal CA1, strong LEC and weak MEC inputs prefer CA1sup (Masurkar et al. 2017). MEC provide predominantly spatial information and the LEC provide primarily nonspatial information to CA1PCs (Knierim, Lee, and Hargreaves 2006; Knierim, Neunuebel, and Deshmukh 2014). These results provide a potential circuit mechanism for the findings that CA1deep are more likely to have place fields during spatial navigation, due to the stronger excitation of CA1deep by MEC inputs, at least in the proximal part of CA1. The increased stability of superficial place maps—where proximal cues and landmarks are more relevant—is also consistent with the preferential innervation of CA1sup by LEC.

Do cells with such segregated anatomical, physiological, and functional properties also form separate assemblies? One possibility is that while hippocampal pyramidal cells exhibit distinct spatio-temporally localized functional dynamics, these differences do not extend to the level of cell assemblies. The other scenario posits that functionally distinct

neurons are recruited to specific learning-related assemblies, each with a biased organization toward one group of functional cell types or the other.

Similar to recent observations in rat hippocampal CA1 (Harvey et al. 2023), the cellular composition of detected cell assemblies within monkey CA1 revealed a pronounced anatomical bias. In majority of the assemblies, all members belonged to the same sublayer of the hippocampus, superficial or deep, indicating a higher synchronization among cells from the same sublayer. This indicate that across species, the anatomical identity of pyramidal cells is a major organizing principle of CA1 assembly dynamics. This might not be the case for all hippocampal subfields. In CA3, neurons within a given cell assembly are sparsely distributed, and the distribution of distances between neurons within the same assembly does not differ from that of neurons in different assemblies, indicating an absence of spatial bias in synchronous spike patterns (N. Takahashi et al. 2010; Harris et al. 2003). During sharp-wave ripples, similar to rat findings (Harvey et al. 2023; Valero et al. 2015), monkey CA1sup cell assemblies activated with significantly higher strength compared to CA1deep cells. CA1sup also had a significantly higher participation probability compared to their deep peers. The functional gradient of superficial and deep is speculated to rely on timed PV-mediated perisomatic inhibition (Valero et al. 2015). In rodents, GABAergic inhibition is consistently stronger in deep cells (Valero et al. 2015; S.-H. Lee et al. 2014). Because SWR active interneurons, such as PV+ basket cells and bistratified cells, enable the phasic firing of active pyramidal cells during ripple cycles (Stark et al. 2014), the variability in activation strength and participation probability might be explained by unbalanced target-selective inhibition in local connections in CA1 pyramidal cells. This can also potentially explain previous observations on the heterogeneous contribution of hippocampal cells to memory replay. Previous reports identified a subset of CA1 pyramidal cells whose reactivation dynamics after a new experience or during learning remained relatively unaltered. On the other hand, a different subset of CA1 pyramidal cells were selectively recruited into postexperience memory replay (Grosmark and Buzsáki 2016; Hall and Wang 2022). The rigid and plastic subpopulations of pyramidal cells can correspond to the deep and superficial cells.

Differences in long-range projection specificity in deep and superficial CA1 pyramidal cells further amplify their segregated functional roles. Earlier studies have demonstrated that during hippocampal SWRs, the reactivation of cell ensembles in several target regions are synchronized (Peyrache et al. 2009; Girardeau, Inema, and Buzsáki 2017; Sosa, Joo, and Frank 2020; Siapas and Wilson 1998; Nitzan et al. 2020; Opalka et al. 2020). However, until recently, it was not known whether memory representations broadcast by SWRs are similarly read out in all cortical target regions or whether these show selective responses. Recent studies in rats suggest that distinct behavior-contingent information is processed in parallel by subpopulations along the radial axis of the hippocampus and is selectively routed to distinct target regions during sharp-wave ripples (Harvey et al. 2023). CA1sup cells mainly target MEC monosynaptically, while much sparser projections to PFC originated from CA1deep cells, with minimal overlap between the two subpopulations. Moreover, MEC responds preferentially to SWRs enriched in CA1sup spikes, while PFC responds preferentially to SWRs dominated by CA1deep activity. Furthermore, the temporal dynamics of MEC and PFC ensemble reactivation were better predicted by the activity of CA1sup and CA1deep, respectively, indicating selective cortical responses to SWRs depending on the anatomical distribution of the hippocampal cells generating them (Harvey et al. 2023). Several lines of evidence suggest that target-selective segregation of function might also exist in the primates. Both monkey and human hippocampal ripples are associated with widespread modulation of cortical and subcortical activity (Cox et al. 2019; Kaplan et al. 2016; Turesson, Logothetis, and Hoffman 2012; Skelin et al. 2020). Additionally, CA1 efferents in monkeys have a radial organization. Projections from the medial prefrontal (Barbas and Blatt 1995; Insausti and Muñoz 2001; Roberts et al. 2007) and orbitofrontal cortices (Cavada et al. 2000) mainly stem from the deep CA1 layer and projections to the medial temporal cortex originates from the superficial CA1 layer (Yukie 2000; Insausti and Muñoz 2001). Given that the neural dynamics of the orbitofrontal cortex support reward processing, reward-associated signals from these deep pyramidal cells may reach the orbitofrontal cortex in primates. These anatomical findings combined with the current results in this dissertation suggest that, in primates, similar to rodents, cell assemblies arise from functionally distinct cell types in the hippocampus, are differentially activated

during SWRs, and possibly interact with different downstream areas during these network oscillatory episodes.

The organization of pyramidal cell assemblies during learning is sculpted by the intricate operations of the inhibitory circuits in the hippocampus (Assisi, Stopfer, and Bazhenov 2011; György Buzsáki 2010). I found that putative inhibitory cell groups form significant members of some of the assemblies in the macaque hippocampus. The assembly participation rate of inhibitory cell groups was significantly lower than pyramidal cell groups indicating a selective role in formation of cell assemblies. The role of inhibitory microcircuits in dynamics reconfiguration of cell assemblies have previously been investigated in the rodent hippocampus (Dupret, O'Neill, and Csicsvari 2013). Hippocampal cell assembly patterns in these animals can alternate rapidly between the representation of different maps across consecutive theta oscillatory cycles when environmental cues or task parameters are abruptly changed (Kay et al. 2020; Jezek et al. 2011; Jadin Jackson and Redish 2007; Brandon et al. 2013). During the course of learning, the expression strength of the new assemblies improve, suggesting their refinement (Dupret, O'Neill, and Csicsvari 2013). The firing rate of many interneurons also fluctuated on a fast time scale that followed this assembly alternation. Some CA1 interneurons exhibited significant positive correlations and increased their instantaneous rate at times when the new representation was preferentially expressed while the ones with negative correlation decreased their firing during the same moments. These firing associations, manifested by rapid fluctuations of the interneurons firing rate, were mirrored by changes of their monosynaptic connection weight. Interneurons that increased their firing associations to new pyramidal assemblies overall received strengthened inputs from pyramidal cells that were members of a new assembly. Moreover, the opposite trend was observed for interneurons that decreased their associations to new assemblies, these received weaker local pyramidal inputs following learning. Importantly, this circuit reconfiguration took place during the learning session and it remained stable in subsequent sleep and memory probe sessions (Dupret, O'Neill, and Csicsvari 2013). These results provided direct evidence that learning engages circuit modifications in the hippocampus that incorporate a redistribution of inhibitory activity that might assist in the segregation of competing pyramidal cell assembly patterns in space

and time. A question that arises from these observations is whether all inhibitory cell types contribute indiscriminately to the cell assembly formation or inhibitory cell classes have behavioral-state dependent patterns that changes during state transitions?

SOM-expressing, dendrite-targeting INs, including OLM and BiCs, and perisomatic-targeting PV+ INs, which comprises basket and AACs are strongly modulated by locomotion (Geiller et al. 2020; Dudok, Klein, et al. 2021). On the other hand, NPY-expressing and SOM-immunonegative, dendrite-targeting INs, which includes Ivy and neurogliaform cells, shows overall weaker modulation by locomotion (Geiller et al. 2020) and CCK+ basket cells (CCK BCs) are suppressed during running and non-locomotory movements (Dudok, Klein, et al. 2021). The CCK and PV GABAergic systems show precise inverse coupling that arises through powerful inhibitory control of CCK BCs by PV cells (Dudok, Klein, et al. 2021). While PV IN activity scales with activity of the CA1 neuronal ensemble, CCK BC activity is inversely scaled. CCK BCs and PV+ INs have distinct synaptic properties that enables them to provide unique forms of perisomatic inhibition during discrete brain states. These fast-spiking PV cells have specific intrinsic and synaptic mechanisms that are optimized for rapid synaptic signaling and temporal precision of firing. PV-BCs receive a high density of excitatory inputs and provide highly divergent feedforward and feedback inhibition to pyramidal cells. In contrast to PV-BCs, CCK-BCs receive sparse excitatory inputs, which they integrate sequentially over a larger temporal window to provide feedback inhibition via asynchronous GABA release (Hu, Gan, and Jonas 2014; Armstrong and Soltesz 2012). During brain states with rapidly alternating rhythmic activity (such as theta, gamma, and ripple oscillations), perisomatic inhibition by PV BCs efficiently suppresses PC activity at specific oscillatory phases with high temporal precision and in some cases promotes subsequent rebound spiking (Klausberger et al. 2003; C. Varga, Golshani, and Soltesz 2012; Stark et al. 2013; Lapray et al. 2012; Gan et al. 2017). However, during episodes of irregular circuit activity, a perisomatic inhibitory tone provided by CCK BCs may exert prolonged control of PC firing, which is necessary even in the absence of strong excitatory inputs to suppress spurious noise correlations (Cardin 2018; Renart et al. 2010). Importantly, the firing of CCK-expressing interneurons, on average, shows no correlation to ripple episodes. However, during single ripple episodes, the same CCK cell appears to be sometimes

specifically silenced and sometimes excited. Such an episode-dependent firing pattern might reflect a subtle balance of incoming excitation and inhibition. The participation of CCK cells in certain ripples may be influenced by the recent history of the network, as shown for pyramidal cells. Therefore, CCK-expressing interneurons might specifically contribute to selecting which pyramidal cells are active in a certain ripple episode as part of a cell assembly (Klausberger et al. 2005). This is consistent with the observation that during locomotion perisomatic-targeting PV+ INs exhibit less disinhibitory control (Geiller et al. 2020), and they participate in almost all SWR episodes (C. Varga, Golshani, and Soltesz 2012), suggesting that these INs predominantly regulate behavioral state and network oscillation-related activity dynamics of the overall pyramidal cell population (Geiller et al. 2020). In contrast, during locomotion, SOM+ dendrite-targeting INs are under strong disinhibitory control suggesting a close, bi-directional interaction of these INs with active CA1 ensembles during exploration and a major role for these INs in regulating experience and learning-related reorganization of CA1 dynamics (Geiller et al. 2020). Moreover, axoaxonic cells may also be a part of inhibitory circuits that regulate the expression of specific cell assemblies. A subset of these inhibitory cell classes show suppression during SWR episodes and the postsynaptic effect of AACs on PC spike generation can remap place fields in the CA1 network (Dudok, Szoboszlay, et al. 2021). In a separate study, basket and ivy cells showed distinct spike-timing dynamics, firing at different rates and times during theta and ripple oscillations. Basket, but not ivy, cells changed their firing rates during movement, sleep and quiet wakefulness, suggesting that basket cells coordinate cell assemblies in a behavioral state–contingent manner, whereas persistently firing ivy cells might control network excitability and homeostasis (Lapray et al. 2012).

In conclusion, the intricate orchestration of synchronized activity within the hippocampus results in the emergence of distinct spatiotemporally organized cell assemblies. These cell assemblies are formed by the interplay of functional cell types, such as pyramidal cells from different substrata, and the intricate regulation by inhibitory cells, thereby shaping the dynamic landscape of hippocampal neural circuits. The differential engagement of inhibitory and pyramidal cell classes in various behavioral states emphasizes the behavioral-state-dependent nature of hippocampal activity.

9.5 Summary

In summary, this dissertation presented novel, fundamental insights into the neural organization of hippocampal CA1 in non-human primates. The findings emphasize the significance of studying complex behavior and cognition under less constrained task conditions and the importance of comparative electrophysiological approaches in elucidating the underlying neural mechanisms of flexible learning and memory.

Table 1 Physiological properties of superficial and deep pyramidal cells

Study	Baseline Firing rate	CV2	Bursting	SWR firing	SWR participation	Ripple phase mod	Ripple phase
Abbaspoor, Hoffman	Sup>Deep	Sup>Deep	Deep>Sup	Sup>Deep	Sup>Deep	-	Differences in phase
Harvey 2023	Deep>Sup	Sup>Deep	Deep>Sup	Deep>Sup	Deep>Sup	-	-
Gu 2023	Deep>Sup (Run only)	-	Sup>Deep (all conditions)	Deep>Sup	Deep>Sup	Sup> Deep	No Differences in phase
Valero 2015	Sup=Deep	-	-	Sup=Deep	Sup>Deep	-	-
Mizuseki 2011	Deep>Sup (RUN, SWS, and REM)	-	Deep>Sup (all conditions)	-	-	-	-
Berndt 2023	Deep>Sup	-	Deep>Sup	-	-	-	Differences in phase

Table 2 Functional properties of superficial and deep pyramidal cells

Study	Prop. Place Cells	Field Width	Prop. Of multi-field	In field firing rate	Spatial Information content (bits/spk)	Reward gain	Context Selectivity
Harvey 2023	Deep>Sup	Sup=Deep	Deep>Sup	Deep>Sup	Sup=Deep	Deep>Sup	Sup>Deep
Gu 2023	Deep>Sup	Sup=Deep	Sup>Deep	Sup=Deep	Sup>Deep	-	-
Mizuseki 2011	Deep>Sup	-	-	-	-	-	-
Danielson 2016	Deep>Sup	Deep>Sup	-	-	-	Deep>Sup	-
Sharif 2021	-	-	-	-	Sup>Deep	-	-
Geiller 2017	-	-	Deep>Sup	-	-	-	Sup>Deep

10. References

Abbaspoor, Saman, Ahmed T Hussin, and Kari L Hoffman. 2023. “Theta- and Gamma-Band Oscillatory Uncoupling in the Macaque Hippocampus.” *ELife* 12 (May). https://doi.org/10.7554/eLife.86548.

Abbott, L F, and S B Nelson. 2000. “Synaptic Plasticity: Taming the Beast.” *Nature Neuroscience* 3 Suppl (November): 1178–83. https://doi.org/10.1038/81453.

Adey, W R. 1960. “Hippocampal Slow Waves.” *Archives of Neurology* 3 (1): 74. https://doi.org/10.1001/archneur.1960.00450010074007.

Aggleton, J P, and M W Brown. 1999. “Episodic Memory, Amnesia, and the Hippocampal-Anterior Thalamic Axis.” *Behavioral and Brain Sciences* 22 (3): 425–44; discussion 444. https://doi.org/10.1017/S0140525X99002034.

Aggleton, J P, N Neave, S Nagle, and P R Hunt. 1995. “A Comparison of the Effects of Anterior Thalamic, Mamillary Body and Fornix Lesions on Reinforced Spatial Alternation.” *Behavioural Brain Research* 68 (1): 91–101. https://doi.org/10.1016/0166-4328(94)00163-a.

Aghajan, Zahra M, Lavanya Acharya, Jason J Moore, Jesse D Cushman, Cliff Vuong, and Mayank R Mehta. 2015. “Impaired Spatial Selectivity and Intact Phase Precession in Two-Dimensional Virtual Reality.” *Nature Neuroscience* 18 (1): 121–28. https://doi.org/10.1038/nn.3884.

Agster, Kara L, Norbert J Fortin, and Howard Eichenbaum. 2002. “The Hippocampus and Disambiguation of Overlapping Sequences.” *The Journal of Neuroscience* 22 (13): 5760–68. https://doi.org/20026559.

Alexander, Georgia M, Shannon Farris, Jason R Pirone, Chenguang Zheng, Laura L Colgin, and Serena M Dudek. 2016. “Social and Novel Contexts Modify Hippocampal CA2 Representations of Space.” *Nature Communications* 7 (January): 10300. https://doi.org/10.1038/ncomms10300.

Allen, Timothy A, and Norbert J Fortin. 2013. “The Evolution of Episodic Memory.” *Proceedings of the National Academy of Sciences of the United States of America* 110 Suppl 2 (Suppl 2): 10379–86. https://doi.org/10.1073/pnas.1301199110.

Allen, Timothy A, Andrea M Morris, Aaron T Mattfeld, Craig E L Stark, and Norbert J Fortin. 2014. “A Sequence of Events Model of Episodic Memory Shows Parallels in Rats and Humans.” *Hippocampus* 24 (10): 1178–88. https://doi.org/10.1002/hipo.22301.

Allen, Timothy A, Daniel M Salz, Sam McKenzie, and Norbert J Fortin. 2016. “Nonspatial Sequence Coding in CA1 Neurons.” *The Journal of Neuroscience* 36 (5): 1547–63. https://doi.org/10.1523/JNEUROSCI.2874-15.2016.

Altemus, K L, P Lavenex, N Ishizuka, and D G Amaral. 2005. “Morphological Characteristics and Electrophysiological Properties of CA1 Pyramidal Neurons in Macaque Monkeys.” *Neuroscience* 136 (3): 741–56. https://doi.org/10.1016/j.neuroscience.2005.07.001.

Amilhon, Bénédicte, Carey Y L Huh, Frédéric Manseau, Guillaume Ducharme, Heather Nichol, Antoine Adamantidis, and Sylvain Williams. 2015. “Parvalbumin Interneurons of Hippocampus Tune Population Activity at Theta Frequency.” *Neuron* 86 (5): 1277–89. https://doi.org/10.1016/j.neuron.2015.05.027.

Andersen, Per, Richard Morris, David Amaral, Tim Bliss, and John O’Keefe, eds. 2006. *The Hippocampus Book*. Oxford University Press.

Andolina, Ian Max. 2023. “Opticka: Psychophysics-Toolbox Based Experiment Manager.” *Zenodo*. https://doi.org/10.5281/zenodo.7787740.

Andrillon, Thomas, Yuval Nir, Chiara Cirelli, Giulio Tononi, and Itzhak Fried. 2015. “Single-Neuron Activity and Eye Movements during Human REM Sleep and Awake Vision.” *Nature Communications* 6 (August): 7884. https://doi.org/10.1038/ncomms8884.

Angeli, S J, E A Murray, and M Mishkin. 1993. “Hippocampectomized Monkeys Can Remember One Place but Not Two.” *Neuropsychologia* 31 (10): 1021–30. https://doi.org/10.1016/0028-3932(93)90030-4.

Armstrong, Caren, and Ivan Soltesz. 2012. “Basket Cell Dichotomy in Microcircuit Function.” *The Journal of Physiology* 590 (4): 683–94. https://doi.org/10.1113/jphysiol.2011.223669.

Arnolds, D E, F H Lopes da Silva, J W Aitink, A Kamp, and P Boeijinga. 1980. “The Spectral Properties of Hippocampal EEG Related to Behaviour in Man.” *Electroencephalography and Clinical Neurophysiology* 50 (3–4): 324–28. https://doi.org/10.1016/0013-4694(80)90160-1.

Aru, Juhan, Jaan Aru, Viola Priesemann, Michael Wibral, Luiz Lana, Gordon Pipa, Wolf Singer, and Raul Vicente. 2015. “Untangling Cross-Frequency Coupling in Neuroscience.” *Current Opinion in Neurobiology* 31 (April): 51–61. https://doi.org/10.1016/j.conb.2014.08.002.

Assisi, Collins, Mark Stopfer, and Maxim Bazhenov. 2011. “Using the Structure of Inhibitory Networks to Unravel Mechanisms of Spatiotemporal Patterning.” *Neuron* 69 (2): 373–86. https://doi.org/10.1016/j.neuron.2010.12.019.

Axmacher, Nikolai, Christian E Elger, and Juergen Fell. 2008. “Ripples in the Medial Temporal Lobe Are Relevant for Human Memory Consolidation.” *Brain: A Journal of Neurology* 131 (Pt 7): 1806–17. https://doi.org/10.1093/brain/awn103.

Axmacher, Nikolai, Melanie M Henseler, Ole Jensen, Ilona Weinreich, Christian E Elger, and Juergen Fell. 2010. “Cross-Frequency Coupling Supports Multi-Item Working Memory in the Human Hippocampus.” *Proceedings of the National Academy of Sciences of the United States of America* 107 (7): 3228–33. https://doi.org/10.1073/pnas.0911531107.

Bachevalier, Jocelyne, Sarah Nemanic, and Maria C Alvarado. 2015. “The Influence of Context on Recognition Memory in Monkeys: Effects of Hippocampal, Parahippocampal and Perirhinal Lesions.” *Behavioural Brain Research* 285 (May): 89–98. https://doi.org/10.1016/j.bbr.2014.07.010.

Bailey, Craig H, Eric R Kandel, and Kristen M Harris. 2015. “Structural Components of Synaptic Plasticity and Memory Consolidation.” *Cold Spring Harbor Perspectives in Biology* 7 (7): a021758. https://doi.org/10.1101/cshperspect.a021758.

Baimbridge, K G, and J J Miller. 1982. “Immunohistochemical Localization of Calcium-Binding Protein in the Cerebellum, Hippocampal Formation and Olfactory Bulb of the Rat.” *Brain Research* 245 (2): 223–29. https://doi.org/10.1016/0006-8993(82)90804-6.

Bala, Praneet C, Benjamin R Eisenreich, Seng Bum Michael Yoo, Benjamin Y Hayden, Hyun Soo Park, and Jan Zimmermann. 2020. “Automated Markerless Pose Estimation in Freely Moving Macaques with OpenMonkeyStudio.” *Nature Communications* 11 (1): 4560. https://doi.org/10.1038/s41467-020-18441-5.

Bannister, N J, and A U Larkman. 1995. “Dendritic Morphology of CA1 Pyramidal Neurones from the Rat Hippocampus: I. Branching Patterns.” *The Journal of Comparative Neurology* 360 (1): 150–60. https://doi.org/10.1002/cne.903600111.

Banta Lavenex, Pamela, and Pierre Lavenex. 2009. “Spatial Memory and the Monkey Hippocampus: Not All Space Is Created Equal.” *Hippocampus* 19 (1): 8–19. https://doi.org/10.1002/hipo.20485.

Barbas, H, and G J Blatt. 1995. “Topographically Specific Hippocampal Projections Target Functionally Distinct Prefrontal Areas in the Rhesus Monkey.” *Hippocampus* 5 (6): 511–33. https://doi.org/10.1002/hipo.450050604.

Bartolini, Giorgia, Gabriele Ciceri, and Oscar Marín. 2013. “Integration of GABAergic Interneurons into Cortical Cell Assemblies: Lessons from Embryos and Adults.” *Neuron* 79 (5): 849–64. https://doi.org/10.1016/j.neuron.2013.08.014.

Bartos, Marlene, Imre Vida, and Peter Jonas. 2007. “Synaptic Mechanisms of Synchronized Gamma Oscillations in Inhibitory Interneuron Networks.” *Nature Reviews. Neuroscience* 8 (1): 45–56. https://doi.org/10.1038/nrn2044.

Başar, E, C Başar-Eroğlu, S Karakaş, and M Schürmann. 2000. “Brain Oscillations in Perception and Memory.” *International Journal of Psychophysiology* 35 (2–3): 95–124. https://doi.org/10.1016/S0167-8760(99)00047-1.

Basile, Benjamin M, Victoria L Templer, Regina Paxton Gazes, and Robert R Hampton. 2020. “Preserved Visual Memory and Relational Cognition Performance in Monkeys with Selective Hippocampal Lesions.” *Science Advances* 6 (29): eaaz0484. https://doi.org/10.1126/sciadv.aaz0484.

Battaglia, Demian, Annette Witt, Fred Wolf, and Theo Geisel. 2012. “Dynamic Effective Connectivity of Inter-Areal Brain Circuits.” *PLoS Computational Biology* 8 (3): e1002438. https://doi.org/10.1371/journal.pcbi.1002438.

Bédard, Claude, and Alain Destexhe. 2009. “Macroscopic Models of Local Field Potentials and the Apparent 1/f Noise in Brain Activity.” *Biophysical Journal* 96 (7): 2589–2603. https://doi.org/10.1016/j.bpj.2008.12.3951.

Belluscio, Mariano A, Kenji Mizuseki, Robert Schmidt, Richard Kempter, and György Buzsáki. 2012. “Cross-Frequency Phase-Phase Coupling between θ and γ Oscillations in the Hippocampus.” *The Journal of Neuroscience* 32 (2): 423–35. https://doi.org/10.1523/JNEUROSCI.4122-11.2012.

Benchenane, Karim, Adrien Peyrache, Mehdi Khamassi, Patrick L Tierney, Yves Gioanni, Francesco P Battaglia, and Sidney I Wiener. 2010. “Coherent Theta Oscillations and Reorganization of Spike Timing in the Hippocampal- Prefrontal Network upon Learning.” *Neuron* 66 (6): 921–36. https://doi.org/10.1016/j.neuron.2010.05.013.

Bennett, M R, W G Gibson, and J Robinson. 1994. “Dynamics of the CA3 Pyramidal Neuron Autoassociative Memory Network in the Hippocampus.” *Philosophical Transactions of the Royal Society of London. Series B, Biological Sciences* 343 (1304): 167–87. https://doi.org/10.1098/rstb.1994.0019.

Berens, Philipp. 2009. “Circstat : A *MATLAB* Toolbox for Circular Statistics.” *Journal of Statistical Software* 31 (10). https://doi.org/10.18637/jss.v031.i10.

Berger, Michael, Naubahar Shahryar Agha, and Alexander Gail. 2020. “Wireless Recording from Unrestrained Monkeys Reveals Motor Goal Encoding beyond Immediate Reach in Frontoparietal Cortex.” *ELife* 9 (May). https://doi.org/10.7554/eLife.51322.

Berg, Rune W, Diane Whitmer, and David Kleinfeld. 2006. “Exploratory Whisking by Rat Is Not Phase Locked to the Hippocampal Theta Rhythm.” *The Journal of Neuroscience* 26 (24): 6518–22. https://doi.org/10.1523/JNEUROSCI.0190-06.2006.

Berndt, Marcus, Massimo Trusel, Todd F Roberts, Brad E Pfeiffer, and Lenora J Volk. 2023. “Bidirectional Synaptic Changes in Deep and Superficial Hippocampal Neurons Following in Vivo Activity.” *Neuron* 111 (19): 2984-2994.e4. https://doi.org/10.1016/j.neuron.2023.08.014.

Berndt, Marcus, Massimo Trusel, Todd F. Roberts, Lenora J. Volk, and Brad E. Pfeiffer. 2022. “Bidirectional Synaptic Changes in Deep and Superficial Hippocampal Neurons Following *in Vivo* Activity.” *BioRxiv*, October. https://doi.org/10.1101/2022.10.27.514077.

Berry, S D, and M A Seager. 2001. “Hippocampal Theta Oscillations and Classical Conditioning.” *Neurobiology of Learning and Memory* 76 (3): 298–313. https://doi.org/10.1006/nlme.2001.4025.

Berry, S D, and R F Thompson. 1978. “Prediction of Learning Rate from the Hippocampal Electroencephalogram.” *Science* 200 (4347): 1298–1300. https://doi.org/10.1126/science.663612.

Besserve, Michel, Scott C Lowe, Nikos K Logothetis, Bernhard Schölkopf, and Stefano Panzeri. 2015. “Shifts of Gamma Phase across Primary Visual Cortical Sites Reflect Dynamic Stimulus-Modulated Information Transfer.” *PLoS Biology* 13 (9): e1002257. https://doi.org/10.1371/journal.pbio.1002257.

Bezaire, Marianne J, and Ivan Soltesz. 2013. “Quantitative Assessment of CA1 Local Circuits: Knowledge Base for Interneuron-Pyramidal Cell Connectivity.” *Hippocampus* 23 (9): 751–85. https://doi.org/10.1002/hipo.22141.

Bieri, Kevin Wood, Katelyn N Bobbitt, and Laura Lee Colgin. 2014. “Slow and Fast γ Rhythms Coordinate Different Spatial Coding Modes in Hippocampal Place Cells.” *Neuron* 82 (3): 670–81. https://doi.org/10.1016/j.neuron.2014.03.013.

Bi, G, and M Poo. 1999. “Distributed Synaptic Modification in Neural Networks Induced by Patterned Stimulation.” *Nature* 401 (6755): 792–96. https://doi.org/10.1038/44573.

Blair, R C, and W Karniski. 1993. “An Alternative Method for Significance Testing of Waveform Difference Potentials.” *Psychophysiology* 30 (5): 518–24. https://doi.org/10.1111/j.1469-8986.1993.tb02075.x.

Bland, B H, and S D Oddie. 2001. “Theta Band Oscillation and Synchrony in the Hippocampal Formation and Associated Structures: The Case for Its Role in Sensorimotor Integration.” *Behavioural Brain Research* 127 (1–2): 119–36. https://doi.org/10.1016/s0166-4328(01)00358-8.

Bliss, T V, and G L Collingridge. 1993. “A Synaptic Model of Memory: Long-Term Potentiation in the Hippocampus.” *Nature* 361 (6407): 31–39. https://doi.org/10.1038/361031a0.

Bliss, T V, and T Lomo. 1973. “Long-Lasting Potentiation of Synaptic Transmission in the Dentate Area of the Anaesthetized Rabbit Following Stimulation of the Perforant Path.” *The Journal of Physiology* 232 (2): 331–56. https://doi.org/10.1113/jphysiol.1973.sp010273.

Bocchio, Marco, Sadegh Nabavi, and Marco Capogna. 2017. “Synaptic Plasticity, Engrams, and Network Oscillations in Amygdala Circuits for Storage and Retrieval of Emotional Memories.” *Neuron* 94 (4): 731–43. https://doi.org/10.1016/j.neuron.2017.03.022.

Bódizs, R, S Kántor, G Szabó, A Szûcs, L Erõss, and P Halász. 2001. “Rhythmic Hippocampal Slow Oscillation Characterizes REM Sleep in Humans.” *Hippocampus* 11 (6): 747–53. https://doi.org/10.1002/hipo.1090.

Bohbot, Véronique D, Milagros S Copara, Jean Gotman, and Arne D Ekstrom. 2017. “Low-Frequency Theta Oscillations in the Human Hippocampus during Real-World and Virtual Navigation.” *Nature Communications* 8 (February): 14415. https://doi.org/10.1038/ncomms14415.

Bontempi, B, C Laurent-Demir, C Destrade, and R Jaffard. 1999. “Time-Dependent Reorganization of Brain Circuitry Underlying Long-Term Memory Storage.” *Nature* 400 (6745): 671–75. https://doi.org/10.1038/23270.

Börgers, Christoph, and Nancy Kopell. 2003. “Synchronization in Networks of Excitatory and Inhibitory Neurons with Sparse, Random Connectivity.” *Neural Computation* 15 (3): 509–38. https://doi.org/10.1162/089976603321192059.

Borhegyi, Zsolt, Viktor Varga, Nóra Szilágyi, Dániel Fabo, and Tamás F Freund. 2004. “Phase Segregation of Medial Septal GABAergic Neurons during Hippocampal Theta Activity.” *The Journal of Neuroscience* 24 (39): 8470–79. https://doi.org/10.1523/JNEUROSCI.1413-04.2004.

Boucly, Céline J, Marco N Pompili, Ralitsa Todorova, Eulalie M Leroux, Sidney Wiener, and Michaël Zugaro. 2022. “Flexible Communication between Cell Assemblies and ‘reader’ Neurons.” *BioRxiv*, September. https://doi.org/10.1101/2022.09.06.506754.

Bragin, A, G Jandó, Z Nádasdy, J Hetke, K Wise, and G Buzsáki. 1995. “Gamma (40-100 Hz) Oscillation in the Hippocampus of the Behaving Rat.” *The Journal of Neuroscience* 15 (1 Pt 1): 47–60. https://doi.org/10.1523/JNEUROSCI.15-01-00047.1995.

Bragin, A, G Jandó, Z Nádasdy, M van Landeghem, and G Buzsáki. 1995. “Dentate EEG Spikes and Associated Interneuronal Population Bursts in the Hippocampal Hilar Region of the Rat.” *Journal of Neurophysiology* 73 (4): 1691–1705. https://doi.org/10.1152/jn.1995.73.4.1691.

Brainard, D H. 1997. “The Psychophysics Toolbox.” *Spatial Vision* 10 (4): 433–36. https://doi.org/10.1163/156856897X00357.

Brandon, Mark P, Andrew R Bogaard, Nathan W Schultheiss, and Michael E Hasselmo. 2013. “Segregation of Cortical Head Direction Cell Assemblies on Alternating θ Cycles.” *Nature Neuroscience* 16 (6): 739–48. https://doi.org/10.1038/nn.3383.

Brandstatt, Kelly L, and Joel L Voss. 2014. “Age-Related Impairments in Active Learning and Strategic Visual Exploration.” *Frontiers in Aging Neuroscience* 6 (February): 19. https://doi.org/10.3389/fnagi.2014.00019.

Bressler, S L, and J A S Kelso. 2001. “Cortical Coordination Dynamics and Cognition.” *Trends in Cognitive Sciences* 5 (1): 26–36. https://doi.org/10.1016/s1364-6613(00)01564-3.

Brincat, Scott L, and Earl K Miller. 2015. “Frequency-Specific Hippocampal-Prefrontal Interactions during Associative Learning.” *Nature Neuroscience* 18 (4): 576–81. https://doi.org/10.1038/nn.3954.

Brooks, B M, E A Attree, F D Rose, B R Clifford, and A G Leadbetter. 1999. “The Specificity of Memory Enhancement during Interaction with a Virtual Environment.” *Memory* 7 (1): 65–78. https://doi.org/10.1080/741943713.

Brown, Emily Kathryn, Benjamin M Basile, Victoria L Templer, and Robert R Hampton. 2019. “Dissociation of Memory Signals for Metamemory in Rhesus Monkeys (Macaca Mulatta).” *Animal Cognition* 22 (3): 331–41. https://doi.org/10.1007/s10071-019-01246-5.

Bugeon, Stéphane, Joshua Duffield, Mario Dipoppa, Anne Ritoux, Isabelle Prankerd, Dimitris Nicoloutsopoulos, David Orme, et al. 2022. “A Transcriptomic Axis Predicts State Modulation of Cortical Interneurons.” *Nature* 607 (7918): 330–38. https://doi.org/10.1038/s41586-022-04915-7.

Bukhtiyarova, Olga, Sylvain Chauvette, Josée Seigneur, and Igor Timofeev. 2022. “Brain States in Freely Behaving Marmosets.” *Sleep* 45 (8). https://doi.org/10.1093/sleep/zsac106.

Bullock, T H, J Z Achimowicz, R B Duckrow, S S Spencer, and V J Iragui-Madoz. 1997. “Bicoherence of Intracranial EEG in Sleep, Wakefulness and Seizures.” *Electroencephalography and Clinical Neurophysiology* 103 (6): 661–78. https://doi.org/10.1016/s0013-4694(97)00087-4.

Bunsey, M, and H Eichenbaum. 1996. “Conservation of Hippocampal Memory Function in Rats and Humans.” *Nature* 379 (6562): 255–57. https://doi.org/10.1038/379255a0.

Burke, John F, Nicole M Long, Kareem A Zaghloul, Ashwini D Sharan, Michael R Sperling, and Michael J Kahana. 2014. “Human Intracranial High-Frequency Activity Maps Episodic Memory Formation in Space and Time.” *Neuroimage* 85 Pt 2 (January): 834–43. https://doi.org/10.1016/j.neuroimage.2013.06.067.

Burns, Samuel P, Dajun Xing, and Robert M Shapley. 2011. “Is Gamma-Band Activity in the Local Field Potential of V1 Cortex a ‘Clock’ or Filtered Noise?” *The Journal of Neuroscience* 31 (26): 9658–64. https://doi.org/10.1523/JNEUROSCI.0660-11.2011.

Burn, Charlotte C. 2008. “What Is It like to Be a Rat? Rat Sensory Perception and Its Implications for Experimental Design and Rat Welfare.” *Applied Animal Behaviour Science* 112 (1–2): 1–32. https://doi.org/10.1016/j.applanim.2008.02.007.

Bush, Daniel, and Neil Burgess. 2020. “Advantages and Detection of Phase Coding in the Absence of Rhythmicity.” *Hippocampus*, February. https://doi.org/10.1002/hipo.23199.

Buzsáki, G, D L Buhl, K D Harris, J Csicsvari, B Czéh, and A Morozov. 2003. “Hippocampal Network Patterns of Activity in the Mouse.” *Neuroscience* 116 (1): 201–11. https://doi.org/10.1016/s0306-4522(02)00669-3.

Buzsáki, G, J Czopf, I Kondákor, and L Kellényi. 1986. “Laminar Distribution of Hippocampal Rhythmic Slow Activity (RSA) in the Behaving Rat: Current-Source Density Analysis, Effects of Urethane and Atropine.” *Brain Research* 365 (1): 125–37. https://doi.org/10.1016/0006-8993(86)90729-8.

Buzsàki, G, and E Eidelberg. 1983. “Phase Relations of Hippocampal Projection Cells and Interneurons to Theta Activity in the Anesthetized Rat.” *Brain Research* 266 (2): 334–39. https://doi.org/10.1016/0006-8993(83)90665-0.

Buzsáki, G, Z Horváth, R Urioste, J Hetke, and K Wise. 1992. “High-Frequency Network Oscillation in the Hippocampus.” *Science* 256 (5059): 1025–27. https://doi.org/10.1126/science.1589772.

Buzsáki, G, L W Leung, and C H Vanderwolf. 1983. “Cellular Bases of Hippocampal EEG in the Behaving Rat.” *Brain Research* 287 (2): 139–71. https://doi.org/10.1016/0165-0173(83)90037-1.

Buzsáki, G. 1986. “Hippocampal Sharp Waves: Their Origin and Significance.” *Brain Research* 398 (2): 242–52. https://doi.org/10.1016/0006-8993(86)91483-6.

———. 1989. “Two-Stage Model of Memory Trace Formation: A Role for ‘Noisy’ Brain States.” *Neuroscience* 31 (3): 551–70. https://doi.org/10.1016/0306-4522(89)90423-5.

———. 1996. “The Hippocampo-Neocortical Dialogue.” *Cerebral Cortex* 6 (2): 81–92. https://doi.org/10.1093/cercor/6.2.81.

Buzsáki, György, Costas A Anastassiou, and Christof Koch. 2012. “The Origin of Extracellular Fields and Currents--EEG, ECoG, LFP and Spikes.” *Nature Reviews. Neuroscience* 13 (6): 407–20. https://doi.org/10.1038/nrn3241.

Buzsáki, György, and Andreas Draguhn. 2004. “Neuronal Oscillations in Cortical Networks.” *Science* 304 (5679): 1926–29. https://doi.org/10.1126/science.1099745.

Buzsáki, György, and Rodolfo Llinás. 2017. “Space and Time in the Brain.” *Science* 358 (6362): 482–85. https://doi.org/10.1126/science.aan8869.

Buzsáki, György, Sam McKenzie, and Lila Davachi. 2022. “Neurophysiology of Remembering.” *Annual Review of Psychology* 73 (January): 187–215. https://doi.org/10.1146/annurev-psych-021721-110002.

Buzsáki, György, and Kenji Mizuseki. 2014. “The Log-Dynamic Brain: How Skewed Distributions Affect Network Operations.” *Nature Reviews. Neuroscience* 15 (4): 264–78. https://doi.org/10.1038/nrn3687.

Buzsáki, György, and Edvard I Moser. 2013. “Memory, Navigation and Theta Rhythm in the Hippocampal-Entorhinal System.” *Nature Neuroscience* 16 (2): 130–38. https://doi.org/10.1038/nn.3304.

Buzsáki, György, and David Tingley. 2018. “Space and Time: The Hippocampus as a Sequence Generator.” *Trends in Cognitive Sciences* 22 (10): 853–69. https://doi.org/10.1016/j.tics.2018.07.006.

Buzsáki, György, and Xiao-Jing Wang. 2012. “Mechanisms of Gamma Oscillations.” *Annual Review of Neuroscience* 35 (March): 203–25. https://doi.org/10.1146/annurev-neuro-062111-150444.

Buzsáki, György. 2002. “Theta Oscillations in the Hippocampus.” *Neuron* 33 (3): 325–40. https://doi.org/10.1016/S0896-6273(02)00586-X.

———. 2004. “Large-Scale Recording of Neuronal Ensembles.” *Nature Neuroscience* 7 (5): 446–51. https://doi.org/10.1038/nn1233.

———. 2006. *Rhythms of the Brain*. Oxford University Press. https://doi.org/10.1093/acprof:oso/9780195301069.001.0001.

———. 2010. “Neural Syntax: Cell Assemblies, Synapsembles, and Readers.” *Neuron* 68 (3): 362–85. https://doi.org/10.1016/j.neuron.2010.09.023.

———. 2015. “Hippocampal Sharp Wave-Ripple: A Cognitive Biomarker for Episodic Memory and Planning.” *Hippocampus* 25 (10): 1073–1188. https://doi.org/10.1002/hipo.22488.

Cabral, Henrique O, Martin Vinck, Celine Fouquet, Cyriel M A Pennartz, Laure Rondi-Reig, and Francesco P Battaglia. 2014. “Oscillatory Dynamics and Place Field Maps Reflect Hippocampal Ensemble Processing of Sequence and Place Memory under NMDA Receptor Control.” *Neuron* 81 (2): 402–15. https://doi.org/10.1016/j.neuron.2013.11.010.

Cacucci, Francesca, Colin Lever, Thomas J Wills, Neil Burgess, and John O’Keefe. 2004. “Theta-Modulated Place-by-Direction Cells in the Hippocampal Formation in the Rat.” *The Journal of Neuroscience* 24 (38): 8265–77. https://doi.org/10.1523/JNEUROSCI.2635-04.2004.

Cantero, Jose L, Mercedes Atienza, Robert Stickgold, Michael J Kahana, Joseph R Madsen, and Bernat Kocsis. 2003. “Sleep-Dependent Theta Oscillations in the Human Hippocampus and Neocortex.” *The Journal of Neuroscience* 23 (34): 10897–903. https://doi.org/10.1523/JNEUROSCI.23-34-10897.2003.

Caplan, J B, J R Madsen, S Raghavachari, and M J Kahana. 2001. “Distinct Patterns of Brain Oscillations Underlie Two Basic Parameters of Human Maze Learning.” *Journal of Neurophysiology* 86 (1): 368–80. https://doi.org/10.1152/jn.2001.86.1.368.

Caporale, Natalia, and Yang Dan. 2008. “Spike Timing-Dependent Plasticity: A Hebbian Learning Rule.” *Annual Review of Neuroscience* 31: 25–46. https://doi.org/10.1146/annurev.neuro.31.060407.125639.

Carassa, A, G Geminiani, F Morganti, and D Varotto. 2002. “Active and Passive Spatial Learning in a Complex Virtual Environment: The Effect of Effcient Exploration.”

Cardin, Jessica A. 2018. “Inhibitory Interneurons Regulate Temporal Precision and Correlations in Cortical Circuits.” *Trends in Neurosciences* 41 (10): 689–700. https://doi.org/10.1016/j.tins.2018.07.015.

Carrillo-Reid, Luis, Jae-Eun Kang Miller, Jordan P Hamm, Jesse Jackson, and Rafael Yuste. 2015. “Endogenous Sequential Cortical Activity Evoked by Visual Stimuli.” *The Journal of Neuroscience* 35 (23): 8813–28. https://doi.org/10.1523/JNEUROSCI.5214-14.2015.

Carr, Margaret F, Shantanu P Jadhav, and Loren M Frank. 2011. “Hippocampal Replay in the Awake State: A Potential Substrate for Memory Consolidation and Retrieval.” *Nature Neuroscience* 14 (2): 147–53. https://doi.org/10.1038/nn.2732.

Cavada, C, T Compañy, J Tejedor, R J Cruz-Rizzolo, and F Reinoso-Suárez. 2000. “The Anatomical Connections of the Macaque Monkey Orbitofrontal Cortex. A Review.” *Cerebral Cortex* 10 (3): 220–42. https://doi.org/10.1093/cercor/10.3.220.

Cembrowski, Mark S, and Nelson Spruston. 2019. “Heterogeneity within Classical Cell Types Is the Rule: Lessons from Hippocampal Pyramidal Neurons.” *Nature Reviews. Neuroscience* 20 (4): 193–204. https://doi.org/10.1038/s41583-019-0125-5.

Chaieb, Leila, Marcin Leszczynski, Nikolai Axmacher, Marlene Höhne, Christian E Elger, and Juergen Fell. 2015. “Theta-Gamma Phase-Phase Coupling during Working Memory Maintenance in the Human Hippocampus.” *Cognitive Neuroscience* 6 (4): 149–57. https://doi.org/10.1080/17588928.2015.1058254.

Charles, David P, David Gaffan, and Mark J Buckley. 2004. “Impaired Recency Judgments and Intact Novelty Judgments after Fornix Transection in Monkeys.” *The Journal of Neuroscience* 24 (8): 2037–44. https://doi.org/10.1523/JNEUROSCI.3796-03.2004.

Chau, Vivian L, Emily F Murphy, R Shayna Rosenbaum, Jennifer D Ryan, and Kari L Hoffman. 2011. “A Flicker Change Detection Task Reveals Object-in-Scene Memory Across Species.” *Frontiers in Behavioral Neuroscience* 5 (September): 58. https://doi.org/10.3389/fnbeh.2011.00058.

Chen, Guifen, John A King, Neil Burgess, and John O’Keefe. 2013. “How Vision and Movement Combine in the Hippocampal Place Code.” *Proceedings of the National Academy of Sciences of the United States of America* 110 (1): 378–83. https://doi.org/10.1073/pnas.1215834110.

Chenani, Alireza, Marta Sabariego, Magdalene I Schlesiger, Jill K Leutgeb, Stefan Leutgeb, and Christian Leibold. 2019. “Hippocampal CA1 Replay Becomes Less Prominent but More Rigid without Inputs from Medial Entorhinal Cortex.” *Nature Communications* 10 (1): 1341. https://doi.org/10.1038/s41467-019-09280-0.

Chen, Yvonne Y, Daniel Yoshor, Sameer A Sheth, and Brett L Foster. 2020. “Stability of Ripple Events during Task Engagement in Human Hippocampus.” *BioRxiv*, October. https://doi.org/10.1101/2020.10.17.342881.

Chen, Zhe Sage, and Matthew A Wilson. 2023. “How Our Understanding of Memory Replay Evolves.” *Journal of Neurophysiology* 129 (3): 552–80. https://doi.org/10.1152/jn.00454.2022.

Cheveigné, Alain de, and Israel Nelken. 2019. “Filters: When, Why, and How (Not) to Use Them.” *Neuron* 102 (2): 280–93. https://doi.org/10.1016/j.neuron.2019.02.039.

Choi, Jun-Hyeok, Su-Eon Sim, Ji-Il Kim, Dong Il Choi, Jihae Oh, Sanghyun Ye, Jaehyun Lee, et al. 2018. “Interregional Synaptic Maps among Engram Cells Underlie Memory Formation.” *Science* 360 (6387): 430–35. https://doi.org/10.1126/science.aas9204.

Chrobak, J J, and G Buzsáki. 1998. “Gamma Oscillations in the Entorhinal Cortex of the Freely Behaving Rat.” *The Journal of Neuroscience* 18 (1): 388–98. https://doi.org/10.1523/JNEUROSCI.18-01-00388.1998.

Chronister, R B, and J F DeFrance. 1979. “Organization of Projection Neurons of the Hippocampus.” *Experimental Neurology* 66 (3): 509–23. https://doi.org/10.1016/0014-4886(79)90198-5.

Clayton, Nicola S, Timothy J Bussey, and Anthony Dickinson. 2003. “Can Animals Recall the Past and Plan for the Future?” *Nature Reviews. Neuroscience* 4 (8): 685–91. https://doi.org/10.1038/nrn1180.

Clayton, N S, and A Dickinson. 1998. “Episodic-like Memory during Cache Recovery by Scrub Jays.” *Nature* 395 (6699): 272–74. https://doi.org/10.1038/26216.

Cobb, S R, E H Buhl, K Halasy, O Paulsen, and P Somogyi. 1995. “Synchronization of Neuronal Activity in Hippocampus by Individual GABAergic Interneurons.” *Nature* 378 (6552): 75–78. https://doi.org/10.1038/378075a0.

Colgin, Laura Lee, Tobias Denninger, Marianne Fyhn, Torkel Hafting, Tora Bonnevie, Ole Jensen, May-Britt Moser, and Edvard I Moser. 2009. “Frequency of Gamma Oscillations Routes Flow of Information in the Hippocampus.” *Nature* 462 (7271): 353–57. https://doi.org/10.1038/nature08573.

Colgin, Laura Lee, and Edvard I Moser. 2010. “Gamma Oscillations in the Hippocampus.” *Physiology* 25 (5): 319–29. https://doi.org/10.1152/physiol.00021.2010.

Colgin, Laura Lee. 2013. “Mechanisms and Functions of Theta Rhythms.” *Annual Review of Neuroscience* 36 (July): 295–312. https://doi.org/10.1146/annurev-neuro-062012-170330.

———. 2016. “Rhythms of the Hippocampal Network.” *Nature Reviews. Neuroscience* 17 (4): 239–49. https://doi.org/10.1038/nrn.2016.21.

Courellis, Hristos S, Samuel U Nummela, Michael Metke, Geoffrey W Diehl, Robert Bussell, Gert Cauwenberghs, and Cory T Miller. 2019. “Spatial Encoding in Primate Hippocampus during Free Navigation.” *PLoS Biology* 17 (12): e3000546. https://doi.org/10.1371/journal.pbio.3000546.

Cox, Roy, Theodor Rüber, Bernhard P Staresina, and Juergen Fell. 2019. “Heterogeneous Profiles of Coupled Sleep Oscillations in Human Hippocampus.” *Neuroimage* 202 (November): 116178. https://doi.org/10.1016/j.neuroimage.2019.116178.

Craig, Michael T, and Chris J McBain. 2015. “Fast Gamma Oscillations Are Generated Intrinsically in CA1 without the Involvement of Fast-Spiking Basket Cells.” *The Journal of Neuroscience* 35 (8): 3616–24. https://doi.org/10.1523/JNEUROSCI.4166-14.2015.

Crystal, Jonathon D. 2021. “Evaluating Evidence from Animal Models of Episodic Memory.” *Journal of Experimental Psychology. Animal Learning and Cognition* 47 (3): 337–56. https://doi.org/10.1037/xan0000294.

Csicsvari, J, H Hirase, A Czurkó, A Mamiya, and G Buzsáki. 1999a. “Oscillatory Coupling of Hippocampal Pyramidal Cells and Interneurons in the Behaving Rat.” *The Journal of Neuroscience* 19 (1): 274–87. https://doi.org/10.1523/JNEUROSCI.19-01-00274.1999.

———. 1999b. “Fast Network Oscillations in the Hippocampal CA1 Region of the Behaving Rat.” *The Journal of Neuroscience* 19 (16): RC20. https://doi.org/10.1523/JNEUROSCI.19-16-j0001.1999.

Csicsvari, Jozsef, Brian Jamieson, Kensall D Wise, and György Buzsáki. 2003. “Mechanisms of Gamma Oscillations in the Hippocampus of the Behaving Rat.” *Neuron* 37 (2): 311–22. https://doi.org/10.1016/s0896-6273(02)01169-8.

Cunningham, Mark O, Ceri H Davies, Eberhard H Buhl, Nancy Kopell, and Miles A Whittington. 2003. “Gamma Oscillations Induced by Kainate Receptor Activation in the Entorhinal Cortex in Vitro.” *The Journal of Neuroscience* 23 (30): 9761–69. https://doi.org/10.1523/JNEUROSCI.23-30-09761.2003.

Cutsuridis, Vassilis, and Michael Hasselmo. 2012. “GABAergic Contributions to Gating, Timing, and Phase Precession of Hippocampal Neuronal Activity during Theta Oscillations.” *Hippocampus* 22 (7): 1597–1621. https://doi.org/10.1002/hipo.21002.

Danielson, Nathan B, Jeffrey D Zaremba, Patrick Kaifosh, John Bowler, Max Ladow, and Attila Losonczy. 2016. “Sublayer-Specific Coding Dynamics during Spatial Navigation and Learning in Hippocampal Area CA1.” *Neuron* 91 (3): 652–65. https://doi.org/10.1016/j.neuron.2016.06.020.

Davachi, Lila, and Sarah DuBrow. 2015. “How the Hippocampus Preserves Order: The Role of Prediction and Context.” *Trends in Cognitive Sciences* 19 (2): 92–99. https://doi.org/10.1016/j.tics.2014.12.004.

Davidson, Thomas J, Fabian Kloosterman, and Matthew A Wilson. 2009. “Hippocampal Replay of Extended Experience.” *Neuron* 63 (4): 497–507. https://doi.org/10.1016/j.neuron.2009.07.027.

Dede, Adam J O, Jennifer C Frascino, John T Wixted, and Larry R Squire. 2016. “Learning and Remembering Real-World Events after Medial Temporal Lobe Damage.” *Proceedings of the National Academy of Sciences of the United States of America* 113 (47): 13480–85. https://doi.org/10.1073/pnas.1617025113.

Demanuele, Charmaine, Christopher J James, and Edmund Js Sonuga-Barke. 2007. “Distinguishing Low Frequency Oscillations within the 1/f Spectral Behaviour of Electromagnetic Brain Signals.” *Behavioral and Brain Functions* 3 (December): 62. https://doi.org/10.1186/1744-9081-3-62.

Devito, Loren M, Benjamin R Kanter, and Howard Eichenbaum. 2010. “The Hippocampus Contributes to Memory Expression during Transitive Inference in Mice.” *Hippocampus* 20 (1): 208–17. https://doi.org/10.1002/hipo.20610.

Diba, Kamran, and György Buzsáki. 2007. “Forward and Reverse Hippocampal Place-Cell Sequences during Ripples.” *Nature Neuroscience* 10 (10): 1241–42. https://doi.org/10.1038/nn1961.

Dickson, C T, J Magistretti, M H Shalinsky, E Fransén, M E Hasselmo, and A Alonso. 2000. “Properties and Role of I(h) in the Pacing of Subthreshold Oscillations in Entorhinal Cortex Layer II Neurons.” *Journal of Neurophysiology* 83 (5): 2562–79. https://doi.org/10.1152/jn.2000.83.5.2562.

Diekelmann, Susanne, and Jan Born. 2010. “The Memory Function of Sleep.” *Nature Reviews. Neuroscience* 11 (2): 114–26. https://doi.org/10.1038/nrn2762.

Donoghue, Thomas, Matar Haller, Erik J Peterson, Paroma Varma, Priyadarshini Sebastian, Richard Gao, Torben Noto, et al. 2020. “Parameterizing Neural Power Spectra into Periodic and Aperiodic Components.” *Nature Neuroscience* 23 (12): 1655–65. https://doi.org/10.1038/s41593-020-00744-x.

Doucet, Guillaume, Roberto A Gulli, Benjamin W Corrigan, Lyndon R Duong, and Julio C Martinez-Trujillo. 2020. “Modulation of Local Field Potentials and Neuronal Activity in Primate Hippocampus during Saccades.” *Hippocampus* 30 (3): 192–209. https://doi.org/10.1002/hipo.23140.

Doucet, Guillaume, Roberto A Gulli, and Julio C Martinez-Trujillo. 2016. “Cross-Species 3D Virtual Reality Toolbox for Visual and Cognitive Experiments.” *Journal of Neuroscience Methods* 266 (June): 84–93. https://doi.org/10.1016/j.jneumeth.2016.03.009.

Douchamps, Vincent, Ali Jeewajee, Pam Blundell, Neil Burgess, and Colin Lever. 2013. “Evidence for Encoding versus Retrieval Scheduling in the Hippocampus by Theta Phase and Acetylcholine.” *The Journal of Neuroscience* 33 (20): 8689–8704. https://doi.org/10.1523/JNEUROSCI.4483-12.2013.

Douglas, R J. 1967. “The Hippocampus and Behavior.” *Psychological Bulletin* 67 (6): 416–22. https://doi.org/10.1037/h0024599.

Dragoi, George, and György Buzsáki. 2006. “Temporal Encoding of Place Sequences by Hippocampal Cell Assemblies.” *Neuron* 50 (1): 145–57. https://doi.org/10.1016/j.neuron.2006.02.023.

Dragoi, George, and Susumu Tonegawa. 2011. “Preplay of Future Place Cell Sequences by Hippocampal Cellular Assemblies.” *Nature* 469 (7330): 397–401. https://doi.org/10.1038/nature09633.

———. 2013. “Distinct Preplay of Multiple Novel Spatial Experiences in the Rat.” *Proceedings of the National Academy of Sciences of the United States of America* 110 (22): 9100–9105. https://doi.org/10.1073/pnas.1306031110.

———. 2014. “Selection of Preconfigured Cell Assemblies for Representation of Novel Spatial Experiences.” *Philosophical Transactions of the Royal Society of London. Series B, Biological Sciences* 369 (1635): 20120522. https://doi.org/10.1098/rstb.2012.0522.

Dragoi, George. 2020. “Cell Assemblies, Sequences and Temporal Coding in the Hippocampus.” *Current Opinion in Neurobiology* 64 (October): 111–18. https://doi.org/10.1016/j.conb.2020.03.003.

Drieu, Céline, Ralitsa Todorova, and Michaël Zugaro. 2018. “Nested Sequences of Hippocampal Assemblies during Behavior Support Subsequent Sleep Replay.” *Science* 362 (6415): 675–79. https://doi.org/10.1126/science.aat2952.

Drieu, Céline, and Michaël Zugaro. 2019. “Hippocampal Sequences during Exploration: Mechanisms and Functions.” *Frontiers in Cellular Neuroscience* 13 (June): 232. https://doi.org/10.3389/fncel.2019.00232.

Dudai, Yadin. 2004. “The Neurobiology of Consolidations, or, How Stable Is the Engram?” *Annual Review of Psychology* 55: 51–86. https://doi.org/10.1146/annurev.psych.55.090902.142050.

Dudok, Barna, Peter M Klein, Ernie Hwaun, Brian R Lee, Zizhen Yao, Olivia Fong, John C Bowler, et al. 2021. “Alternating Sources of Perisomatic Inhibition during Behavior.” *Neuron* 109 (6): 997-1012.e9. https://doi.org/10.1016/j.neuron.2021.01.003.

Dudok, Barna, Miklos Szoboszlay, Anirban Paul, Peter M Klein, Zhenrui Liao, Ernie Hwaun, Gergely G Szabo, et al. 2021. “Recruitment and Inhibitory Action of Hippocampal Axo-Axonic Cells during Behavior.” *Neuron* 109 (23): 3838-3850.e8. https://doi.org/10.1016/j.neuron.2021.09.033.

Dunn, Soraya L S, Stephen M Town, Jennifer K Bizley, and Daniel Bendor. 2022. “Behaviourally Modulated Hippocampal Theta Oscillations in the Ferret Persist during Both Locomotion and Immobility.” *Nature Communications* 13 (1): 5905. https://doi.org/10.1038/s41467-022-33507-2.

Dupret, David, Joseph O’Neill, and Jozsef Csicsvari. 2013. “Dynamic Reconfiguration of Hippocampal Interneuron Circuits during Spatial Learning.” *Neuron* 78 (1): 166–80. https://doi.org/10.1016/j.neuron.2013.01.033.

Dupret, David, Barty Pleydell-Bouverie, and Jozsef Csicsvari. 2008. “Inhibitory Interneurons and Network Oscillations.” *Proceedings of the National Academy of Sciences of the United States of America* 105 (47): 18079–80. https://doi.org/10.1073/pnas.0810064105.

Dusek, J A, and H Eichenbaum. 1997. “The Hippocampus and Memory for Orderly Stimulus Relations.” *Proceedings of the National Academy of Sciences of the United States of America* 94 (13): 7109–14. https://doi.org/10.1073/pnas.94.13.7109.

Eastman, Kyler M, and Alexander C Huk. 2012. “PLDAPS: A Hardware Architecture and Software Toolbox for Neurophysiology Requiring Complex Visual Stimuli and Online Behavioral Control.” *Frontiers in Neuroinformatics* 6 (January): 1. https://doi.org/10.3389/fninf.2012.00001.

Edeline, J M, G Dutrieux, Y Manunta, and E Hennevin. 2001. “Diversity of Receptive Field Changes in Auditory Cortex during Natural Sleep.” *The European Journal of Neuroscience* 14 (11): 1865–80. https://doi.org/10.1046/j.0953-816x.2001.01821.x.

Ego-Stengel, Valérie, and Matthew A Wilson. 2010. “Disruption of Ripple-Associated Hippocampal Activity during Rest Impairs Spatial Learning in the Rat.” *Hippocampus* 20 (1): 1–10. https://doi.org/10.1002/hipo.20707.

Eichenbaum, H, P Dudchenko, E Wood, M Shapiro, and H Tanila. 1999. “The Hippocampus, Memory, and Place Cells: Is It Spatial Memory or a Memory Space?” *Neuron* 23 (2): 209–26. https://doi.org/10.1016/s0896-6273(00)80773-4.

Eichenbaum, Howard. 2014. “Time Cells in the Hippocampus: A New Dimension for Mapping Memories.” *Nature Reviews. Neuroscience* 15 (11): 732–44. https://doi.org/10.1038/nrn3827.

———. 2017a. “The Role of the Hippocampus in Navigation Is Memory.” *Journal of Neurophysiology* 117 (4): 1785–96. https://doi.org/10.1152/jn.00005.2017.

———. 2017b. “Time (and Space) in the Hippocampus.” *Current Opinion in Behavioral Sciences* 17 (October): 65–70. https://doi.org/10.1016/j.cobeha.2017.06.010.

Ekstrom, Arne D, Jeremy B Caplan, Emily Ho, Kirk Shattuck, Itzhak Fried, and Michael J Kahana. 2005. “Human Hippocampal Theta Activity during Virtual Navigation.” *Hippocampus* 15 (7): 881–89. https://doi.org/10.1002/hipo.20109.

Eliav, Tamir, Maya Geva-Sagiv, Michael M Yartsev, Arseny Finkelstein, Alon Rubin, Liora Las, and Nachum Ulanovsky. 2018. “Nonoscillatory Phase Coding and Synchronization in the Bat Hippocampal Formation.” *Cell* 175 (4): 1119-1130.e15. https://doi.org/10.1016/j.cell.2018.09.017.

Ellender, Tommas J, Wiebke Nissen, Laura L Colgin, Edward O Mann, and Ole Paulsen. 2010. “Priming of Hippocampal Population Bursts by Individual Perisomatic-Targeting Interneurons.” *The Journal of Neuroscience* 30 (17): 5979–91. https://doi.org/10.1523/JNEUROSCI.3962-09.2010.

English, Daniel Fine, Sam McKenzie, Talfan Evans, Kanghwan Kim, Euisik Yoon, and György Buzsáki. 2017. “Pyramidal Cell-Interneuron Circuit Architecture and Dynamics in Hippocampal Networks.” *Neuron* 96 (2): 505-520.e7. https://doi.org/10.1016/j.neuron.2017.09.033.

Eschenko, Oxana, Wiâm Ramadan, Matthias Mölle, Jan Born, and Susan J Sara. 2008. “Sustained Increase in Hippocampal Sharp-Wave Ripple Activity during Slow-Wave Sleep after Learning.” *Learning & Memory* 15 (4): 222–28. https://doi.org/10.1101/lm.726008.

Etter, Guillaume, Suzanne van der Veldt, Frédéric Manseau, Iman Zarrinkoub, Emilie Trillaud-Doppia, and Sylvain Williams. 2019. “Optogenetic Gamma Stimulation Rescues Memory Impairments in an Alzheimer’s Disease Mouse Model.” *Nature Communications* 10 (1): 5322. https://doi.org/10.1038/s41467-019-13260-9.

Farooq, Usman, Jeremie Sibille, Kefei Liu, and George Dragoi. 2019. “Strengthened Temporal Coordination within Pre-Existing Sequential Cell Assemblies Supports Trajectory Replay.” *Neuron* 103 (4): 719-733.e7. https://doi.org/10.1016/j.neuron.2019.05.040.

Fell, J, P Klaver, K Lehnertz, T Grunwald, C Schaller, C E Elger, and G Fernández. 2001. “Human Memory Formation Is Accompanied by Rhinal-Hippocampal Coupling and Decoupling.” *Nature Neuroscience* 4 (12): 1259–64. https://doi.org/10.1038/nn759.

Fellner, Marie-Christin, Stephanie Gollwitzer, Stefan Rampp, Gernot Kreiselmeyr, Daniel Bush, Beate Diehl, Nikolai Axmacher, Hajo Hamer, and Simon Hanslmayr. 2019. “Spectral Fingerprints or Spectral Tilt? Evidence for Distinct Oscillatory Signatures of Memory Formation.” *PLoS Biology* 17 (7): e3000403. https://doi.org/10.1371/journal.pbio.3000403.

Fernández-Ruiz, Antonio, Valeri A Makarov, Nuria Benito, and Oscar Herreras. 2012. “Schaffer-Specific Local Field Potentials Reflect Discrete Excitatory Events at Gamma Frequency That May Fire Postsynaptic Hippocampal CA1 Units.” *The Journal of Neuroscience* 32 (15): 5165–76. https://doi.org/10.1523/JNEUROSCI.4499-11.2012.

Fernández-Ruiz, Antonio, Azahara Oliva, Eliezyer Fermino de Oliveira, Florbela Rocha-Almeida, David Tingley, and György Buzsáki. 2019. “Long-Duration Hippocampal Sharp Wave Ripples Improve Memory.” *Science* 364 (6445): 1082–86. https://doi.org/10.1126/science.aax0758.

Fernández-Ruiz, Antonio, Azahara Oliva, Marisol Soula, Florbela Rocha-Almeida, Gergo A Nagy, Gonzalo Martin-Vazquez, and György Buzsáki. 2021. “Gamma Rhythm Communication between Entorhinal Cortex and Dentate Gyrus Neuronal Assemblies.” *Science* 372 (6537). https://doi.org/10.1126/science.abf3119.

Fontanini, Alfredo, and Donald B Katz. 2008. “Behavioral States, Network States, and Sensory Response Variability.” *Journal of Neurophysiology* 100 (3): 1160–68. https://doi.org/10.1152/jn.90592.2008.

Forro, Thomas, and Thomas Klausberger. 2023. “Differential Behavior-Related Activity of Distinct Hippocampal Interneuron Types during Odor-Associated Spatial Navigation.” *Neuron* 111 (15): 2399-2413.e5. https://doi.org/10.1016/j.neuron.2023.05.007.

Fortin, Norbert J, Kara L Agster, and Howard B Eichenbaum. 2002. “Critical Role of the Hippocampus in Memory for Sequences of Events.” *Nature Neuroscience* 5 (5): 458–62. https://doi.org/10.1038/nn834.

Fortin, Norbert J, Sean P Wright, and Howard Eichenbaum. 2004. “Recollection-like Memory Retrieval in Rats Is Dependent on the Hippocampus.” *Nature* 431 (7005): 188–91. https://doi.org/10.1038/nature02853.

Foster, David J, and Matthew A Wilson. 2006. “Reverse Replay of Behavioural Sequences in Hippocampal Place Cells during the Awake State.” *Nature* 440 (7084): 680–83. https://doi.org/10.1038/nature04587.

———. 2007. “Hippocampal Theta Sequences.” *Hippocampus* 17 (11): 1093–99. https://doi.org/10.1002/hipo.20345.

Foster, David J. 2017. “Replay Comes of Age.” *Annual Review of Neuroscience* 40 (July): 581–602. https://doi.org/10.1146/annurev-neuro-072116-031538.

Foster, T C, C A Castro, and B L McNaughton. 1989. “Spatial Selectivity of Rat Hippocampal Neurons: Dependence on Preparedness for Movement.” *Science* 244 (4912): 1580–82. https://doi.org/10.1126/science.2740902.

Fotowat, Haleh, Candice Lee, James Jaeyoon Jun, and Len Maler. 2019. “Neural Activity in a Hippocampus-like Region of the Teleost Pallium Is Associated with Active Sensing and Navigation.” *ELife* 8 (April). https://doi.org/10.7554/eLife.44119.

Fox, S E, S Wolfson, and J B Ranck. 1986. “Hippocampal Theta Rhythm and the Firing of Neurons in Walking and Urethane Anesthetized Rats.” *Experimental Brain Research* 62 (3): 495–508. https://doi.org/10.1007/BF00236028.

França, Arthur S C, Nils Z Borgesius, Bryan C Souza, and Michael X Cohen. 2021. “Beta2 Oscillations in Hippocampal-Cortical Circuits During Novelty Detection.” *Frontiers in Systems Neuroscience* 15 (February): 617388. https://doi.org/10.3389/fnsys.2021.617388.

França, Arthur S C, George C do Nascimento, Vítor Lopes-dos-Santos, Larissa Muratori, Sidarta Ribeiro, Bruno Lobão-Soares, and Adriano B L Tort. 2014. “Beta2 Oscillations (23-30 Hz) in the Mouse Hippocampus during Novel Object Recognition.” *The European Journal of Neuroscience* 40 (11): 3693–3703. https://doi.org/10.1111/ejn.12739.

Franjic, Daniel, Mario Skarica, Shaojie Ma, Jon I Arellano, Andrew T N Tebbenkamp, Jinmyung Choi, Chuan Xu, et al. 2022. “Transcriptomic Taxonomy and Neurogenic Trajectories of Adult Human, Macaque, and Pig Hippocampal and Entorhinal Cells.” *Neuron* 110 (3): 452-469.e14. https://doi.org/10.1016/j.neuron.2021.10.036.

Frankland, Paul W, and Bruno Bontempi. 2005. “The Organization of Recent and Remote Memories.” *Nature Reviews. Neuroscience* 6 (2): 119–30. https://doi.org/10.1038/nrn1607.

Freund, T F, and M Antal. 1988. “GABA-Containing Neurons in the Septum Control Inhibitory Interneurons in the Hippocampus.” *Nature* 336 (6195): 170–73. https://doi.org/10.1038/336170a0.

Freund, T F, and G Buzsáki. 1996. “Interneurons of the Hippocampus.” *Hippocampus* 6 (4): 347–470. https://doi.org/10.1002/(SICI)1098-1063(1996)6:4<347::AID-HIPO1>3.0.CO;2-I.

Freund, T F. 1989. “GABAergic Septohippocampal Neurons Contain Parvalbumin.” *Brain Research* 478 (2): 375–81. https://doi.org/10.1016/0006-8993(89)91520-5.

Freund, Tamás F, and István Katona. 2007. “Perisomatic Inhibition.” *Neuron* 56 (1): 33–42. https://doi.org/10.1016/j.neuron.2007.09.012.

Friston, Karl, and Gyorgy Buzsáki. 2016. “The Functional Anatomy of Time: What and When in the Brain.” *Trends in Cognitive Sciences* 20 (7): 500–511. https://doi.org/10.1016/j.tics.2016.05.001.

Frotscher, M, and C Léránth. 1985. “Cholinergic Innervation of the Rat Hippocampus as Revealed by Choline Acetyltransferase Immunocytochemistry: A Combined Light and Electron Microscopic Study.” *The Journal of Comparative Neurology* 239 (2): 237–46. https://doi.org/10.1002/cne.902390210.

Froudist-Walsh, Sean, Philip G F Browning, Paula L Croxson, Kathy L Murphy, Jul Lea Shamy, Tess L Veuthey, Charles R E Wilson, and Mark G Baxter. 2018. “The Rhesus Monkey Hippocampus Critically Contributes to Scene Memory Retrieval, but Not New Learning.” *The Journal of Neuroscience* 38 (36): 7800–7808. https://doi.org/10.1523/JNEUROSCI.0832-18.2018.

Fuchs, A F. 1967. “Saccadic and Smooth Pursuit Eye Movements in the Monkey.” *The Journal of Physiology* 191 (3): 609–31. https://doi.org/10.1113/jphysiol.1967.sp008271.

Fuentealba, Pablo, Rahima Begum, Marco Capogna, Shozo Jinno, László F Márton, Jozsef Csicsvari, Alex Thomson, Peter Somogyi, and Thomas Klausberger. 2008. “Ivy Cells: A Population of Nitric-Oxide-Producing, Slow-Spiking GABAergic Neurons and Their Involvement in Hippocampal Network Activity.” *Neuron* 57 (6): 917–29. https://doi.org/10.1016/j.neuron.2008.01.034.

Fuhrmann, Falko, Daniel Justus, Liudmila Sosulina, Hiroshi Kaneko, Tatjana Beutel, Detlef Friedrichs, Susanne Schoch, Martin Karl Schwarz, Martin Fuhrmann, and Stefan Remy. 2015. “Locomotion, Theta Oscillations, and the Speed-Correlated Firing of Hippocampal Neurons Are Controlled by a Medial Septal Glutamatergic Circuit.” *Neuron* 86 (5): 1253–64. https://doi.org/10.1016/j.neuron.2015.05.001.

Gaffan, D. 1991. “Spatial Organization of Episodic Memory.” *Hippocampus* 1 (3): 262–64. https://doi.org/10.1002/hipo.450010311.

———. 1994. “Scene-Specific Memory for Objects: A Model of Episodic Memory Impairment in Monkeys with Fornix Transection.” *Journal of Cognitive Neuroscience* 6 (4): 305–20. https://doi.org/10.1162/jocn.1994.6.4.305.

Gais, Steffen, and Jan Born. 2004a. “Declarative Memory Consolidation: Mechanisms Acting during Human Sleep.” *Learning & Memory* 11 (6): 679–85. https://doi.org/10.1101/lm.80504.

———. 2004b. “Low Acetylcholine during Slow-Wave Sleep Is Critical for Declarative Memory Consolidation.” *Proceedings of the National Academy of Sciences of the United States of America* 101 (7): 2140–44. https://doi.org/10.1073/pnas.0305404101.

Gan, Jian, Shih-Ming Weng, Alejandro J Pernía-Andrade, Jozsef Csicsvari, and Peter Jonas. 2017. “Phase-Locked Inhibition, but Not Excitation, Underlies Hippocampal Ripple Oscillations in Awake Mice In Vivo.” *Neuron* 93 (2): 308–14. https://doi.org/10.1016/j.neuron.2016.12.018.

Gangadharan, Gireesh, Jonghan Shin, Seong-Wook Kim, Angela Kim, Afshin Paydar, Duk-Soo Kim, Taisuke Miyazaki, et al. 2016. “Medial Septal GABAergic Projection Neurons Promote Object Exploration Behavior and Type 2 Theta Rhythm.” *Proceedings of the National Academy of Sciences of the United States of America* 113 (23): 6550–55. https://doi.org/10.1073/pnas.1605019113.

Geiller, Tristan, Mohammad Fattahi, June-Seek Choi, and Sébastien Royer. 2017. “Place Cells Are More Strongly Tied to Landmarks in Deep than in Superficial CA1.” *Nature Communications* 8 (February): 14531. https://doi.org/10.1038/ncomms14531.

Geiller, Tristan, Sebastien Royer, and June-Seek Choi. 2017. “Segregated Cell Populations Enable Distinct Parallel Encoding within the Radial Axis of the CA1 Pyramidal Layer.” *Experimental Neurobiology* 26 (1): 1–10. https://doi.org/10.5607/en.2017.26.1.1.

Geiller, Tristan, Bert Vancura, Satoshi Terada, Eirini Troullinou, Spyridon Chavlis, Grigorios Tsagkatakis, Panagiotis Tsakalides, et al. 2020. “Large-Scale 3D Two-Photon Imaging of Molecularly Identified CA1 Interneuron Dynamics in Behaving Mice.” *Neuron* 108 (5): 968-983.e9. https://doi.org/10.1016/j.neuron.2020.09.013.

Geisler, Caroline, David Robbe, Michaël Zugaro, Anton Sirota, and György Buzsáki. 2007. “Hippocampal Place Cell Assemblies Are Speed-Controlled Oscillators.” *Proceedings of the National Academy of Sciences of the United States of America* 104 (19): 8149–54. https://doi.org/10.1073/pnas.0610121104.

Gelbard-Sagiv, Hagar, Roy Mukamel, Michal Harel, Rafael Malach, and Itzhak Fried. 2008. “Internally Generated Reactivation of Single Neurons in Human Hippocampus during Free Recall.” *Science* 322 (5898): 96–101. https://doi.org/10.1126/science.1164685.

Giehl, Janet, Nima Noury, and Markus Siegel. 2021. “Dissociating Harmonic and Non-Harmonic Phase-Amplitude Coupling in the Human Brain.” *Neuroimage* 227 (February): 117648. https://doi.org/10.1016/j.neuroimage.2020.117648.

Gilboa, Asaf, and Hannah Marlatte. 2017. “Neurobiology of Schemas and Schema-Mediated Memory.” *Trends in Cognitive Sciences* 21 (8): 618–31. https://doi.org/10.1016/j.tics.2017.04.013.

Giocomo, Lisa M, and Michael E Hasselmo. 2009. “Knock-out of HCN1 Subunit Flattens Dorsal-Ventral Frequency Gradient of Medial Entorhinal Neurons in Adult Mice.” *The Journal of Neuroscience* 29 (23): 7625–30. https://doi.org/10.1523/JNEUROSCI.0609-09.2009.

Girardeau, Gabrielle, Karim Benchenane, Sidney I Wiener, György Buzsáki, and Michaël B Zugaro. 2009. “Selective Suppression of Hippocampal Ripples Impairs Spatial Memory.” *Nature Neuroscience* 12 (10): 1222–23. https://doi.org/10.1038/nn.2384.

Girardeau, Gabrielle, Ingrid Inema, and György Buzsáki. 2017. “Reactivations of Emotional Memory in the Hippocampus-Amygdala System during Sleep.” *Nature Neuroscience* 20 (11): 1634–42. https://doi.org/10.1038/nn.4637.

Girardeau, Gabrielle, and Vítor Lopes-Dos-Santos. 2021. “Brain Neural Patterns and the Memory Function of Sleep.” *Science* 374 (6567): 560–64. https://doi.org/10.1126/science.abi8370.

Givens, Bennet S., and David S. Olton. 1990. “Cholinergic and GABAergic Modulation of Medial Septal Area: Effect on Working Memory.” *Behavioral Neuroscience* 104 (6): 849–55. https://doi.org/10.1037/0735-7044.104.6.849.

Givens, B. 1996. “Stimulus-Evoked Resetting of the Dentate Theta Rhythm: Relation to Working Memory.” *Neuroreport* 8 (1): 159–63. https://doi.org/10.1097/00001756-199612200-00032.

Glenberg, A M. 1997. “What Memory Is For.” *Behavioral and Brain Sciences* 20 (1): 1–19; discussion 19. https://doi.org/10.1017/s0140525x97000010.

Gloveli, Tengis, Tamar Dugladze, Sikha Saha, Hannah Monyer, Uwe Heinemann, Roger D Traub, Miles A Whittington, and Eberhard H Buhl. 2005. “Differential Involvement of Oriens/Pyramidale Interneurones in Hippocampal Network Oscillations in Vitro.” *The Journal of Physiology* 562 (Pt 1): 131–47. https://doi.org/10.1113/jphysiol.2004.073007.

Gomez-Marin, Alex, and Asif A Ghazanfar. 2019. “The Life of Behavior.” *Neuron* 104 (1): 25–36. https://doi.org/10.1016/j.neuron.2019.09.017.

Gomez-Marin, Alex, Joseph J Paton, Adam R Kampff, Rui M Costa, and Zachary F Mainen. 2014. “Big Behavioral Data: Psychology, Ethology and the Foundations of Neuroscience.” *Nature Neuroscience* 17 (11): 1455–62. https://doi.org/10.1038/nn.3812.

Gondan, Matthias. 2010. “A Permutation Test for the Race Model Inequality.” *Behavior Research Methods* 42 (1): 23–28. https://doi.org/10.3758/BRM.42.1.23.

Gottlieb, Jacqueline, and Pierre-Yves Oudeyer. 2018. “Towards a Neuroscience of Active Sampling and Curiosity.” *Nature Reviews. Neuroscience* 19 (12): 758–70. https://doi.org/10.1038/s41583-018-0078-0.

Goutagny, Romain, Jesse Jackson, and Sylvain Williams. 2009. “Self-Generated Theta Oscillations in the Hippocampus.” *Nature Neuroscience* 12 (12): 1491–93. https://doi.org/10.1038/nn.2440.

Goyal, Abhinav, Jonathan Miller, Salman E Qasim, Andrew J Watrous, Honghui Zhang, Joel M Stein, Cory S Inman, et al. 2020. “Functionally Distinct High and Low Theta Oscillations in the Human Hippocampus.” *Nature Communications* 11 (1): 2469. https://doi.org/10.1038/s41467-020-15670-6.

Greenberg, Jeffrey A, John F Burke, Rafi Haque, Michael J Kahana, and Kareem A Zaghloul. 2015. “Decreases in Theta and Increases in High Frequency Activity Underlie Associative Memory Encoding.” *Neuroimage* 114 (July): 257–63. https://doi.org/10.1016/j.neuroimage.2015.03.077.

Green, J D, and A A Arduini. 1954. “Hippocampal Electrical Activity in Arousal.” *Journal of Neurophysiology* 17 (6): 533–57. https://doi.org/10.1152/jn.1954.17.6.533.

Griffin, Amy L, Yukiko Asaka, Ryan D Darling, and Stephen D Berry. 2004. “Theta-Contingent Trial Presentation Accelerates Learning Rate and Enhances Hippocampal Plasticity during Trace Eyeblink Conditioning.” *Behavioral Neuroscience* 118 (2): 403–11. https://doi.org/10.1037/0735-7044.118.2.403.

Griffiths, Benjamin J, and Ole Jensen. 2023. “Gamma Oscillations and Episodic Memory.” *Trends in Neurosciences* 46 (10): 832–46. https://doi.org/10.1016/j.tins.2023.07.003.

Griffiths, Benjamin J, George Parish, Frederic Roux, Sebastian Michelmann, Mircea van der Plas, Luca D Kolibius, Ramesh Chelvarajah, et al. 2019. “Directional Coupling of Slow and Fast Hippocampal Gamma with Neocortical Alpha/Beta Oscillations in Human Episodic Memory.” *Proceedings of the National Academy of Sciences of the United States of America* 116 (43): 21834–42. https://doi.org/10.1073/pnas.1914180116.

Griffiths, D, A Dickinson, and N Clayton. 1999. “Episodic Memory: What Can Animals Remember about Their Past?” *Trends in Cognitive Sciences* 3 (2): 74–80. https://doi.org/10.1016/s1364-6613(98)01272-8.

Grinvald, Amiram, Amos Arieli, Misha Tsodyks, and Tal Kenet. 2003. “Neuronal Assemblies: Single Cortical Neurons Are Obedient Members of a Huge Orchestra.” *Biopolymers* 68 (3): 422–36. https://doi.org/10.1002/bip.10273.

Grion, Natalia, Athena Akrami, Yangfang Zuo, Federico Stella, and Mathew E Diamond. 2016. “Coherence between Rat Sensorimotor System and Hippocampus Is Enhanced during Tactile Discrimination.” *PLoS Biology* 14 (2): e1002384. https://doi.org/10.1371/journal.pbio.1002384.

Groppe, David M, Thomas P Urbach, and Marta Kutas. 2011a. “Mass Univariate Analysis of Event-Related Brain Potentials/Fields I: A Critical Tutorial Review.” *Psychophysiology* 48 (12): 1711–25. https://doi.org/10.1111/j.1469-8986.2011.01273.x.

———. 2011b. “Mass Univariate Analysis of Event-Related Brain Potentials/Fields II: Simulation Studies.” *Psychophysiology* 48 (12): 1726–37. https://doi.org/10.1111/j.1469-8986.2011.01272.x.

Grosmark, Andres D, and György Buzsáki. 2016. “Diversity in Neural Firing Dynamics Supports Both Rigid and Learned Hippocampal Sequences.” *Science* 351 (6280): 1440–43. https://doi.org/10.1126/science.aad1935.

Gulli, Roberto A, Lyndon R Duong, Benjamin W Corrigan, Guillaume Doucet, Sylvain Williams, Stefano Fusi, and Julio C Martinez-Trujillo. 2020. “Context-Dependent Representations of Objects and Space in the Primate Hippocampus during Virtual Navigation.” *Nature Neuroscience* 23 (1): 103–12. https://doi.org/10.1038/s41593-019-0548-3.

Guzowski, John F, James J Knierim, and Edvard I Moser. 2004. “Ensemble Dynamics of Hippocampal Regions CA3 and CA1.” *Neuron* 44 (4): 581–84. https://doi.org/10.1016/j.neuron.2004.11.003.

Gu, Liqin, Minglong Ren, Longnian Lin, and Jiamin Xu. 2023. “Calbindin-Expressing CA1 Pyramidal Neurons Encode Spatial Information More Efficiently.” *ENeuro*, February. https://doi.org/10.1523/ENEURO.0411-22.2023.

Guzman, Segundo Jose, Alois Schlögl, Michael Frotscher, and Peter Jonas. 2016. “Synaptic Mechanisms of Pattern Completion in the Hippocampal CA3 Network.” *Science* 353 (6304): 1117–23. https://doi.org/10.1126/science.aaf1836.

Haggard, Patrick, and Valerian Chambon. 2012. “Sense of Agency.” *Current Biology* 22 (10): R390-2. https://doi.org/10.1016/j.cub.2012.02.040.

Hahn, Gerald, Adrian Ponce-Alvarez, Gustavo Deco, Ad Aertsen, and Arvind Kumar. 2019. “Portraits of Communication in Neuronal Networks.” *Nature Reviews. Neuroscience* 20 (2): 117–27. https://doi.org/10.1038/s41583-018-0094-0.

Halgren, E, T L Babb, and P H Crandall. 1978. “Human Hippocampal Formation EEG Desynchronizes during Attentiveness and Movement.” *Electroencephalography and Clinical Neurophysiology* 44 (6): 778–81. https://doi.org/10.1016/0013-4694(78)90212-2.

Hall, Arron F, and Dong V Wang. 2022. “The Two Tales of Hippocampal Sharp-Wave Ripple Content: The Rigid and the Plastic.” *Progress in Neurobiology* 221 (December): 102396. https://doi.org/10.1016/j.pneurobio.2022.102396.

Hampton, Robert R, Jonathan W M Engelberg, and Ryan J Brady. 2020. “Explicit Memory and Cognition in Monkeys.” *Neuropsychologia* 138 (February): 107326. https://doi.org/10.1016/j.neuropsychologia.2019.107326.

Hampton, Robert R, Benjamin M Hampstead, and Elisabeth A Murray. 2004. “Selective Hippocampal Damage in Rhesus Monkeys Impairs Spatial Memory in an Open-Field Test.” *Hippocampus* 14 (7): 808–18. https://doi.org/10.1002/hipo.10217.

Hampton, Robert R., Benjamin M. Hampstead, and Elisabeth A. Murray. 2005. “Rhesus Monkeys (Macaca Mulatta) Demonstrate Robust Memory for What and Where, but Not When, in an Open-Field Test of Memory.” *Learning and Motivation* 36 (2): 245–59. https://doi.org/10.1016/j.lmot.2005.02.004.

Hampton, Robert R., and Sara J. Shettleworth. 1996. “Hippocampal Lesions Impair Memory for Location but Not Color in Passerine Birds.” *Behavioral Neuroscience* 110 (4): 831–35. https://doi.org/10.1037/0735-7044.110.4.831.

Hangya, Balázs, Zsolt Borhegyi, Nóra Szilágyi, Tamás F Freund, and Viktor Varga. 2009. “GABAergic Neurons of the Medial Septum Lead the Hippocampal Network during Theta Activity.” *The Journal of Neuroscience* 29 (25): 8094–8102. https://doi.org/10.1523/JNEUROSCI.5665-08.2009.

Harris, Kenneth D, Jozsef Csicsvari, Hajime Hirase, George Dragoi, and György Buzsáki. 2003. “Organization of Cell Assemblies in the Hippocampus.” *Nature* 424 (6948): 552–56. https://doi.org/10.1038/nature01834.

Harris, Kenneth D, Hannah Hochgerner, Nathan G Skene, Lorenza Magno, Linda Katona, Carolina Bengtsson Gonzales, Peter Somogyi, Nicoletta Kessaris, Sten Linnarsson, and Jens Hjerling-Leffler. 2018. “Classes and Continua of Hippocampal CA1 Inhibitory Neurons Revealed by Single-Cell Transcriptomics.” *PLoS Biology* 16 (6): e2006387. https://doi.org/10.1371/journal.pbio.2006387.

Harris, Kenneth D. 2005. “Neural Signatures of Cell Assembly Organization.” *Nature Reviews. Neuroscience* 6 (5): 399–407. https://doi.org/10.1038/nrn1669.

Harvey, Ryan E, Heath L Robinson, Can Liu, Azahara Oliva, and Antonio Fernandez-Ruiz. 2023. “Hippocampo-Cortical Circuits for Selective Memory Encoding, Routing, and Replay.” *Neuron* 111 (13): 2076-2090.e9. https://doi.org/10.1016/j.neuron.2023.04.015.

Hasselmo, Michael E, and Chantal E Stern. 2014. “Theta Rhythm and the Encoding and Retrieval of Space and Time.” *Neuroimage* 85 Pt 2 (0 2): 656–66. https://doi.org/10.1016/j.neuroimage.2013.06.022.

Hasselmo, M E. 1999. “Neuromodulation: Acetylcholine and Memory Consolidation.” *Trends in Cognitive Sciences* 3 (9): 351–59. https://doi.org/10.1016/s1364-6613(99)01365-0.

Hasselmo, Michael E, Clara Bodelón, and Bradley P Wyble. 2002. “A Proposed Function for Hippocampal Theta Rhythm: Separate Phases of Encoding and Retrieval Enhance Reversal of Prior Learning.” *Neural Computation* 14 (4): 793–817. https://doi.org/10.1162/089976602317318965.

Hasselmo, Michael E. 2005. “What Is the Function of Hippocampal Theta Rhythm?--Linking Behavioral Data to Phasic Properties of Field Potential and Unit Recording Data.” *Hippocampus* 15 (7): 936–49. https://doi.org/10.1002/hipo.20116.

Hazama, Yutaro, and Ryoi Tamura. 2019. “Effects of Self-Locomotion on the Activity of Place Cells in the Hippocampus of a Freely Behaving Monkey.” *Neuroscience Letters* 701 (May): 32–37. https://doi.org/10.1016/j.neulet.2019.02.009.

Hebb, D O. 1949. “The Organization of Behavior; A Neuropsychological Theory.” *The American Journal of Psychology* 63 (4): 633. https://doi.org/10.2307/1418888.

Herweg, Nora A, Ethan A Solomon, and Michael J Kahana. 2020. “Theta Oscillations in Human Memory.” *Trends in Cognitive Sciences* 24 (3): 208–27. https://doi.org/10.1016/j.tics.2019.12.006.

He, Hongshen, Yi Wang, and Thomas J McHugh. 2023. “Behavioral Status Modulates CA2 Influence on Hippocampal Network Dynamics.” *Hippocampus* 33 (3): 252–65. https://doi.org/10.1002/hipo.23498.

Henze, D A, Z Borhegyi, J Csicsvari, A Mamiya, K D Harris, and G Buzsáki. 2000. “Intracellular Features Predicted by Extracellular Recordings in the Hippocampus in Vivo.” *Journal of Neurophysiology* 84 (1): 390–400. https://doi.org/10.1152/jn.2000.84.1.390.

Hirase, H, X Leinekugel, A Czurkó, J Csicsvari, and G Buzsáki. 2001. “Firing Rates of Hippocampal Neurons Are Preserved during Subsequent Sleep Episodes and Modified by Novel Awake Experience.” *Proceedings of the National Academy of Sciences of the United States of America* 98 (16): 9386–90. https://doi.org/10.1073/pnas.161274398.

Hoffman, Kari L, Michelle C Dragan, Timothy K Leonard, Cristiano Micheli, Rodrigo Montefusco-Siegmund, and Taufik A Valiante. 2013. “Saccades during Visual Exploration Align Hippocampal 3-8 Hz Rhythms in Human and Non-Human Primates.” *Frontiers in Systems Neuroscience* 7 (August): 43. https://doi.org/10.3389/fnsys.2013.00043.

Hölscher, C, R Anwyl, and M J Rowan. 1997. “Stimulation on the Positive Phase of Hippocampal Theta Rhythm Induces Long-Term Potentiation That Can Be Depotentiated by Stimulation on the Negative Phase in Area CA1 in Vivo.” *The Journal of Neuroscience* 17 (16): 6470–77. https://doi.org/10.1523/JNEUROSCI.17-16-06470.1997.

Holt, G R, W R Softky, C Koch, and R J Douglas. 1996. “Comparison of Discharge Variability in Vitro and in Vivo in Cat Visual Cortex Neurons.” *Journal of Neurophysiology* 75 (5): 1806–14. https://doi.org/10.1152/jn.1996.75.5.1806.

Hori, Etsuro, Eiichi Tabuchi, Nobuhisa Matsumura, Ryoi Tamura, Satoshi Eifuku, Shunro Endo, Hisao Nishijo, and Taketoshi Ono. 2003. “Representation of Place by Monkey Hippocampal Neurons in Real and Virtual Translocation.” *Hippocampus* 13 (2): 190–96. https://doi.org/10.1002/hipo.10062.

Hsiao, Yi-Tse, Chenguang Zheng, and Laura Lee Colgin. 2016. “Slow Gamma Rhythms in CA3 Are Entrained by Slow Gamma Activity in the Dentate Gyrus.” *Journal of Neurophysiology* 116 (6): 2594–2603. https://doi.org/10.1152/jn.00499.2016.

Hsieh, Liang-Tien, Matthias J Gruber, Lucas J Jenkins, and Charan Ranganath. 2014. “Hippocampal Activity Patterns Carry Information about Objects in Temporal Context.” *Neuron* 81 (5): 1165–78. https://doi.org/10.1016/j.neuron.2014.01.015.

Huerta, P T, and J E Lisman. 1995. “Bidirectional Synaptic Plasticity Induced by a Single Burst during Cholinergic Theta Oscillation in CA1 in Vitro.” *Neuron* 15 (5): 1053–63. https://doi.org/10.1016/0896-6273(95)90094-2.

Hughes, Adam M, Tara A Whitten, Jeremy B Caplan, and Clayton T Dickson. 2012. “BOSC: A Better Oscillation Detection Method, Extracts Both Sustained and Transient Rhythms from Rat Hippocampal Recordings.” *Hippocampus* 22 (6): 1417–28. https://doi.org/10.1002/hipo.20979.

Hussin, Ahmed T, Saman Abbaspoor, and Kari L Hoffman. 2022. “Retrosplenial and Hippocampal Synchrony during Retrieval of Old Memories in Macaques.” *The Journal of Neuroscience* 42 (42): 7947–56. https://doi.org/10.1523/JNEUROSCI.0001-22.2022.

Hussin, Ahmed T, Timothy K Leonard, and Kari L Hoffman. 2020. “Sharp-Wave Ripple Features in Macaques Depend on Behavioral State and Cell-Type Specific Firing.” *Hippocampus* 30 (1): 50–59. https://doi.org/10.1002/hipo.23046.

Hu, Hua, Jian Gan, and Peter Jonas. 2014. “Fast-Spiking, Parvalbumin^{+} GABAergic Interneurons: From Cellular Design to Microcircuit Function.” *Science* 345 (6196): 1255263. https://doi.org/10.1126/science.1255263.

Hyafil, Alexandre. 2015. “Misidentifications of Specific Forms of Cross-Frequency Coupling: Three Warnings.” *Frontiers in Neuroscience* 9 (October): 370. https://doi.org/10.3389/fnins.2015.00370.

Hyman, James M, Bradley P Wyble, Vikas Goyal, Christina A Rossi, and Michael E Hasselmo. 2003. “Stimulation in Hippocampal Region CA1 in Behaving Rats Yields Long-Term Potentiation When Delivered to the Peak of Theta and Long-Term Depression When Delivered to the Trough.” *The Journal of Neuroscience* 23 (37): 11725–31. https://doi.org/10.1523/JNEUROSCI.23-37-11725.2003.

Igarashi, Kei M, Li Lu, Laura L Colgin, May-Britt Moser, and Edvard I Moser. 2014. “Coordination of Entorhinal-Hippocampal Ensemble Activity during Associative Learning.” *Nature* 510 (7503): 143–47. https://doi.org/10.1038/nature13162.

Imbrosci, Barbara, Noam Nitzan, Sam McKenzie, José R Donoso, Aarti Swaminathan, Claudia Böhm, Nikolaus Maier, and Dietmar Schmitz. 2021. “Subiculum as a Generator of Sharp Wave-Ripples in the Rodent Hippocampus.” *Cell Reports* 35 (3): 109021. https://doi.org/10.1016/j.celrep.2021.109021.

Insausti, R, and M Muñoz. 2001. “Cortical Projections of the Non-Entorhinal Hippocampal Formation in the Cynomolgus Monkey (Macaca Fascicularis).” *The European Journal of Neuroscience* 14 (3): 435–51. https://doi.org/10.1046/j.0953-816x.2001.01662.x.

Ison, Matias J, Florian Mormann, Moran Cerf, Christof Koch, Itzhak Fried, and Rodrigo Quian Quiroga. 2011. “Selectivity of Pyramidal Cells and Interneurons in the Human Medial Temporal Lobe.” *Journal of Neurophysiology* 106 (4): 1713–21. https://doi.org/10.1152/jn.00576.2010.

Jackson, Jadin, and A David Redish. 2007. “Network Dynamics of Hippocampal Cell-Assemblies Resemble Multiple Spatial Maps within Single Tasks.” *Hippocampus* 17 (12): 1209–29. https://doi.org/10.1002/hipo.20359.

Jackson, Jesse, Bénédicte Amilhon, Romain Goutagny, Jean-Bastien Bott, Frédéric Manseau, Christian Kortleven, Steven L Bressler, and Sylvain Williams. 2014. “Reversal of Theta Rhythm Flow through Intact Hippocampal Circuits.” *Nature Neuroscience* 17 (10): 1362–70. https://doi.org/10.1038/nn.3803.

Jacobs, Joshua. 2014. “Hippocampal Theta Oscillations Are Slower in Humans than in Rodents: Implications for Models of Spatial Navigation and Memory.” *Philosophical Transactions of the Royal Society of London. Series B, Biological Sciences* 369 (1635): 20130304. https://doi.org/10.1098/rstb.2013.0304.

Jadhav, Shantanu P, Caleb Kemere, P Walter German, and Loren M Frank. 2012. “Awake Hippocampal Sharp-Wave Ripples Support Spatial Memory.” *Science* 336 (6087): 1454–58. https://doi.org/10.1126/science.1217230.

Jang, Yoonhee, and David E Huber. 2008. “Context Retrieval and Context Change in Free Recall: Recalling from Long-Term Memory Drives List Isolation.” *Journal of Experimental Psychology. Learning, Memory, and Cognition* 34 (1): 112–27. https://doi.org/10.1037/0278-7393.34.1.112.

Jayachandran, Maanasa, Tatiana D Viena, Andy Garcia, Abdiel Vasallo Veliz, Sofia Leyva, Valentina Roldan, Robert P Vertes, and Timothy A Allen. 2023. “Nucleus Reuniens Transiently Synchronizes Memory Networks at Beta Frequencies.” *Nature Communications* 14 (1): 4326. https://doi.org/10.1038/s41467-023-40044-z.

Jezek, Karel, Espen J Henriksen, Alessandro Treves, Edvard I Moser, and May-Britt Moser. 2011. “Theta-Paced Flickering between Place-Cell Maps in the Hippocampus.” *Nature* 478 (7368): 246–49. https://doi.org/10.1038/nature10439.

Ji, Daoyun, and Matthew A Wilson. 2008. “Firing Rate Dynamics in the Hippocampus Induced by Trajectory Learning.” *The Journal of Neuroscience* 28 (18): 4679–89. https://doi.org/10.1523/JNEUROSCI.4597-07.2008.

Jones, Stephanie R. 2016. “When Brain Rhythms Aren’t ‘Rhythmic’: Implication for Their Mechanisms and Meaning.” *Current Opinion in Neurobiology* 40 (October): 72–80. https://doi.org/10.1016/j.conb.2016.06.010.

Joshi, Abhilasha, Eric L Denovellis, Abhijith Mankili, Yagiz Meneksedag, Thomas J Davidson, Anna K Gillespie, Jennifer A Guidera, Demetris Roumis, and Loren M Frank. 2023. “Dynamic Synchronization between Hippocampal Representations and Stepping.” *Nature* 617 (7959): 125–31. https://doi.org/10.1038/s41586-023-05928-6.

Juavinett, Ashley L, Jeffrey C Erlich, and Anne K Churchland. 2018. “Decision-Making Behaviors: Weighing Ethology, Complexity, and Sensorimotor Compatibility.” *Current Opinion in Neurobiology* 49 (April): 42–50. https://doi.org/10.1016/j.conb.2017.11.001.

Jung, Richard, and A E Kornmüller. 1938. “Eine Methodik Der Ableitung Iokalisierter Potentialschwankungen Aus Subcorticalen Hirngebieten.” *Archiv Für Psychiatrie Und Nervenkrankheiten* 109 (1): 1–30. https://doi.org/10.1007/BF02157817.

Jutras, Michael J, Pascal Fries, and Elizabeth A Buffalo. 2009. “Gamma-Band Synchronization in the Macaque Hippocampus and Memory Formation.” *The Journal of Neuroscience* 29 (40): 12521–31. https://doi.org/10.1523/JNEUROSCI.0640-09.2009.

———. 2013. “Oscillatory Activity in the Monkey Hippocampus during Visual Exploration and Memory Formation.” *Proceedings of the National Academy of Sciences of the United States of America* 110 (32): 13144–49. https://doi.org/10.1073/pnas.1302351110.

Kaas, Jon H, Hui-Xin Qi, and Iwona Stepniewska. 2022. “Escaping the Nocturnal Bottleneck, and the Evolution of the Dorsal and Ventral Streams of Visual Processing in Primates.” *Philosophical Transactions of the Royal Society of London. Series B, Biological Sciences* 377 (1844): 20210293. https://doi.org/10.1098/rstb.2021.0293.

Kamondi, Anita, László Acsády, Xiao-Jing Wang, and György Buzsáki. 1998. “Theta Oscillations in Somata and Dendrites of Hippocampal Pyramidal Cells in Vivo: Activity-Dependent Phase-Precession of Action Potentials.” *Hippocampus*, January.

Kang, Daesung, Mingzhou Ding, Irina Topchiy, and Bernat Kocsis. 2017. “Reciprocal Interactions between Medial Septum and Hippocampus in Theta Generation: Granger Causality Decomposition of Mixed Spike-Field Recordings.” *Frontiers in Neuroanatomy* 11 (December): 120. https://doi.org/10.3389/fnana.2017.00120.

Kaplan, Raphael, Mohit H Adhikari, Rikkert Hindriks, Dante Mantini, Yusuke Murayama, Nikos K Logothetis, and Gustavo Deco. 2016. “Hippocampal Sharp-Wave Ripples Influence Selective Activation of the Default Mode Network.” *Current Biology* 26 (5): 686–91. https://doi.org/10.1016/j.cub.2016.01.017.

Katona, Linda, Damien Lapray, Tim J Viney, Abderrahim Oulhaj, Zsolt Borhegyi, Benjamin R Micklem, Thomas Klausberger, and Peter Somogyi. 2014. “Sleep and Movement Differentiates Actions of Two Types of Somatostatin-Expressing GABAergic Interneuron in Rat Hippocampus.” *Neuron* 82 (4): 872–86. https://doi.org/10.1016/j.neuron.2014.04.007.

Katz, Chaim N, Kramay Patel, Omid Talakoub, David Groppe, Kari Hoffman, and Taufik A Valiante. 2020. “Differential Generation of Saccade, Fixation, and Image-Onset Event-Related Potentials in the Human Mesial Temporal Lobe.” *Cerebral Cortex* 30 (10): 5502–16. https://doi.org/10.1093/cercor/bhaa132.

Katz, Chaim N, Andrea G P Schjetnan, Kramay Patel, Victoria Barkley, Kari L Hoffman, Suneil K Kalia, Katherine D Duncan, and Taufik A Valiante. 2022. “A Corollary Discharge Mediates Saccade-Related Inhibition of Single Units in Mnemonic Structures of the Human Brain.” *Current Biology* 32 (14): 3082-3094.e4. https://doi.org/10.1016/j.cub.2022.06.015.

Kay, Kenneth, Jason E Chung, Marielena Sosa, Jonathan S Schor, Mattias P Karlsson, Margaret C Larkin, Daniel F Liu, and Loren M Frank. 2020. “Constant Sub-Second Cycling between Representations of Possible Futures in the Hippocampus.” *Cell* 180 (3): 552-567.e25. https://doi.org/10.1016/j.cell.2020.01.014.

Kemere, Caleb, Margaret F Carr, Mattias P Karlsson, and Loren M Frank. 2013. “Rapid and Continuous Modulation of Hippocampal Network State during Exploration of New Places.” *Plos One* 8 (9): e73114. https://doi.org/10.1371/journal.pone.0073114.

Klausberger, Thomas, Peter J Magill, László F Márton, J David B Roberts, Philip M Cobden, György Buzsáki, and Peter Somogyi. 2003. “Brain-State- and Cell-Type-Specific Firing of Hippocampal Interneurons in Vivo.” *Nature* 421 (6925): 844–48. https://doi.org/10.1038/nature01374.

Klausberger, Thomas, László F Márton, Agnes Baude, J David B Roberts, Peter J Magill, and Peter Somogyi. 2004. “Spike Timing of Dendrite-Targeting Bistratified Cells during Hippocampal Network Oscillations in Vivo.” *Nature Neuroscience* 7 (1): 41–47. https://doi.org/10.1038/nn1159.

Klausberger, Thomas, Laszlo F Marton, Joseph O’Neill, Jojanneke H J Huck, Yannis Dalezios, Pablo Fuentealba, Wai Yee Suen, et al. 2005. “Complementary Roles of Cholecystokinin- and Parvalbumin-Expressing GABAergic Neurons in Hippocampal Network Oscillations.” *The Journal of Neuroscience* 25 (42): 9782–93. https://doi.org/10.1523/JNEUROSCI.3269-05.2005.

Klausberger, Thomas, and Peter Somogyi. 2008. “Neuronal Diversity and Temporal Dynamics: The Unity of Hippocampal Circuit Operations.” *Science* 321 (5885): 53–57. https://doi.org/10.1126/science.1149381.

Kleen, Jonathan K, Jason E Chung, Kristin K Sellers, Jenny Zhou, Michael Triplett, Kye Lee, Angela Tooker, Razi Haque, and Edward F Chang. 2021. “Bidirectional Propagation of Low Frequency Oscillations over the Human Hippocampal Surface.” *Nature Communications* 12 (1): 2764. https://doi.org/10.1038/s41467-021-22850-5.

Klinzing, Jens G, Niels Niethard, and Jan Born. 2019. “Mechanisms of Systems Memory Consolidation during Sleep.” *Nature Neuroscience* 22 (10): 1598–1610. https://doi.org/10.1038/s41593-019-0467-3.

Knierim, James J, Inah Lee, and Eric L Hargreaves. 2006. “Hippocampal Place Cells: Parallel Input Streams, Subregional Processing, and Implications for Episodic Memory.” *Hippocampus* 16 (9): 755–64. https://doi.org/10.1002/hipo.20203.

Knierim, James J, Joshua P Neunuebel, and Sachin S Deshmukh. 2014. “Functional Correlates of the Lateral and Medial Entorhinal Cortex: Objects, Path Integration and Local-Global Reference Frames.” *Philosophical Transactions of the Royal Society of London. Series B, Biological Sciences* 369 (1635): 20130369. https://doi.org/10.1098/rstb.2013.0369.

Kohara, Keigo, Michele Pignatelli, Alexander J Rivest, Hae-Yoon Jung, Takashi Kitamura, Junghyup Suh, Dominic Frank, et al. 2014. “Cell Type-Specific Genetic and Optogenetic Tools Reveal Hippocampal CA2 Circuits.” *Nature Neuroscience* 17 (2): 269–79. https://doi.org/10.1038/nn.3614.

Komisaruk, B R. 1970. “Synchrony between Limbic System Theta Activity and Rhythmical Behavior in Rats.” *Journal of Comparative and Physiological Psychology* 70 (3): 482–92. https://doi.org/10.1037/h0028709.

Koriat, Asher, and Shiri Pearlman-Avnion. 2003. “Memory Organization of Action Events and Its Relationship to Memory Performance.” *Journal of Experimental Psychology: General* 132 (3): 435–54. https://doi.org/10.1037/0096-3445.132.3.435.

Kovach, Christopher K, Hiroyuki Oya, and Hiroto Kawasaki. 2018. “The Bispectrum and Its Relationship to Phase-Amplitude Coupling.” *Neuroimage* 173 (February): 518–39. https://doi.org/10.1016/j.neuroimage.2018.02.033.

Krakauer, John W, Asif A Ghazanfar, Alex Gomez-Marin, Malcolm A MacIver, and David Poeppel. 2017. “Neuroscience Needs Behavior: Correcting a Reductionist Bias.” *Neuron* 93 (3): 480–90. https://doi.org/10.1016/j.neuron.2016.12.041.

Kramis, R, C H Vanderwolf, and B H Bland. 1975. “Two Types of Hippocampal Rhythmical Slow Activity in Both the Rabbit and the Rat: Relations to Behavior and Effects of Atropine, Diethyl Ether, Urethane, and Pentobarbital.” *Experimental Neurology* 49 (1 Pt 1): 58–85. https://doi.org/10.1016/0014-4886(75)90195-8.

Kraus, Benjamin J, Robert J Robinson, John A White, Howard Eichenbaum, and Michael E Hasselmo. 2013. “Hippocampal ‘Time Cells’: Time versus Path Integration.” *Neuron* 78 (6): 1090–1101. https://doi.org/10.1016/j.neuron.2013.04.015.

Krook-Magnuson, Esther, Csaba Varga, Sang-Hun Lee, and Ivan Soltesz. 2012. “New Dimensions of Interneuronal Specialization Unmasked by Principal Cell Heterogeneity.” *Trends in Neurosciences* 35 (3): 175–84. https://doi.org/10.1016/j.tins.2011.10.005.

Kullmann, Dimitri M, and Karri P Lamsa. 2007. “Long-Term Synaptic Plasticity in Hippocampal Interneurons.” *Nature Reviews. Neuroscience* 8 (9): 687–99. https://doi.org/10.1038/nrn2207.

Kunec, Steve, Michael E Hasselmo, and Nancy Kopell. 2005. “Encoding and Retrieval in the CA3 Region of the Hippocampus: A Model of Theta-Phase Separation.” *Journal of Neurophysiology* 94 (1): 70–82. https://doi.org/10.1152/jn.00731.2004.

Lansink, Carien S, Guido T Meijer, Jan V Lankelma, Martin A Vinck, Jadin C Jackson, and Cyriel M A Pennartz. 2016. “Reward Expectancy Strengthens CA1 Theta and Beta Band Synchronization and Hippocampal-Ventral Striatal Coupling.” *The Journal of Neuroscience* 36 (41): 10598–610. https://doi.org/10.1523/JNEUROSCI.0682-16.2016.

Lapray, Damien, Balint Lasztoczi, Michael Lagler, Tim James Viney, Linda Katona, Ornella Valenti, Katja Hartwich, Zsolt Borhegyi, Peter Somogyi, and Thomas Klausberger. 2012. “Behavior-Dependent Specialization of Identified Hippocampal Interneurons.” *Nature Neuroscience* 15 (9): 1265–71. https://doi.org/10.1038/nn.3176.

Lasztóczi, Bálint, and Thomas Klausberger. 2014. “Layer-Specific GABAergic Control of Distinct Gamma Oscillations in the CA1 Hippocampus.” *Neuron* 81 (5): 1126–39. https://doi.org/10.1016/j.neuron.2014.01.021.

Laubach, M, J Wessberg, and M A Nicolelis. 2000. “Cortical Ensemble Activity Increasingly Predicts Behaviour Outcomes during Learning of a Motor Task.” *Nature* 405 (6786): 567–71. https://doi.org/10.1038/35014604.

Lavenex, Pamela Banta, David G Amaral, and Pierre Lavenex. 2006. “Hippocampal Lesion Prevents Spatial Relational Learning in Adult Macaque Monkeys.” *The Journal of Neuroscience* 26 (17): 4546–58. https://doi.org/10.1523/JNEUROSCI.5412-05.2006.

Le Van Quyen, Michel, Anatol Bragin, Richard Staba, Benoit Crépon, Charles L Wilson, and Jerome Engel. 2008. “Cell Type-Specific Firing during Ripple Oscillations in the Hippocampal Formation of Humans.” *The Journal of Neuroscience* 28 (24): 6104–10. https://doi.org/10.1523/JNEUROSCI.0437-08.2008.

Leão, Richardson N, Sanja Mikulovic, Katarina E Leão, Hermany Munguba, Henrik Gezelius, Anders Enjin, Kalicharan Patra, et al. 2012. “OLM Interneurons Differentially Modulate CA3 and Entorhinal Inputs to Hippocampal CA1 Neurons.” *Nature Neuroscience* 15 (11): 1524–30. https://doi.org/10.1038/nn.3235.

Lecoq, Jérôme, Michael Oliver, Joshua H Siegle, Natalia Orlova, Peter Ledochowitsch, and Christof Koch. 2021. “Removing Independent Noise in Systems Neuroscience Data Using DeepInterpolation.” *Nature Methods* 18 (11): 1401–8. https://doi.org/10.1038/s41592-021-01285-2.

Lee, Eric Kenji, Hymavathy Balasubramanian, Alexandra Tsolias, Stephanie Udochukwu Anakwe, Maria Medalla, Krishna V Shenoy, and Chandramouli Chandrasekaran. 2021. “Non-Linear Dimensionality Reduction on Extracellular Waveforms Reveals Cell Type Diversity in Premotor Cortex.” *ELife* 10 (August). https://doi.org/10.7554/eLife.67490.

Lee, Sang-Hun, Ivan Marchionni, Marianne Bezaire, Csaba Varga, Nathan Danielson, Matthew Lovett-Barron, Attila Losonczy, and Ivan Soltesz. 2014. “Parvalbumin-Positive Basket Cells Differentiate among Hippocampal Pyramidal Cells.” *Neuron* 82 (5): 1129–44. https://doi.org/10.1016/j.neuron.2014.03.034.

Lega, Bradley, John Burke, Joshua Jacobs, and Michael J Kahana. 2016. “Slow-Theta-to-Gamma Phase-Amplitude Coupling in Human Hippocampus Supports the Formation of New Episodic Memories.” *Cerebral Cortex* 26 (1): 268–78. https://doi.org/10.1093/cercor/bhu232.

Lega, Bradley C, Joshua Jacobs, and Michael Kahana. 2012. “Human Hippocampal Theta Oscillations and the Formation of Episodic Memories.” *Hippocampus* 22 (4): 748–61. https://doi.org/10.1002/hipo.20937.

Lehn, Hanne, Hill-Aina Steffenach, Niels M van Strien, Dick J Veltman, Menno P Witter, and Asta K Håberg. 2009. “A Specific Role of the Human Hippocampus in Recall of Temporal Sequences.” *The Journal of Neuroscience* 29 (11): 3475–84. https://doi.org/10.1523/JNEUROSCI.5370-08.2009.

Leonard, Timothy K, and Kari L Hoffman. 2017. “Sharp-Wave Ripples in Primates Are Enhanced near Remembered Visual Objects.” *Current Biology* 27 (2): 257–62. https://doi.org/10.1016/j.cub.2016.11.027.

Leonard, Timothy K, Jonathan M Mikkila, Emad N Eskandar, Jason L Gerrard, Daniel Kaping, Shaun R Patel, Thilo Womelsdorf, and Kari L Hoffman. 2015. “Sharp Wave Ripples during Visual Exploration in the Primate Hippocampus.” *The Journal of Neuroscience* 35 (44): 14771–82. https://doi.org/10.1523/JNEUROSCI.0864-15.2015.

Leung, L S. 1998. “Generation of Theta and Gamma Rhythms in the Hippocampus.” *Neuroscience and Biobehavioral Reviews* 22 (2): 275–90. https://doi.org/10.1016/s0149-7634(97)00014-6.

Leutgeb, S, and S J Mizumori. 1999. “Excitotoxic Septal Lesions Result in Spatial Memory Deficits and Altered Flexibility of Hippocampal Single-Unit Representations.” *The Journal of Neuroscience* 19 (15): 6661–72. https://doi.org/10.1523/JNEUROSCI.19-15-06661.1999.

Leutgeb, Stefan, Jill K Leutgeb, Alessandro Treves, May-Britt Moser, and Edvard I Moser. 2004. “Distinct Ensemble Codes in Hippocampal Areas CA3 and CA1.” *Science* 305 (5688): 1295–98. https://doi.org/10.1126/science.1100265.

Levy, W B, and O Steward. 1983. “Temporal Contiguity Requirements for Long-Term Associative Potentiation/Depression in the Hippocampus.” *Neuroscience* 8 (4): 791–97. https://doi.org/10.1016/0306-4522(83)90010-6.

Li, X G, P Somogyi, A Ylinen, and G Buzsáki. 1994. “The Hippocampal CA3 Network: An in Vivo Intracellular Labeling Study.” *The Journal of Comparative Neurology* 339 (2): 181–208. https://doi.org/10.1002/cne.903390204.

Libby, Laura A, Zachariah M Reagh, Nichole R Bouffard, J Daniel Ragland, and Charan Ranganath. 2019. “The Hippocampus Generalizes across Memories That Share Item and Context Information.” *Journal of Cognitive Neuroscience* 31 (1): 24–35. https://doi.org/10.1162/jocn_a_01345.

Lisman, John E, and Ole Jensen. 2013. “The θ-γ Neural Code.” *Neuron* 77 (6): 1002–16. https://doi.org/10.1016/j.neuron.2013.03.007.

Liu, Anli A, Simon Henin, Saman Abbaspoor, Anatol Bragin, Elizabeth A Buffalo, Jordan S Farrell, David J Foster, et al. 2022. “A Consensus Statement on Detection of Hippocampal Sharp Wave Ripples and Differentiation from Other Fast Oscillations.” *Nature Communications* 13 (1): 6000. https://doi.org/10.1038/s41467-022-33536-x.

Liu, Can, Ralitsa Todorova, Wenbo Tang, Azahara Oliva, and Antonio Fernandez-Ruiz. 2023. “Associative and Predictive Hippocampal Codes Support Memory-Guided Behaviors.” *Science* 382 (6668): eadi8237. https://doi.org/10.1126/science.adi8237.

Livingstone, M S, and D H Hubel. 1981. “Effects of Sleep and Arousal on the Processing of Visual Information in the Cat.” *Nature* 291 (5816): 554–61. https://doi.org/10.1038/291554a0.

Long, Nicole M, and Michael J Kahana. 2015. “Successful Memory Formation Is Driven by Contextual Encoding in the Core Memory Network.” *Neuroimage* 119 (October): 332–37. https://doi.org/10.1016/j.neuroimage.2015.06.073.

———. 2019. “Hippocampal Contributions to Serial-Order Memory.” *Hippocampus* 29 (3): 252–59. https://doi.org/10.1002/hipo.23025.

Lopes-dos-Santos, Vitor, Demi Brizee, and David Dupret. 2023. “Spatio-Temporal Organization of Network Activity Patterns in the Hippocampus.” *BioRxiv*, October. https://doi.org/10.1101/2023.10.17.562689.

Lopes-dos-Santos, Vítor, Sergio Conde-Ocazionez, Miguel A L Nicolelis, Sidarta T Ribeiro, and Adriano B L Tort. 2011. “Neuronal Assembly Detection and Cell Membership Specification by Principal Component Analysis.” *Plos One* 6 (6): e20996. https://doi.org/10.1371/journal.pone.0020996.

Lopes-dos-Santos, Vítor, Sidarta Ribeiro, and Adriano B L Tort. 2013. “Detecting Cell Assemblies in Large Neuronal Populations.” *Journal of Neuroscience Methods* 220 (2): 149–66. https://doi.org/10.1016/j.jneumeth.2013.04.010.

Lopes-Dos-Santos, Vítor, Gido M van de Ven, Alexander Morley, Stéphanie Trouche, Natalia Campo-Urriza, and David Dupret. 2018. “Parsing Hippocampal Theta Oscillations by Nested Spectral Components during Spatial Exploration and Memory-Guided Behavior.” *Neuron* 100 (4): 940-952.e7. https://doi.org/10.1016/j.neuron.2018.09.031.

Lovett-Barron, Matthew, Patrick Kaifosh, Mazen A Kheirbek, Nathan Danielson, Jeffrey D Zaremba, Thomas R Reardon, Gergely F Turi, René Hen, Boris V Zemelman, and Attila Losonczy. 2014. “Dendritic Inhibition in the Hippocampus Supports Fear Learning.” *Science* 343 (6173): 857–63. https://doi.org/10.1126/science.1247485.

Luczak, Artur, Peter Barthó, and Kenneth D Harris. 2009. “Spontaneous Events Outline the Realm of Possible Sensory Responses in Neocortical Populations.” *Neuron* 62 (3): 413–25. https://doi.org/10.1016/j.neuron.2009.03.014.

Lynch, M A. 2004. “Long-Term Potentiation and Memory.” *Physiological Reviews* 84 (1): 87–136. https://doi.org/10.1152/physrev.00014.2003.

Maccaferri, G, and C J McBain. 1995. “Passive Propagation of LTD to Stratum Oriens-Alveus Inhibitory Neurons Modulates the Temporoammonic Input to the Hippocampal CA1 Region.” *Neuron* 15 (1): 137–45. https://doi.org/10.1016/0896-6273(95)90071-3.

———. 1996. “The Hyperpolarization-Activated Current (Ih) and Its Contribution to Pacemaker Activity in Rat CA1 Hippocampal Stratum Oriens-Alveus Interneurones.” *The Journal of Physiology* 497 (Pt 1) (Pt 1): 119–30. https://doi.org/10.1113/jphysiol.1996.sp021754.

Macrides, F, H B Eichenbaum, and W B Forbes. 1982. “Temporal Relationship between Sniffing and the Limbic Theta Rhythm during Odor Discrimination Reversal Learning.” *The Journal of Neuroscience* 2 (12): 1705–17. https://doi.org/10.1523/JNEUROSCI.02-12-01705.1982.

Magee, Jeffrey C, and Christine Grienberger. 2020. “Synaptic Plasticity Forms and Functions.” *Annual Review of Neuroscience* 43 (July): 95–117. https://doi.org/10.1146/annurev-neuro-090919-022842.

Magee, J C, and D Johnston. 1997. “A Synaptically Controlled, Associative Signal for Hebbian Plasticity in Hippocampal Neurons.” *Science* 275 (5297): 209–13. https://doi.org/10.1126/science.275.5297.209.

Maier, Nikolaus, Volker Nimmrich, and Andreas Draguhn. 2003. “Cellular and Network Mechanisms Underlying Spontaneous Sharp Wave-Ripple Complexes in Mouse Hippocampal Slices.” *The Journal of Physiology* 550 (Pt 3): 873–87. https://doi.org/10.1113/jphysiol.2003.044602.

Malenka, R C, and R A Nicoll. 1999. “Long-Term Potentiation--a Decade of Progress?” *Science* 285 (5435): 1870–74. https://doi.org/10.1126/science.285.5435.1870.

Malkova, Ludise, and Mortimer Mishkin. 2003. “One-Trial Memory for Object-Place Associations after Separate Lesions of Hippocampus and Posterior Parahippocampal Region in the Monkey.” *The Journal of Neuroscience* 23 (5): 1956–65. https://doi.org/10.1523/JNEUROSCI.23-05-01956.2003.

Mankin, Emily A, Fraser T Sparks, Begum Slayyeh, Robert J Sutherland, Stefan Leutgeb, and Jill K Leutgeb. 2012. “Neuronal Code for Extended Time in the Hippocampus.” *Proceedings of the National Academy of Sciences of the United States of America* 109 (47): 19462–67. https://doi.org/10.1073/pnas.1214107109.

Manns, Joseph R, Marc W Howard, and Howard Eichenbaum. 2007. “Gradual Changes in Hippocampal Activity Support Remembering the Order of Events.” *Neuron* 56 (3): 530–40. https://doi.org/10.1016/j.neuron.2007.08.017.

Mao, Dun, Eric Avila, Baptiste Caziot, Jean Laurens, J David Dickman, and Dora E Angelaki. 2021. “Spatial Modulation of Hippocampal Activity in Freely Moving Macaques.” *Neuron* 109 (21): 3521-3534.e6. https://doi.org/10.1016/j.neuron.2021.09.032.

Mao, Dun. 2022. “Neural Correlates of Spatial Navigation in Primate Hippocampus.” *Neuroscience Bulletin*, November. https://doi.org/10.1007/s12264-022-00968-w.

Maren, S, G Aharonov, and M S Fanselow. 1997. “Neurotoxic Lesions of the Dorsal Hippocampus and Pavlovian Fear Conditioning in Rats.” *Behavioural Brain Research* 88 (2): 261–74. https://doi.org/10.1016/s0166-4328(97)00088-0.

Mark, Shirley, and Misha Tsodyks. 2012. “Population Spikes in Cortical Networks during Different Functional States.” *Frontiers in Computational Neuroscience* 6 (July): 43. https://doi.org/10.3389/fncom.2012.00043.

Markram, H, W Gerstner, and P J Sjöström. 2012. “Spike-Timing-Dependent Plasticity: A Comprehensive Overview.” *Frontiers in Synaptic Neuroscience* 4 (July): 2. https://doi.org/10.3389/fnsyn.2012.00002.

Markram, H, J Lübke, M Frotscher, and B Sakmann. 1997. “Regulation of Synaptic Efficacy by Coincidence of Postsynaptic APs and EPSPs.” *Science* 275 (5297): 213–15. https://doi.org/10.1126/science.275.5297.213.

Markram, Henry, Wulfram Gerstner, and Per Jesper Sjöström. 2011. “A History of Spike-Timing-Dependent Plasticity.” *Frontiers in Synaptic Neuroscience* 3 (August): 4. https://doi.org/10.3389/fnsyn.2011.00004.

Marr, D, David Willshaw, and Bruce McNaughton. 1991. “Simple Memory: A Theory for Archicortex.” In *From the Retina to the Neocortex*, edited by Lucia Vaina, 59–128. Boston, MA: Birkhäuser Boston. https://doi.org/10.1007/978-1-4684-6775-8_5.

Marshall, Lisa, Halla Helgadóttir, Matthias Mölle, and Jan Born. 2006. “Boosting Slow Oscillations during Sleep Potentiates Memory.” *Nature* 444 (7119): 610–13. https://doi.org/10.1038/nature05278.

Martinez-Trujillo, Julio, Diego Piza, Benjamin Corrigan, Roberto Gulli, Sonia Do Carmo, A. Claudio Cuello, and Lyle Muller. 2023. “Primacy of Vision Shapes Behavioral Strategies and Neural Substrates of Spatial Navigation in the Hippocampus of the Common Marmoset.” *Research Square*, October. https://doi.org/10.21203/rs.3.rs-3231892/v1.

Martinez-Trujillo, Julio. 2022. “Corollary Discharge: Linking Saccades and Memory Circuits in the Human Brain.” *Current Biology* 32 (14): R774–76. https://doi.org/10.1016/j.cub.2022.06.006.

Masimore, B, J Kakalios, and A D Redish. 2004. “Measuring Fundamental Frequencies in Local Field Potentials.” *Journal of Neuroscience Methods* 138 (1–2): 97–105. https://doi.org/10.1016/j.jneumeth.2004.03.014.

Masurkar, Arjun V, Kalyan V Srinivas, David H Brann, Richard Warren, Daniel C Lowes, and Steven A Siegelbaum. 2017. “Medial and Lateral Entorhinal Cortex Differentially Excite Deep versus Superficial CA1 Pyramidal Neurons.” *Cell Reports* 18 (1): 148–60. https://doi.org/10.1016/j.celrep.2016.12.012.

Maurer, Andrew P, Sara N Burke, Peter Lipa, William E Skaggs, and Carol A Barnes. 2012. “Greater Running Speeds Result in Altered Hippocampal Phase Sequence Dynamics.” *Hippocampus* 22 (4): 737–47. https://doi.org/10.1002/hipo.20936.

Maurer, Andrew P, Shea R Vanrhoads, Gary R Sutherland, Peter Lipa, and Bruce L McNaughton. 2005. “Self-Motion and the Origin of Differential Spatial Scaling along the Septo-Temporal Axis of the Hippocampus.” *Hippocampus* 15 (7): 841–52. https://doi.org/10.1002/hipo.20114.

Mayford, Mark, Steven A Siegelbaum, and Eric R Kandel. 2012. “Synapses and Memory Storage.” *Cold Spring Harbor Perspectives in Biology* 4 (6). https://doi.org/10.1101/cshperspect.a005751.

McCartney, Holly, Andrew D Johnson, Zachary M Weil, and Bennet Givens. 2004. “Theta Reset Produces Optimal Conditions for Long-Term Potentiation.” *Hippocampus* 14 (6): 684–87. https://doi.org/10.1002/hipo.20019.

McClelland, J L, B L McNaughton, and R C O’Reilly. 1995. “Why There Are Complementary Learning Systems in the Hippocampus and Neocortex: Insights from the Successes and Failures of Connectionist Models of Learning and Memory.” *Psychological Review* 102 (3): 419–57. https://doi.org/10.1037/0033-295X.102.3.419.

McFarland, W L, H Teitelbaum, and E K Hedges. 1975. “Relationship between Hippocampal Theta Activity and Running Speed in the Rat.” *Journal of Comparative and Physiological Psychology* 88 (1): 324–28. https://doi.org/10.1037/h0076177.

McInnes, Leland, John Healy, and James Melville. 2018. “UMAP: Uniform Manifold Approximation and Projection for Dimension Reduction.” *ArXiv*. https://doi.org/10.48550/arxiv.1802.03426.

McKenzie, Sam, Andrea J Frank, Nathaniel R Kinsky, Blake Porter, Pamela D Rivière, and Howard Eichenbaum. 2014. “Hippocampal Representation of Related and Opposing Memories Develop within Distinct, Hierarchically Organized Neural Schemas.” *Neuron* 83 (1): 202–15. https://doi.org/10.1016/j.neuron.2014.05.019.

McKenzie, Sam. 2018. “Inhibition Shapes the Organization of Hippocampal Representations.” *Hippocampus* 28 (9): 659–71. https://doi.org/10.1002/hipo.22803.

McQuiston, A Rory. 2014. “Acetylcholine Release and Inhibitory Interneuron Activity in Hippocampal CA1.” *Frontiers in Synaptic Neuroscience* 6 (September): 20. https://doi.org/10.3389/fnsyn.2014.00020.

Meador, K J, J L Thompson, D W Loring, A M Murro, D W King, B B Gallagher, G P Lee, J R Smith, and H F Flanigin. 1991. “Behavioral State-Specific Changes in Human Hippocampal Theta Activity.” *Neurology* 41 (6): 869–72. https://doi.org/10.1212/wnl.41.6.869.

Meister, Miriam L R, and Elizabeth A Buffalo. 2016. “Getting Directions from the Hippocampus: The Neural Connection between Looking and Memory.” *Neurobiology of Learning and Memory* 134 Pt A (Pt A): 135–44. https://doi.org/10.1016/j.nlm.2015.12.004.

Miller, Cory T, David Gire, Kim Hoke, Alexander C Huk, Darcy Kelley, David A Leopold, Matthew C Smear, Frederic Theunissen, Michael Yartsev, and Cristopher M Niell. 2022. “Natural Behavior Is the Language of the Brain.” *Current Biology* 32 (10): R482–93. https://doi.org/10.1016/j.cub.2022.03.031.

Mitzdorf, U. 1985. “Current Source-Density Method and Application in Cat Cerebral Cortex: Investigation of Evoked Potentials and EEG Phenomena.” *Physiological Reviews* 65 (1): 37–100. https://doi.org/10.1152/physrev.1985.65.1.37.

Miyawaki, Hiroyuki, and Kenji Mizuseki. 2022. “De Novo Inter-Regional Coactivations of Preconfigured Local Ensembles Support Memory.” *Nature Communications* 13 (1): 1272. https://doi.org/10.1038/s41467-022-28929-x.

Mizuseki, Kenji, and György Buzsáki. 2013. “Preconfigured, Skewed Distribution of Firing Rates in the Hippocampus and Entorhinal Cortex.” *Cell Reports* 4 (5): 1010–21. https://doi.org/10.1016/j.celrep.2013.07.039.

Mizuseki, Kenji, Kamran Diba, Eva Pastalkova, and György Buzsáki. 2011. “Hippocampal CA1 Pyramidal Cells Form Functionally Distinct Sublayers.” *Nature Neuroscience* 14 (9): 1174–81. https://doi.org/10.1038/nn.2894.

Montefusco-Siegmund, Rodrigo, Timothy K Leonard, and Kari L Hoffman. 2017. “Hippocampal Gamma-Band Synchrony and Pupillary Responses Index Memory during Visual Search.” *Hippocampus* 27 (4): 425–34. https://doi.org/10.1002/hipo.22702.

Moroni, Fabio, Lino Nobili, Giuseppe Curcio, Fabrizio De Carli, Fabiana Fratello, Cristina Marzano, Luigi De Gennaro, et al. 2007. “Sleep in the Human Hippocampus: A Stereo-EEG Study.” *Plos One* 2 (9): e867. https://doi.org/10.1371/journal.pone.0000867.

Moscovitch, Morris, R Shayna Rosenbaum, Asaf Gilboa, Donna Rose Addis, Robyn Westmacott, Cheryl Grady, Mary Pat McAndrews, et al. 2005. “Functional Neuroanatomy of Remote Episodic, Semantic and Spatial Memory: A Unified Account Based on Multiple Trace Theory.” *Journal of Anatomy* 207 (1): 35–66. https://doi.org/10.1111/j.1469-7580.2005.00421.x.

Murty, Vishnu P, Sarah DuBrow, and Lila Davachi. 2015. “The Simple Act of Choosing Influences Declarative Memory.” *The Journal of Neuroscience* 35 (16): 6255–64. https://doi.org/10.1523/JNEUROSCI.4181-14.2015.

M Aghajan, Zahra, Peter Schuette, Tony A Fields, Michelle E Tran, Sameed M Siddiqui, Nicholas R Hasulak, Thomas K Tcheng, et al. 2017. “Theta Oscillations in the Human Medial Temporal Lobe during Real-World Ambulatory Movement.” *Current Biology* 27 (24): 3743-3751.e3. https://doi.org/10.1016/j.cub.2017.10.062.

Mizuseki, Kenji, Anton Sirota, Eva Pastalkova, and György Buzsáki. 2009. “Theta Oscillations Provide Temporal Windows for Local Circuit Computation in the Entorhinal-Hippocampal Loop.” *Neuron* 64 (2): 267–80. https://doi.org/10.1016/j.neuron.2009.08.037.

Montgomery, Sean M, Anton Sirota, and György Buzsáki. 2008. “Theta and Gamma Coordination of Hippocampal Networks during Waking and Rapid Eye Movement Sleep.” *The Journal of Neuroscience* 28 (26): 6731–41. https://doi.org/10.1523/JNEUROSCI.1227-08.2008.

Muessig, Laurenz, Michal Lasek, Isabella Varsavsky, Francesca Cacucci, and Thomas Joseph Wills. 2019. “Coordinated Emergence of Hippocampal Replay and Theta Sequences during Post-Natal Development.” *Current Biology* 29 (5): 834-840.e4. https://doi.org/10.1016/j.cub.2019.01.005.

Muller, Lyle, Romain Brette, and Boris Gutkin. 2011. “Spike-Timing Dependent Plasticity and Feed-Forward Input Oscillations Produce Precise and Invariant Spike Phase-Locking.” *Frontiers in Computational Neuroscience* 5 (November): 45. https://doi.org/10.3389/fncom.2011.00045.

Murray, Elisabeth A., Mark G. Baxter, and David Gaffan. 1998. “Monkeys with Rhinal Cortex Damage or Neurotoxic Hippocampal Lesions Are Impaired on Spatial Scene Learning and Object Reversals.” *Behavioral Neuroscience* 112 (6): 1291–1303. https://doi.org/10.1037/0735-7044.112.6.1291.

Murray, E A, and M Mishkin. 1998. “Object Recognition and Location Memory in Monkeys with Excitotoxic Lesions of the Amygdala and Hippocampus.” *The Journal of Neuroscience* 18 (16): 6568–82. https://doi.org/10.1523/JNEUROSCI.18-16-06568.1998.

Nádasdy, Z, H Hirase, A Czurkó, J Csicsvari, and G Buzsáki. 1999. “Replay and Time Compression of Recurring Spike Sequences in the Hippocampus.” *The Journal of Neuroscience* 19 (21): 9497–9507. https://doi.org/10.1523/JNEUROSCI.19-21-09497.1999.

Nadel, Lynn, and Oliver Hardt. 2011. “Update on Memory Systems and Processes.” *Neuropsychopharmacology* 36 (1): 251–73. https://doi.org/10.1038/npp.2010.169.

Nagahara, Alan H, Tim Bernot, and Mark H Tuszynski. 2010. “Age-Related Cognitive Deficits in Rhesus Monkeys Mirror Human Deficits on an Automated Test Battery.” *Neurobiology of Aging* 31 (6): 1020–31. https://doi.org/10.1016/j.neurobiolaging.2008.07.007.

Nakahara, Kiyoshi, Toshihiro Hayashi, Seiki Konishi, and Yasushi Miyashita. 2002. “Functional MRI of Macaque Monkeys Performing a Cognitive Set-Shifting Task.” *Science* 295 (5559): 1532–36. https://doi.org/10.1126/science.1067653.

Navas-Olive, Andrea, Manuel Valero, Teresa Jurado-Parras, Adan de Salas-Quiroga, Robert G Averkin, Giuditta Gambino, Elena Cid, and Liset M de la Prida. 2020. “Multimodal Determinants of Phase-Locked Dynamics across Deep-Superficial Hippocampal Sublayers during Theta Oscillations.” *Nature Communications* 11 (1): 2217. https://doi.org/10.1038/s41467-020-15840-6.

Newman, Ehren L, Shea N Gillet, Jason R Climer, and Michael E Hasselmo. 2013. “Cholinergic Blockade Reduces Theta-Gamma Phase Amplitude Coupling and Speed Modulation of Theta Frequency Consistent with Behavioral Effects on Encoding.” *The Journal of Neuroscience* 33 (50): 19635–46. https://doi.org/10.1523/JNEUROSCI.2586-13.2013.

Nicolelis, M A, L A Baccala, R C Lin, and J K Chapin. 1995. “Sensorimotor Encoding by Synchronous Neural Ensemble Activity at Multiple Levels of the Somatosensory System.” *Science* 268 (5215): 1353–58. https://doi.org/10.1126/science.7761855.

Nitzan, Noam, Sam McKenzie, Prateep Beed, Daniel Fine English, Silvia Oldani, John J Tukker, György Buzsáki, and Dietmar Schmitz. 2020. “Propagation of Hippocampal Ripples to the Neocortex by Way of a Subiculum-Retrosplenial Pathway.” *Nature Communications* 11 (1): 1947. https://doi.org/10.1038/s41467-020-15787-8.

Norman, Yitzhak, Omri Raccah, Su Liu, Josef Parvizi, and Rafael Malach. 2021. “Hippocampal Ripples and Their Coordinated Dialogue with the Default Mode Network during Recent and Remote Recollection.” *Neuron* 109 (17): 2767-2780.e5. https://doi.org/10.1016/j.neuron.2021.06.020.

Norman, Yitzhak, Erin M Yeagle, Simon Khuvis, Michal Harel, Ashesh D Mehta, and Rafael Malach. 2019. “Hippocampal Sharp-Wave Ripples Linked to Visual Episodic Recollection in Humans.” *Science* 365 (6454). https://doi.org/10.1126/science.aax1030.

Numan, R, and J R Quaranta. 1990. “Effects of Medial Septal Lesions on Operant Delayed Alternation in Rats.” *Brain Research* 531 (1–2): 232–41. https://doi.org/10.1016/0006-8993(90)90779-b.

Nuñez, Angel, and Washington Buño. 2021. “The Theta Rhythm of the Hippocampus: From Neuronal and Circuit Mechanisms to Behavior.” *Frontiers in Cellular Neuroscience* 15 (March): 649262. https://doi.org/10.3389/fncel.2021.649262.

O’Keefe, J, and M L Recce. 1993. “Phase Relationship between Hippocampal Place Units and the EEG Theta Rhythm.” *Hippocampus* 3 (3): 317–30. https://doi.org/10.1002/hipo.450030307.

O’Keefe, J. 1976. “Place Units in the Hippocampus of the Freely Moving Rat.” *Experimental Neurology* 51 (1): 78–109. https://doi.org/10.1016/0014-4886(76)90055-8.

O'Keefe, John, and Julija Krupic. 2021. "Do Hippocampal Pyramidal Cells Respond to Non-Spatial Stimuli?" *Physiological Reviews*, February. https://doi.org/10.1152/physrev.00014.2020.

O'Neill, Joseph, Barty Pleydell-Bouverie, David Dupret, and Jozsef Csicsvari. 2010. "Play It Again: Reactivation of Waking Experience and Memory." *Trends in Neurosciences* 33 (5): 220–29. https://doi.org/10.1016/j.tins.2010.01.006.

Ognjanovski, Nicolette, Samantha Schaeffer, Jiaxing Wu, Sima Mofakham, Daniel Maruyama, Michal Zochowski, and Sara J Aton. 2017. "Parvalbumin-Expressing Interneurons Coordinate Hippocampal Network Dynamics Required for Memory Consolidation." *Nature Communications* 8 (April): 15039. https://doi.org/10.1038/ncomms15039.

Ólafsdóttir, H Freyja, Daniel Bush, and Caswell Barry. 2018. "The Role of Hippocampal Replay in Memory and Planning." *Current Biology* 28 (1): R37–50. https://doi.org/10.1016/j.cub.2017.10.073.

Oliva, Azahara, Antonio Fernández-Ruiz, György Buzsáki, and Antal Berényi. 2016. "Role of Hippocampal CA2 Region in Triggering Sharp-Wave Ripples." *Neuron* 91 (6): 1342–55. https://doi.org/10.1016/j.neuron.2016.08.008.

Oliva, Azahara, Antonio Fernandez-Ruiz, and Lindsay A Karaba. 2023. "CA2 Orchestrates Hippocampal Network Dynamics." *Hippocampus* 33 (3): 241–51. https://doi.org/10.1002/hipo.23495.

Opalka, Ashley N, Wen-Qiang Huang, Jun Liu, Hualou Liang, and Dong V Wang. 2020. "Hippocampal Ripple Coordinates Retrosplenial Inhibitory Neurons during Slow-Wave Sleep." *Cell Reports* 30 (2): 432-441.e3. https://doi.org/10.1016/j.celrep.2019.12.038.

Orban, Guy A, David Van Essen, and Wim Vanduffel. 2004. "Comparative Mapping of Higher Visual Areas in Monkeys and Humans." *Trends in Cognitive Sciences* 8 (7): 315–24. https://doi.org/10.1016/j.tics.2004.05.009.

Pachitariu, Marius, Nicholas Steinmetz, Shabnam Kadir, Matteo Carandini, and Kenneth D Harris. 2016. "Kilosort: Realtime Spike-Sorting for Extracellular Electrophysiology with Hundreds of Channels." *BioRxiv*, June. https://doi.org/10.1101/061481.

Palmigiano, Agostina, Theo Geisel, Fred Wolf, and Demian Battaglia. 2017. "Flexible Information Routing by Transient Synchrony." *Nature Neuroscience* 20 (7): 1014–22. https://doi.org/10.1038/nn.4569.

Papatheodoropoulos, C. 2010. "Patterned Activation of Hippocampal Network (Approximately 10 Hz) during in Vitro Sharp Wave-Ripples." *Neuroscience* 168 (2): 429–42. https://doi.org/10.1016/j.neuroscience.2010.03.058.

Parkinson, J K, E A Murray, and M Mishkin. 1988. "A Selective Mnemonic Role for the Hippocampus in Monkeys: Memory for the Location of Objects." *The Journal of Neuroscience* 8 (11): 4159–67. https://doi.org/10.1523/JNEUROSCI.08-11-04159.1988.

Park, Jin-Yong, and Nelson Spruston. 2012. "Synergistic Actions of Metabotropic Acetylcholine and Glutamate Receptors on the Excitability of Hippocampal CA1 Pyramidal Neurons." *The Journal of Neuroscience* 32 (18): 6081–91. https://doi.org/10.1523/JNEUROSCI.6519-11.2012.

Parra, P, A I Gulyás, and R Miles. 1998. "How Many Subtypes of Inhibitory Cells in the Hippocampus?" *Neuron* 20 (5): 983–93. https://doi.org/10.1016/s0896-6273(00)80479-1.

Passingham, Richard. 2009. "How Good Is the Macaque Monkey Model of the Human Brain?" *Current Opinion in Neurobiology* 19 (1): 6–11. https://doi.org/10.1016/j.conb.2009.01.002.

Pastalkova, Eva, Vladimir Itskov, Asohan Amarasingham, and György Buzsáki. 2008. "Internally Generated Cell Assembly Sequences in the Rat Hippocampus." *Science* 321 (5894): 1322–27. https://doi.org/10.1126/science.1159775.

Pavlides, C, and J Winson. 1989. "Influences of Hippocampal Place Cell Firing in the Awake State on the Activity of These Cells during Subsequent Sleep Episodes." *The Journal of Neuroscience* 9 (8): 2907–18. https://doi.org/10.1523/JNEUROSCI.09-08-02907.1989.

Peigneux, Philippe, Steven Laureys, Sonia Fuchs, Fabienne Collette, Fabien Perrin, Jean Reggers, Christophe Phillips, et al. 2004. "Are Spatial Memories Strengthened in the Human Hippocampus during Slow Wave Sleep?" *Neuron* 44 (3): 535–45. https://doi.org/10.1016/j.neuron.2004.10.007.

Pelkey, Kenneth A, Ramesh Chittajallu, Michael T Craig, Ludovic Tricoire, Jason C Wester, and Chris J McBain. 2017. "Hippocampal Gabaergic Inhibitory Interneurons." *Physiological Reviews* 97 (4): 1619–1747. https://doi.org/10.1152/physrev.00007.2017.

Pelli, D G. 1997. "The VideoToolbox Software for Visual Psychophysics: Transforming Numbers into Movies." *Spatial Vision* 10 (4): 437–42. https://doi.org/10.1163/156856897X00366.

Penaud, S, N Jebara, M Zaoui, E Orriols, A Berthoz, and P Piolino. 2022. "Episodic Memory and Self-Reference in a Naturalistic Context: New Insights Based on a Virtual Walk in the Latin Quarter of Paris." *Journal of Environmental Psychology* 81 (June): 101801. https://doi.org/10.1016/j.jenvp.2022.101801.

Penner, Cooper, Juri Minxha, Nand Chandravadia, Adam N Mamelak, and Ueli Rutishauser. 2022. "Properties and Hemispheric Differences of Theta Oscillations in the Human Hippocampus." *Hippocampus* 32 (5): 335–41. https://doi.org/10.1002/hipo.23412.

Perentos, Nikolas, Marino Krstulovic, and A Jennifer Morton. 2022. "Deep Brain Electrophysiology in Freely Moving Sheep." *Current Biology* 32 (4): 763-774.e4. https://doi.org/10.1016/j.cub.2021.12.035.

Pesaran, Bijan, Martin Vinck, Gaute T Einevoll, Anton Sirota, Pascal Fries, Markus Siegel, Wilson Truccolo, Charles E Schroeder, and Ramesh Srinivasan. 2018. "Investigating Large-Scale Brain Dynamics Using Field Potential Recordings: Analysis and Interpretation." *Nature Neuroscience* 21 (7): 903–19. https://doi.org/10.1038/s41593-018-0171-8.

Peters, A, D L Rosene, M B Moss, T L Kemper, C R Abraham, J Tigges, and M S Albert. 1996. "Neurobiological Bases of Age-Related Cognitive Decline in the Rhesus Monkey." *Journal of Neuropathology and Experimental Neurology* 55 (8): 861–74. https://doi.org/10.1097/00005072-199608000-00001.

Petersen, Peter C, Joshua H Siegle, Nicholas A Steinmetz, Sara Mahallati, and György Buzsáki. 2021. "CellExplorer: A Framework for Visualizing and Characterizing Single Neurons." *Neuron* 109 (22): 3594-3608.e2. https://doi.org/10.1016/j.neuron.2021.09.002.

Petersen, Peter Christian, and György Buzsáki. 2020. "Cooling of Medial Septum Reveals Theta Phase Lag Coordination of Hippocampal Cell Assemblies." *Neuron* 107 (4): 731-744.e3. https://doi.org/10.1016/j.neuron.2020.05.023.

Peyrache, Adrien, Karim Benchenane, Mehdi Khamassi, Sidney I Wiener, and Francesco P Battaglia. 2010. "Principal Component Analysis of Ensemble Recordings Reveals Cell Assemblies at High Temporal Resolution." *Journal of Computational Neuroscience* 29 (1–2): 309–25. https://doi.org/10.1007/s10827-009-0154-6.

Peyrache, Adrien, Mehdi Khamassi, Karim Benchenane, Sidney I Wiener, and Francesco P Battaglia. 2009. "Replay of Rule-Learning Related Neural Patterns in the Prefrontal Cortex during Sleep." *Nature Neuroscience* 12 (7): 919–26. https://doi.org/10.1038/nn.2337.

Pezzulo, Giovanni, Caleb Kemere, and Matthijs A A van der Meer. 2017. "Internally Generated Hippocampal Sequences as a Vantage Point to Probe Future-Oriented Cognition." *Annals of the New York Academy of Sciences* 1396 (1): 144–65. https://doi.org/10.1111/nyas.13329.

Pine, Daniel S, Steven P Wise, and Elisabeth A Murray. 2021. "Evolution, Emotion, and Episodic Engagement." *The American Journal of Psychiatry* 178 (8): 701–14. https://doi.org/10.1176/appi.ajp.2020.20081187.

Plancher, Gaën, Julien Barra, Eric Orriols, and Pascale Piolino. 2013. "The Influence of Action on Episodic Memory: A Virtual Reality Study." *Quarterly Journal of Experimental Psychology* 66 (5): 895–909. https://doi.org/10.1080/17470218.2012.722657.

Plihal, W, and J Born. 1997. "Effects of Early and Late Nocturnal Sleep on Declarative and Procedural Memory." *Journal of Cognitive Neuroscience* 9 (4): 534–47. https://doi.org/10.1162/jocn.1997.9.4.534.

Poo, Mu-Ming, Michele Pignatelli, Tomás J Ryan, Susumu Tonegawa, Tobias Bonhoeffer, Kelsey C Martin, Andrii Rudenko, et al. 2016. "What Is Memory? The Present State of the Engram." *BMC Biology* 14 (May): 40. https://doi.org/10.1186/s12915-016-0261-6.

Qasim, Salman E, Itzhak Fried, and Joshua Jacobs. 2021. "Phase Precession in the Human Hippocampus and Entorhinal Cortex." *Cell* 184 (12): 3242-3255.e10. https://doi.org/10.1016/j.cell.2021.04.017.

Quirk, G J, C Repa, and J E LeDoux. 1995. “Fear Conditioning Enhances Short-Latency Auditory Responses of Lateral Amygdala Neurons: Parallel Recordings in the Freely Behaving Rat.” *Neuron* 15 (5): 1029–39. https://doi.org/10.1016/0896-6273(95)90092-6.

Rajji, Tarek, David Chapman, Howard Eichenbaum, and Robert Greene. 2006. “The Role of CA3 Hippocampal NMDA Receptors in Paired Associate Learning.” *The Journal of Neuroscience* 26 (3): 908–15. https://doi.org/10.1523/JNEUROSCI.4194-05.2006.

Rami, A, A Bréhier, M Thomasset, and A Rabié. 1987. “Cholecalcin (28-KDa Calcium-Binding Protein) in the Rat Hippocampus: Development in Normal Animals and in Altered Thyroid States. An Immunocytochemical Study.” *Developmental Biology* 124 (1): 228–38. https://doi.org/10.1016/0012-1606(87)90474-x.

Ranade, Sachin, Balázs Hangya, and Adam Kepecs. 2013. “Multiple Modes of Phase Locking between Sniffing and Whisking during Active Exploration.” *The Journal of Neuroscience* 33 (19): 8250–56. https://doi.org/10.1523/JNEUROSCI.3874-12.2013.

Ranck, J B. 1973. “Studies on Single Neurons in Dorsal Hippocampal Formation and Septum in Unrestrained Rats. I. Behavioral Correlates and Firing Repertoires.” *Experimental Neurology* 41 (2): 461–531. https://doi.org/10.1016/0014-4886(73)90290-2.

Ranganath, C. 2010. “Binding Items and Contexts: The Cognitive Neuroscience of Episodic Memory.” *Current Directions in Psychological Science* 19 (3): 131–37. https://doi.org/10.1177/0963721410368805.

Rangel, Lara M, Andrea A Chiba, and Laleh K Quinn. 2015. “Theta and Beta Oscillatory Dynamics in the Dentate Gyrus Reveal a Shift in Network Processing State during Cue Encounters.” *Frontiers in Systems Neuroscience* 9 (July): 96. https://doi.org/10.3389/fnsys.2015.00096.

Rangel, L M, A S Alexander, J B Aimone, J Wiles, F H Gage, A A Chiba, and L K Quinn. 2014. “Temporally Selective Contextual Encoding in the Dentate Gyrus of the Hippocampus.” *Nature Communications* 5: 3181. https://doi.org/10.1038/ncomms4181.

Rapp, P R, and D G Amaral. 1989. “Evidence for Task-Dependent Memory Dysfunction in the Aged Monkey.” *The Journal of Neuroscience* 9 (10): 3568–76. https://doi.org/10.1523/JNEUROSCI.09-10-03568.1989.

Rasch, Björn, Christian Büchel, Steffen Gais, and Jan Born. 2007. “Odor Cues during Slow-Wave Sleep Prompt Declarative Memory Consolidation.” *Science* 315 (5817): 1426–29. https://doi.org/10.1126/science.1138581.

Ravassard, Pascal, Ashley Kees, Bernard Willers, David Ho, Daniel A Aharoni, Jesse Cushman, Zahra M Aghajan, and Mayank R Mehta. 2013. “Multisensory Control of Hippocampal Spatiotemporal Selectivity.” *Science* 340 (6138): 1342–46. https://doi.org/10.1126/science.1232655.

Raven, Frank, and Sara J Aton. 2021. “The Engram’s Dark Horse: How Interneurons Regulate State-Dependent Memory Processing and Plasticity.” *Frontiers in Neural Circuits* 15 (September): 750541. https://doi.org/10.3389/fncir.2021.750541.

Rawlins, J N, J Feldon, and J A Gray. 1979. “Septo-Hippocampal Connections and the Hippocampal Theta Rhythm.” *Experimental Brain Research* 37 (1): 49–63. https://doi.org/10.1007/BF01474253.

Ray, Supratim, and John H R Maunsell. 2010. “Differences in Gamma Frequencies across Visual Cortex Restrict Their Possible Use in Computation.” *Neuron* 67 (5): 885–96. https://doi.org/10.1016/j.neuron.2010.08.004.

Renart, Alfonso, Jaime de la Rocha, Peter Bartho, Liad Hollender, Néstor Parga, Alex Reyes, and Kenneth D Harris. 2010. “The Asynchronous State in Cortical Circuits.” *Science* 327 (5965): 587–90. https://doi.org/10.1126/science.1179850.

Rex, Christopher S, Laura L Colgin, Yousheng Jia, Malcolm Casale, Theodore K Yanagihara, Maria Debenedetti, Christine M Gall, Eniko A Kramar, and Gary Lynch. 2009. “Origins of an Intrinsic Hippocampal EEG Pattern.” *Plos One* 4 (11): e7761. https://doi.org/10.1371/journal.pone.0007761.

Rey, Hernan Gonzalo, Itzhak Fried, and Rodrigo Quian Quiroga. 2014. “Timing of Single-Neuron and Local Field Potential Responses in the Human Medial Temporal Lobe.” *Current Biology* 24 (3): 299–304. https://doi.org/10.1016/j.cub.2013.12.004.

Rhesus Macaque Genome Sequencing and Analysis Consortium, Richard A Gibbs, Jeffrey Rogers, Michael G Katze, Roger Bumgarner, George M Weinstock, Elaine R Mardis, et al. 2007. “Evolutionary and Biomedical Insights from the Rhesus Macaque Genome.” *Science* 316 (5822): 222–34. https://doi.org/10.1126/science.1139247.

Richardson, Andrew G, Xilin Liu, Pauline K Weigand, Eric D Hudgins, Joel M Stein, Sandhitsu R Das, Alexander Proekt, et al. 2017. “Hippocampal Gamma-Slow Oscillation Coupling in Macaques during Sedation and Sleep.” *Hippocampus* 27 (11): 1125–39. https://doi.org/10.1002/hipo.22757.

Ringo, J L, S Sobotka, M D Diltz, and C M Bunce. 1994. “Eye Movements Modulate Activity in Hippocampal, Parahippocampal, and Inferotemporal Neurons.” *Journal of Neurophysiology* 71 (3): 1285–88. https://doi.org/10.1152/jn.1994.71.3.1285.

Robbe, David, Sean M Montgomery, Alexander Thome, Pavel E Rueda-Orozco, Bruce L McNaughton, and György Buzsaki. 2006. “Cannabinoids Reveal Importance of Spike Timing Coordination in Hippocampal Function.” *Nature Neuroscience* 9 (12): 1526–33. https://doi.org/10.1038/nn1801.

Roberts, Angela C, Davorka L Tomic, Caroline H Parkinson, Tom A Roeling, David J Cutter, Trevor W Robbins, and Barry J Everitt. 2007. “Forebrain Connectivity of the Prefrontal Cortex in the Marmoset Monkey (Callithrix Jacchus): An Anterograde and Retrograde Tract-Tracing Study.” *The Journal of Comparative Neurology* 502 (1): 86–112. https://doi.org/10.1002/cne.21300.

Robin, Jessica, and Morris Moscovitch. 2017. “Details, Gist and Schema: Hippocampal–Neocortical Interactions Underlying Recent and Remote Episodic and Spatial Memory.” *Current Opinion in Behavioral Sciences* 17 (October): 114–23. https://doi.org/10.1016/j.cobeha.2017.07.016.

Rolls, Edmund T. 1999. “Spatial View Cells and the Representation of Place in the Primate Hippocampus.” *Hippocampus*, January.

Rolls, Edmund T. 2013. “The Mechanisms for Pattern Completion and Pattern Separation in the Hippocampus.” *Frontiers in Systems Neuroscience* 7 (October): 74. https://doi.org/10.3389/fnsys.2013.00074.

———. 2023. “Hippocampal Spatial View Cells for Memory and Navigation, and Their Underlying Connectivity in Humans.” *Hippocampus* 33 (5): 533–72. https://doi.org/10.1002/hipo.23467.

Rotem-Turchinski, Nuphar, Ayelet Ramaty, and Avi Mendelsohn. 2019. “The Opportunity to Choose Enhances Long-Term Episodic Memory.” *Memory* 27 (4): 431–40. https://doi.org/10.1080/09658211.2018.1515317.

Rothschild, Gideon, Elad Eban, and Loren M Frank. 2017. “A Cortical-Hippocampal-Cortical Loop of Information Processing during Memory Consolidation.” *Nature Neuroscience* 20 (2): 251–59. https://doi.org/10.1038/nn.4457.

Roux, Frédéric, George Parish, Ramesh Chelvarajah, David T Rollings, Vijay Sawlani, Hajo Hamer, Stephanie Gollwitzer, et al. 2022. “Oscillations Support Short Latency Co-Firing of Neurons during Human Episodic Memory Formation.” *ELife* 11 (November). https://doi.org/10.7554/eLife.78109.

Roy, Dheeraj S, Young-Gyun Park, Minyoung E Kim, Ying Zhang, Sachie K Ogawa, Nicholas DiNapoli, Xinyi Gu, et al. 2022. “Brain-Wide Mapping Reveals That Engrams for a Single Memory Are Distributed across Multiple Brain Regions.” *Nature Communications* 13 (1): 1799. https://doi.org/10.1038/s41467-022-29384-4.

Royer, Sébastien, Anton Sirota, Jagdish Patel, and György Buzsáki. 2010. “Distinct Representations and Theta Dynamics in Dorsal and Ventral Hippocampus.” *The Journal of Neuroscience* 30 (5): 1777–87. https://doi.org/10.1523/JNEUROSCI.4681-09.2010.

Royer, Sébastien, Boris V Zemelman, Attila Losonczy, Jinhyun Kim, Frances Chance, Jeffrey C Magee, and György Buzsáki. 2012. “Control of Timing, Rate and Bursts of Hippocampal Place Cells by Dendritic and Somatic Inhibition.” *Nature Neuroscience* 15 (5): 769–75. https://doi.org/10.1038/nn.3077.

Russo, Eleonora, and Daniel Durstewitz. 2017. “Cell Assemblies at Multiple Time Scales with Arbitrary Lag Constellations.” *ELife* 6 (January). https://doi.org/10.7554/eLife.19428.

Rutishauser, Ueli, Ian B Ross, Adam N Mamelak, and Erin M Schuman. 2010. “Human Memory Strength Is Predicted by Theta-Frequency Phase-Locking of Single Neurons.” *Nature* 464 (7290): 903–7. https://doi.org/10.1038/nature08860.

Ryan, J D, R R Althoff, S Whitlow, and N J Cohen. 2000. “Amnesia Is a Deficit in Relational Memory.” *Psychological Science* 11 (6): 454–61. https://doi.org/10.1111/1467-9280.00288.

Sainsbury, R S, J L Harris, and G L Rowland. 1987. “Sensitization and Hippocampal Type 2 Theta in the Rat.” *Physiology & Behavior* 41 (5): 489–93. https://doi.org/10.1016/0031-9384(87)90085-0.

Sainsbury, R S, A Heynen, and C P Montoya. 1987. “Behavioral Correlates of Hippocampal Type 2 Theta in the Rat.” *Physiology & Behavior* 39 (4): 513–19. https://doi.org/10.1016/0031-9384(87)90382-9.

Sainsbury, R S. 1998. “Hippocampal Theta: A Sensory-Inhibition Theory of Function.” *Neuroscience and Biobehavioral Reviews* 22 (2): 237–41. https://doi.org/10.1016/s0149-7634(97)00011-0.

Salinas, E, and T J Sejnowski. 2001. “Correlated Neuronal Activity and the Flow of Neural Information.” *Nature Reviews. Neuroscience* 2 (8): 539–50. https://doi.org/10.1038/35086012.

Salz, Daniel M, Zoran Tiganj, Srijesa Khasnabish, Annalyse Kohley, Daniel Sheehan, Marc W Howard, and Howard Eichenbaum. 2016. “Time Cells in Hippocampal Area CA3.” *The Journal of Neuroscience* 36 (28): 7476–84. https://doi.org/10.1523/JNEUROSCI.0087-16.2016.

Sayer, R J, M J Friedlander, and S J Redman. 1990. “The Time Course and Amplitude of EPSPs Evoked at Synapses between Pairs of CA3/CA1 Neurons in the Hippocampal Slice.” *The Journal of Neuroscience* 10 (3): 826–36. https://doi.org/10.1523/JNEUROSCI.10-03-00826.1990.

Sayer, R J, S J Redman, and P Andersen. 1989. “Amplitude Fluctuations in Small EPSPs Recorded from CA1 Pyramidal Cells in the Guinea Pig Hippocampal Slice.” *The Journal of Neuroscience* 9 (3): 840–50. https://doi.org/10.1523/JNEUROSCI.09-03-00840.1989.

Scheffer-Teixeira, Robson, Hindiael Belchior, Fábio V Caixeta, Bryan C Souza, Sidarta Ribeiro, and Adriano B L Tort. 2012. “Theta Phase Modulates Multiple Layer-Specific Oscillations in the CA1 Region.” *Cerebral Cortex* 22 (10): 2404–14. https://doi.org/10.1093/cercor/bhr319.

Schlingloff, Dániel, Szabolcs Káli, Tamás F Freund, Norbert Hájos, and Attila I Gulyás. 2014. “Mechanisms of Sharp Wave Initiation and Ripple Generation.” *The Journal of Neuroscience* 34 (34): 11385–98. https://doi.org/10.1523/JNEUROSCI.0867-14.2014.

Schneider, Aidan, Mehdi Azabou, Louis McDougall-Vigier, David F Parks, Sahara Ensley, Kiran Bhaskaran-Nair, Tomasz Nowakowski, Eva L Dyer, and Keith B Hengen. 2023. “Transcriptomic Cell Type Structures in Vivo Neuronal Activity across Multiple Timescales.” *Cell Reports* 42 (4): 112318. https://doi.org/10.1016/j.celrep.2023.112318.

Schomburg, Erik W, Antonio Fernández-Ruiz, Kenji Mizuseki, Antal Berényi, Costas A Anastassiou, Christof Koch, and György Buzsáki. 2014. “Theta Phase Segregation of Input-Specific Gamma Patterns in Entorhinal-Hippocampal Networks.” *Neuron* 84 (2): 470–85. https://doi.org/10.1016/j.neuron.2014.08.051.

Schroeder, Charles E, Donald A Wilson, Thomas Radman, Helen Scharfman, and Peter Lakatos. 2010. “Dynamics of Active Sensing and Perceptual Selection.” *Current Opinion in Neurobiology* 20 (2): 172–76. https://doi.org/10.1016/j.conb.2010.02.010.

Schultheiss, Nathan W, Maximilian Schlecht, Maanasa Jayachandran, Deborah R Brooks, Jennifer L McGlothan, Tomás R Guilarte, and Timothy A Allen. 2020. “Awake Delta and Theta-Rhythmic Hippocampal Network Modes during Intermittent Locomotor Behaviors in the Rat.” *Behavioral Neuroscience* 134 (6): 529–46. https://doi.org/10.1037/bne0000409.

Schwarz, David A, Mikhail A Lebedev, Timothy L Hanson, Dragan F Dimitrov, Gary Lehew, Jim Meloy, Sankaranarayani Rajangam, et al. 2014. “Chronic, Wireless Recordings of Large-Scale Brain Activity in Freely Moving Rhesus Monkeys.” *Nature Methods* 11 (6): 670–76. https://doi.org/10.1038/nmeth.2936.

Scoville, W B, and B Milner. 1957. “Loss of Recent Memory after Bilateral Hippocampal Lesions.” *Journal of Neurology, Neurosurgery, and Psychiatry* 20 (1): 11–21. https://doi.org/10.1136/jnnp.20.1.11.

Sederberg, Per B, Michael J Kahana, Marc W Howard, Elizabeth J Donner, and Joseph R Madsen. 2003. “Theta and Gamma Oscillations during Encoding Predict Subsequent Recall.” *The Journal of Neuroscience* 23 (34): 10809–14. https://doi.org/10.1523/JNEUROSCI.23-34-10809.2003.

Sederberg, Per B, Andreas Schulze-Bonhage, Joseph R Madsen, Edward B Bromfield, David C McCarthy, Armin Brandt, Michele S Tully, and Michael J Kahana. 2007. “Hippocampal and Neocortical Gamma Oscillations Predict Memory Formation in Humans.” *Cerebral Cortex* 17 (5): 1190–96. https://doi.org/10.1093/cercor/bhl030.

Segal, M, J F Disterhoft, and J Olds. 1972. “Hippocampal Unit Activity during Classical Aversive and Appetitive Conditioning.” *Science* 175 (4023): 792–94. https://doi.org/10.1126/science.175.4023.792.

Seidenbecher, Thomas, T Rao Laxmi, Oliver Stork, and Hans-Christian Pape. 2003. “Amygdalar and Hippocampal Theta Rhythm Synchronization during Fear Memory Retrieval.” *Science* 301 (5634): 846–50. https://doi.org/10.1126/science.1085818.

Sejnowski, T J. 1999. “The Book of Hebb.” *Neuron* 24 (4): 773–76. https://doi.org/10.1016/s0896-6273(00)81025-9.

Semba, K, and B R Komisaruk. 1984. “Neural Substrates of Two Different Rhythmical Vibrissal Movements in the Rat.” *Neuroscience* 12 (3): 761–74. https://doi.org/10.1016/0306-4522(84)90168-4.

Senior, Timothy J, John R Huxter, Kevin Allen, Joseph O’Neill, and Jozsef Csicsvari. 2008. “Gamma Oscillatory Firing Reveals Distinct Populations of Pyramidal Cells in the CA1 Region of the Hippocampus.” *The Journal of Neuroscience* 28 (9): 2274–86. https://doi.org/10.1523/JNEUROSCI.4669-07.2008.

Seress, L, A I Gulyás, I Ferrer, T Tunon, E Soriano, and T F Freund. 1993. “Distribution, Morphological Features, and Synaptic Connections of Parvalbumin- and Calbindin D28k-Immunoreactive Neurons in the Human Hippocampal Formation.” *The Journal of Comparative Neurology* 337 (2): 208–30. https://doi.org/10.1002/cne.903370204.

Seress, L, A I Gulyás, and T F Freund. 1991. “Parvalbumin- and Calbindin D28k-Immunoreactive Neurons in the Hippocampal Formation of the Macaque Monkey.” *The Journal of Comparative Neurology* 313 (1): 162–77. https://doi.org/10.1002/cne.903130112.

Shamay-Tsoory, Simone G, and Avi Mendelsohn. 2019. “Real-Life Neuroscience: An Ecological Approach to Brain and Behavior Research.” *Perspectives on Psychological Science* 14 (5): 841–59. https://doi.org/10.1177/1745691619856350.

Sharif, Farnaz, Behnam Tayebi, György Buzsáki, Sébastien Royer, and Antonio Fernandez-Ruiz. 2021. “Subcircuits of Deep and Superficial CA1 Place Cells Support Efficient Spatial Coding across Heterogeneous Environments.” *Neuron* 109 (2): 363-376.e6. https://doi.org/10.1016/j.neuron.2020.10.034.

Sheremet, Alex, Sara N Burke, and Andrew P Maurer. 2016. “Movement Enhances the Nonlinearity of Hippocampal Theta.” *The Journal of Neuroscience* 36 (15): 4218–30. https://doi.org/10.1523/JNEUROSCI.3564-15.2016.

Shirvalkar, Prasad R, Peter R Rapp, and Matthew L Shapiro. 2010. “Bidirectional Changes to Hippocampal Theta-Gamma Comodulation Predict Memory for Recent Spatial Episodes.” *Proceedings of the National Academy of Sciences of the United States of America* 107 (15): 7054–59. https://doi.org/10.1073/pnas.0911184107.

Siapas, A G, and M A Wilson. 1998. “Coordinated Interactions between Hippocampal Ripples and Cortical Spindles during Slow-Wave Sleep.” *Neuron* 21 (5): 1123–28. https://doi.org/10.1016/s0896-6273(00)80629-7.

Siegle, Joshua H, and Matthew A Wilson. 2014. “Enhancement of Encoding and Retrieval Functions through Theta Phase-Specific Manipulation of Hippocampus.” *ELife* 3 (July): e03061. https://doi.org/10.7554/eLife.03061.

Silva, Delia, Ting Feng, and David J Foster. 2015. “Trajectory Events across Hippocampal Place Cells Require Previous Experience.” *Nature Neuroscience* 18 (12): 1772–79. https://doi.org/10.1038/nn.4151.

Simon, Axelle Pascale, Frédérique Poindessous-Jazat, Patrick Dutar, Jacques Epelbaum, and Marie-Hélène Bassant. 2006. “Firing Properties of Anatomically Identified Neurons in the Medial Septum of Anesthetized and Unanesthetized Restrained Rats.” *The Journal of Neuroscience* 26 (35): 9038–46. https://doi.org/10.1523/JNEUROSCI.1401-06.2006.

Singer, W. 1993. “Synchronization of Cortical Activity and Its Putative Role in Information Processing and Learning.” *Annual Review of Physiology* 55: 349–74. https://doi.org/10.1146/annurev.ph.55.030193.002025.

Sjöström, P J, G G Turrigiano, and S B Nelson. 2001. “Rate, Timing, and Cooperativity Jointly Determine Cortical Synaptic Plasticity.” *Neuron* 32 (6): 1149–64. https://doi.org/10.1016/s0896-6273(01)00542-6.

Skaggs, William E, Bruce L McNaughton, Michele Permenter, Matthew Archibeque, Julie Vogt, David G Amaral, and Carol A Barnes. 2007. “EEG Sharp Waves and Sparse Ensemble Unit Activity in the Macaque Hippocampus.” *Journal of Neurophysiology* 98 (2): 898–910. https://doi.org/10.1152/jn.00401.2007.

Skaggs, William E., Bruce L. McNaughton, Matthew A. Wilson, and Carol A. Barnes. 1996. “Theta Phase Precession in Hippocampal Neuronal Populations and the Compression of Temporal Sequences.” *Hippocampus*, January.

Skaggs, W E, B L McNaughton, M A Wilson, and C A Barnes. 1996. “Theta Phase Precession in Hippocampal Neuronal Populations and the Compression of Temporal Sequences.” *Hippocampus* 6 (2): 149–72. https://doi.org/10.1002/(SICI)1098-1063(1996)6:2<149::AID-HIPO6>3.0.CO;2-K.

Skaggs, W E, and B L McNaughton. 1996. “Replay of Neuronal Firing Sequences in Rat Hippocampus during Sleep Following Spatial Experience.” *Science* 271 (5257): 1870–73. https://doi.org/10.1126/science.271.5257.1870.

Skelin, Ivan, Haoxin Zhang, Jie Zheng, Shiting Ma, Bryce A. Mander, Olivia Kim Mcmanus, Sumeet Vadera, Robert T. Knight, Bruce L. McNaughton, and Jack J. Lin. 2020. “Coupling between Slow-Waves and Sharp-Wave Ripples Organizes Distributed Neural Activity during Sleep in Humans.” *BioRxiv*, May. https://doi.org/10.1101/2020.05.24.113480.

Slomianka, Lutz, Irmgard Amrein, Irene Knuesel, Jens Christian Sørensen, and David P Wolfer. 2011. “Hippocampal Pyramidal Cells: The Reemergence of Cortical Lamination.” *Brain Structure & Function* 216 (4): 301–17. https://doi.org/10.1007/s00429-011-0322-0.

Smith, Anne C, Loren M Frank, Sylvia Wirth, Marianna Yanike, Dan Hu, Yasuo Kubota, Ann M Graybiel, Wendy A Suzuki, and Emery N Brown. 2004. “Dynamic Analysis of Learning in Behavioral Experiments.” *The Journal of Neuroscience* 24 (2): 447–61. https://doi.org/10.1523/JNEUROSCI.2908-03.2004.

Sobotka, S, and J L Ringo. 1997. “Saccadic Eye Movements, Even in Darkness, Generate Event-Related Potentials Recorded in Medial Sputum and Medial Temporal Cortex.” *Brain Research* 756 (1–2): 168–73. https://doi.org/10.1016/s0006-8993(97)00145-5.

Sobotka, Stanislaw, Wei Zuo, and James L Ringo. 2002. “Is the Functional Connectivity within Temporal Lobe Influenced by Saccadic Eye Movements?” *Journal of Neurophysiology* 88 (4): 1675–84. https://doi.org/10.1152/jn.2002.88.4.1675.

Soltesz, I, and M Deschênes. 1993. “Low- and High-Frequency Membrane Potential Oscillations during Theta Activity in CA1 and CA3 Pyramidal Neurons of the Rat Hippocampus under Ketamine-Xylazine Anesthesia.” *Journal of Neurophysiology* 70 (1): 97–116. https://doi.org/10.1152/jn.1993.70.1.97.

Soltesz, Ivan, and Attila Losonczy. 2018. “CA1 Pyramidal Cell Diversity Enabling Parallel Information Processing in the Hippocampus.” *Nature Neuroscience* 21 (4): 484–93. https://doi.org/10.1038/s41593-018-0118-0.

Sosa, Marielena, Hannah R Joo, and Loren M Frank. 2020. “Dorsal and Ventral Hippocampal Sharp-Wave Ripples Activate Distinct Nucleus Accumbens Networks.” *Neuron* 105 (4): 725-741.e8. https://doi.org/10.1016/j.neuron.2019.11.022.

Sotty, F, M Danik, F Manseau, F Laplante, R Quirion, and S Williams. 2003. “Distinct Electrophysiological Properties of Glutamatergic, Cholinergic and GABAergic Rat Septohippocampal Neurons: Novel Implications for Hippocampal Rhythmicity.” *The Journal of Physiology* 551 (3): 927–43. https://doi.org/10.1111/j.1469-7793.2003.00927.x.

Squire, Larry R, Lisa Genzel, John T Wixted, and Richard G Morris. 2015. “Memory Consolidation.” *Cold Spring Harbor Perspectives in Biology* 7 (8): a021766. https://doi.org/10.1101/cshperspect.a021766.

Squire, L R. 1992. “Memory and the Hippocampus: A Synthesis from Findings with Rats, Monkeys, and Humans.” *Psychological Review* 99 (2): 195–231. https://doi.org/10.1037/0033-295X.99.2.195.

Stangl, Matthias, Sabrina L Maoz, and Nanthia Suthana. 2023. “Mobile Cognition: Imaging the Human Brain in the ‘Real World’.” *Nature Reviews. Neuroscience* 24 (6): 347–62. https://doi.org/10.1038/s41583-023-00692-y.

Stangl, Matthias, Uros Topalovic, Cory S Inman, Sonja Hiller, Diane Villaroman, Zahra M Aghajan, Leonardo Christov-Moore, et al. 2021. “Boundary-Anchored Neural Mechanisms of Location-Encoding for Self and Others.” *Nature* 589 (7842): 420–25. https://doi.org/10.1038/s41586-020-03073-y.

Stanley, Emily M, Marlene A Wilson, and Jim R Fadel. 2012. “Hippocampal Neurotransmitter Efflux during One-Trial Novel Object Recognition in Rats.” *Neuroscience Letters* 511 (1): 38–42. https://doi.org/10.1016/j.neulet.2012.01.033.

Staresina, Bernhard P, Sebastian Michelmann, Mathilde Bonnefond, Ole Jensen, Nikolai Axmacher, and Juergen Fell. 2016. “Hippocampal Pattern Completion Is Linked to Gamma Power Increases and Alpha Power Decreases during Recollection.” *ELife* 5 (August). https://doi.org/10.7554/eLife.17397.

Stark, Eran, and Moshe Abeles. 2009. “Unbiased Estimation of Precise Temporal Correlations between Spike Trains.” *Journal of Neuroscience Methods* 179 (1): 90–100. https://doi.org/10.1016/j.jneumeth.2008.12.029.

Stark, Eran, Ronny Eichler, Lisa Roux, Shigeyoshi Fujisawa, Horacio G Rotstein, and György Buzsáki. 2013. “Inhibition-Induced Theta Resonance in Cortical Circuits.” *Neuron* 80 (5): 1263–76. https://doi.org/10.1016/j.neuron.2013.09.033.

Stark, Eran, Lisa Roux, Ronny Eichler, Yuta Senzai, Sebastien Royer, and György Buzsáki. 2014. “Pyramidal Cell-Interneuron Interactions Underlie Hippocampal Ripple Oscillations.” *Neuron* 83 (2): 467–80. https://doi.org/10.1016/j.neuron.2014.06.023.

Steinschneider, M, C E Tenke, C E Schroeder, D C Javitt, G V Simpson, J C Arezzo, and H G Vaughan. 1992. “Cellular Generators of the Cortical Auditory Evoked Potential Initial Component.” *Electroencephalography and Clinical Neurophysiology* 84 (2): 196–200. https://doi.org/10.1016/0168-5597(92)90026-8.

Steriade, M, D A McCormick, and T J Sejnowski. 1993. “Thalamocortical Oscillations in the Sleeping and Aroused Brain.” *Science* 262 (5134): 679–85. https://doi.org/10.1126/science.8235588.

Stevens, C F, and A M Zador. 1998. “Input Synchrony and the Irregular Firing of Cortical Neurons.” *Nature Neuroscience* 1 (3): 210–17. https://doi.org/10.1038/659.

Stewart, M, and S E Fox. 1991. “Hippocampal Theta Activity in Monkeys.” *Brain Research* 538 (1): 59–63. https://doi.org/10.1016/0006-8993(91)90376-7.

Sullivan, David, Jozsef Csicsvari, Kenji Mizuseki, Sean Montgomery, Kamran Diba, and György Buzsáki. 2011. “Relationships between Hippocampal Sharp Waves, Ripples, and Fast Gamma Oscillation: Influence of Dentate and Entorhinal Cortical Activity.” *The Journal of Neuroscience* 31 (23): 8605–16. https://doi.org/10.1523/JNEUROSCI.0294-11.2011.

Sun, Yanjun, Amanda Q Nguyen, Joseph P Nguyen, Luc Le, Dieter Saur, Jiwon Choi, Edward M Callaway, and Xiangmin Xu. 2014. “Cell-Type-Specific Circuit Connectivity of Hippocampal CA1 Revealed through Cre-Dependent Rabies Tracing.” *Cell Reports* 7 (1): 269–80. https://doi.org/10.1016/j.celrep.2014.02.030.

Sutherland, R J, R J McDonald, C R Hill, and J W Rudy. 1989. “Damage to the Hippocampal Formation in Rats Selectively Impairs the Ability to Learn Cue Relationships.” *Behavioral and Neural Biology* 52 (3): 331–56. https://doi.org/10.1016/S0163-1047(89)90457-3.

Szabo, Gergely G, Jordan S Farrell, Barna Dudok, Wen-Hsien Hou, Anna L Ortiz, Csaba Varga, Prannath Moolchand, et al. 2022. “Ripple-Selective GABAergic Projection Cells in the Hippocampus.” *Neuron* 110 (12): 1959-1977.e9. https://doi.org/10.1016/j.neuron.2022.04.002.

Tai, Siew Kian, Jingyi Ma, Klaus-Peter Ossenkopp, and L Stan Leung. 2012. “Activation of Immobility-Related Hippocampal Theta by Cholinergic Septohippocampal Neurons during Vestibular Stimulation.” *Hippocampus* 22 (4): 914–25. https://doi.org/10.1002/hipo.20955.

Takahashi, Muneyoshi, Hiroshi Nishida, A David Redish, and Johan Lauwereyns. 2014. “Theta Phase Shift in Spike Timing and Modulation of Gamma Oscillation: A Dynamic Code for Spatial Alternation during Fixation in Rat Hippocampal Area CA1.” *Journal of Neurophysiology* 111 (8): 1601–14. https://doi.org/10.1152/jn.00395.2013.

Takahashi, Naoya, Takuya Sasaki, Wataru Matsumoto, Norio Matsuki, and Yuji Ikegaya. 2010. “Circuit Topology for Synchronizing Neurons in Spontaneously Active Networks.” *Proceedings of the National Academy of Sciences of the United States of America* 107 (22): 10244–49. https://doi.org/10.1073/pnas.0914594107.

Takeuchi, Saori, Tatsuya Mima, Rie Murai, Hideki Shimazu, Yoshikazu Isomura, and Toru Tsujimoto. 2015. “Gamma Oscillations and Their Cross-Frequency Coupling in the Primate Hippocampus during Sleep.” *Sleep* 38 (7): 1085–91. https://doi.org/10.5665/sleep.4818.

Talakoub, Omid, Andrea Gomez Palacio Schjetnan, Taufik A Valiante, Milos R Popovic, and Kari L Hoffman. 2016. “Closed-Loop Interruption of Hippocampal Ripples through Fornix Stimulation in the Non-Human Primate.” *Brain Stimulation* 9 (6): 911–18. https://doi.org/10.1016/j.brs.2016.07.010.

Talakoub, Omid, Patricia F Sayegh, Thilo Womelsdorf, Wolf Zinke, Pascal Fries, Christopher M Lewis, and Kari L Hoffman. 2019. “Hippocampal and Neocortical Oscillations Are Tuned to Behavioral State in Freely-Behaving Macaques.” *BioRxiv*, February. https://doi.org/10.1101/552877.

Tamura, Ryoi, Hiroshi Nishida, Satoshi Eifuku, Hiroaki Fushiki, Yukio Watanabe, and Kumiko Uchiyama. 2013. “Sleep-Stage Correlates of Hippocampal Electroencephalogram in Primates.” *Plos One* 8 (12): e82994. https://doi.org/10.1371/journal.pone.0082994.

Templer, Victoria L, and Robert R Hampton. 2012. “Rhesus Monkeys (Macaca Mulatta) Show Robust Evidence for Memory Awareness across Multiple Generalization Tests.” *Animal Cognition* 15 (3): 409–19. https://doi.org/10.1007/s10071-011-0468-4.

———. 2013a. “Cognitive Mechanisms of Memory for Order in Rhesus Monkeys (Macaca Mulatta).” *Hippocampus* 23 (3): 193–201. https://doi.org/10.1002/hipo.22082.

———. 2013b. “Episodic Memory in Nonhuman Animals.” *Current Biology* 23 (17): R801-6. https://doi.org/10.1016/j.cub.2013.07.016.

Tenke, C E, C E Schroeder, J C Arezzo, and H G Vaughan. 1993. “Interpretation of High-Resolution Current Source Density Profiles: A Simulation of Sublaminar Contributions to the Visual Evoked Potential.” *Experimental Brain Research* 94 (2): 183–92. https://doi.org/10.1007/BF00230286.

Teyler, T J, and P DiScenna. 1986. “The Hippocampal Memory Indexing Theory.” *Behavioral Neuroscience* 100 (2): 147–54. https://doi.org/10.1037/0735-7044.100.2.147.

Thammasan, Nattapong, and Makoto Miyakoshi. 2020. “Cross-Frequency Power-Power Coupling Analysis: A Useful Cross-Frequency Measure to Classify ICA-Decomposed EEG.” *Sensors (Basel, Switzerland)* 20 (24). https://doi.org/10.3390/s20247040.

Thome, Alexander, Diano F Marrone, Timothy M Ellmore, Monica K Chawla, Peter Lipa, Victor Ramirez-Amaya, Sarah H Lisanby, Bruce L McNaughton, and Carol A Barnes. 2017. “Evidence for an Evolutionarily Conserved Memory Coding Scheme in the Mammalian Hippocampus.” *The Journal of Neuroscience* 37 (10): 2795–2801. https://doi.org/10.1523/JNEUROSCI.3057-16.2017.

Tingley, David, and Adrien Peyrache. 2020. “On the Methods for Reactivation and Replay Analysis.” *Philosophical Transactions of the Royal Society of London. Series B, Biological Sciences* 375 (1799): 20190231. https://doi.org/10.1098/rstb.2019.0231.

Tong, Ai Phuong S, Alex P Vaz, John H Wittig, Sara K Inati, and Kareem A Zaghloul. 2021. “Ripples Reflect a Spectrum of Synchronous Spiking Activity in Human Anterior Temporal Lobe.” *ELife* 10 (November). https://doi.org/10.7554/eLife.68401.

Topolnik, Lisa, and Suhel Tamboli. 2022. “The Role of Inhibitory Circuits in Hippocampal Memory Processing.” *Nature Reviews. Neuroscience* 23 (8): 476–92. https://doi.org/10.1038/s41583-022-00599-0.

Torrence, Christopher, and Gilbert P. Compo. 1998. “A Practical Guide to Wavelet Analysis.” *Bulletin of the American Meteorological Society* 79 (1): 61–78. https://doi.org/10.1175/1520-0477(1998)079<0061:APGTWA>2.0.CO;2.

Tort, Adriano B L, Robert Komorowski, Howard Eichenbaum, and Nancy Kopell. 2010. “Measuring Phase-Amplitude Coupling between Neuronal Oscillations of Different Frequencies.” *Journal of Neurophysiology* 104 (2): 1195–1210. https://doi.org/10.1152/jn.00106.2010.

Tort, Adriano B L, Robert W Komorowski, Joseph R Manns, Nancy J Kopell, and Howard Eichenbaum. 2009. “Theta-Gamma Coupling Increases during the Learning of Item-Context Associations.” *Proceedings of the National Academy of Sciences of the United States of America* 106 (49): 20942–47. https://doi.org/10.1073/pnas.0911331106.

Tort, Adriano B L, Mark A Kramer, Catherine Thorn, Daniel J Gibson, Yasuo Kubota, Ann M Graybiel, and Nancy J Kopell. 2008. “Dynamic Cross-Frequency Couplings of Local Field Potential Oscillations in Rat Striatum and Hippocampus during Performance of a T-Maze Task.” *Proceedings of the National Academy of Sciences of the United States of America* 105 (51): 20517–22. https://doi.org/10.1073/pnas.0810524105.

Tóth, K, T F Freund, and R Miles. 1997. “Disinhibition of Rat Hippocampal Pyramidal Cells by GABAergic Afferents from the Septum.” *The Journal of Physiology* 500 (Pt 2) (Pt 2): 463–74. https://doi.org/10.1113/jphysiol.1997.sp022033.

Trainito, Caterina, Constantin von Nicolai, Earl K Miller, and Markus Siegel. 2019. “Extracellular Spike Waveform Dissociates Four Functionally Distinct Cell Classes in Primate Cortex.” *Current Biology* 29 (18): 2973-2982.e5. https://doi.org/10.1016/j.cub.2019.07.051.

Traub, R D, M O Cunningham, T Gloveli, F E N LeBeau, A Bibbig, E H Buhl, and M A Whittington. 2003. “GABA-Enhanced Collective Behavior in Neuronal Axons Underlies Persistent Gamma-Frequency Oscillations.” *Proceedings of the National Academy of Sciences of the United States of America* 100 (19): 11047–52. https://doi.org/10.1073/pnas.1934854100.

Traub, R D, M A Whittington, S B Colling, G Buzsáki, and J G Jefferys. 1996. “Analysis of Gamma Rhythms in the Rat Hippocampus in Vitro and in Vivo.” *The Journal of Physiology* 493 (Pt 2) (Pt 2): 471–84. https://doi.org/10.1113/jphysiol.1996.sp021397.

Trimper, John B, Claire R Galloway, Andrew C Jones, Kaavya Mandi, and Joseph R Manns. 2017. “Gamma Oscillations in Rat Hippocampal Subregions Dentate Gyrus, CA3, CA1, and Subiculum Underlie Associative Memory Encoding.” *Cell Reports* 21 (9): 2419–32. https://doi.org/10.1016/j.celrep.2017.10.123.

Trimper, John B, Roxana A Stefanescu, and Joseph R Manns. 2014. “Recognition Memory and Theta-Gamma Interactions in the Hippocampus.” *Hippocampus* 24 (3): 341–53. https://doi.org/10.1002/hipo.22228.

Tse, Dorothy, Rosamund F Langston, Masaki Kakeyama, Ingrid Bethus, Patrick A Spooner, Emma R Wood, Menno P Witter, and Richard G M Morris. 2007. “Schemas and Memory Consolidation.” *Science* 316 (5821): 76–82. https://doi.org/10.1126/science.1135935.

Tsodyks, M, T Kenet, A Grinvald, and A Arieli. 1999. “Linking Spontaneous Activity of Single Cortical Neurons and the Underlying Functional Architecture.” *Science* 286 (5446): 1943–46. https://doi.org/10.1126/science.286.5446.1943.

Tukker, John J, Pablo Fuentealba, Katja Hartwich, Peter Somogyi, and Thomas Klausberger. 2007. “Cell Type-Specific Tuning of Hippocampal Interneuron Firing during Gamma Oscillations in Vivo.” *The Journal of Neuroscience* 27 (31): 8184–89. https://doi.org/10.1523/JNEUROSCI.1685-07.2007.

Tulving, and E. 1972. “Episodic Memory and Semantic Memory.” *Organization of Memory*.

Tulving, Endel, and Hans J. Markowitsch. 1998. “Episodic and Declarative Memory: Role of the Hippocampus.” *Hippocampus*, January.

Turesson, Hjalmar K, Nikos K Logothetis, and Kari L Hoffman. 2012. “Category-Selective Phase Coding in the Superior Temporal Sulcus.” *Proceedings of the National Academy of Sciences of the United States of America* 109 (47): 19438–43. https://doi.org/10.1073/pnas.1217012109.

Uchida, S, T Maehara, N Hirai, Y Okubo, and H Shimizu. 2001. “Cortical Oscillations in Human Medial Temporal Lobe during Wakefulness and All-Night Sleep.” *Brain Research* 891 (1–2): 7–19. https://doi.org/10.1016/s0006-8993(00)03154-1.

Ulanovsky, Nachum, and Cynthia F Moss. 2007. “Hippocampal Cellular and Network Activity in Freely Moving Echolocating Bats.” *Nature Neuroscience* 10 (2): 224–33. https://doi.org/10.1038/nn1829.

Umbach, Gray, Ryan Tan, Joshua Jacobs, Brad E Pfeiffer, and Bradley Lega. 2022. “Flexibility of Functional Neuronal Assemblies Supports Human Memory.” *Nature Communications* 13 (1): 6162. https://doi.org/10.1038/s41467-022-33587-0.

“Unable to Find Information for 13050334.” n.d.

Valero, Manuel, Elena Cid, Robert G Averkin, Juan Aguilar, Alberto Sanchez-Aguilera, Tim J Viney, Daniel Gomez-Dominguez, Elisa Bellistri, and Liset Menendez de la Prida. 2015. “Determinants of Different Deep and Superficial CA1 Pyramidal Cell Dynamics during Sharp-Wave Ripples.” *Nature Neuroscience* 18 (9): 1281–90. https://doi.org/10.1038/nn.4074.

Vandecasteele, Marie, Viktor Varga, Antal Berényi, Edit Papp, Péter Barthó, Laurent Venance, Tamás F Freund, and György Buzsáki. 2014. “Optogenetic Activation of Septal Cholinergic Neurons Suppresses Sharp Wave Ripples and Enhances Theta Oscillations in the Hippocampus.” *Proceedings of the National Academy of Sciences of the United States of America* 111 (37): 13535–40. https://doi.org/10.1073/pnas.1411233111.

Vanderwolf, C H. 1969. “Hippocampal Electrical Activity and Voluntary Movement in the Rat.” *Electroencephalography and Clinical Neurophysiology* 26 (4): 407–18. https://doi.org/10.1016/0013-4694(69)90092-3.

Vanduffel, W, D Fize, H Peuskens, K Denys, S Sunaert, J T Todd, and G A Orban. 2002. “Extracting 3D from Motion: Differences in Human and Monkey Intraparietal Cortex.” *Science* 298 (5592): 413–15. https://doi.org/10.1126/science.1073574.

Varela, F, J P Lachaux, E Rodriguez, and J Martinerie. 2001. “The Brainweb: Phase Synchronization and Large-Scale Integration.” *Nature Reviews. Neuroscience* 2 (4): 229–39. https://doi.org/10.1038/35067550.

Varga, Csaba, Peyman Golshani, and Ivan Soltesz. 2012. “Frequency-Invariant Temporal Ordering of Interneuronal Discharges during Hippocampal Oscillations in Awake Mice.” *Proceedings of the National Academy of Sciences of the United States of America* 109 (40): E2726-34. https://doi.org/10.1073/pnas.1210929109.

Varga, Csaba, Mikko Oijala, Jonathan Lish, Gergely G Szabo, Marianne Bezaire, Ivan Marchionni, Peyman Golshani, and Ivan Soltesz. 2014. “Functional Fission of Parvalbumin Interneuron Classes during Fast Network Events.” *ELife* 3 (November). https://doi.org/10.7554/eLife.04006.

Varga, Viktor, Balázs Hangya, Kinga Kránitz, Anikó Ludányi, Rita Zemankovics, István Katona, Ryuichi Shigemoto, Tamás F Freund, and Zsolt Borhegyi. 2008. “The Presence of Pacemaker HCN Channels Identifies Theta Rhythmic GABAergic Neurons in the Medial Septum.” *The Journal of Physiology* 586 (16): 3893–3915. https://doi.org/10.1113/jphysiol.2008.155242.

Vaz, Alex P, Sara K Inati, Nicolas Brunel, and Kareem A Zaghloul. 2019. “Coupled Ripple Oscillations between the Medial Temporal Lobe and Neocortex Retrieve Human Memory.” *Science* 363 (6430): 975–78. https://doi.org/10.1126/science.aau8956.

Vaz, Alex P, John H Wittig, Sara K Inati, and Kareem A Zaghloul. 2020. “Replay of Cortical Spiking Sequences during Human Memory Retrieval.” *Science* 367 (6482): 1131–34. https://doi.org/10.1126/science.aba0672.

Ven, Gido M van de, Stéphanie Trouche, Colin G McNamara, Kevin Allen, and David Dupret. 2016. “Hippocampal Offline Reactivation Consolidates Recently Formed Cell Assembly Patterns during Sharp Wave-Ripples.” *Neuron* 92 (5): 968–74. https://doi.org/10.1016/j.neuron.2016.10.020.

Vinck, Martin, Cem Uran, and Marius Schneider. 2022. “Aperiodic Processes Explaining Rhythms in Behavior: A Matter of False Detection or Definition?,” July. https://doi.org/10.31234/osf.io/wzvfh.

Vinck, Martin, Marijn van Wingerden, Thilo Womelsdorf, Pascal Fries, and Cyriel M A Pennartz. 2010. “The Pairwise Phase Consistency: A Bias-Free Measure of Rhythmic Neuronal Synchronization.” *Neuroimage* 51 (1): 112–22. https://doi.org/10.1016/j.neuroimage.2010.01.073.

Viney, Tim J, Balint Lasztoczi, Linda Katona, Michael G Crump, John J Tukker, Thomas Klausberger, and Peter Somogyi. 2013. “Network State-Dependent Inhibition of Identified Hippocampal CA3 Axo-Axonic Cells in Vivo.” *Nature Neuroscience* 16 (12): 1802–11. https://doi.org/10.1038/nn.3550.

Vivekananda, Umesh, Daniel Bush, James A Bisby, Sallie Baxendale, Roman Rodionov, Beate Diehl, Fahmida A Chowdhury, et al. 2021. “Theta Power and Theta-Gamma Coupling Support Long-Term Spatial Memory Retrieval.” *Hippocampus* 31 (2): 213–20. https://doi.org/10.1002/hipo.23284.

Voloh, Benjamin, David J-N Maisson, Roberto Lopez Cervera, Indirah Conover, Mrunal Zambre, Benjamin Hayden, and Jan Zimmermann. 2023. “Hierarchical Action Encoding in Prefrontal Cortex of Freely Moving Macaques.” *Cell Reports* 42 (9): 113091. https://doi.org/10.1016/j.celrep.2023.113091.

Wagner, Ferdinand. 2006. *Modeling Software with Finite State Machines: A Practical Approach*. Auerbach Publications. https://doi.org/10.1201/9781420013641.

Wallace, Damian J, and Jason Nd Kerr. 2010. “Chasing the Cell Assembly.” *Current Opinion in Neurobiology*, May. https://doi.org/10.1016/j.conb.2010.05.003.

Wallenstein, G V, and M E Hasselmo. 1997. “GABAergic Modulation of Hippocampal Population Activity: Sequence Learning, Place Field Development, and the Phase Precession Effect.” *Journal of Neurophysiology* 78 (1): 393–408. https://doi.org/10.1152/jn.1997.78.1.393.

Wang, X J, and G Buzsáki. 1996. “Gamma Oscillation by Synaptic Inhibition in a Hippocampal Interneuronal Network Model.” *The Journal of Neuroscience* 16 (20): 6402–13. https://doi.org/10.1523/JNEUROSCI.16-20-06402.1996.

Wang, Yingxue, Sandro Romani, Brian Lustig, Anthony Leonardo, and Eva Pastalkova. 2015. “Theta Sequences Are Essential for Internally Generated Hippocampal Firing Fields.” *Nature Neuroscience* 18 (2): 282–88. https://doi.org/10.1038/nn.3904.

Watrous, Andrew J, Darrin J Lee, Ali Izadi, Gene G Gurkoff, Kiarash Shahlaie, and Arne D Ekstrom. 2013. “A Comparative Study of Human and Rat Hippocampal Low-Frequency Oscillations during Spatial Navigation.” *Hippocampus* 23 (8): 656–61. https://doi.org/10.1002/hipo.22124.

Weidemann, Christoph T, James E Kragel, Bradley C Lega, Gregory A Worrell, Michael R Sperling, Ashwini D Sharan, Barbara C Jobst, et al. 2019. “Neural Activity Reveals Interactions between Episodic and Semantic Memory Systems during Retrieval.” *Journal of Experimental Psychology: General* 148 (1): 1–12. https://doi.org/10.1037/xge0000480.

Wespatat, Valérie, Frank Tennigkeit, and Wolf Singer. 2004. “Phase Sensitivity of Synaptic Modifications in Oscillating Cells of Rat Visual Cortex.” *The Journal of Neuroscience* 24 (41): 9067–75. https://doi.org/10.1523/JNEUROSCI.2221-04.2004.

Whishaw, I Q, and C H Vanderwolf. 1973. “Hippocampal EEG and Behavior: Changes in Amplitude and Frequency of RSA (Theta Rhythm) Associated with Spontaneous and Learned Movement Patterns in Rats and Cats.” *Behavioral Biology* 8 (4): 461–84. https://doi.org/10.1016/S0091-6773(73)80041-0.

Whittington, M A, I M Stanford, S B Colling, J G Jefferys, and R D Traub. 1997. “Spatiotemporal Patterns of Gamma Frequency Oscillations Tetanically Induced in the Rat Hippocampal Slice.” *The Journal of Physiology* 502 (Pt 3) (Pt 3): 591–607. https://doi.org/10.1111/j.1469-7793.1997.591bj.x.

Whittington, M A, R D Traub, and J G Jefferys. 1995. “Synchronized Oscillations in Interneuron Networks Driven by Metabotropic Glutamate Receptor Activation.” *Nature* 373 (6515): 612–15. https://doi.org/10.1038/373612a0.

Whittington, M A, R D Traub, N Kopell, B Ermentrout, and E H Buhl. 2000. “Inhibition-Based Rhythms: Experimental and Mathematical Observations on Network Dynamics.” *International Journal of Psychophysiology* 38 (3): 315–36. https://doi.org/10.1016/S0167-8760(00)00173-2.

Wilson, M A, and B L McNaughton. 1993. “Dynamics of the Hippocampal Ensemble Code for Space.” *Science* 261 (5124): 1055–58. https://doi.org/10.1126/science.8351520.

———. 1994. “Reactivation of Hippocampal Ensemble Memories during Sleep.” *Science* 265 (5172): 676–79. https://doi.org/10.1126/science.8036517.

Winson, J. 1972. “Interspecies Differences in the Occurrence of Theta.” *Behavioral Biology* 7 (4): 479–87. https://doi.org/10.1016/S0091-6773(72)80210-4.

———. 1978. “Loss of Hippocampal Theta Rhythm Results in Spatial Memory Deficit in the Rat.” *Science* 201 (4351): 160–63. https://doi.org/10.1126/science.663646.

Wintzer, Marie E, Roman Boehringer, Denis Polygalov, and Thomas J McHugh. 2014. “The Hippocampal CA2 Ensemble Is Sensitive to Contextual Change.” *The Journal of Neuroscience* 34 (8): 3056–66. https://doi.org/10.1523/JNEUROSCI.2563-13.2014.

Wójtowicz, Tomasz, and Jerzy W Mozrzymas. 2015. “Diverse Impact of Neuronal Activity at θ Frequency on Hippocampal Long-Term Plasticity.” *Journal of Neuroscience Research* 93 (9): 1330–44. https://doi.org/10.1002/jnr.23581.

Womelsdorf, Thilo, Christopher Thomas, Adam Neumann, Marcus R Watson, Kianoush Banaie Boroujeni, Seyed A Hassani, Jeremy Parker, and Kari L Hoffman. 2021. “A Kiosk Station for the Assessment of Multiple Cognitive Domains and Cognitive Enrichment of Monkeys.” *Frontiers in Behavioral Neuroscience* 15 (August): 721069. https://doi.org/10.3389/fnbeh.2021.721069.

Wood, E R, P A Dudchenko, and H Eichenbaum. 1999. “The Global Record of Memory in Hippocampal Neuronal Activity.” *Nature* 397 (6720): 613–16. https://doi.org/10.1038/17605.

Wood, E R, P A Dudchenko, R J Robitsek, and H Eichenbaum. 2000. “Hippocampal Neurons Encode Information about Different Types of Memory Episodes Occurring in the Same Location.” *Neuron* 27 (3): 623–33. https://doi.org/10.1016/s0896-6273(00)00071-4.

Wulff, Peer, Alexey A Ponomarenko, Marlene Bartos, Tatiana M Korotkova, Elke C Fuchs, Florian Bähner, Martin Both, et al. 2009. “Hippocampal Theta Rhythm and Its Coupling with Gamma Oscillations Require Fast Inhibition onto Parvalbumin-Positive Interneurons.” *Proceedings of the National Academy of Sciences of the United States of America* 106 (9): 3561–66. https://doi.org/10.1073/pnas.0813176106.

Xia, Frances, Blake A Richards, Matthew M Tran, Sheena A Josselyn, Kaori Takehara-Nishiuchi, and Paul W Frankland. 2017. “Parvalbumin-Positive Interneurons Mediate Neocortical-Hippocampal Interactions That Are Necessary for Memory Consolidation.” *ELife* 6 (September). https://doi.org/10.7554/eLife.27868.

Xing, Dajun, Yutai Shen, Samuel Burns, Chun-I Yeh, Robert Shapley, and Wu Li. 2012. “Stochastic Generation of Gamma-Band Activity in Primary Visual Cortex of Awake and Anesthetized Monkeys.” *The Journal of Neuroscience* 32 (40): 13873–80a. https://doi.org/10.1523/JNEUROSCI.5644-11.2012.

Yamamoto, Jun, Junghyup Suh, Daigo Takeuchi, and Susumu Tonegawa. 2014. “Successful Execution of Working Memory Linked to Synchronized High-Frequency Gamma Oscillations.” *Cell* 157 (4): 845–57. https://doi.org/10.1016/j.cell.2014.04.009.

Yang, Scott Cheng-Hsin, Máté Lengyel, and Daniel M Wolpert. 2016. “Active Sensing in the Categorization of Visual Patterns.” *ELife* 5 (February). https://doi.org/10.7554/eLife.12215.

Yang, Scott Cheng-Hsin, Daniel M Wolpert, and Máté Lengyel. 2018. “Theoretical Perspectives on Active Sensing.” *Current Opinion in Behavioral Sciences* 11 (October): 100–108. https://doi.org/10.1016/j.cobeha.2016.06.009.

Yartsev, Michael M, Menno P Witter, and Nachum Ulanovsky. 2011. “Grid Cells without Theta Oscillations in the Entorhinal Cortex of Bats.” *Nature* 479 (7371): 103–7. https://doi.org/10.1038/nature10583.

Ylinen, A, A Bragin, Z Nádasdy, G Jandó, I Szabó, A Sik, and G Buzsáki. 1995. “Sharp Wave-Associated High-Frequency Oscillation (200 Hz) in the Intact Hippocampus: Network and Intracellular Mechanisms.” *The Journal of Neuroscience* 15 (1 Pt 1): 30–46. https://doi.org/10.1523/JNEUROSCI.15-01-00030.1995.

Yukie, M. 2000. “Connections between the Medial Temporal Cortex and the CA1 Subfield of the Hippocampal Formation in the Japanese Monkey (Macaca Fuscata).” *The Journal of Comparative Neurology* 423 (2): 282–98. https://doi.org/10.1002/1096-9861(20000724)423:2<282::aid-cne7>3.0.co;2-z.

Zhang, Hao, Shih-Chieh Lin, and Miguel A L Nicolelis. 2010. “Spatiotemporal Coupling between Hippocampal Acetylcholine Release and Theta Oscillations in Vivo.” *The Journal of Neuroscience* 30 (40): 13431–40. https://doi.org/10.1523/JNEUROSCI.1144-10.2010.

Zhang, Xin-Jun, Zhizhong Li, Zhi Han, Khadeejah T Sultan, Kun Huang, and Song-Hai Shi. 2017. “Precise Inhibitory Microcircuit Assembly of Developmentally Related Neocortical Interneurons in Clusters.” *Nature Communications* 8 (July): 16091. https://doi.org/10.1038/ncomms16091.

Zheng, Chenguang, Kevin Wood Bieri, Yi-Tse Hsiao, and Laura Lee Colgin. 2016. “Spatial Sequence Coding Differs during Slow and Fast Gamma Rhythms in the Hippocampus.” *Neuron* 89 (2): 398–408. https://doi.org/10.1016/j.neuron.2015.12.005.

Zhou, Y, A Sheremet, Y Qin, J P Kennedy, N M DiCola, S N Burke, and A P Maurer. 2019. “Methodological Considerations on the Use of Different Spectral Decomposition Algorithms to Study Hippocampal Rhythms.” *ENeuro* 6 (4). https://doi.org/10.1523/ENEURO.0142-19.2019.

Zhu, Seren L, Kaushik J Lakshminarasimhan, and Dora E Angelaki. 2023. “Computational Cross-Species Views of the Hippocampal Formation.” *Hippocampus* 33 (5): 586–99. https://doi.org/10.1002/hipo.23535.

Zutshi, Ipshita, Manuel Valero, Antonio Fernández-Ruiz, and György Buzsáki. 2022. “Extrinsic Control and Intrinsic Computation in the Hippocampal CA1 Circuit.” *Neuron* 110 (4): 658-673.e5. https://doi.org/10.1016/j.neuron.2021.11.015.